UNIVERSITÀ DEGLI STUDI DI MILANO
FACOLTÀ DI SCIENZE E TECNOLOGIE
CARL VON OSSIETZKY UNIVERSITÄT OLDENBURG
Doctoral Program in Mathematical Sciences
PhD in Mathematics

The *hp* version of the Virtual Element Method

Advisors:
Prof. Dr. Alexey Chernov
Prof. Dr. Simone Scacchi

Coadvisor:
Prof. Dr. Lourenço Beirão da Veiga

Coordinator:
Prof. Dr. Vieri Mastropietro

PhD thesis of:
Lorenzo Mascotto
MAT 08, XXX cycle

Academic Year 2016/2017

Contents

Chapter 1

Introduction

1.1 Aim of the thesis

The interest in Galerkin methods for the approximation of solutions to partial differential equations (PDEs in short) based on polytopal (i.e. polygonal, polyhedral, ...) meshes has recently grown, due to the high-flexibility that such meshes allow. In fact, employing polytopal meshes automatically includes the possibility of using nonconvex elements, hanging nodes (enabling natural handling of interface problems with nonmatching grids), easy construction of adaptive meshes and efficient approximations of geometric data features.

We provide here an (incomplete and short) list of polytopal methods: hybrid high-order methods (HHO) [62], mimetic finite difference (MFD) [34, 50], hybrid discontinuous Galerkin methods (HDGM) [60], polygonal finite element method (PFEM) [69, 86, 99], polygonal discontinuous Galerkin methods (DG-FEM) [53, 104], boundary element method-based FEM (BEM-based FEM) [92], weak Galerkin methods (WGM) [103].

The virtual element method (VEM in short) is an alternative (and among the most successful) approach enabling computation on polygonal (polyhedral in 3D) meshes [25, 30]. It is based on globally continuous discretization spaces that generally consist locally of Trefftz-like functions. More precisely, the key idea of the VEM is that trial and test spaces consists of functions that are solutions to local PDE problems in each element. Since these local problems do not admit closed-form solutions, the bilinear form, and thereby the entries of the stiffness matrix, are not computable in general. The computable version involves an approximate discrete bilinear form consisting of two additive parts: the first one involves local projections on polynomial spaces, the second one is a *computable* stabilizing bilinear form. We emphasize that the approximated discrete bilinear form can be evaluated without explicit knowledge of local basis functions in the interior of the polygonal element: an indirect description via the associated set of internal degrees of freedom suffices.

Among the properties of the VEM, in addition to the employment of polytopal meshes, we recall the possibility of handling approximation spaces of arbitrary $\mathcal{C}^k$ global regularity [37,51] and approximation spaces that satisfy exactly the divergence-free constraint [36].

Although the VEM is a very recent technology, the associated literature is widespread. We recall only some of the topics covered by this new methodology: implementation issues [30], general linear second-order elliptic problems [4,26,28,56], Stokes problem [6,36,52,55], Cahn-Hillard equation [7], locking-free linear elasticity problem [29, 67], small deformation problems in structural mechanics [24], plate bending problem [51], Steklov eigenvalue problem [87], residual based a-posteriori error estimation [38, 54, 88], serendipity VEM [27], application to discrete fracture network simulations [39–41], contact problem [105], comparison with the smoothed finite element method [89], topology optimization [66], geomechanics problem [5], Helmoltz problem [91].

In all the above mentioned works, the target was always the h version of the VEM, i.e. the convergence of the method is obtained by keeping fixed the dimension of local spaces, while refining the mesh.

Contrarily, the p version of a Galerkin method consists in achieving convergence by keeping fixed the decomposition of the domain and increasing the dimension of local spaces. The combination

of the h and p strategies goes by the name of hp version of the method under consideration.

The present thesis aims to combine the technology of the VEM with the p and the hp strategies. More precisely, we transfer the classical analysis of [14, 20, 96] to the VEM framework. Particular emphasis is giben to the approximation of two dimensional Poisson and Laplace problems, a priori and a posteriori error analysis, multrigrid solvers, stabilization of the method and conditioning of the stiffness matrix. Part of the topics covered by this thesis can be found in the following works: [10, 31, 32, 58, 79].

It is worth to point out that the only other polygonal methods (at least to the best of our knowledge) where the p and hp versions have been investigated so far are DG-FEM, see e.g. [53,104], and Hybrid High Order Methods, see e.g. [3].

Among the other reasons for which polygonal methods are useful within the hp framework, there is the fact that they allow for extremely flexible geometries when refining towards the corners of the domain and for an easy handling of refinement-derefinement strategies in adaptive algorithms.

The structure of the remainder of this chapter is the following. In Section 1.2, we fix some notations involving various functional spaces and associated norms. The model problems are introduced in Section 1.3, whereas, in Section 1.4, we discuss admissible polygonal decompositions along with their properties. Finally, in Section 1.5, we present in detail the outline of the thesis.

We highlight that, since we are going to demand many assumptions on the polygonal decomposition, we collect the all of them in a separate chapter at page 123.

1.2 Some useful notations

In this section, we collect some useful notations regarding the functional spaces employed throughout this thesis.

First of all, we underline that we mainly employ Lipschitz domains in $\mathbb{R}^2$; by Lipschitz domain we heuristically define a domain whose boundary is locally the graph of a Lipschitz function; for a more precise definition, we refer e.g. to [96, Appendix A].

Given Ω a Lipschitz domain in $\mathbb{R}^2$, we denote by $\partial\Omega$ the boundary of Ω. We firstly define the Lebesgue space of square integrable functions over Ω as:

$$L^2(\Omega) = \left\{ u : \Omega \to \mathbb{R} \mid u \text{ is Lebesgue measurable, } \int_\Omega |u|^2 < \infty \right\}. \tag{1.1}$$

We endow the space $L^2(\Omega)$ with the following inner product and norm:

$$(u, v)_{0,\Omega} = \int_\Omega u\, v, \qquad \|u\|_{0,\Omega}^2 = \int_\Omega |u|^2 \qquad \forall\, u,\, v \in L^2(\Omega). \tag{1.2}$$

Next, we introduce the Sobolev spaces. Let us denote, for a sufficiently regular function u, by:

$$D^{\boldsymbol{\alpha}} u = \partial_x^{\alpha_1} \partial_y^{\alpha_2} u \qquad \forall\, \boldsymbol{\alpha} = (\alpha_1, \alpha_2) \in \mathbb{N}^2 \tag{1.3}$$

the $\boldsymbol{\alpha}$ derivative of u, where here and henceforth by $\mathbb{N}$ we denote the set of natural numbers including 0. Having set:

$$\mathcal{C}_0^\infty(\Omega) = \{ u \in \mathcal{C}^\infty(\Omega) \mid \operatorname{supp}(u) \text{ is a compact subset of } \Omega \},$$

we define the concept of $\boldsymbol{\alpha}$ weak derivative. Given $u \in L^2(\Omega)$, we say that $v \in L^2(\Omega)$ is the $\boldsymbol{\alpha}$ weak derivative of u if:

$$\int_\Omega u\, D^{\boldsymbol{\alpha}} \varphi = (-1)^{|\boldsymbol{\alpha}|} \int_\Omega v\, \varphi \qquad \forall\, \varphi \in \mathcal{C}_0^\infty(\Omega), \tag{1.4}$$

where $|\cdot|$ denotes the ℓ^1 norm:

$$|\boldsymbol{\alpha}| = \alpha_1 + \alpha_2 \qquad \forall\, \boldsymbol{\alpha} = (\alpha_1, \alpha_2) \in \mathbb{N}^2. \tag{1.5}$$

Given $k \in \mathbb{N}$, we now define the Sobolev space of integer order k over Ω as follows:

$$H^k(\Omega) = \left\{ u \in L^2(\Omega) \mid \|u\|_{k,\Omega} < \infty \right\}, \tag{1.6}$$

where the Sobolev inner product and norm of integer order k read:

$$(u,v)_{k,\Omega} = \sum_{\boldsymbol{\alpha}\in\mathbb{N}^2\ |\boldsymbol{\alpha}|\leq k} (D^{\boldsymbol{\alpha}}u, D^{\boldsymbol{\alpha}}v)_{0,\Omega}, \quad \|v\|^2_{k,\Omega} = \sum_{\boldsymbol{\alpha}\in\mathbb{N}^2\ |\boldsymbol{\alpha}|\leq k} \|D^{\boldsymbol{\alpha}}u\|^2_{0,\Omega} \qquad \forall\, u,\, v \in H^k(\Omega). \tag{1.7}$$

It is also possible to define Sobolev spaces with fractional order. This can be done e.g. using interpolation theory [101, 102]. Equivalently, one can use an explicit definition. More precisely, let $k \in \mathbb{N}$ and $\theta \in (0,1)$. Then, $H^{k+\theta}(\Omega)$ is the subspace of $H^k(\Omega)$ consisting of functions having finite Aronszajn-Slobodeckij norm:

$$\|u\|^2_{k+\theta,\Omega} = \|u\|^2_{k,\Omega} + \sum_{|\boldsymbol{\alpha}|=k,\ \boldsymbol{\alpha}\in\mathbb{N}^2} \int_\Omega \int_\Omega \frac{|D^{\boldsymbol{\alpha}}u(\mathbf{x}) - D^{\boldsymbol{\alpha}}u(\mathbf{y})|^2}{|\mathbf{x}-\mathbf{y}|^{2+2\theta}} d\mathbf{x}\, d\mathbf{y}. \tag{1.8}$$

Analogously, it is possible to define Lebesgue and Sobolev spaces over $\partial\Omega$ as well as on straight edges.

The definition of Lebesgue spaces on the boundary, along with their inner products and norms, is a trivial extension of (1.1) and (1.2). For what instead concerns Sobolev spaces on a straight edge s, one defines:

$$H^k(s) = \left\{ u \in L^2(s) \mid |u|_{k,s} < \infty \right\}, \tag{1.9}$$

where the Sobolev inner product and norm of integer order k read:

$$(u,v)_{k,s} = \sum_{j\leq k} (\partial^j u, \partial^j v)_{0,s}, \quad |u|^2_{k,s} = (u,u)_{k,s}, \tag{1.10}$$

where $\partial^j u$ denotes the j-th tangential derivative of u on edge e.

We also explicitly write the definition of fractional space $H^\theta(\partial\Omega)$, $\theta \in (0,1)$, by imposing the finiteness of the Aronszajn-Slobodeckij norm over $\partial\Omega$:

$$\|u\|^2_{\theta,\partial\Omega} = \|u\|^2_{0,\partial\Omega} + |u|^2_{\theta,\partial\Omega} = \int_{\partial\Omega} |u|^2 + \int_{\partial\Omega}\int_{\partial\Omega} \frac{|u(\xi)-u(\eta)|^2}{|\xi-\eta|^{1+2\theta}} d\xi\, d\eta. \tag{1.11}$$

We recall the following classical result, which goes by the name of *Trace Theorem*, see e.g. [96].

Theorem 1.2.1. *Given Ω Lipschitz domain, there exists a linear, continuous and surjective map, which goes by the name of* trace operator*:*

$$\gamma: \quad H^1(\Omega) \quad \longrightarrow \quad H^{\frac{1}{2}}(\partial\Omega). \tag{1.12}$$

Having defined the trace, we denote, for some $g \in H^{\frac{1}{2}}(\partial\Omega)$:

$$H^1_g(\Omega) = \left\{ u \in H^1(\Omega) \mid \gamma(u) = g \right\}, \tag{1.13}$$

highlighting with a separate symbol the particular case of vanishing trace:

$$H^1_0(\Omega) = \left\{ u \in H^1(\Omega) \mid \gamma(u) = 0 \right\}. \tag{1.14}$$

It is possible also to define negative order Sobolev spaces. We explicitly give the definition of two of them. $H^{-1}(\Omega)$ is the dual of $H^1_0(\Omega)$ defined in (1.14) and is endowed with the following norm:

$$\|u\|_{-1,\Omega} = \sup_{\Phi\in H^1_0(\Omega),\, \Phi\neq 0} \frac{{}_{-1}\langle u, \Phi\rangle_1}{|\Phi|_{1,\Omega}}, \tag{1.15}$$

where ${}_{-1}\langle u, \cdot\rangle_1$ denotes the duality pairing of functional u on functions in $H^1_0(\Omega)$.

Instead, $H^{-\frac{1}{2}}(\partial\Omega)$ is the dual space of $H^{\frac{1}{2}}(\partial\Omega)$, which is defined through the finiteness of norm (1.11), and is endowed with the following norm:

$$\|u\|_{-\frac{1}{2},\partial\Omega} = \sup_{\Phi\in H^{\frac{1}{2}}(\partial\Omega),\, \Phi\neq 0} \frac{{}_{-\frac{1}{2}}\langle u, \Phi\rangle_{\frac{1}{2}}}{\|\Phi\|_{\frac{1}{2},\partial\Omega}}. \tag{1.16}$$

where ${}_{-\frac{1}{2}}\langle u, \cdot \rangle_{\frac{1}{2}}$ denotes the duality pairing of functional u on functions in $H^{\frac{1}{2}}(\partial\Omega)$.

In case we apply negative norms (1.15) and (1.16) to functions u in $L^2(\Omega)$ and $L^2(\partial\Omega)$ respectively, Riesz theorem, see e.g. [49, Theorem 2.4.2] implies:

$$\|u\|_{-1,\Omega} = \sup_{\Phi\in H^1_0(\Omega),\, \Phi\neq 0} \frac{(u,\Phi)_{0,\Omega}}{|\Phi|_{1,\Omega}}, \qquad \|u\|_{-\frac{1}{2},\Omega} = \sup_{\Phi\in H^{\frac{1}{2}}(\partial\Omega),\, \Phi\neq 0} \frac{(u,\Phi)_{0,\partial\Omega}}{\|\Phi\|_{\frac{1}{2},\partial\Omega}}.$$

In addition to the standard Lebesgue and (possibly fractional) Sobolev spaces, we will also employ more specific spaces, which arise naturally in the regularity analysis of elliptic PDEs on polygonal domains, see Appendix A. To this purpose, we henceforth assume that Ω is a polygonal domain with N_Ω vertices and edges. Let:

$$\{\mathbf{A}_i\}_{i=1}^{N_\Omega} \qquad \text{and} \qquad \{\omega_i\}_{i=1}^{N_\Omega}, \tag{1.17}$$

be the set of vertices and the width of the associated angles of Ω, see Figure 1.1. We can now

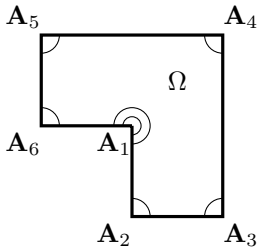

Figure 1.1: Vertices of domain Ω.

define the so-called weighted Sobolev spaces. To this purpose, we consider, given a vector $\boldsymbol{\beta} = (\beta_1, \ldots, \beta_{N_\Omega}) \in \mathbb{R}_+^{N_\Omega}$, a weight-function:

$$\Phi_{\boldsymbol{\beta}}(\mathbf{x}) = \Pi_{i=1}^{N_\Omega} \min(1, |\mathbf{x} - \mathbf{A}_i|)^{\beta_i}. \tag{1.18}$$

The weight function $\Phi_{\boldsymbol{\beta}}$ has the property of tending to 0 whenever $\mathbf{x}$ tends to any of the vertices of Ω; the rate of convergence to 0 at vertex $\mathbf{A}_i$ is described by the associated entry in the weight vector $\boldsymbol{\beta}$.

Given now $m, \ell \in \mathbb{N}$ with $m \geq \ell$ and $\boldsymbol{\beta} \in [0,1)^{N_\Omega}$, we define the *weighted Sobolev spaces* $H^{m,\ell}_{\boldsymbol{\beta}}(\Omega)$, as the completion of $\mathcal{C}^\infty(\overline{\Omega})$ with respect to the norm:

$$\|u\|^2_{H^{m,\ell}_{\boldsymbol{\beta}}(\Omega)} = \|u\|^2_{\ell-1,\Omega} + |u|^2_{H^{m,\ell}_{\boldsymbol{\beta}}(\Omega)} = \|u\|^2_{\ell-1,\Omega} + \sum_{k=\ell}^{m} \|\Phi_{\boldsymbol{\beta}+k-\ell}\, |D^k u|\|^2_{0,\Omega}, \tag{1.19}$$

where we have set, for $k \in \mathbb{N}$:

$$|D^k u| = \sum_{|\boldsymbol{\alpha}|=k,\ \boldsymbol{\alpha}\in\mathbb{N}^2} |D^{\boldsymbol{\alpha}} u|.$$

Here, we are using, with an abuse of notation, the following notation:

$$\boldsymbol{\beta} + k - \ell = (\beta_1 + k - \ell, \ldots, \beta_{N_\Omega} + k - \ell). \tag{1.20}$$

For future usage, we also define, for $m, \ell \in \mathbb{N}$ with $m \geq \ell$ and $\boldsymbol{\beta} \in [0,1)^{N_\Omega}$, weighted Sobolev norms and seminorms over straight edges $s \in \mathcal{E}_n$:

$$\|u\|^2_{H^{m,\ell}_{\boldsymbol{\beta}}(s)} = \|u\|^2_{\ell-1,s} + |u|^2_{H^{m,\ell}_{\boldsymbol{\beta}}(s)} = \|u\|^2_{\ell-1,s} + \sum_{k=\ell}^{m} \|\Phi_{\boldsymbol{\beta}+k-\ell}\, |\partial_t^k u|\|^2_{0,s}, \tag{1.21}$$

where $\partial_t u$ denotes the k-th tangential derivative of u.

Example 1.2.1. Examples of functions in weighted-Sobolev spaces are provided in (A.6) and (A.7).

At this point, we define the *countably normed spaces*, also known as *Babuška spaces*. Given $\ell \in \mathbb{N}$ and $\boldsymbol{\beta} \in [0,1)^{N_\Omega}$:

$$\begin{aligned}\mathcal{B}^{\ell}_{\boldsymbol{\beta}}(\Omega) &= \Big\{ u \in H^{m,\ell}_{\boldsymbol{\beta}}(\Omega)\, \forall\, m \geq \ell \geq 0 \mid \|\Phi_{\boldsymbol{\beta}+k-\ell}|D^k u|\|_{0,\Omega} \leq c_u\, d_u^{k-\ell}(k-\ell)!,\ \forall k \in \mathbb{N},\ k \geq \ell \Big\},\\ \mathcal{O}^{2}_{\boldsymbol{\beta}}(\Omega) &= \Big\{ u \in H^{m,2}_{\boldsymbol{\beta}}(\Omega)\, \forall\, m \geq 2 \mid |D^k u(\mathbf{x})| \leq c_u\, d_u^{k}(k)!\Phi^{-1}_{\boldsymbol{\beta}+k-1}(\mathbf{x}),\ \forall k \in \mathbb{N},\ k \geq 2,\ \forall \mathbf{x} \in \Omega \Big\},\end{aligned} \tag{1.22}$$

where c_u and d_u are two positive constants greater than 1 and depending only on function u.

It was proven in [17, Thorem 2.2], that the following inclusion holds true:

$$\mathcal{B}^2_{\boldsymbol{\beta}}(\Omega) \subset \mathcal{O}^2_{\boldsymbol{\beta}}(\Omega) \qquad \forall \boldsymbol{\beta} \in [0,1)^{N_\Omega}. \tag{1.23}$$

By:

$$\mathcal{B}^{\frac{3}{2}}_{\boldsymbol{\beta}}(\partial\Omega) \quad \text{and} \quad \mathcal{O}^{\frac{3}{2}}_{\boldsymbol{\beta}}(\partial\Omega), \tag{1.24}$$

we denote the spaces of traces of functions in spaces $\mathcal{B}^2_{\boldsymbol{\beta}}(\Omega)$ and $\mathcal{O}^2_{\boldsymbol{\beta}}(\Omega)$ respectively.

We also define the set of polynomials and harmonic polynomials of given degree $\ell \in \mathbb{N}$ over a domain $D \subseteq \mathbb{R}^2$ with the following symbols:

$$\mathbb{P}_\ell(D), \qquad \mathbb{H}_\ell(D). \tag{1.25}$$

1.3 The model problems

Throughout this thesis, we will focus our attention to the following model problem. Given $\Omega \subset \mathbb{R}^2$ polygonal domain, $f : \Omega \to \mathbb{R}$ and $g : \partial\Omega \to \mathbb{R}$ sufficiently regular, the aim is to find u such that:

$$\begin{cases} -\Delta u = f & \text{in } \Omega \\ u = g & \text{on } \partial\Omega \end{cases}. \tag{1.26}$$

Most of the time, we will consider the Poisson problem endowed with homogeneous boundary conditions, i.e. by imposing $g = 0$. The associated weak formulation reads:

$$\begin{cases} \text{find } u \in V \quad \text{such that} \\ a(u,v) = (f,v)_{0,\Omega} \quad \forall\, v \in V \end{cases}, \tag{1.27}$$

where:

$$V = H^1_0(\Omega), \qquad a(u,v) = (\nabla u, \nabla v)_{0,\Omega} \qquad \forall\, u,\, v \in V. \tag{1.28}$$

A particular situation occurs in Chapter 4, where the target problem is instead a Laplace problem, which is, problem (1.26) with $f = 0$ and $g \neq 0$. In this case, the weak formulation reads a bit differently:

$$\begin{cases} \text{find } u \in V_g \quad \text{such that} \\ a(u,v) = 0 \quad \forall\, v \in V \end{cases} \tag{1.29}$$

where:

$$V_g = H^1_g(\Omega). \tag{1.30}$$

It is well-known, see e.g. [49], that the Lax-Milgram lemma implies the well-posedness of problem (1.27), assuming $f \in L^2(\Omega)$.

The well-posedness of problem (1.29), assuming $g \in H^{\frac{1}{2}}(\partial K)$, is known as well; nonetheless, we briefly recall here its proof. Owing to Theorem 1.2.1 and in particular to the surjectivity of the trace operator, there exists a function $G \in V_g$. Moreover, problem (1.29) is equivalent to:

$$\begin{cases} \text{find } \widetilde{u} \in V \quad \text{such that} \\ a(\widetilde{u},v) = a(-G,v) \quad \forall\, v \in V \end{cases}, \tag{1.31}$$

where $\widetilde{u}$ has the form $\widetilde{u} = u - G$. Obviously, one has that $\widetilde{u} \in V$.

Using the fact that $a(-G, v)$ is a linear continuous functional, we can apply again the Lax-Milgram lemma for proving the well-posedness of problem (1.31). In order to conclude, it suffices to pick $u = \widetilde{u} + G$.

For the sake of completeness, the weak formulation of the full problem (1.26) (with nonhomogeneous Dirichlet boundary conditions) reads, for $f \in L^2(\Omega)$ and $g \in H^{\frac{1}{2}}(\partial\Omega)$:

$$\begin{cases} \text{find } u \in V_g \quad \text{such that} \\ a(u, v) = (f, v) \quad \forall\, v \in V \end{cases} . \tag{1.32}$$

The issue of the regularity of the weak solution to problem (1.32) is addressed in Appendix A.

1.4 Polygonal decompositions

The VEM, as already emphasized, can be considered as a generalization of the FEM to polytopal meshes. In this section, we introduce regularity assumptions on sequences of meshes $\{\mathcal{T}_n\}_{n\in\mathbb{N}}$ that are instrumental for the theoretical analysis in the next chapters.

Preliminarily, we highlight two facts. The first one is that, in the following, we will need "locally" stricter assumptions; we postpone the description of such assumptions when needed. The second one is that it is possible to weaken the regularity assumptions that we present here, as done in [35], but for the sake of simplicity we stick to simpler ones.

Let us firstly fix some notations. Let $\{\mathcal{T}_n\}_{n\in\mathbb{N}}$ be a sequence of polygonal decompositions of Ω. Let $\mathcal{V}_n$ ($\mathcal{V}_n^b$) and $\mathcal{E}_n$ ($\mathcal{E}_n^b$) be the set of (boundary vertices) and edges of decomposition $\mathcal{T}_n$ for all $n \in \mathbb{N}$.

To each edge $s \in \mathcal{E}_n$, we associate a tangential vector $\boldsymbol{\tau}_s = \boldsymbol{\tau}$ and a normal versor $\mathbf{n}_s = \mathbf{n}$ obtained by a counterclock-wise rotation of $\boldsymbol{\tau}_s$. When no confusion occurs, we denote $\boldsymbol{\tau}_s$ and $\mathbf{n}_s$ by $\boldsymbol{\tau}$ and $\mathbf{n}$.

We demand the following very basic assumption on $\mathcal{T}_n$, for all $n \in \mathbb{N}$:

(**G0**) $\mathcal{T}_n$ is a conforming polygonal decomposition of Ω, i.e. each boundary edge $s \in \mathcal{E}_n^b$ is an edge of *only one* element $K \in \mathcal{T}_n$, whereas each internal edge $s \in \mathcal{E}_n \setminus \mathcal{E}_n^b$ is an edge of *exactly two* elements K_1 and K_2 of $\mathcal{T}_n$.

Note that, since in our construction it is possible to have angles with magnitude 180°, assumption (**G0**) implies that hanging nodes are automatically included in the geometry of the decomposition, see Figure 1.2. We also fix the notation for the mesh size function of an edge, of an element and

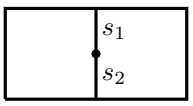

Figure 1.2: Two pentagons with two distinct adjacent edges s_1 and s_2 as interface.

of a mesh. Given $\mathcal{T}_n$ polygonal decomposition, $K \in \mathcal{T}_n$ and $s \in \mathcal{E}_n$, we define:

$$h_s = \text{length}(s), \qquad h_K = \text{diam}(K), \qquad h_{\mathcal{T}_n} = h = \max_{K\in\mathcal{T}_n} h_K. \tag{1.33}$$

Moreover, given $K \in \mathcal{T}_n$, we also define:

$$x_K, \qquad \text{the barycenter of polygon } K. \tag{1.34}$$

1.4.1 Regular and quasi-uniform polygonal meshes

We introduce next two additional assumptions under which we will say that $\{\mathcal{T}_n\}_{n\in\mathbb{N}}$ is a regular sequence of polygonal meshes. For all $n \in \mathbb{N}$:

(**G1**) every $K \in \mathcal{T}_n$ is star-shaped (see [49, (4.2.2)]) with respect to a ball of radius greater than or equal to $\rho_0 h_K$, where ρ_0 is a universal positive constant;

(**G2**) given any $K \in \mathcal{T}_n$, for all edges s of K, it holds that $h_s \geq \rho_0 h_K$, where ρ_0 is a universal positive constant; without loss of generality, we assume that ρ_0 is the same constant of assumption (**G1**); besides, the number of edges in K is uniformly bounded independently of the geometry of the domain.

In addition to (**G1**)-(**G2**), we occasionally demand an additional assumption, which allows us to define the concept of quasi-uniform meshes. For all $n \in \mathbb{N}$:

(**G3**) for all $K \in \mathcal{T}_n$, $h \leq c h_K$, being c a universal positive constant.

Under (**G0**)-(**G1**)-(**G2**)-(**G3**), we will discuss in Chapter 2 the h and p version of the VEM with quasi-uniform meshes. In Figure 1.3, we depict four possible meshes originating sequences of quasi-uniform meshes.

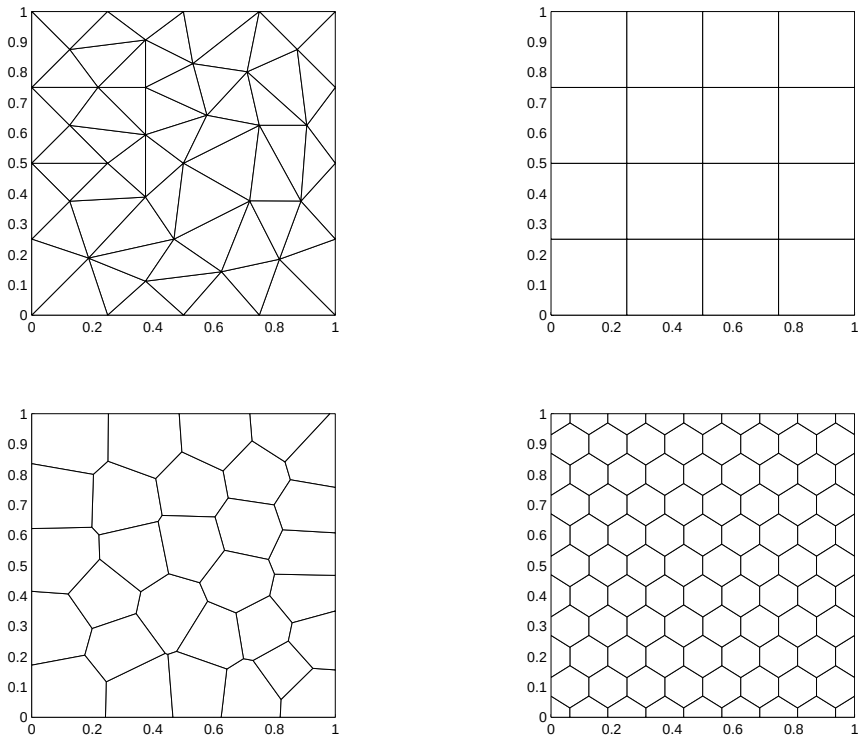

Figure 1.3: Up-left: unstructured triangular mesh. Up-right: square mesh. Down-left: Voronoi-Lloyd mesh. Down-right: regular-hexagonal mesh.

1.4.2 Geometrically graded meshes

When employing the full *hp* strategy, one needs to use meshes that are geometrically refined towards the vertices of domain Ω. More specifically, such meshes will be employed in Chapters 3 and 4. Here, we want to present a formal construction of such meshes.

In order to define geometrically graded meshes, we assume the following (actually non mandatory) simplifying requirement:

(**G4**) $\mathbf{0}$ is a vertex of Ω and is denoted by $\mathbf{A}_1$, see (1.17); moreover, the geometric refinements are performed only towards vertex $\mathbf{0}$ and not towards the other vertices. We also denote by

$H^{m,\ell}_{\beta}(\Omega,\mathbf{0})$, $\beta\in\mathbb{R}$, the weighted Sobolev and Babuška spaces with a unique singular vertex, the spaces obtained by the completion of $\mathcal{C}^{\infty}(\overline{\Omega})$ using the norm:

$$\|u\|^2_{H^{m,\ell}_{\beta}(\Omega)}=\|u\|^2_{\ell-1,\Omega}+|u|^2_{H^{m,\ell}_{\beta}(\Omega)}=\|u\|^2_{\ell-1,\Omega}+\sum_{k=\ell}^{m}\|\Phi_{\beta+k-\ell}|D^k u|\|^2_{0,\Omega} \tag{1.35}$$

and:

$$\mathcal{B}^{\ell}_{\beta}(\Omega,\mathbf{0})=\left\{u\in\mathcal{B}^{\ell}_{\boldsymbol{\beta}}(\Omega)\mid\boldsymbol{\beta}=(\beta,0,0,\ldots,0)\right\} \tag{1.36}$$

respectively, where the weight function Φ_{β} has been modified to:

$$\Phi_{\beta}(\mathbf{x})=\min(1,|\mathbf{x}-\mathbf{0}|^{\beta}). \tag{1.37}$$

We deem that under (**G4**) the presentation of the forthcoming theoretical results simpler.

Let assumptions (**G0**)-(**G1**)-(**G2**)-(**G4**) hold true and let $\sigma\in(0,1)$ be a given parameter; σ is related to the "rate of refinement" towards vertex $\mathbf{0}$.

We assume that, for all $n\in\mathbb{N}$, $\mathcal{T}_n$ consists of $n+1$ "layers", where the concept of "layer" is defined as follows.

We set the 0-th layer $L_{n,0}=L_0$ as the set of all polygons $K\in\mathcal{T}_n$ abutting $\mathbf{0}$, which we recall by (**G4**) is the unique "singular corner" of Ω. The other layers are defined by induction as:

$$L_{n,j}=L_j:=\left\{K_1\in\mathcal{T}_n\mid\overline{K}_1\cap\overline{K}_2\neq\emptyset\text{ for some }K_2\in L_{j-1}\text{ and }K_1\nsubseteq\cup_{i=0}^{j-1}L_i\right\}\quad\forall j=1,\ldots,n. \tag{1.38}$$

Next, we describe a procedure for building geometric (polygonal) graded meshes. Let $\mathcal{T}_0=\{\Omega\}$. The decomposition $\mathcal{T}_{n+1}$ is obtained by refining decomposition $\mathcal{T}_n$ *only* at the elements in the finest layer L_0. In order to have a proper geometric graded sequence of meshes, we demand for the following assumption.

(**G5**)

$$h_K\approx\begin{cases}\sigma^n & \text{if } K\in L_0\\ \frac{1-\sigma}{\sigma}\mathrm{dist}(K,\mathbf{0}) & \text{if } K\in L_j,\quad j=1,\ldots,n\end{cases}. \tag{1.39}$$

A consequence of (**G5**) is that $h_K\approx\sigma^{n-j}$, j being the layer to which K belongs. This, in addition to (1.39) guarantees that the distance between $K\in L_j$, $j=1,\ldots,n$ and $\mathbf{0}$ is proportional to σ^{n-j}. Moreover, following [72, equation (5.6)], it can be shown that the number of elements in each layer is uniformly bounded with respect to the geometric parameters discussed so far.

The sequence of meshes that we build is then characterized by very small elements near the singularity, while the size of the elements increases proportionally with the distance between the elements themselves and $\mathbf{0}$.

Example 1.4.1. In Figure 1.4, we present three polygonal meshes extrapolated from sequences of meshes satisfying assumption (**G0**)-(**G2**)-(**G4**)-(**G5**). We observe that the the sequence of meshes generated by the mesh in Figure 1.4 (right) does not fulfill the star-shapedness assumption (**G1**), whereas the other two meshes do.

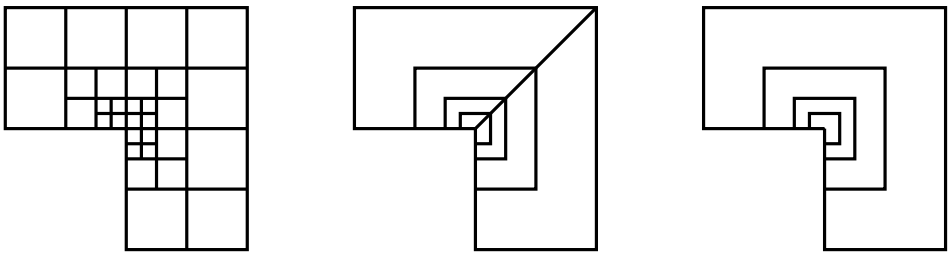

Figure 1.4: Decomposition $\mathcal{T}_n$, $n=3$, made of: squares (left), nonconvex hexagons and quadrilaterals (center), nonstar-shaped/nonconvex decagons and nonstar-shaped/nonconvex hexagons (right).

In Figure 1.5, we depict instead the first three elements associated with the mesh depicted in Figure 1.4 (center); as an example, we fix the geometric parameter σ to $\frac{1}{2}$.

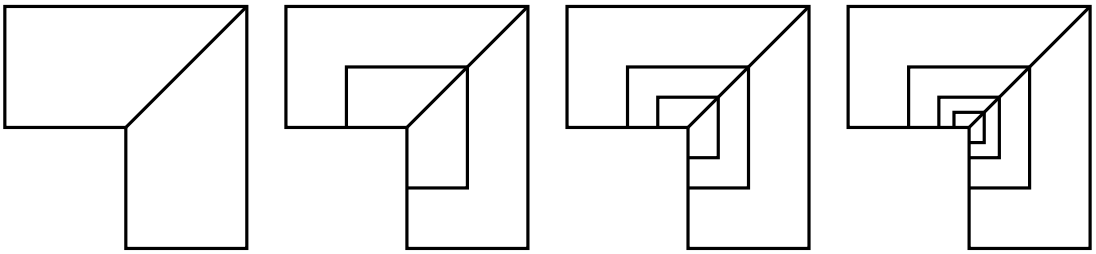

Figure 1.5: First three elements $\mathcal{T}_1$ (left), $\mathcal{T}_2$ (left-center), $\mathcal{T}_3$ (right-center), $\mathcal{T}_4$ (right) associated with the mesh depicted in Figure 1.4 (center). Here, geometric parameter σ is fixed to $\frac{1}{2}$.

1.4.3 Additional notation

Given $\mathcal{T}_n$, polygonal decomposition, we introduce some notations concerning $\mathcal{T}_n$.

In particular, we can split the bilinear form a defined in 1.28 as a sum of local contributions:

$$a(u,v) = \sum_{K\in\mathcal{T}_n} a^K(u,v) = \sum_{K\in\mathcal{T}_n} (\nabla u, \nabla v)_{0,K} \qquad \forall\, u,\, v \in V. \tag{1.40}$$

Moreover, we can also define the broken-H^1 seminorm and norm as:

$$|u|^2_{1,\mathcal{T}_n} = \sum_{K\in\mathcal{T}_n} |u|^2_{1,K}, \qquad \|u\|^2_{1,\mathcal{T}_n} = \sum_{K\in\mathcal{T}_n} \|u\|^2_{1,K} \qquad \forall\, u \in L^2(\Omega)\cap H^1(K) \quad \forall\, K \in \mathcal{T}_n. \tag{1.41}$$

Finally, we associate to each element $K \in \mathcal{T}_n$ a number $p_K \in \mathbb{N}$. We collect all these numbers in a vector $\mathbf{p} \in \mathbb{N}^{\mathrm{card}(\mathcal{T}_n)}$ and we consider the bijection:

$$\mathcal{T}_n \longleftrightarrow \mathbf{p} \qquad \text{with} \qquad K \longleftrightarrow p_K. \tag{1.42}$$

Then, we can define the space of continuous and discontinuous piecewise polynomials over decomposition $\mathcal{T}_n$ with polynomial distribution given by $\mathbf{p}$, as:

$$\mathcal{S}^{\mathbf{p},0}(\Omega,\mathcal{T}_n) = \big\{q \in \mathcal{C}^0(\overline{\Omega}) \mid q|_K \in \mathbb{P}_{p_K}(K)\big\}, \quad \mathcal{S}^{\mathbf{p},-1}(\Omega,\mathcal{T}_n) = \big\{q \in L^2(\Omega) \mid q|_K \in \mathbb{P}_{p_K}(K)\big\}. \tag{1.43}$$

In case $\mathbf{p}_i = p$ for all $i = 1,\dots,\mathrm{card}(\mathcal{T}_n)$, we use the notation $\mathcal{S}^{p,k}(\Omega,\mathcal{T}_n) = \mathcal{S}^{\mathbf{p},k}(\Omega,\mathcal{T}_n)$, $k = -1, 0$.

Analogously, we can define the space of continuous and discontinuous piecewise harmonic polynomials over decomposition $\mathcal{T}_n$ with polynomial distribution given by $\mathbf{p}$, as:

$$\mathcal{S}^{\mathbf{p},0}_\Delta(\Omega,\mathcal{T}_n) = \big\{q \in \mathcal{C}^0(\overline{\Omega}) \mid q|_K \in \mathbb{H}_{p_K}(K)\big\}, \quad \mathcal{S}^{\mathbf{p},-1}_\Delta(\Omega,\mathcal{T}_n) = \big\{q \in L^2(\Omega) \mid q|_K \in \mathbb{H}_{p_K}(K)\big\}. \tag{1.44}$$

In case $\mathbf{p}_i = p$ for all $i = 1,\dots,\mathrm{card}(\mathcal{T}_n)$, we use the notation $\mathcal{S}^{p,k}_\Delta(\Omega,\mathcal{T}_n) = \mathcal{S}^{\mathbf{p},k}_\Delta(\Omega,\mathcal{T}_n)$, $k = -1, 0$.

Throughout the thesis, we write $f \lesssim g$ for two positive quantities f and g depending on a discretization parameter (typically h or p) if there exists a parameter-independent positive constant c such that $f \le cg$ holds for all values of the parameter. We write $f \approx g$ if $f \lesssim g$ and $g \lesssim f$ hold.

1.5 Structure of the thesis

In this section, we describe the topics covered in the thesis. For a more detailed description of such topics, we refer to the introduction of the forthcoming chapters.

- The h and p version of the VEM on quasi-uniform meshes is investigated in Chapter 2; here, the issue of the regularity of the solution in not taken into account and we limit ourselves to prove convergence results for solutions with "desired" finite Sobolev regularity or, even, analytic solution.

- The case of solutions having instead the "natural" Sobolev regularity on polygons (thus taking corners into account) along with the full *hp* technology employing geometrically refined meshes, is addressed in Chapter 3, while in Chapter 4 the same issues are investigated for the solution to Laplace problems. The reason for which we split the analysis of the Poisson and Laplace equations is that in the latter case the structure of the approximation space takes advantages from the structure of the problem, leading in fact to a very efficient method.

- The a posteriori analysis of the *hp* VEM is studied in Chapter 5; we anticipate that this is a very preliminary investigation of this topic (no numerical tests are performed, no optimal bounds in terms of p for L^2 approximation by means of functions in local VE spaces, ...); a deeper analysis concerning a posteriori *hp* VEM is the subject of future works.

- In the previous parts, the issue of choosing a proper stabilization of the method, typical of the construction of the VEM, was not addressed. For this reason, Chapter 6 is devoted to introduce various stabilizations along with, both theoretical and numerical, explicit bounds in terms of the polynomial degree p.

- Having introduced various stabilizations, we present in Chapter 7 a number of numerical experiments aimed to validate the approximation results shown in Chapters 2, 3 and 4.

- It is well-known that the p version of triangular FEM is haunted by ill-conditioning of the stiffness matrix, see [90]; the p version of the VEM makes no exception. Therefore, in Chapter 8, we suggests possible remedies in order to alleviate such ill-conditioning.

- The issue of having fast solvers for the solution to the final system is also important, e.g. in view of 3D problems; for this reason, we discuss in Chapter 9 a multigrid algorithm (with non-inherited sublevel solvers) for the pure p version of the VEM.

- Finally, we briefly describe future challenges, related to the topics discussed so far, in Chapter 10.

- Two appendices are also presented. Appendix A is committed to recall regularity results of elliptic PDEs on polygonal domains. A number of *hp* inverse estimates on triangles and general polygons are discussed and proven in Appendix B.

Chapter 2

The h and p version of the virtual element method for the Poisson problem on quasi-uniform meshes

The aim of this chapter is to study the approximation of Poisson problem (1.32); for simplicity, we assume homogeneous Dirichlet boundary conditions and therefore we look at the weak formulation (1.27). The treatment of inhomogeneous boundary conditions can be dealt with as in Chapter 4.

The standard h and p versions of VEM on quasi-uniform meshes are discussed; the issue of approximating solutions with the "natural" regularity, i.e. with a proper singular behaviour at the vertices of the computational domain, cf. Appendix A, is not here addressed but postponed to Chapters 3 and 4.

Here, we assume either that the solution to problem (1.27) has a finite Sobolev regularity, or that it is analytic (on a proper enlarged domain). As in the standard h and p FEM framework [14, 96], in the former case both the h and the p version lead to an algebraic decay of the error, whereas, in the latter, exponential convergence in terms of p can be achieved.

The outline of the present chapter follows. In Section 2.1, we introduce the VEM with uniform degree of accuracy and we prove an abstract error analysis result asserting that the error of the method is bounded, up to a pollution factor due to the stabilization typical of VEM, with three terms involving oscillation of the right-hand side, best error approximation by means of piecewise discontinuous polynomials and by means of functions in the VE space; moreover, we recall from [25] the convergence result for the h version of the method. In Section 2.2, under the assumption that the solution to (1.27) has finite Sobolev regularity, we discuss algebraic convergence in terms of p of the error of the method; for the purpose, we discuss local hp local approximation properties of polynomials and of functions in the VE space on polygons. Such algebraic convergence is proven in a different fashion in Section 2.3; here, we additionally prove exponential convergence in terms of p assuming that the solution is analytic on a proper enlarged domain. A hint regarding the double rate of convergence employing the p version of VEM is given in Section 2.4.

We highlight that the topics here discussed are presented in [31].

2.1 Virtual elements for the Poisson problem with uniform degree of accuracy

Let $\{\mathcal{T}_n\}_{n\in\mathbb{N}}$ be a sequence of (quasi-uniform) polyhedral meshes satisfying assumptions (**G0**)-(**G1**)-(**G2**)-(**G3**). Let $p \in \mathbb{N}$ be given.

The aim of the present section is to introduce V_{hp}, a finite dimensional space of V defined in (1.28), $a_{hp} : V_{hp} \times V_{hp} \to \mathbb{R}$, a discrete bilinear form mimicking its continuous counterpart a defined in (1.28) and finally f_{hp}, an element of V_{hp}^*, the dual space of V_{hp}, and a duality pairing $\langle f_{hp}, \cdot \rangle_{hp}$,

such that the following VEM:

$$\begin{cases} \text{find } u_{hp} \in V_{hp} \text{ such that} \\ a_{hp}(u_{hp}, v_{hp}) = \langle f_{hp}, v_{hp} \rangle_{hp} \quad \forall\, v_{hp} \in V_{hp} \end{cases} \tag{2.1}$$

is well-posed and it is possible to prove some h and p approximation estimates.

We begin with the definition of the approximation space. Having set the space of piecewise continuous polynomials of degree p over the boundary of each element K:

$$\mathbb{B}_{hp}(\partial K) := \left\{ v_{hp} \in \mathcal{C}^0(\partial K) \mid v_{hp}|_s \in \mathbb{P}_p(s), \text{for all } s \text{ edge of } K \right\}, \tag{2.2}$$

we define the local VE spaces:

$$V_{hp}(K) = \left\{ v_{hp} \in H^1(K) \mid \Delta v_{hp} \in \mathbb{P}_{p-2}(K), v_{hp}|_{\partial K} \in \mathbb{B}_{hp}(\partial K) \right\} \qquad \forall\, K \in \mathcal{T}_n. \tag{2.3}$$

Importantly, we observe that $\mathbb{P}_p(K) \subseteq V_{hp}(K)$ for any $K \in \mathcal{T}_n$. For every function $v_{hp} \in V_{hp}(K)$, we identify the following set of local degrees of freedom:

- the values of v_{hp} at vertices of K,
- the values of v_{hp} at $(p-1)$ distinct internal nodes of each edge s of K (for instance at the $p-1$ internal Gauß-Lobatto nodes),
- the internal moments

$$\frac{1}{|K|} \int_K q_\alpha v_{hp}, \tag{2.4}$$

  where $\{q_\alpha\}_{\alpha=1}^{\dim \mathbb{P}_{p-2}(K)}$ is a basis of $\mathbb{P}_{p-2}(K)$. Various choices for the polynomial basis $\{q_\alpha\}_{\alpha=1}^{\dim \mathbb{P}_{p-2}(K)}$ are presented in Section 8.1.2.

In order to show that this is a set of unisolvent degrees of freedom, we refer to [25, Proposition 4.1].

In Figure 2.1, we depict on a polygon the degrees of freedom for $p = 1, 2, 3$.

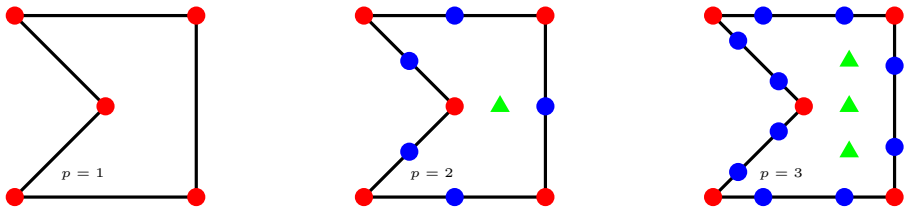

Figure 2.1: Degrees of freedom on a nonconvex pentagon for $p = 1$ (left), $p = 2$ (center), $p = 3$ (right). The red and blue dots denote vertex and edge dofs respectively, the green triangles denote internal moments.

The dimension of local VE spaces with uniform degree p is therefore given by:

$$\dim(V_{hp}(K)) = N_K p + \frac{(p-1)(p-2)}{2}, \tag{2.5}$$

where:

$$N_K = \#\text{ of vertices and edges of polygon } K. \tag{2.6}$$

A possible way to describe the construction of local VE spaces is the following.

One wants to have a space containing polynomials, since it is well-known that they have good approximation properties.

Next, one observes that polynomials satisfy a local Poisson problem with prescribed polynomial right-hand side and boundary datum. Nonetheless, employing piecewise polynomial spaces over a polygonal decomposition does not enable in general the construction of H^1 conforming approximation spaces.

In order to recover H^1 conformity, one enriches the polynomial space over an element by adding the non polynomial solutions to local PDEs with completely general polynomial right-hand side and boundary datum, getting thus the local VE space.

The global Virtual Space is consequently obtained by the continuous matching of the local spaces over the element boundaries:

$$V_{hp} = \left\{ v_{hp} \in C^0(\overline{\Omega}) \mid v_{hp}|_K \in V_{hp}(K), v_{hp}|_{\partial\Omega} = 0 \right\}, \tag{2.7}$$

with the natural definition of the global degrees of freedom obtained from the local ones.

Importantly, functions in the local VE space $V_{hp}(K)$ are known explicitly *only* on the boundary of K and *not* at the interior. For this reason, it is not possible to compute exactly the $H^1(K)$ inner product of two functions in $V_{hp}(K)$.

Therefore, we proceed as follows. We begin with introducing the following operator:

$$\Pi_p^{\nabla,K} : V_{hp}(K) \to \mathbb{P}_p(K) \text{ s. t. } \begin{cases} a^K(q_p, v_{hp} - \Pi_p^{\nabla,K} v_{hp}) = 0 \\ P^0(v_{hp} - \Pi_p^{\nabla,K} v_{hp}) = 0 \end{cases} \qquad \forall\, q_p \in \mathbb{P}_p(K), \quad \forall\, v_{hp} \in V_{hp}(K), \tag{2.8}$$

where $P_0 : V_{hp}(K) \to \mathbb{R}$ is a functional having the role of fixing the constant part of energy projector $\Pi_p^{\nabla,K}$.

Typically, functional P_0 has the following form. For $p = 1$, one sets for instance:

$$P_0(v_{hp}) = \frac{1}{N_K} \sum_{i=1}^{N_K} v_{hp}(\nu_j), \tag{2.9}$$

where $\{\nu_j\}_{j=1}^{N_K}$ denotes the set of vertices of K, whereas, for $p \geq 2$, one sets:

$$P_0(v_{hp}) = \frac{1}{|K|} \int_K v_{hp}. \tag{2.10}$$

The reason for the double choice (2.9)-(2.10) is that when employing low-order VEM, i.e. VEM with $p = 1$, the quantity (2.10) is not computable since the set of degrees of freedom does not contain any sort of internal moments.

It is worth to stress that operator $\Pi_p^{\nabla,K}$ is computable via the degrees of freedom as discussed in [25, 30]. In fact, it suffices to compute:

$$a^K(q_p, v_{hp}) = \int_{\partial K} (\partial_n q_p) v_{hp} - \int_K \Delta q_p \; v_{hp}.$$

The boundary term is computable through the boundary degrees of freedom, while the bulk term via the internal degrees of freedom (2.4).

When no confusion occurs, we denote by Π_p^∇ the energy projector $\Pi_p^{\nabla,K}$.

Having defined operator Π_p^∇, we observe that Pythagorean theorem in Hilbert spaces asserts:

$$a^K(u_{hp}, v_{hp}) = a^K(\Pi_p^\nabla u_{hp}, \Pi_p^\nabla v_{hp}) + a^K((I - \Pi_p^\nabla)u_{hp}, (I - \Pi_p^\nabla)v_{hp}) \qquad \forall\, u_{hp},\, v_{hp} \in V_{hp}(K). \tag{2.11}$$

The first term on the right-hand side of (2.11) is now actually computable owing to the computability of Π_p^∇, whereas the second is still not. Therefore, we substitute the second term with:

$$a^K((I - \Pi_p^\nabla)u_{hp}, (I - \Pi_p^\nabla)v_{hp}) \longrightarrow S^K((I - \Pi_p^\nabla)u_{hp}, (I - \Pi_p^\nabla)v_{hp}),$$

where $S^K : \ker(\Pi_p^\nabla) \times \ker(\Pi_p^\nabla) \to \mathbb{R}$ is any *computable* bilinear form, which goes by the name of stabilization of the method, on which we assume that:

$$c_*(p)|v_{hp}|_{1,K}^2 \leq S^K(v_{hp}, v_{hp}) \leq c^*(p)|v_{hp}|_{1,K}^2 \qquad \forall\, v_{hp} \in \ker(\Pi_p^\nabla), \tag{2.12}$$

where $c_*(p)$ and $c^*(p)$ are two positive constants depending only on p and the parameter ρ_0 introduced in assumptions (**G1**)-(**G2**).

Importantly, we allow constants $c_*(p)$ and $c^*(p)$, which henceforth will go under the name of *stability constants*, to depend on p.

Specific choices for S^K and explicit bounds in terms of p of the stability constants are not the target of the present section, but are postponed to Chapter 6.

To summarize, we have built a local discrete bilinear form of the following sort:

$$a_{hp}^K(u_{hp}, v_{hp}) = a^K(\Pi_p^\nabla u_{hp}, \Pi_p^\nabla v_{hp}) + S^K((I - \Pi_p^\nabla)u_{hp}, (I - \Pi_p^\nabla)v_{hp}) \qquad \forall\, u_{hp},\, v_{hp} \in V_{hp}(K). \tag{2.13}$$

It is also possible to prove, owing to (2.12), the following two properties of a_{hp}^K:

($\mathbf{A}_{hp}\mathbf{1}$) **polynomial consistency**: for all $K \in \mathcal{T}_n$, it must hold:

$$a^K(q_p, v_{hp}) = a_{hp}^K(q_p, v_{hp}) \quad \forall\, q_p \in \mathbb{P}_p(K),\, \forall\, v_{hp} \in V_{hp}(K); \tag{2.14}$$

($\mathbf{A}_{hp}\mathbf{2}$) **stability**: for all $K \in \mathcal{T}_n$, it must hold:

$$\alpha_*(p)|v_{hp}|_{1,K}^2 \leq a_{hp}^K(v_{hp}, v_{hp}) \leq \alpha^*(p)|v_{hp}|_{1,K}^2, \quad \forall\, v_{hp} \in V_{hp}(K), \tag{2.15}$$

where $0 < \alpha_*(p) \leq \alpha^*(p) < +\infty$ are two constants which may depend on p.

More precisely, it holds true that:

$$\alpha_*(p) = \min(1, c_*(p)), \qquad \alpha^*(p) = \max(1, c^*(p)). \tag{2.16}$$

Assumptions ($\mathbf{A}_{hp}\mathbf{1}$)-($\mathbf{A}_{hp}\mathbf{2}$) are instrumental for proving the forthcoming abstract error result Lemma 2.1.1. In addition to that, assumption ($\mathbf{A}_{hp}\mathbf{1}$) guarantees that the method passes the so-called patch test; this means that if the solution to problem (1.27) is a polynomial, then the method returns the exact solution, assuming to work in exact arithmetic. On the other hand, assumption ($\mathbf{A}_{hp}\mathbf{2}$) is needed in order to have the well-posedness of method (2.1).

The global discrete bilinear form reads:

$$a_{hp}(u_{hp}, v_{hp}) = \sum_{K \in \mathcal{T}_n} a_{hp}^K(u_{hp}, v_{hp}), \quad \forall\, u_{hp},\, v_{hp} \in V_{hp}. \tag{2.17}$$

Analogously to what we said for the bilinear form, also the right-hand side of (1.27) is not explicitly computable, since functions in the VE space are not known pointwise at the interior of each element. For this reason, we introduce a discrete bilinear form, which is based on another (piecewise defined) projector.

Given $K \in \mathcal{T}_n$, we define $\Pi_{p-2}^{0,K}$ as the $L^2(K)$ projection:

$$\Pi_{p-2}^{0,K} : V_{hp}(K) \to \mathbb{P}_{p-2}(K) \quad \text{s. t.} \quad (q_{p-2}, v_{hp} - \Pi_{p-2}^{0,K} v_{hp})_{0,K} \quad \forall\, q_{p-2} \in \mathbb{P}_{p-2}(K),\, \forall\, v_{hp} \in V_{hp}(K). \tag{2.18}$$

We stress that the projector $\Pi_{p-2}^{0,K}$ is computable via the internal dofs (2.4). When no confusion occurs, we write Π_{p-2}^0 in lieu of $\Pi_{p-2}^{0,K}$.

We are now in business for defining the discrete right-hand side. In particular, we set:

$$\langle f_{hp}, v_{hp} \rangle_{hp} = \sum_{K \in \mathcal{T}_n} \langle f_{hp}, v_{hp} \rangle_{K,hp}, \tag{2.19}$$

where:

$$\langle f_{hp}, v_{hp} \rangle_{K,hp} = \begin{cases} \int_K f\left(\Pi_{p-2}^0 v_{hp}\right) & \text{if } p \geq 2 \\ \int_K f\left(P_0(v_{hp})\right) & \text{if } p = 1 \end{cases} \qquad \forall\, v_{hp} \in V_{hp}(K), \tag{2.20}$$

where we recall that P_0 is defined in (2.9).

With the choice performed for space V_{hp} defined in (2.7), the discrete bilinear form a_{hp} defined in (2.17) and discrete right-hand side f_{hp} defined in (2.19), it is clear that method (2.1) is well-posed for all $\mathcal{T}_n$ and $p \in \mathbb{N}$.

Before concluding this section, we recall the following abstract error analysis result, which can be regarded as a Strang-like lemma in the framework of VEM. Let $\mathcal{F}_{hp}$ be the smallest constant satisfying:

$$|(f, v_{hp})_{0,\Omega} - \langle f_{hp}, v_{hp} \rangle_{hp}| \leq \mathcal{F}_{hp}|v_{hp}|_{1,\Omega} \qquad \forall\, v_{hp} \in V_{hp}. \tag{2.21}$$

Then, the following holds true.

Lemma 2.1.1. *Under assumptions (**A_{hp}1**)-(**A_{hp}2**), let u and u_{hp} be the solution to (1.27) and (2.1) respectively. Let u_π be any function in $\mathcal{S}^{p,-1}(\Omega,\mathcal{T}_n)$ defined in (1.44) and let u_I be any function in V_{hp} defined in (2.7). Then, the following estimate is valid:*

$$|u-u_{hp}|_{1,\Omega} \lesssim \frac{\alpha^*(p)}{\alpha_*(p)}\{|u-u_\pi|_{1,\mathcal{T}_n} + |u-u_I|_{1,\Omega} + \mathcal{F}_{hp}\}. \tag{2.22}$$

Proof. See [25, Theorem 3.1]. □

Lemma 2.1.1 states that, up to the pollution factor $\frac{\alpha^*(p)}{\alpha_*(p)}$ due to the choice of the stabilization, the error of the method is bounded by the sum of three terms:

- a best error term with respect to piecewise discontinuous polynomials over $\mathcal{T}_n$;
- a best error term with respect to functions in the global VE space V_{hp} defined in (2.7);
- a term due to the oscillation of the right-hand side.

The two forthcoming sections are devoted to estimate these three terms, assuming either that the solution has finite Sobolev regularity, see Section 2.2, or analytic regularity on a proper enlarged domain, see Section 2.3.

It is worth to stress that the convergence results in terms of h have been already discussed in [25].

2.2 Algebraic convergence for finite Sobolev regularity solutions

In this section, we study the convergence of method (2.1) assuming that u, the solution to problem (1.27), belongs to $H^{k+1}(\Omega)$ for some $k \in \mathbb{N}$.

The section is organized as follows. In Sections 2.2.1, 2.2.2 and 2.2.3, we bound respectively the first, the second and the third terms appearing on the right-hand side of (2.22); in Section 2.2.4, we collect all these local bounds in order to achieve h and p convergence of the method.

2.2.1 Polynomial approximation term

We start by bounding the term $|u-u_\pi|_{1,\mathcal{T}_n}$ of the right-hand side of (2.22). In order to derive the bound, we need to prove a generalized-polygonal version of a classic result, namely [20, Lemma 4.1]. In this lemma, it was shown the existence of a sequence of polynomials which approximate functions in H^{k+1} over the triangular and square reference elements. We extend this result for generic polygons having diameter equal to 1. Thus, we are ready to show the following result.

Lemma 2.2.1. *Let $\widehat{K} \subseteq \mathbb{R}^2$ be a polygon with diam($\widehat{K}$)=1. Moreover, assume that $\widehat{K}$ is star-shaped with respect to a ball of radius greater than or equal to ρ_0 and the distance between any two vertices of $\widehat{K}$ is greater than or equal to ρ_0, ρ_0 being the constant introduced in assumptions (**G1**)-(**G2**). Then, there exists a family of approximation operators $\{\widehat{\Pi}_p^{\widehat{K}}\}_{p\in\mathbb{N}}$, with $\widehat{\Pi}_p^{\widehat{K}} : H^{k+1}(\widehat{K}) \to \mathbb{P}_p(\widehat{K})$ for all $p \in \mathbb{N}$ such that, for each $0 \le \ell \le k+1$, $\widehat{u} \in H^{k+1}(\widehat{K})$, $k \in \mathbb{N}$, it holds:*

$$\|\widehat{u} - \widehat{\Pi}_p^{\widehat{K}}\widehat{u}\|_{\ell,\widehat{K}} \le cp^{-(k+1-\ell)}\|\widehat{u}\|_{k+1,\widehat{K}}, \tag{2.23}$$

where c is a positive constant independent of u and p.

Proof. We assume without loss of generality that $\mathbf{x}_K$, the barycenter of $\widehat{K}$ defined in (1.34), coincides with the origin $\mathbf{0}$. For a given $r > 0$, we define:

$$R(r) := \left\{(x,y) \in \mathbb{R}^2 \mid |x| < r,\, |y| < r\right\}. \tag{2.24}$$

Thanks to the fact that diam($\widehat{K}$)=1 and $\mathbf{x}_{\widehat{K}} = \mathbf{0}$, we have $R(1) \supset \overline{\widehat{K}}$. Let $r_0 > 1$. Then, it obviously holds $\overline{\widehat{K}} \subset R(r_0)$. We note that $\partial\widehat{K}$ is Lipschitz; consequently, using [98, Chapter VI,

Theorem 5], there exists $E : H^{k+1}(\widehat{K}) \to H^{k+1}(R(2r_0))$ extension operator such that $E(\widehat{u}) = 0$ on $R(2r_0) \setminus R(\frac{3}{2}r_0)$ and $\|E(\widehat{u})\|_{k+1,R(2r_0)} \leq c\|\widehat{u}\|_{k+1,\widehat{K}}$. A careful inspection of [98, Chapter VI, Theorem 5] shows that the constant c depends only on k, the involved Sobolev order, and on the "worst angle" value:

$$\theta_{\widehat{K}} = \min_{\theta \in \mathcal{A}_{\widehat{K}}} \min\{\theta, 2\pi - \theta\},$$

where $\mathcal{A}_{\widehat{K}}$ denotes the set of the (magnitude of) internal angles of $\widehat{K}$. In particular, the constant c may explode when $\theta_{\widehat{K}} \to 0$. It is possible to check that, under the regularity hypotheses on K, the angle parameter $\theta_{\widehat{K}}$ is bounded from below by a constant depending only on the star-shapedness parameter of polygon $\widehat{K}$.

Therefore, it holds $\|E(\widehat{u})\|_{k+1,R(2r_0)} \leq c(k,\rho_0)\|\widehat{u}\|_{k+1,\widehat{K}}$. The remaining part of the proof, that is based on the approximation of the extended function $E(\widehat{u})$, follows exactly the same steps as in [20, Lemma 4.1], and is therefore not shown. □

Using this result, we are able to give a generalized-polygonal version of [20, Lemma 4.5], which will play the role of local *hp* estimate result on $|u - u_\pi|_{1,K}$, where K is a polygon of the decomposition $\mathcal{T}_n$.

Lemma 2.2.2. *Let $K \in \mathcal{T}_n$ satisfying assumptions (**G0**)-(**G1**)-(**G2**) and $u \in H^{k+1}(K)$. Then there exists a sequence of approximation operators $\{\Pi_p^K\}_{p\in\mathbb{N}}$, with $\Pi_p^K : H^{k+1}(K) \to \mathbb{P}_p(K)$ for all $p \in \mathbb{N}$ such that for any $0 \leq \ell \leq k+1$, $k \in \mathbb{N}$, the following holds true:*

$$|u - \Pi_p^K u|_{\ell,K} \leq c\frac{h_K^{\mu+1-\ell}}{p^{k+1-\ell}}\|u\|_{k+1,K}, \tag{2.25}$$

where $\mu = \min(p,k)$ and c is a positive constant independent of u, h and p.

Proof. We consider the mapping $F(\mathbf{x}) = \frac{1}{h_K}(\mathbf{x} - \mathbf{x}_K)$ and let $\widehat{K} = F(K)$. Clearly, $\mathrm{diam}(\widehat{K}) = 1$ and the barycenter of $\widehat{K}$ is in the origin, $\mathbf{x}_{\widehat{K}} = \mathbf{0}$. We denote the pull-back of a function by adding a hat at the top of it.

Let $\widehat{\Pi}_p^{\widehat{K}}\widehat{u}$ be the sequence of approximating polynomials of degree p of $\widehat{u}$ associated with polygon $\widehat{K}$ introduced in Lemma 2.2.1. We set $\Pi_p^K u$ to be the push-forward of the above sequence with respect to the transformation F, i.e. $\Pi_p^K u = (\widehat{\Pi}_p^{\widehat{K}}(\widehat{u})) \circ F$, where $\widehat{\varphi} = \varphi \circ F^{-1}$ for a sufficiently regular function φ. Then, it is possible to check, by a simple change of variables argument that:

$$|u - \Pi_p^K u|_{\ell,K} \leq c h_K^{1-\ell}|\widehat{u} - \widehat{\Pi}_p^{\widehat{K}}\widehat{u}|_{\ell,\widehat{K}},$$

where c is a constant independent of K (hence on $\widehat{K}$), h, u and p. Besides, c is independent also of ℓ, thanks to the fact that F is the composition of a translation with a dilatation.
We apply Lemma 2.2.1 and we obtain, by adding and subtracting any $\widehat{q}_p \in \mathbb{P}_p(\widehat{K})$:

$$\begin{aligned} |u - \Pi_p^K u|_{\ell,K} &\leq c h_K^{1-\ell}\|(\widehat{u} - \widehat{q}_p) - \widehat{\Pi}_p^{\widehat{K}}(\widehat{u} - \widehat{q}_p)\|_{\ell,\widehat{K}} \\ &\leq c\frac{h_K^{1-\ell}}{p^{k+1-\ell}}\|\widehat{u} - \widehat{q}_p\|_{k+1,\widehat{K}} \quad \forall \widehat{q}_p \in \mathbb{P}_p(\widehat{K}), \end{aligned} \tag{2.26}$$

where c on the right-hand side of (2.26) is a constant depending on k. Using the classical Scott-Dupont theory (see e.g. [65]) and a scaling argument, bound (2.26) yields:

$$|u - \Pi_p^K u|_{\ell,K} \leq c\frac{h_K^{1-\ell}}{p^{k+1-\ell}}\left(\sum_{i=\mu+1}^{k+1}|\widehat{u}|_{i,\widehat{K}}^2\right)^{\frac{1}{2}} \leq c\frac{h_K^{\mu+1-\ell}}{p^{k+1-\ell}}\|u\|_{k+1,K}, \quad \mu = \min(p,k), \tag{2.27}$$

where c is independent of u, p and h. □

Remark 1. We note that if $k \leq p$ then it is possible to take the seminorm on the right-hand side of (2.25), yielding:

$$|u - \Pi_p^K u|_{\ell,K} \leq c\frac{h_K^{k+1-\ell}}{p^{k+1-\ell}}|u|_{k+1,K},$$

where c is a constant independent of h, p and u. This automatically follows from (2.27).

We are now able to give a global estimate on $|u - u_\pi|_{1,\mathcal{T}_n}$, in (2.22), where $u_\pi \in \mathcal{S}^{p,-1}(\Omega, \mathcal{T}_n)$ defined in (1.44). In fact, by choosing $u_\pi|_K = \Pi_p^K u$ for all $K \in \mathcal{T}_n$ and recalling the shape-regularity property (**G1**), we obtain:

$$\begin{aligned} |u - u_\pi|_{1,\mathcal{T}_n} &\leq c\frac{h^\mu}{p^k}\|u\|_{k+1,\Omega}, \quad \mu = \min(p,k), \\ |u - u_\pi|_{1,\mathcal{T}_n} &\leq c\frac{h^k}{p^k}|u|_{k+1,\Omega}, \quad \text{for } p \geq k, \end{aligned} \tag{2.28}$$

where c is a constant independent of h, p and u.

2.2.2 Virtual interpolation term

We turn now to the term $|u - u_I|_{1,\Omega}$ of the right-hand side of (2.22).

Remark 2. Assumptions (**G1**)-(**G2**)-(**G3**) imply that there exists $\widetilde{\mathcal{T}}_n$, an auxiliary conforming triangulation that refines $\mathcal{T}_n$, obtained by connecting, for all $K \in \mathcal{T}_n$, the N_K vertices of K to the center of the ball that realizes assumption (**G1**) for K. Moreover, it is possible to check that $\widetilde{\mathcal{T}}_n$ forms a shape-regular sequence, with shape-regularity constant depending solely on the parameters ρ_0 and c introduced in assumptions (**G1**)-(**G2**)-(**G3**).

In fact, assume by contradiction that $\left\{\widetilde{\mathcal{T}}_n\right\}_{n\in\mathbb{N}}$ is not a shape-regular sequence of subtriangulations. This means that it is possible to build sequences of triangles such that:

(i) the magnitudes of a sequence of angles tend to 0, see Figure 2.2 (left);

(ii) the magnitudes of a sequence of angles tend to π, see Figure 2.2 (right).

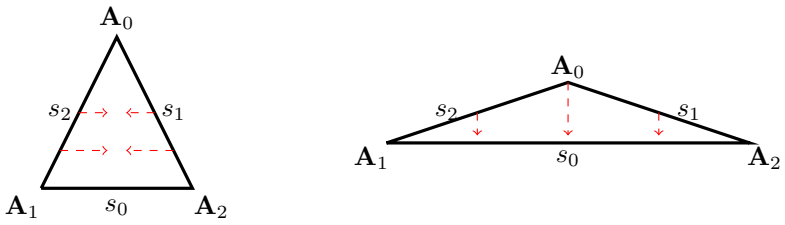

Figure 2.2: Left: (i) the magnitudes of a sequence of angles tend to 0. Right: (ii) the magnitudes of an angle tend to π.

We distinguish what happens in the three cases. We denote by $\mathbf{C}$ and r the radius and the center of the ball with respect to which K is star-shaped; moreover, in order to ease the proof, we employ the notation in Figure 2.2.

If (i) holds, then:

- if $\mathbf{C} = \mathbf{A}_0$, we have:
$$1 \approx \frac{|s_0|}{h_K} \leq \frac{|s_0|}{|s_1|} \to 0 \qquad \lightning;$$
- if $\mathbf{C} = \mathbf{A}_1$ (analogously one treats the case $\mathbf{C} = \mathbf{A}_2$), we have:
$$1 \approx \frac{h_K}{|s_1|} \approx \frac{r}{|s_1|} \leq \frac{|s_0|}{|s_1|} \to 0 \qquad \lightning.$$

Instead, if (ii) holds, then:

- if $\mathbf{C} = \mathbf{A}_0$, we have:
$$1 \approx \frac{h_K}{|s_0|} \approx \frac{r}{|s_0|} \leq \frac{\text{dist}(\mathbf{A}_0, s_0)}{|s_0|} \to 0 \qquad \lightning;$$

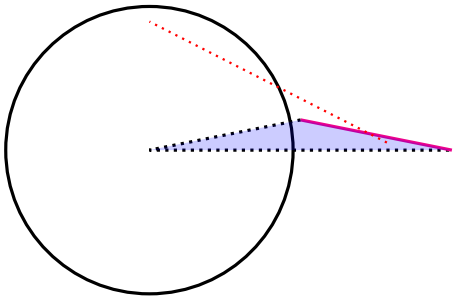

Figure 2.3: Failure of the star-shapedness assumption with respect to a ball. The red segment necessarily sticks out the polygon under consideration, whatever the polygon is. In fact, the magenta edge of the light-blue triangle is by assumption an edge of the original polygon.

- if $\mathbf{C} = \mathbf{A}_1$ (analogously one treats the case $\mathbf{C} = \mathbf{A}_2$) we argue saying that, if this case holds true, then the polygons in the sequence $\mathcal{T}_n$ associated with $\widetilde{\mathcal{T}}_n$ are definitively not star-shaped with respect to a ball with radius comparable to h_K, see Figure 2.3.

We denote by $\mathcal{S}^{p,0}(\Omega, \widetilde{\mathcal{T}}_n)$ the set of piecewise continuous polynomials of degree p over the auxiliary triangular decomposition $\widetilde{\mathcal{T}}_n$. It is well-known, see [20, Theorem 4.6] that there exists $\varphi_{hp} \in \mathcal{S}^{p,0}(\Omega, \widetilde{\mathcal{T}}_n)$ with $\varphi_{hp}|_{\partial\Omega} = 0$ such that, for any $u \in H^{k+1}(\Omega)$, $k \in \mathbb{R}^+$, the following holds true:

$$\begin{aligned} &\|u - \varphi_{hp}\|_{1,\Omega} \leq c_1 \frac{h^\mu}{p^k} \|u\|_{k+1,\Omega} \quad \text{with } k > \frac{1}{2}, \\ &|u - \varphi_{hp}|_{1,\Omega} \leq c_2 \frac{h^k}{p^k} |u|_{k+1,\Omega} \quad \text{with } k > \frac{1}{2} \text{ and } p \geq k, \end{aligned} \tag{2.29}$$

where c_1 and c_2 are two constants independent of u, p and h and where $\mu = \min(p, k)$.

Now, we use φ_{hp} in (2.29) in order to construct a virtual interpolant $u_I \in V_{hp}$ of u. To this purpose, we modify a particular technique which was firstly introduced in [87].

Lemma 2.2.3. *Under assumptions **(G0)**-**(G1)**-**(G2)**-**(G3)** and given $u \in H^{k+1}(\Omega)$, $k \in \mathbb{N}$, there exists $u_I \in V_{hp}$ such that:*

$$|u - u_I|_{1,\Omega} \leq c \frac{h^\mu}{p^k} \|u\|_{k+1,\Omega}, \quad \mu = \min(p, k), \tag{2.30}$$

where c is independent of h, p and u.

Proof. Let u_π be the function defined in (2.28) and let φ_{hp} be the function described in (2.29). For each $K \in \mathcal{T}_n$, we define $u_I|_K$ the solution to the following problem:

$$\begin{cases} -\Delta u_I = -\Delta u_\pi & \text{in } K \\ u_I = \varphi_{hp} & \text{on } \partial K \end{cases}. \tag{2.31}$$

Clearly one has that $u_I|_E \in V_{hp}(K)$. Moreover, since $u_I \in \mathcal{C}^0(\overline{\Omega}) \cap H_0^1(\Omega)$, it holds that $u_I \in V_{hp}$. Using (2.31), we can write:

$$\begin{cases} -\Delta(u_I - u_\pi) = 0 & \text{in } K \\ u_I - u_\pi = \varphi_{hp} - u_\pi & \text{on } \partial K \end{cases}.$$

Therefore, since $u_I - u_\pi$ is harmonic, it holds:

$$|u_I - u_\pi|_{1,K} = \inf \left\{ |z|_{1,K},\ z \in H^1(K) \mid z = \varphi_{hp} - u_\pi \text{ on } \partial K \right\} \leq |\varphi_{hp} - u_\pi|_{1,K}. \tag{2.32}$$

Finally, by (2.32), we obtain:

$$\begin{aligned} |u - u_I|_{1,K} &\leq |u - u_\pi|_{1,K} + |u_\pi - u_I|_{1,K} \leq |u - u_\pi|_{1,K} + |u_\pi - \varphi_{hp}|_{1,K} \\ &\leq 2|u - u_\pi|_{1,K} + |u - \varphi_{hp}|_{1,K}. \end{aligned} \tag{2.33}$$

The proof is completed by summing on all the elements in (2.33) and using (2.28), (2.29). □

The proof of Lemma 2.2.3 is somehow standard, since it combines known results from [21, 87]. In the two forthcoming chapters, we present novel strategies for proving best approximation results in terms of functions in the VE space.

Remark 3. We point out that if $k \leq p$ and under the hypothesis of Lemma 2.2.3, the following holds true:

$$|u - u_I|_{1,\Omega} \leq c\frac{h^k}{p^k}|u|_{k+1,\Omega},$$

where c is a constant independent of h, p and u.

2.2.3 Oscillation of the right-hand side

It remains to estimate the term $\mathcal{F}_{hp}$ in (2.22). We have the following result.

Lemma 2.2.4. *Under assumptions (**G0**)–(**G1**)-(**G2**)–(**G3**), let the loading term $f \in H^{\widetilde{k}+1}(K)$ for all $K \in \mathcal{T}_h$, $\widetilde{k} \in \mathbb{N}$. Then, the following holds true:*

$$\mathcal{F}_{hp} \leq c\frac{h^{\widetilde{\mu}}}{p^{\widetilde{k}+2}}\left(\sum_{K\in\mathcal{T}_h}\|f\|^2_{\widetilde{k},K}\right)^{\frac{1}{2}}, \quad \widetilde{\mu} = \min(p, \widetilde{k}+2). \tag{2.34}$$

where c is a constant independent of h, p and u.

Proof. Since the case $p = 1$ has been already analysed in [25], we only consider the case $p \geq 2$. Let $v_{hp} \in V_{hp}$. Let Π^0_{p-2} be the L^2 projector over the polygon K defined in (2.18), for all $K \in \mathcal{T}_n$. Using the definition of the discrete right-hand side (2.19), we get:

$$\begin{aligned}(f, v_{hp})_{0,\Omega} - \langle f_{hp}, v_{hp}\rangle_{hp} &= \sum_{K\in\mathcal{T}_h}(f - \Pi^0_{p-2}f, v_{hp})_{0,K} = \sum_{K\in\mathcal{T}_n}(f - \Pi^0_{p-2}f, v_{hp} - \Pi^0_{p-2}v_{hp})_{0,K}\\ &\leq \sum_{K\in\mathcal{T}_h}\|f - \Pi^0_{p-2}f\|_{0,K}\|v_{hp} - \Pi^0_{p-2}v_{hp}\|_{0,K}\\ &\leq \sum_{K\in\mathcal{T}_h}\|f - f^\pi_{p-2}\|_{0,K}\|v_{hp} - v^\pi_{p-2}\|_{0,K},\end{aligned}$$

where f^π_{p-2} and v^π_{p-2} are the piecewise polynomial functions of degree $p-2$ that realize the bound (2.27) with $\ell = 0$ on each $K \in \mathcal{T}_n$.

An adaptation of Lemma 2.2.1 (and thus also of [20, Lemma 4.1] or [21, Lemma 3.1]) implies that, given $\widetilde{p} = \max(1, p-2)$:

$$\begin{aligned}|(f, v_{hp})_{0,\Omega} - \langle f_{hp}, v_{hp}\rangle_{hp}| &\leq c\sum_{K\in\mathcal{T}_n}\frac{h_K^{\min((p-2)+1,\widetilde{k}+1)}}{\widetilde{p}^{\widetilde{k}+1}}\|f\|_{\widetilde{k}+1,K}\frac{h_K}{\widetilde{p}}|v_{hp}|_{1,K}\\ &\leq c\frac{h^{\min(p,\widetilde{k}+2)}}{\widetilde{p}^{\widetilde{k}+2}}\left(\sum_{K\in\mathcal{T}_n}\|f\|^2_{\widetilde{k}+1,K}\right)^{\frac{1}{2}}|v_{hp}|_{1,K}.\end{aligned}$$

The final result follows by the definition of $\mathcal{F}_{hp}$ in (2.21) and substituting $\widetilde{p}$ with p, up to a change of the constant c. □

By observing that, if the solution u of (1.27) is in $H^{k+1}(\Omega)$ then $f \in H^{k-1}(\Omega)$, Lemma 2.2.4 immediately gives also the following corollary.

Corollary 2.2.5. *Under assumptions (**G0**)-(**G1**)-(**G2**)-(**G3**) introduced in Section 1.4, let the solution u of (1.27) be in $H^{k+1}(\Omega)$, $k \in \mathbb{N}$. Then, the following holds true:*

$$\mathcal{F}_{hp} \leq \frac{h^\mu}{p^k}\|u\|_{k+1,\Omega}, \quad \mu = \min(p, k), \tag{2.35}$$

where c is a constant independent of h, p and u.

Finally, we note that an analogous observation as in Remark 1 and Remark 3 holds also for Corollary 2.2.5, yielding:

$$\mathcal{F}_{hp} \leq \frac{h^k}{p^k}|u|_{k+1,\Omega}\,, \quad 1 \leq k+1 \leq p+1, \tag{2.36}$$

where c is a constant independent of h, p and u.

2.2.4 Convergence of the method for finite Sobolev regularity solutions

Finally, we are able to show the following convergence result.

Theorem 2.2.6. *Let $k \in \mathbb{N}$, $k > \frac{1}{2}$ and let the mesh assumptions (**$A_{hp}1$**)-(**$A_{hp}2$**)-(**G0**)-(**G1**)-(**G2**)-(**G3**) hold true. Let u and u_{hp} be respectively the solutions to problems* (1.27) *and* (2.1)*, with $u \in H^{k+1}(\Omega)$. Then, the following hp estimates are valid:*

$$|u - u_{hp}|_{1,\Omega} \leq c\frac{\alpha^*(p)}{\alpha_*(p)}\frac{h^\mu}{p^k}\|u\|_{k+1,\Omega}, \quad \mu = \min(p,k), \tag{2.37}$$

$$|u - u_{hp}|_{1,\Omega} \leq c\frac{\alpha^*(p)}{\alpha_*(p)}\frac{h^k}{p^k}|u|_{k+1,\Omega}, \quad \textit{if } k \leq p, \tag{2.38}$$

where c is a positive constant independent of h, p and u.

Proof. It suffices to combine (2.21), (2.22), (2.28), (2.30) and (2.35). □

We highlight that the constants appearing on the right-hand side of (2.37)-(2.38) are linear in the ratio $\frac{\alpha^*(p)}{\alpha_*(p)}$, $\alpha_*(p)$ and $\alpha^*(p)$ being the stability constants introduced in (2.15), and therefore, in principle, a pollution effect due to the stabilization is expected. We anticipate that, although in Chapter 6 we are not able to provide fully p independent stabilization, the numerical results in Section 7.1.1 show that the pollution effect has a mild impact on the convergence of the error.

Remark 4. Let the domain Ω be convex. Following the argument shown in [29] (and, if $p = 1, 2$ suitably changing the definition of the discrete loading term (2.19)) and applying approximation results similar to those shown above, one can also easily derive L^2 estimates of the form:

$$\|u - u_{hp}\|_{0,\Omega} \leq c\frac{\alpha^*(p)}{\alpha_*(p)}\frac{h^{\mu+1}}{p^{k+1}}\|u\|_{k+1,\Omega}, \quad \mu = \min(p,k), \tag{2.39}$$

where c is a constant independent of h, p and u, with the usual modification for the case $k \leq p$.

2.3 Exponential convergence with p VEM for analytic solutions

In this section, we study the convergence of method (2.1) assuming that u, the solution to problem (1.27), is analytic on a proper enlarged domain.

In order to obtain exponential convergence estimates for analytic functions, we must show bounds analogous to (2.37) and (2.38) by expliciting the dependence of the constants c_1 and c_2 on k, i.e. on the Sobolev regularity of the solution u. To this purpose, we will follow an approach which is slightly different with respect to the one of Section 2.2.

The outline of this section follows. In Section 2.3.1, we discuss additional regularity assumptions on the sequence of meshes that will be instrumental for proving the exponential convergence in terms of p of the method. Next, in Sections 2.3.2, 2.3.3 and 2.3.4, we bound respectively the first, second and third terms appearing on the right-hand side of (2.22). Finally, in Section 2.3.5, we prove the exponential convergence in terms of p of the method.

2.3.1 Additional regularity assumptions on the sequence of meshes

In this section, we demand additional regularity assumptions on the sequence of meshes $\{\mathcal{T}_n\}_{n\in\mathbb{N}}$ under which we will be able to prove the main result of this section, namely the exponential convergence in terms of p of the method, see Section 2.3.5.

We recall that, given a sequence of polygonal decompositions $\{\mathcal{T}_n\}_{n\in\mathbb{N}}$, there exists a sequence of regular subtriangulations $\left\{\widetilde{\mathcal{T}}_n\right\}_{n\in\mathbb{N}}$ described in Remark 2.

Given K polygon in $\mathcal{T}_n$, we define $Q = Q(K)$ as any of the squares containing K having smallest diameter; besides, given $\widetilde{K}$ triangle in $\widetilde{\mathcal{T}}_n$, we define $\widetilde{Q} = \widetilde{Q}(\widetilde{K})$ the parallelogram given by $\widetilde{Q} = \overline{\widetilde{K} \cup \widetilde{K}^*}$, where $\widetilde{K}^*$ is the reflection of $\widetilde{K}$ with respect to a midpoint of one of its edges. We point out that there are three possible $\widetilde{Q}(\widetilde{K})$, see figure 2.4; we fix arbitrarily one of them. Next,

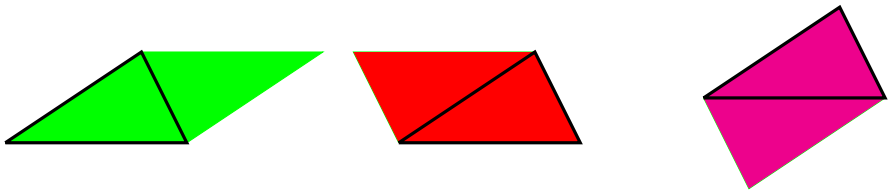

Figure 2.4: The three possible "covering" parallelograms associated with a given triangle.

we define:

$$\Omega^{ext} = \Omega^{ext}(n) := \Omega \cup \left(\bigcup_{K\in\mathcal{T}_n} Q(K) \right) \cup \left(\bigcup_{\widetilde{K}\in\widetilde{\mathcal{T}}_n} \widetilde{Q}(\widetilde{K}) \right). \tag{2.40}$$

We observe that $\sup_{\mathbf{x}\in\Omega^{ext}} \mathrm{dist}(\mathbf{x},\Omega) \leq d(n)$, being $d(\cdot)$ a decreasing function of n, where we recall that n denotes the index of the mesh $\mathcal{T}_n$ that we are employing. Therefore, given $\overline{n} \in \mathbb{N}$, $\forall n \geq \overline{n}$ one has $d(n) \leq d(\overline{n})$ and thus Ω^{ext} is an uniformly bounded domain in terms of n, also if n is unbounded.

We demand the following additional regularity assumption on sequence $\{\mathcal{T}_n\}_{n\in\mathbb{N}}$:

(**G6**) for all $n \in \mathbb{N}$, there exists a positive universal constant $N \in \mathbb{N}$ such that there are at most N overlapping squares in the collection $\{Q(K)\}$ and N parallelograms in the collection $\{\widetilde{Q}(\widetilde{K})\}$, i.e. for all $Q(K)$ in $\{Q(K)\}_{K\in\mathcal{T}_n}$ and for all $\widetilde{Q}(\widetilde{K})$ in $\{\widetilde{Q}(\widetilde{K})\}_{\widetilde{K}\in\widetilde{\mathcal{T}}_n}$, given $I_{K'} := \{Q(K) \mid Q(K) \cap Q(K') \neq \emptyset\}$ and $\widetilde{I}_{\widetilde{K}'} := \{\widetilde{Q}(\widetilde{K}) \mid \widetilde{Q}(\widetilde{K}) \cap \widetilde{Q}(\widetilde{K}') \neq \emptyset\}$, it holds that $\mathrm{card}(I_{K'})$, $\mathrm{card}(\widetilde{I}_{\widetilde{K}'}) \leq N$, $\forall\, K \in \mathcal{T}_h$ and $\forall\, \widetilde{K} \in \widetilde{\mathcal{T}}_n$.

We note that, given $u \in H^{k+1}(\Omega^{ext})$, $k \in \mathbb{N}$, assumption (**G6**) implies the crude bounds:

$$\sum_{K\in\mathcal{T}_n} \|u\|^2_{k+1,Q(K)} \leq N\|u\|^2_{k+1,\Omega^{ext}}, \quad \sum_{\widetilde{K}\in\widetilde{\mathcal{T}}_n} \|u\|^2_{k+1,\widetilde{Q}(\widetilde{K})} \leq N\|u\|^2_{k+1,\Omega^{ext}},$$

with Ω^{ext} defined in (2.40).

In the following we will assume that u, the solution to problem (1.27), is in fact the restriction of a regular function on the set Ω^{ext}, Ω^{ext} being defined in (2.40); with an abuse of notation we will call again u such a regular function.

2.3.2 Polynomial approximation term

Here, we give an explicit representation of the constant c in (2.23) in terms of k, k being the Sobolev regularity of the target function u. We start by showing the counterpart of Lemma 2.2.1. As a minor note, we point out that the estimate of Lemma 2.3.1 does not require explicitly a shape regularity condition on the polygons, differently from Lemma 2.2.1.

Lemma 2.3.1. *Let $\widehat{Q}$ be the square $[-1,1]^2$ and let $\widehat{K} \subseteq \widehat{Q}$ be any polygon with barycenter $\mathbf{x}_{\widehat{K}} = \mathbf{0}$. Moreover, assume that $p \geq 2k$, with $k \in \mathbb{N}$. Then, there exists a family of approximation operators $\{\widehat{\Pi}_p^{\widehat{Q}}\}_{p\in\mathbb{N}}$ with $\widehat{\Pi}_p^{\widehat{Q}} : H^2(\widehat{Q}) \to \mathbb{P}_p(\widehat{Q})$ such that, for each $\widehat{u} \in H^{k+1}(\widehat{Q})$, it holds:*

$$|\widehat{u} - \widehat{\Pi}_p^{\widehat{Q}}\widehat{u}|_{1,\widehat{K}} \leq c\, 2^k e^k p^{-k} |\widehat{u}|_{k+1,\widehat{Q}} \tag{2.41}$$

with c a constant independent of u, k and p.

Proof. Given $\widehat{Q} = [-1,1]^2$, let $\{\mathbf{V}_i\}_{i=1}^4$ be the set of vertices of $\widehat{Q}$. Let $\widehat{u} \in H^{k+1}(\widehat{Q})$. Let $\mathbb{Q}_p(\Theta)$ be the set of polynomials of maximum degree p in each variable over a domain $\Theta \in \mathbb{R}^2$. As a consequence of [96, Lemma 4.67], it is possible to show the existence of $\widehat{\varphi}_p \in \mathbb{Q}_p(\widehat{Q})$ such that:

$$\widehat{\varphi}_p(\mathbf{V}_i) = \widehat{u}(\mathbf{V}_i), \quad \forall i = 1, \ldots, 4 \tag{2.42}$$

and

$$|\widehat{u} - \widehat{\varphi}_p|^2_{1,\widehat{Q}} \leq 2 \left\{ \frac{(p-k)!}{(p+k)!} + \frac{1}{p(p+1)} \cdot \frac{(p-k+1)!}{(p+k-1)!} \right\} |\widehat{u}|^2_{k+1,\widehat{Q}}. \tag{2.43}$$

Since $p \geq k$, it is possible to show that (2.43) leads to the following simpler bound:

$$|\widehat{u} - \widehat{\varphi}_p|_{1,\widehat{Q}} \leq c e^k p^{-k} |\widehat{u}|_{k+1,\widehat{Q}}, \text{ with } c = \sqrt{2\,e}. \tag{2.44}$$

In order to show this, we perform the computations only on the first term on the right-hand side of (2.43) since the treatment of the other one is analogous. Using Stirling formula:

$$\frac{(p-k)!}{(p+k)!} = \frac{(p-k)^{(p-k)} \cdot e^{-(p-k)} \cdot \sqrt{2\pi(p-k)} \cdot e^{\theta_{p-k}}}{(p+k)^{(p+k)} \cdot e^{-(p+k)} \cdot \sqrt{2\pi(p+k)} \cdot e^{\theta_{p+k}}},$$

with

$$\frac{1}{12n+1} \leq \theta_n \leq \frac{1}{12n} \qquad \forall\, n \in \mathbb{N}.$$

Then:

$$\frac{(p-k)!}{(p+k)!} \leq p^{-2k} \cdot e^{2k} \cdot e^{\theta_{p-k}} \leq c\, e^{2k} p^{-2k}, \text{ with } c = e. \tag{2.45}$$

At this point, we observe that $\mathbb{Q}_p(\widehat{Q}) \subseteq \mathbb{P}_{2p}(\widehat{Q})$. This fact and (2.44) immediately imply that there exists $\widehat{\varphi}_p \in \mathbb{P}_p(\widehat{Q})$ which interpolates $\widehat{u}$ at the vertices of $\widehat{Q}$ as in (2.42) and which satisfies:

$$|\widehat{u} - \widehat{\varphi}_p|_{1,\widehat{Q}} \leq c\, 2^k e^k p^{-k} |\widehat{u}|_{k+1,\widehat{Q}},$$

provided that $p \geq 2k$.

We note that, owing to the fact that $\widehat{K} \subseteq \widehat{Q}$, it holds:

$$|\widehat{u} - \widehat{\varphi}_p|_{1,\widehat{K}} \leq |\widehat{u} - \widehat{\varphi}_p|_{1,\widehat{Q}} \leq c 2^k e^k p^{-k} |\widehat{u}|_{k+1,\widehat{Q}}.$$

In order to conclude, it suffices to define $\widehat{\Pi}_p^{\widehat{Q}}\widehat{u} := \widehat{\varphi}_p$. □

The counterpart of Lemma 2.2.2 follows.

Lemma 2.3.2. *Given $K \in \mathcal{T}_n$, let $Q = Q(K)$ be the smallest square containing K; moreover, let $u \in H^{k+1}(Q)$ and $p \geq 2k$. Then, there exists a sequence of approximation operators $\{\Pi_p^Q\}_{p\in\mathbb{N}}$ with $\Pi_p^Q : H^2(Q) \longrightarrow \mathbb{P}_p(Q)$ such that, for any $k \in \mathbb{N}$:*

$$|u - \Pi_p^Q u|_{1,K} \leq c M^k \frac{h_K^\mu}{p^k} \|u\|_{k+1,Q}, \quad \mu = \min(p,k),$$

where c and M are two constants independent of k, h, p and u.

Proof. It suffices to apply Lemma 2.3.1 and a classical scaling argument. The mapping F between Q and $\widehat{Q}$ is the composition of a roto-traslation and a dilatation in $\mathbb{R}^2$. The polygon $\widehat{K} \in \widehat{Q}$ and the operator $\Pi_p^Q u$ are simply given by $\widehat{K} = F(K)$ and $\Pi_p^Q u = (\Pi_p^Q(u \circ F^{-1})) \circ F$ respectively. □

We define $u_\pi \in \mathcal{S}^{p,-1}(\Omega,\mathcal{T}_n), \mathcal{S}^{p,-1}(\Omega,\mathcal{T}_n)$ being introduced in (1.44), as:

$$u_\pi|_K = (\Pi_p^Q u)|_K, \text{ with } Q = Q(K) \quad \forall\, K \in \mathcal{T}_n.$$

Owing to assumption (**G6**) and Lemma 2.3.2, we are able to give the following global estimate:

$$|u - u_\pi|_{1,\mathcal{T}_n} \leq cA^k \frac{h^\mu}{p^k} \|u\|_{k+1,\Omega^{ext}},\ \mu = \min(p,k), \tag{2.46}$$

where Ω^{ext} is defined in (2.40) and c and A are two positive constants independent of h, p, k, ρ_0 and u (A is independent also of N), ρ_0 being introduced in assumptions (**G1**)-(**G2**).

2.3.3 Virtual interpolation term

In the present section, we give an explicit representation of the constant c in (2.30) in terms of k. We point out that here the shape regularity assumption is needed; in fact, the usual scaling arguments used herein are based on affine mappings of shape regular triangles into the master triangle.

Lemma 2.3.3. *Let u be the solution to* (1.27) *with $u \in H^{k+1}(\Omega^{ext})$, Ω^{ext} being defined in* (2.40). *Under assumptions (**G0**)-(**G1**)-(**G2**)-(**G3**)-(**G6**), provided that $p \geq 2k$, there exists $u_I \in V_{hp}$ such that:*

$$|u - u_I|_{1,\Omega} \leq c \cdot B^k \frac{h^k}{p^k} |u|_{k+1,\Omega^{ext}}, \tag{2.47}$$

where c and B are two constants independent of k, p, h and u (B is independent also of N).

Proof. The proof of this lemma is a combination of the arguments used in Lemma 2.3.1 and the construction of Lemma 2.2.3. Therefore, we only give the sketch of the proof.

We start by considering a triangle $\widetilde{K}$ in the subtriangulation $\widetilde{\mathcal{T}}_n$, we map it into the master triangle $\widehat{T}$ (e.g. the triangle obtained halving the square $[-1,1]^2$ through one of its two diagonal), we use a Legendre-type approximant in order to derive an estimate in terms of p as in Lemma 2.3.1, we go back to the triangle $\widetilde{K}$.

Let $\widetilde{Q}$ be the parallelogram $\widetilde{Q} = \widetilde{Q}(\widetilde{K})$ (see assumption (**G6**)) and let $\{\widetilde{\mathbf{V}}_i\}_{i=1}^3$ be the set of the vertices of $\widetilde{K}$. Therefore, it is possible to show the existence of a $\varphi_{hp} \in \mathbb{P}_p(\widetilde{K})$ such that $\varphi_{hp}(\widetilde{\mathbf{V}}_i) = u(\widetilde{\mathbf{V}}_i)$, $\forall i = 1,2,3$ and such that:

$$|u - \varphi_{hp}|_{1,\widetilde{K}} \leq c\widetilde{B}^k \frac{h^k}{p^k} |u|_{k+1,\widetilde{Q}}, \tag{2.48}$$

where c and $\widetilde{B}$ are two positive constants independent of p, h, k and u ($\widetilde{B}$ is also independent of N and ρ_0, ρ_0 being introduced in assumptions (**G1**)-(**G2**)). We point out that this estimate holds for all the triangles in the subtriangulation $\widetilde{\mathcal{T}}_n$. We denote, with a little abuse of notation, by $\varphi_{hp} : \Omega \to \mathbb{R}$ the global piecewise polynomial function whose restriction on each triangle $\widetilde{K}$ satisfies (2.48).

So far, we have obtained a piecewise discontinuous polynomials. We set:

$$E = E(\widetilde{K}) := \left(\bigcup_{\left\{\widetilde{\widetilde{K}} \in \widetilde{\mathcal{T}}_n | \widetilde{K} \cap \widetilde{\widetilde{K}} = s\right\}} \widetilde{Q}\left(\widetilde{\widetilde{K}}\right) \right) \cup \widetilde{Q}(\widetilde{K}), \quad s \text{ edge of } \widetilde{K},$$

where we recall that $\widetilde{Q}(\widetilde{\widetilde{K}})$ is defined in assumption (**G6**). We need to modify φ_{hp} in order to get a continuous piecewise polynomial on the subtriangulation $\widetilde{\mathcal{T}}_n$ without changing the approximation property (2.48). This can be done following the same approach as in [20, Theorem 4.6 and Lemma 4.7], i.e. by correcting φ_{hp} with suitable polynomial extensions of its edge jumps. It is possible to check that such step does not introduce constants depending on k.

With another little abuse of notation, we have obtained a $\varphi_{hp} \in H_0^1(\Omega)$ piecewise continuous polynomial of degree p over the subtriangular decomposition $\widetilde{\mathcal{T}}_n$, such that an analogous of (2.48) holds for all $\widetilde{K} \in \widetilde{\mathcal{T}}_n$:

$$|u - \varphi_{hp}|_{1,\widetilde{K}} \leq c\widetilde{\widetilde{B}}^k \frac{h^k}{p^k} |u|_{k+1,E(K)}.$$

Using assumption (**G6**) and summing on all the elements, one can conclude the proof. □

2.3.4 Oscillation of the right-hand side

The counterpart of Lemma 2.2.4 is a consequence of Lemmata 2.2.4 and 2.3.2. In particular the following holds.

Lemma 2.3.4. *Under assumptions (**G0**)-(**G1**)-(**G2**)-(**G3**)-(**G6**), let Ω^{ext} be defined in* (2.40) *and let the loading term $f \in H^{\widetilde{k}+1}(\Omega^{ext})$. Then, the following holds true:*

$$\mathcal{F}_{hp} \leq cD^k \frac{h^{\widetilde{\mu}}}{p^{\widetilde{k}+2}} \|f\|_{\widetilde{k}+1,\Omega^{ext}}, \quad \widetilde{\mu} = \min(p, \widetilde{k}+2), \tag{2.49}$$

*where c and D are two positive constants independent of k, h, p and u (D is also independent of N, N being the parameter introduced in assumption (**G6**) denoting the maximum number of overlapping parallelograms associated with subtriangulation $\widetilde{\mathcal{T}}_n$).*

2.3.5 Exponential convergence of the method for analytic (on an enlarged domain) solutions

Combining bounds (2.22), (2.46), (2.47) and (2.49) yields the following result.

Theorem 2.3.5. *Under the assumptions (**A_{hp}1**)-(**A_{hp}2**)-(**G0**)-(**G1**)-(**G2**)-(**G3**)-(**G6**), let $k \in \mathbb{N}$, $k > \frac{1}{2}$ and let u and u_{hp} be respectively the solutions to problems* (1.27) *and* (2.1). *Let Ω^{ext} be defined as in* (2.40), *$u \in H^{k+1}(\Omega^{ext})$ and ρ_0 and N be defined in assumptions (**G1**), (**G2**) and (**G6**) respectively. Assume also $p \geq 2k$. Then, the following hp estimate holds true:*

$$|u - u_{hp}|_{1,\Omega} \leq c \frac{\alpha^*(p)}{\alpha_*(p)} \widetilde{A}^k \frac{h^k}{p^k} |u|_{k+1,\Omega^{ext}}, \tag{2.50}$$

where c and $\widetilde{A}$ are two positive constants independent of h, p, k and u ($\widetilde{A}$ is also independent of N).

As done in Remark 4, we point out that if the domain Ω is convex it is possible to derive easily, owing to the approximation properties of Legendre polynomials, L^2 estimates of the form:

$$\|u - u_{hp}\|_{0,\Omega} \leq c \frac{\alpha^*(p)}{\alpha_*(p)} \widetilde{A}^k \frac{h^{k+1}}{p^{k+1}} |u|_{k+1,\Omega^{ext}}, \tag{2.51}$$

where c and $\widetilde{A}$ are two constants independent of h, p, k and u ($\widetilde{A}$ is also independent of N).

We have the following exponential convergence result for analytic solutions u over the extended domain Ω^{ext} defined in (2.40).

Theorem 2.3.6. *Under the assumptions (**A_{hp}1**)-(**A_{hp}2**)-(**G0**)-(**G1**)-(**G2**)-(**G3**)-(**G6**), let u and u_{hp} be respectively the solutions to problems* (1.27) *and* (2.1), *with $u \in \mathcal{A}(\overline{\Omega^{ext}})$, $\mathcal{A}(\overline{\Omega^{ext}})$ being the set of analytic function over the closure of Ω^{ext} defined in* (2.40). *Then, the following exponential convergence estimate holds:*

$$\|u - u_{hp}\|_{1,\Omega} \leq c \frac{\alpha^*(p)}{\alpha_*(p)} e^{-b\,p}, \tag{2.52}$$

for some positive constants c and b independent of p.

Proof. We recall (see for instance [47]) that an analytic function u in the closure of a domain $\Theta \in \mathbb{R}^2$ is characterized by the following bound:

$$\|D^{\boldsymbol{\alpha}} u\|_{\infty,\overline{\Theta}} \leq cA^{|\boldsymbol{\alpha}|}\boldsymbol{\alpha}! \qquad \forall\, \boldsymbol{\alpha} = (\alpha_1, \alpha_2) \in \mathbb{N}_0^2, \tag{2.53}$$

where $\boldsymbol{\alpha}! = \alpha_1!\alpha_2!$ and where c and A are constants independent of the multi-index $\boldsymbol{\alpha}$; nevertheless, c and A depends on u and on $\overline{\Theta}$. Recalling (2.50), we have:

$$|u - u_{hp}|_{1,\Omega} \leq c(N)\frac{\alpha^*(p)}{\alpha_*(p)}\widetilde{A}^k\frac{h^k}{p^k}|u|_{k+1,\Omega^{ext}},$$

if $p \geq 2k$.

Using (2.53) yields:

$$|u - u_{hp}|_{1,\Omega} \leq c\frac{\alpha^*(p)}{\alpha_*(p)}\left(\widetilde{A}\frac{h}{p}\right)^k A^{k+1}(k+1)!.$$

By means of Stirling formula, we obtain:

$$|u - u_{hp}|_{1,\Omega} \leq c\frac{\alpha^*(p)}{\alpha_*(p)}\left(\frac{hA\widetilde{A}}{p}\right)^k\left(\frac{k+1}{e}\right)^{k+1}\sqrt{2\pi}(k+1)^{\frac{1}{2}},$$

which leads to:

$$|u - u_{hp}|_{1,\Omega} \leq c\frac{\alpha^*(p)}{\alpha_*(p)}\left(\frac{hA\widetilde{A}}{e\,p}k\right)^k k^{\frac{3}{2}}.$$

By denoting $\delta = \frac{hA\widetilde{A}}{e}$ we can write:

$$|u - u_{hp}|_{1,\Omega} \leq c\frac{\alpha^*(p)}{\alpha_*(p)}\left(\frac{k}{p}\delta\right)^k k^{\frac{3}{2}}.$$

Since this last inequality holds true for all $k \in \mathbb{N}$ such that $2 \leq 2k \leq p$, we may choose $k = \lfloor \frac{p}{2(\delta+1)} \rfloor$, where $\lfloor\cdot\rfloor$ denotes the floor function. Hence:

$$|u - u_{hp}|_{1,\Omega} \leq c\frac{\alpha^*(p)}{\alpha_*(p)}\left(\frac{\delta}{2(\delta+1)}\right)^{\frac{p}{2(\delta+1)}} p^{\frac{3}{2}} = c\frac{\alpha^*(p)}{\alpha_*(p)}e^{-b\,p}p^{\frac{3}{2}}\,, \quad \text{with } b = \frac{\log(\frac{\delta}{2(\delta+1)})}{2(\delta+1)}. \tag{2.54}$$

The multiplier $p^{\frac{3}{2}}$ can be absorbed by $e^{-b\,p}$ by making b a little bit smaller and increasing c; therefore, (2.54) immediately yields:

$$|u - u_{hp}|_{1,\Omega} \leq c\frac{\alpha^*(p)}{\alpha_*(p)}e^{-b\,p}, \tag{2.55}$$

for some constants c and b independent of p. The result follows from the Poincarè inequality. □

Remark 5. We point out that in order to obtain the *hp* estimates of Theorem 2.2.6 and of Theorem 2.3.5, we used two different approximant polynomials.

Throughout Section 2.2, we decided to follow the Babuška-Suri construction (see [20,21]) which is based on a Fourier series expansion on a proper domain. Nevertheless this construction obliges, also in the case of the overlapping square technique related to assumption (**G6**), to use some extension operator (for instance the one described in [98, Chapter VI] for Lipschitz domains). Thus, to give an explicit representation of the dependence of the involved constant on the Sobolev regularity k is a not trivial work. Just to provide an example of possible additional complications, we emphasize that the extension operator from [98, Chapter VI, Theorem 5] is based on a partition of unity argument and thus one should be able to bound Sobolev (semi)norms of the bump-functions appearing in the partition of unity. The problem is that such (semi)norms blow up very rapidly when the Sobolev order grows, even faster than the rate of convergence of the method.

On the other hand, throughout Section 2.3, we made use of Legendre-type approximant (as done for instance in [96]). In this case, owing to Legendre polynomials properties, we are able to obtain exponential estimates, since the dependence in the constant with respect to the Sobolev regularity k can be derived and is mild enough.

We stress that the Legendre approach could be used also in Section 2.2; the choice of Fourier-type approximation, which we recall is not applicable in Section 2.3, is essentially a matter of taste and has the merit of avoiding to use bi-polynomial functions; furthermore, the latter approach is much easier than the former and this is why we show the details of both.

We anticipate that the numerical tests in Section 7.1.2 do not suffer practically of the theoretical pollution effect related to the stability.

2.4 A hint concerning the double rate of convergence in terms of p

Assume now that u, the solution to problem (1.27), is given by:

$$u = r^{\alpha} \sin(\alpha\, \theta), \tag{2.56}$$

where (r, θ) are the polar coordinates associated with a vertex of domain Ω and $\alpha \in \mathbb{R}_+$.

It is well-known, e.g. from [20,21], that one can achieve the so-called double rate of convergence of the p version of FEM, whenever the solution to problem (1.27) has a particular form, e.g. the one in (2.56). This means that in (2.37) and (2.38), instead of getting p^{-k}, it is possible to get a rate of convergence p^{-2k}.

The same sort of double rate of convergence can be recovered in the framework of p VEM under appropriate assumptions on u. Since the aim of the thesis does not consist in investigating this kind of issue, we here give only rough details for the recovering of such double rate.

A function as in (2.56) is provided in (7.4) and is in fact the target of the numerical tests regarding the h and p version of VEM on quasi-uniform meshes.

As a byproduct, we underline that what we are going to discuss can be extended to solutions that are more general than those in (2.56), see e.g. [20, Section 5].

We now sketch the proof of the double rate of convergence in VEM. To this purpose, we need to recall a technical result which is a direct consequence of [20, Lemma 5.1].

Lemma 2.4.1. *Let u the solution to problem* (1.27) *be as in* (2.56) *and let T be a shape-regular triangle. Then, there exists a sequence $\{z_p\}_{p\in\mathbb{N}}$ with $z_p \in \mathbb{P}_p(T)$ for all $p \in \mathbb{N}$ such that:*

$$\|u - z_p\|_{1,T} \leq c \frac{h^{\alpha}}{p^{2\,\alpha}},$$

where c is a positive constant independent of h and p.

Combining Lemma 2.4.1 with Lemma 2.2.2, one is able to bound the first term on the right-hand side of (2.22) that is a best error term with respect to polynomials; instead, in order to bound the second term on the right-hand side of (2.22), that is a best error term with respect to functions in the VE space, one should use the strategy presented in Lemma 2.2.3 and picking as φ_{hp} in (2.31) the function defined in [20, Lemma 5.2] which is nothing but the p-FEM solution on the subtriangulation $\widetilde{\mathcal{T}}_n$ introduced in Remark 2 of u, which also provides double rate of convergence in terms of p.

Chapter 3

The hp version of the virtual element method and approximation of corner singularities for the Poisson problem on geometrically refined meshes

In Chapter 2, we discussed the h and p version of VEM on quasi-uniform meshes assuming either finite Sobolev regularity or analyticity (on a proper enlarged domain) of the solution to such target problem. In the former case, the p version (as well in fact as the h version) of the method leads to an algebraic decay of the error, see Theorem 2.2.6, while in the latter one has exponential convergence, see Theorem 2.3.6.

Nonetheless, solutions to elliptic PDEs on polygons suffer in general a lack of regularity at the corners of the domain and therefore one is not able to obtain exponential convergence of the error both for the h and the p version of the method when employing quasi-uniform meshes. More precisely, as discussed in Appendix A, the solutions to elliptic PDEs typically belong to Babuška spaces $\mathcal{B}^{\ell}_{\boldsymbol{\beta}}(\Omega)$ defined in (1.22) and thus, also with smooth data (analytic right-hand side and homogeneous Dirichlet boundary conditions), such solutions are in general singular at the corners of the domain.

The fact that when the solution has finite Sobolev regularity both the h and the p version of the method return an algebraic decay of the error, which is opposed to exponential convergence when approximating analytic solutions, is also valid in the FEM framework [20, 96]. Here, a remedy in order to recover exponential convergence is given by the full hp version of the method, which consists in combining mesh refinements towards the corners of the domain and by increasing the dimension of local spaces in the interior of the domain.

The present chapter is devoted to extend the technology of VEM to the hp setting, exploiting in this way the great flexibility of polygonal methods in handling meshes that are geometrically refined, see e.g. Figures 1.4 and 1.5.

Throughout the chapter, we assume that the sequences of polygonal decompositions $\{\mathcal{T}_n\}_{n\in\mathbb{N}}$ satisfy assumptions (**G0**)-(**G1**)-(**G2**)-(**G4**)-(**G5**), that is we consider geometric meshes refined towards a single vertex only, namely $\mathbf{0}$. In addition, we will also assume that u and f, the solution and the right-hand side of problem (1.27) respectively, belong to the modified Babuška spaces $\mathcal{B}^2_{\beta}(\Omega,\mathbf{0})$ and $\mathcal{B}^0_{\beta}(\Omega,\mathbf{0})$, where space $\mathcal{B}^{\ell}_{\beta}(\Omega,\mathbf{0})$ is defined in (1.36), where $1-\alpha_{1,1}<\beta$, $\alpha_{1,1}$ being the first singular exponent defined in (A.4) associated with vertex $\mathbf{0}$.

All the results in this chapter hold true also in the case of "multiple singularities", but, for the sake of simplicity, we assume only the singularity at $\mathbf{0}$.

The outline of the chapter follows. In Section 3.1, we deal with the construction of a VEM with nonuniform degrees of accuracy. In Section 3.2, we prove exponential convergence in terms of the total number of degrees of freedom and, under proper assumptions on the stabilization, we prove that, at the theoretical level, there is no pollution effect due to the stabilization.

Finally, we point out that the contents of this chapter are presented in [32].

3.1 Virtual Elements for the Poisson problem with nonuniform degree of accuracy

In this section, we introduce a VEM with nonuniform degree of accuracy for Poisson problem (1.27). Recall that we are given sequences of polygonal decompositions $\{\mathcal{T}_n\}_{n\in\mathbb{N}}$ satisfying assumptions (**G0**)-(**G1**)-(**G2**)-(**G4**)-(**G5**). We associate to each $\mathcal{T}_n$, $n \in \mathbb{N}$, a vector $\mathbf{p} \in \mathbb{N}^{\mathrm{card}(\mathcal{T}_n)}$ which is in bijection with $\mathcal{T}_n$ as follows:

$$\mathbf{p} = (p_1, p_2, \ldots, p_{\mathrm{card}(\mathcal{T}_n)}) \quad \longleftrightarrow \quad \mathcal{T}_n = (K_1, K_2, \ldots, K_{\mathrm{card}(\mathcal{T}_n)}). \tag{3.1}$$

We also write p_K in lieu of p_i whenever $K = K_i$. Vector $\mathbf{p}$ will pay the role of distribution of the local degrees of accuracy over $\mathcal{T}_n$.

For the sake of simplicity, we assume that:

$$p_K \geq 2 \qquad \forall\, K \in \mathcal{T}_n. \tag{3.2}$$

Assumption (3.2) has the merit of simplifying the treatment of the discrete right-hand side (3.15) and in fact is not mandatory.

Even more importantly, we demand the following property on distribution $\mathbf{p}$:

(**P1**) the following holds true:

$$p_{K_1} \approx p_{K_2} \text{ whenever } \overline{K_1} \cap \overline{K_2} \neq \emptyset, \tag{3.3}$$

that is, we demand that two neighbouring elements must have comparable p.

We also associate a "degree of accuracy" to each edge s in the skeleton of $\mathcal{T}_n$ following the so-called *maximum-rule*. This means that:

- if $s \not\subset \partial\Omega$, i.e. if s is an internal edge, then there exists K_1, $K_2 \in \mathcal{T}_n$ such that $\overline{K_1} \cap \overline{K_2} = s$; we fix $p_s = \max(p_{K_1}, p_{K_2})$;
- if $s \subset \partial\Omega$, i.e. if s is a boundary edge, then there exists exactly one $K \in \mathcal{T}_n$ such that $s \subset K$; we fix $p_s = p_K$.

In Figure 3.1, we depict an example where the *maximum-rule* applies.

We are now ready to define the VE space with nonuniform distribution of degrees of freedom. As in Chapter 2, we begin with the definition of the local spaces. Given $K \in \mathcal{T}_n$, we define the space of piecewise continuous polynomials over ∂K as:

$$\mathbb{B}(\partial K) = \big\{ v_n \in \mathcal{C}^0(\partial K) \mid v_n|_s \in \mathbb{P}_{p_s}(s) \text{ for all } s \text{ edge of } K \big\}. \tag{3.4}$$

The local VE space reads:

$$V(K) = \big\{ v_n \in H^1(K) \mid \Delta v_n \in \mathbb{P}_{p_K-2}(K),\ v_n \in \mathbb{B}(\partial K) \big\}. \tag{3.5}$$

The difference between local spaces $V(K)$ defined in (3.5) and $V_{hp}(K)$ defined in (2.3) is that in the former space nonuniform polynomial degree on the boundary is allowed.

The two spaces share the same type of degrees of freedom, see Section 2.1, but we highlight that the number of edge dofs depends here on the distribution of polynomial degrees over the boundary of K. More precisely, the dimension of space $V(K)$ is:

$$\dim(V(K)) = \sum_{j=1}^{N_K} p_{s_j} + \frac{(p_K - 1)p_K}{2}, \tag{3.6}$$

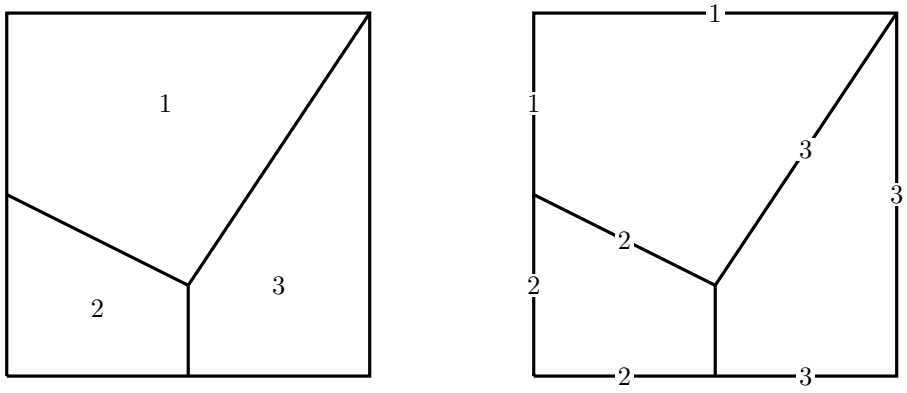

Figure 3.1: Left: distribution of the degrees of accuracy on polygons. Right: distribution of the degrees of accuracy on edges via *maximum rule*.

where we recall that N_K is the number of vertices and edges of K, while $\{s_j\}_{j=1}^{N_K}$ denotes its set of edges.

We observe that, since we are employing the *maximum-rule*, we have $\mathbb{P}_{p_K}(K) \subset V(K)$. In principle, it is possible to pick also the *minimum-rule*; in doing that, no actual changes in the convergence of the method can be seen in numerical tests; yet, since $\mathbb{P}_{p_K}(K) \subset V(K)$ would not hold anymore, the approximation analysis would get more technical.

The global VE space is obtained by matching the boundary dofs on each edge and by imposing homogeneous Dirichlet boundary conditions:

$$V_n = \big\{v_n \in \mathcal{C}^0(\overline{\Omega}) \mid v_n|_K \in V(K),\, v_n|_{\partial\Omega} = 0\big\}. \tag{3.7}$$

Having defined the global VE space and recalling that it consists of functions that are explicitly known only on the skeleton of $\mathcal{T}_n$, we introduce a *computable* global discrete bilinear form (since its continuous counterpart is not computable):

$$a_n(u_n, v_n) = \sum_{K\in\mathcal{T}_n} a_n^K(u_n, v_n) \qquad \forall\, u_n,\, v_n \in V_n, \tag{3.8}$$

where the local discrete bilinear forms read, as in (2.13):

$$a_n^K(u_n, v_n) = a^K(\Pi^\nabla_{p_K} u_n, \Pi^\nabla_{p_K} u_n) + S^K((I - \Pi^\nabla_{p_K})u_n, (I - \Pi^\nabla_{p_K})v_n) \qquad \forall\, u_n,\, v_n \in V(K), \tag{3.9}$$

where $\Pi^\nabla_{p_K}$ is defined as in (2.8) and where

$$S^K : \ker(\Pi^\nabla_{p_K}) \times \ker(\Pi^\nabla_{p_K}) \to \mathbb{R} \tag{3.10}$$

is a computable stabilizing bilinear form satisfying:

$$c_*(p_K)|v_n|^2_{1,K} \le S^K(v_n, v_n) \le c^*(p_K)|v_n|^2_{1,K} \quad \forall v_n \in \ker(\Pi^\nabla_{p_K}). \tag{3.11}$$

Here we demand an additional assumption on the stabilization constants $c_*(p_K)$ and $c^*(p_K)$, namely:

$$c_*(p_K) = c\, p_K^{-r_1}, \qquad c^*(p_K) = c\, p_K^{r_2} \qquad \forall\, K \in \mathcal{T}_n, \tag{3.12}$$

for some universal positive constants c, r_1 and r_2.

The reason for which we demand (3.12) is that under this assumption we are able to prove exponential convergence of *hp* VEM in Section 3.2.4. We anticipate that in Section 6.2 we exhibit explicit choices for S^K satisfying (3.2.4) with explicit r_1 and r_2.

As in Chapter 2, it is possible to prove that the local discrete form a_n^K satisfies the two following properties:

($\mathbf{A}_n\mathbf{1}$) **polynomial consistency**: for all $K \in \mathcal{T}_n$, it must hold:

$$a^K(q_{p_K}, v_n) = a_n^K(q_{p_K}, v_n) \qquad \forall\, q_{p_K} \in \mathbb{P}_{p_K}(K), \quad \forall\, v_n \in V(K); \tag{3.13}$$

($\mathbf{A}_n\mathbf{2}$) **stability**: for all $K \in \mathcal{T}_n$, it must hold:

$$\alpha_*(p_K)|v_n|^2_{1,K} \leq a_n^K(v_n, v_n) \leq \alpha^*(p_K)|v_n|^2_{1,K} \qquad \forall\, v_n \in V(K) \tag{3.14}$$

where $\alpha_*(p_K) = \min(1, c\, p_K^{-r_1})$ and $\alpha^*(p_K) = \max(1, c\, p_K^{r_2})$, c, r_1 and r_2 being introduced in (3.12).

For what concerns the discrete right-hand side (again, we can not keep the continuous one since the functions in the VE space are not known explicitly at the interior of each polygon), we define:

$$\langle f_n, v_n\rangle_n = \sum_{K\in\mathcal{T}_n} \langle f_n, v_n\rangle_{K,n} \qquad \forall\, v_n \in V_n, \tag{3.15}$$

where the local terms are defined as:

$$\langle f_n, v_n\rangle_{K,n} = \int_K f_n\big(\Pi^0_{p_K-2} v_n\big) \qquad \forall\, v_n \in V(K), \tag{3.16}$$

$\Pi^0_{p_K-2}$ being the L^2 projection defined in (2.18), which we recall is computable via only internal dofs (2.4).

At the end of the day, we end up with the following VEM based on a nonuniform distribution of local degrees of accuracy:

$$\begin{cases} \text{find } u_n \in V_n \text{ such that} \\ a_n(u_n, v_n) = \langle f_n, v_n\rangle_n \qquad \forall\, v_n \in V_n \end{cases}, \tag{3.17}$$

which is well-posed, owing to (3.14).

Let now $\mathcal{F}_n^K$, $K \in \mathcal{T}_n$, be be the smallest positive constants such that:

$$|(f, v_n)_{0,K} - \langle f_n, v_n\rangle_{0,K}| = \int_K (f - \Pi^0_{p-2} f)\,(v_n - \Pi^0_{p-2} v_n) =: F_K(v_n) \leq \mathcal{F}_n^K |v_n|_{1,K}\ \forall\, v_n \in V(K) \tag{3.18}$$

and let:

$$\alpha(p_K) := \frac{\alpha^*(p_K)}{\min_{K'\in\mathcal{T}_n} \alpha_*(p'_K)}, \qquad \forall\, K \in \mathcal{T}_n, \tag{3.19}$$

where $\alpha_*(p_K)$ and $\alpha^*(p_K)$ are introduced in (3.14).

We prove now an abstract error analysis which traces Lemma 2.22 but in addition takes here into account the nonuniformity of the distribution of the polynomial degrees of accuracy.

Lemma 3.1.1. *Under assumptions ($\boldsymbol{A}_n\mathbf{1}$)-($\boldsymbol{A}_n\mathbf{2}$), let u and u_n be the solutions to problems* (1.27) *and* (3.17) *respectively. Then, for all $u_I \in V_n$ and for all $u_\pi \in \mathcal{S}^{\mathbf{p},-1}(\Omega, \mathcal{T}_n)$ defined in* (1.44)*, it holds that:*

$$|u - u_n|_{1,\Omega} \lesssim \sum_{K\in\mathcal{T}_n} \alpha(p_K)\left\{|u - u_\pi|_{1,K} + |u - u_I|_{1,K} + \mathcal{F}_n^K\right\}, \tag{3.20}$$

where $\mathcal{F}_n^K$ and $\alpha(p_K)$ are defined in (3.18) *and* (3.19) *respectively.*

Lemma 3.20 states that, up to the pollution factor $\alpha(p_K)$ defined in (3.19) due to the presence of the stabilization, the error of the method is bounded by the sum of three terms:

- a sum of local best error terms with respect to polynomials of degree p_K over each $K \in \mathcal{T}_n$;
- a sum of local best error terms with respect to functions in the local VE spaces $V(K)$;
- a sum of local terms due to the oscillation of the right-hand side.

The forthcoming section, is devoted to estimate these three terms. Thanks to (3.12), we prove exponential convergence of the method in terms of the total number of degrees of freedom without the pollution effect due to the stabilization.

3.2 Exponential convergence with *hp* VEM

In this section, we study the convergence of VEM (3.17), where we recall that we are assuming that u, the solution to problem (1.27), belongs to $\mathcal{B}^2_\beta(\Omega, \mathbf{0})$ defined in (1.36) with $1 - \alpha_{1,1} < \beta$, $\alpha_{1,1}$ being the first singular exponent (A.4) associated with vertex $\mathbf{0}$. In particular, u has the natural regularity that one would expect when solving a Poisson problem on a polygonal domain, see Theorem A.0.4.

We demand additional regularity on the sequences of decompositions $\{\mathcal{T}_n\}_{n\in\mathbb{N}}$. We recall that we are employing sequences of meshes that are geometrically refined toward vertex $\mathbf{0}$, see Section 1.4.2. We also recall that in each $K \in \mathcal{T}_n$, $n \in \mathbb{N}$, we distinguish between polygons belonging to L_0, the layer of polygons abutting $\mathbf{0}$ and all the other layers.

In order to fix the notation, we write:

$$\mathcal{T}_n^0 = L_0 \qquad \mathcal{T}_n^1 = \cup_{j=1}^n L_j. \tag{3.21}$$

See Figure 3.2 for a graphical representation of the two sets defined in (3.21).

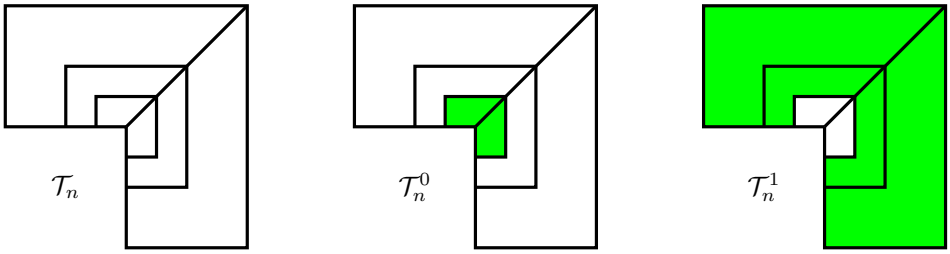

Figure 3.2: Left: $\mathcal{T}_n$, original mesh. Center: $\mathcal{T}_n^0$, layer of polygons abutting $\mathbf{0}$. Right: $\mathcal{T}_n^1$, other layers.

We are now able to demand an additional assumption on the mesh:

(**G7**) given $\mathcal{T}_n$ geometric polygonal decomposition, there exists a collection C_n^1 of squares such that:

- card(C_n^1) = card$(\mathcal{T}_n^1)$; for each $K \in \mathcal{T}_n^1$, there exists $Q = Q(K) \in C_n^1$ such that $Q \supseteq K$ and $h_K \approx h_Q$, being $h_Q = \text{diam}(Q)$; in addition, it must hold dist$(\mathbf{0}, Q(K)) \approx h_K$;
- every $\mathbf{x} \in \Omega$ belong at most to a fixed number of squares Q, independently of all the discretization parameters;
- for all $K \in \mathcal{T}_n^0$, K is star-shaped with respect to $\mathbf{0}$; moreover, the subtriangulation of K obtained by joining $\mathbf{0}$ with the other vertices of the polygon is uniformly shape-regular.

We set $\Omega_n^{ext} = (\cup_{Q\in C_n^1} Q) \cup (\cup_{K\in\mathcal{T}_n^0} K)$.

In Figure 3.3, we depict on the left the fact that the mesh in Figure 1.4 (center) fulfills the covering square requirement (**G7**), on the left the fact that the mesh in Figure 1.4 (right) does not.

We point out that (**G7**) seems to be a rather technical requirement. Indeed, we will show in Section 7.2 that also meshes not satisfying (**G7**) may produce the expected convergence which will be proven in Section 3.2.4.

We note that (**G7**) is in the spirit of the strategy of the overlapping square technique used in Chapter 2. We here additionally require that squares covering polygons in $\mathcal{T}_n^1$ can not cover vertex $\mathbf{0}$; if this were true, then all the approximation results proven in Sections 3.2.1, 3.2.2 and 3.2.3 on polygons not abutting $\mathbf{0}$ would not hold anymore.

Finally, we point out that instead of considering a decomposition of squares C_n, it is possible to consider in (**G7**) a decomposition in sufficiently regular quadrilaterals (e.g. parallelograms), since the same analysis by means of Legendre polynomials used in the forthcoming sections could be performed as well.

The remainder of the section is organized as follows. In Sections 3.2.1, 3.2.2 and 3.2.3, we bound the local contributions due to the first, second and third terms appearing on the right-hand

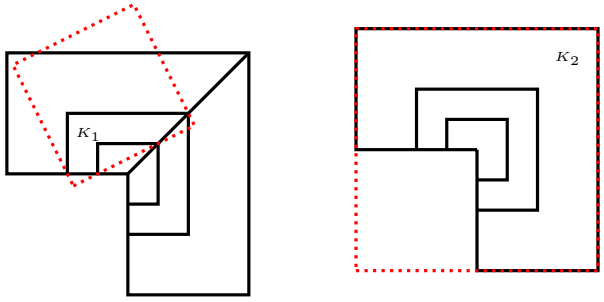

Figure 3.3: Left: the mesh in Figure 1.4 (center) fulfills the covering square requirement in assumption (**G7**); this is shown e.g. for element K_1. Right: the mesh in Figure 1.4 (right) does not; this is shown e.g. for element K_2. In both cases the bounding square has a red dotted boundary.

side of (3.20); finally, in Section 3.2.4, we prove the main result of the chapter, namely exponential convergence of the method in terms of the total number of degrees of freedom; here, thanks to (3.12), it is possible to get rid of the pollution effect of the stabilization.

3.2.1 Local approximation by polynomials

Here, we deal with the approximation of the first local terms on the right-hand side of (3.20). What we are going to prove are *hp* approximation properties by means of local polynomials on polygons. In *hp*-FEM literature, classical approximation of this type is not done on general polygons but only on squares and triangles, see [20, 21, 71, 77, 78, 96] and the references therein.
The basic tool behind this approach is the employment of orthogonal bases, namely tensor product of Legendre polynomials on the square, see [96], and Koornwinder polynomials (that is collapsed tensor product of Jacobi polynomials) on triangles, see [63, 74, 77]; with such basis, explicit computations can be performed, owing to properties of Legendre and Jacobi polynomials. On a generic polygon an explicit basis with good approximation properties is not available, at least to the best of our knowledge.

The first result is a polynomial approximation estimate regarding regular functions on polygons far from the singularity. This result will be used for the approximation of the first local terms on the right-hand side of (3.20) for the elements K separated from the singularity.

Lemma 3.2.1. *Under assumptions (**G0**)-(**G1**)-(**G2**)-(**G4**)-(**G5**)-(**G7**), let $K \in L_j$, $j = 1, \dots, n$. Let $Q(K)$ be defined in (**G7**) and let $u \in H^{s_K+3,2}_\beta(Q(K))$, $1 \le s_K \le p_K$, where we recall that the definition of the weighted Sobolev spaces under consideration can be found in* (1.35)*. Then, there exists $\Phi \in \mathbb{P}_{p_K}(Q(K))$ such that:*

$$\|D^m(u-\Phi)\|^2_{0,K} \lesssim \sigma^{2(n-j)(2-m-\beta)} \frac{\Gamma(p_K - s_K + 1)}{\Gamma(p_K + s_K + 3 - 2m)} \left(\frac{\rho}{2}\right)^{2s_K} |u|^2_{H^{s_K+3,2}_\beta(Q(K))}, \tag{3.22}$$

where $m = 0, 1, 2$; $2 \le j \le n+1$; $\rho = \max(1, \frac{1-\sigma}{\sigma})$, σ is the grading parameter of the mesh introduced in (1.39) *and Γ is the Gamma function.*

Proof. The result follows from classical scaling arguments and [96, Lemma 4.53]. Here, we only sketch the proof.

Firstly one encapsulates polygon K into the corresponding square $Q(K)$. It is possible to bound the left-hand side of inequality (3.22) with the same (semi)norm on the square. After that, the square is mapped into the reference square $\widehat{Q} = [-1, 1]^2$ and a p analysis by means of tensor product of Legendre polynomials is developed (see [96, Theorem 4.46]). Subsequently, the reference square is pushed forward to square Q. Using the property of the geometric mesh and [96, Lemma 4.50], the result follows. □

Estimates on polygons around the singularity are discussed in the following lemma. We point out that for the error control in layer L_0 we can work directly on the element without the need of employing covering squares, as done for the analysis on the polygons of the other layers, see

Lemma 3.2.1. The proof is an extension to polygonal domains of that in Theorem [96, Lemma 4.16].

Lemma 3.2.2. *Under assumptions (**G0**)-(**G1**)-(**G2**)-(**G4**)-(**G5**)-(**G7**), let $K \in L_0$. Let $u \in H^{2,2}_\beta(K)$, $\beta \in [0,1)$, where we recall that the definition of the weighted Sobolev spaces under consideration can be found in* (1.35)*. Then, there exists $\Phi \in \mathbb{P}_1(K)$ such that:*

$$|u-\Phi|^2_{1,K} \lesssim h_K^{2(1-\beta)} \||\mathbf{x}|^\beta D^2 u\|^2_{0,K} \lesssim \sigma^{2(1-\beta)n} \||\mathbf{x}|^\beta D^2 u\|^2_{0,K}, \tag{3.23}$$

where σ is the grading parameter of the mesh introduced in (1.39) *and where the hidden constant depends on the parameters ρ_0 and c introduced in assumptions (**G1**)-(**G2**)-(**G3**).*

Proof. We consider the subtriangulation $\widetilde{\mathcal{T}}_n(K)$ of K described in Remark 2 and we recall that it is shape-regular, with shape-regularity constant depending on the parameters ρ_0 and c introduced in assumptions (**G1**)-(**G2**)-(**G3**). Let $\widehat{T}$ be the reference triangle of vertices $(0,0)$, $(1,0)$ and $(0,1)$ and let $F_T^{-1} : T \to \widehat{T}$ be the standard affine map between the triangle T and the reference triangle $\widehat{T}$ for all $T \in \widetilde{\mathcal{T}}_n(K)$.

Proceeding as in [96, Lemma 4.16], it is possible to prove the validity of the following inequality:

$$|\widehat{U}|^2_{1,\widehat{T}} \le c\left\{ \||\widehat{\mathbf{x}}|^\beta D^2 \widehat{U}\|^2_{0,\widehat{T}} + \|\widehat{\Pi}^0_1 \widehat{U}\|^2_{0,\widehat{T}} \right\} \quad \forall \widehat{U} \in H^{2,2}_\beta(\widehat{T}), \tag{3.24}$$

where c is a positive constant independent of $\widehat{U}$ and where $\widehat{\Pi}^0_1(\cdot) = \Pi^{0,K}_1 \circ F_T(\cdot)$, $\Pi^{0,K}_1$ being the L^2 projector from $L^2(K)$ into $\mathbb{P}_1(K)$.

Given now $U \in H^{2,2}_\beta(K)$, splitting $|U|^2_{1,K}$ into a sum of terms over the triangles in $\widetilde{\mathcal{T}}_n(K)$, using a scaling argument and applying (3.24), yield:

$$|U|^2_{1,K} \le c h_K^{2(1-\beta)} \left\{ \||\mathbf{x}|^\beta D^2 U\|^2_{0,K} + \|\Pi^{0,K}_1 U\|^2_{0,K} \right\},$$

where now c is a positive constant depending only on the shape-regularity of $\widetilde{\mathcal{T}}_n(K)$ and hence on the parameters ρ_0 and c introduced in assumptions (**G1**)-(**G2**)-(**G3**), see Remark 2.

The assertion follows by picking $U = u - \Phi$, where $\Phi = \Pi^{0,K}_1 u$. □

We stress that (3.23) does not rely on p approximation results, but only on scaling argument. This is enough in order to prove the main result of this work, that is Theorem 3.2.8, and it is in accordance with the choice of the vector of local degrees of accuracy that will be done in the forthcoming definition (3.45). We emphasize that this is in the spirit of classical *hp* refinement, see [96].

3.2.2 Local approximation by functions in the VE space

Here, we treat the approximation of the second local terms on the right-hand side of (3.20). We observe that this term has two main differences with respect to the other two. The first difference is that we need an approximant u_I which is globally continuous; the second one is that u_I is not a piecewise polynomial but a function belonging to the virtual space V_n.

As done in Section 3.2.1, we split the analysis into two parts. Firstly, we work on polygons abutting the singularity, see Lemma 3.2.4; secondly, we work on elements K in the first layer L_0, see Lemma 3.2.5.

In order to prove such results, we need an additional technicality.

Lemma 3.2.3. *Under assumptions (**G1**)-(**G2**)-(**G3**), let $K \in \mathcal{T}_n$ with, for simplicity, $h_K = 1$. Then, for all $v \in H^1(K)$ with $\Delta v = 0$, the following holds true:*

$$|v|^2_{1,K} \lesssim \left\{ (\|\Delta v\|_{0,K} + |v|_{1,K}) \|v\|_{\frac{1}{2},\partial K} + \|\Delta v\|_{0,K} \|v\|_{0,K} \right\}, \tag{3.25}$$

*where the hidden constant depends on the parameters ρ_0 and c introduced in assumptions (**G1**)-(**G2**)-(**G3**).*

Proof. A fundamental tool needed for proving the assertion is the fact that the subtriangulation of K obtained by joining its vertices with the center of the ball in assumption (**G1**), is shape-regular with shape-regularity constant depending on the parameters ρ_0 and c introduced in assumptions (**G1**)-(**G2**)-(**G3**), see Remark 2.

Given N_K the number of edges of K, we denote by $\widehat{K}$ the regular polygon centered at $\mathbf{0} = (0,0)$ with N_K edges of length 1. Note that, due to the fact that N_K is uniformly bounded and that $h_K \approx h_s$ for all edges s of K, see assumption (**G2**), $h_K \approx 1$. Let $\widetilde{\mathcal{T}}_n(K)$ be the subtriangulation of $\widehat{K}$ obtained by joining $\mathbf{0}$ with the vertices of $\widehat{K}$.

Then, see for instance [82, Lemma 2.3], there exists a bijection $F_K^{-1} \in W^{1,\infty}(\widehat{K}, K)$, with inverse $F_K \in W^{1,\infty}(K, \widehat{K})$, which maps every $\widehat{T} \in \widetilde{\mathcal{T}}_n(\widehat{K})$ in $T \in \widetilde{\mathcal{T}}_n(K)$ in an affine way. The $W^{1,\infty}$ norms of F_K^{-1} and F_K are bounded solely in terms of the star-shapedness constant of $\widetilde{\mathcal{T}}_n(K)$ and therefore on the parameters ρ_0 and c introduced in assumptions (**G1**)-(**G2**)-(**G3**). Moreover, notice that, since the number of edges is uniformly bounded, see assumption (**G2**), there is a finite number of such reference polygons $\widehat{K}$.

We are now ready to prove the statement of the lemma. We begin by applying an integration by parts, a Cauchy-Schwarz inequality and the definition of the $H^{\frac{1}{2}}(\partial K)$ norm, to get:

$$|v|_{1,K}^2 = \int_K \Delta v\, v + \int_{\partial K} \partial_{\mathbf{n}} v\, v \leq \|\Delta v\|_{0,K}\|v\|_{0,K} + \|\partial_{\mathbf{n}} v\|_{-\frac{1}{2},\partial K}\|v\|_{\frac{1}{2},\partial K}. \tag{3.26}$$

We only need to bound the second term on the right-hand side of (3.26). To this purpose, we recall:

$$\|\partial_{\mathbf{n}} v\|_{-\frac{1}{2},\partial K} = \sup_{\varphi \in H^{\frac{1}{2}}(\partial K),\, \varphi \neq 0} \frac{{}_{-\frac{1}{2}}\langle \partial_{\mathbf{n}} v, \varphi \rangle_{\frac{1}{2}}}{\|\varphi\|_{\frac{1}{2},\partial K}} \tag{3.27}$$

and we bound from below the denominator on the right-hand side of (3.27).

Using the regularity of the maps F_K and F_K^{-1}, it is trivial to show that, for every $\Phi \in H^1(K)$, one has:

$$\|\Phi\|_{1,K} \lesssim \|\widehat{\Phi}\|_{1,\widehat{K}}, \tag{3.28}$$

where the hidden constant depends on the shape-regularity of $\widetilde{\mathcal{T}}_n(K)$ and where $\widehat{\Phi} = \Phi \circ F_K$.

At this point, we recall that the right-inverse trace theorem, see e.g. [80, Theorem 3.37], guarantees that for each $\widehat{\varphi} \in H^{\frac{1}{2}}(\partial\widehat{K})$ there exists $\widehat{\Phi} \in H^1(\widehat{K})$ such that $\widehat{\Phi}|_{\partial\widehat{K}} = \widehat{\varphi}$ and:

$$\|\widehat{\Phi}\|_{1,\widehat{K}} \leq c\|\widehat{\varphi}\|_{\frac{1}{2},\partial\widehat{K}}, \tag{3.29}$$

for some universal positive constant c.

As a further step, we observe that, given $\varphi \in H^{\frac{1}{2}}(\partial K)$ and $\widehat{\varphi} = \varphi \circ F_K^{-1}$, one gets:

$$\|\widehat{\varphi}\|_{\frac{1}{2},\partial\widehat{K}} \lesssim \|\varphi\|_{\frac{1}{2},\partial K}, \tag{3.30}$$

where the hidden constant depends solely on the shape-regularity of the subtriangulation $\widetilde{\mathcal{T}}_n(K)$; in order to see this, it suffices to use interpolation theory [102] and to show that:

$$\|\widehat{v}\|_{0,\partial\widehat{K}} \lesssim \|v\|_{0,\partial K} \qquad |\widehat{v}|_{1,\partial\widehat{K}} \lesssim |v|_{1,\partial K}, \tag{3.31}$$

with hidden constants depending on the shape-regularity of $\widetilde{\mathcal{T}}_n(K)$. Thus, (3.31) follows again from a mapping argument and the regularity of F_K and F_K^{-1}.

Collecting (3.28), (3.29) and (3.30), we deduce that, given $\varphi \in H^{\frac{1}{2}}(\partial K)$, there exists $\Phi \in H^1(K)$ such that $\Phi|_{\partial K} = \varphi$ and:

$$\|\Phi\|_{1,K} \lesssim \|\varphi\|_{\frac{1}{2},\partial K}, \tag{3.32}$$

with hidden constant depending solely on the parameters ρ_0 and c introduced in assumptions (**G1**)-(**G2**)-(**G3**), through Remark 2.

Plugging (3.32) into (3.27), applying an integration by parts and finally using Cauchy-Schwarz inequality, yield:

$$\|\partial_{\mathbf{n}} v\|_{-\frac{1}{2},\partial K} = \sup_{\Phi \in H^1(K),\, \Phi \neq 0} \frac{\int_K \nabla v \cdot \nabla \Phi + \int_K (\Delta v)\Phi}{\|\gamma(\Phi)\|_{\frac{1}{2},\partial K}} \lesssim |v|_{1,K} + \|\Delta v\|_{0,K},$$

where γ denotes the trace operator, whence the claim.

□

Remark 6. A straightforward modification of the proof of Lemma 3.2.3 implies that, in case v is such that Δv has zero average over K, then (3.25) modifies to:

$$|v|^2_{1,K} \lesssim \left\{ (\|\Delta v\|_{0,K} + |v|_{1,K}) \|v - c_1\|_{\frac{1}{2},\partial K} + \|\Delta v\|_{0,K} \|v - c_2\|_{0,K} \right\}, \tag{3.33}$$

where the hidden constant depends on the parameters ρ_0 and c introduced in assumptions (**G1**)-(**G2**)-(**G3**) and where c_1 and c_2 belong to $\mathbb{R}$. If instead v is such that $\Delta v \in \mathbb{P}_p(K)$, $p \in \mathbb{N}$, then (3.25) modifies to:

$$|v|^2_{1,K} \lesssim \left\{ (\|\Delta v\|_{0,K} + |v|_{1,K}) \|v\|_{\frac{1}{2},\partial K} + \|\Delta v\|_{0,K} \|\Pi^0_p v\|_{0,K} \right\}, \tag{3.34}$$

where, once again, the hidden constant depends on the parameters ρ_0 and c introduced in assumptions (**G1**)-(**G2**)-(**G3**) and where we recall that Π^0_p is the L^2 projector defined as in (2.18).

Lemma 3.2.4. *Under assumptions (**G0**)-(**G1**)-(**G2**)-(**G4**)-(**G5**)-(**G7**)-(**P1**), let $K \in L_j$, $j = 1, \dots, n$. Let f, the right-hand side of* (1.27)*, belong to space $\mathcal{B}^0_\beta(\Omega, \mathbf{0})$ and, consequently, u, the solution to problem* (1.27)*, belongs to $\mathcal{B}^2_\beta(\Omega, \mathbf{0})$, where we recall that Babuška spaces under consideration are defined in* (1.36)*, where we are assuming $1 - \alpha_{1,1} < \beta$, $\alpha_{1,1}$ being the singular exponent* (A.4) *associated with vertex $\mathbf{0}$. Assume moreover that if $K \in L_1$, then $p_K \approx 2$. Then, for all $1 \le s_K \le p_K$, there exists $u_I \in V(K)$ such that:*

$$|u - u_I|^2_{1,K} \lesssim \|f - \Pi^0_{p_K - 2} f\|^2_{0,K} + \sigma^{(n-j)(3-2\beta)} p_K^{-2\,s_K - 1} \left(\frac{\rho e}{2}\right)^{2\,s_K + 1} \sum_{s \in \mathcal{E}^K} |u|^2_{H^{s_K+1,2}_\beta(s)}, \tag{3.35}$$

where we recall that $\Pi^0_{p_K-2}$ is the $L^2(K)$ orthogonal projection from $V(K)$ into $\mathbb{P}_{p_K-2}(K)$ defined in (2.18)*, σ is the grading parameter of the mesh introduced in* (1.39)*, $\rho = \max\left(1, \frac{1-\sigma}{\sigma}\right)$ and where we recall that the $H^{s_K+1,2}_\beta(s)$ seminorm is defined in* (1.21)*.*

Proof. Before starting the proof, we observe that the boundary norm on the right-hand side of (3.35) exists, since $u \in \mathcal{B}^2_\beta(\Omega, \mathbf{0})$ implies that $u \in H^t(K)$ for all $t \in \mathbb{N}$ and polygons $K \notin L_0$.

We define u_I as the *weak* solution to the following problem:

$$\begin{cases} -\Delta u_I = \Pi^0_{p_K-2} f & \text{in } K, \\ u_I = \pi u & \text{on } \partial K, \end{cases} \tag{3.36}$$

where $\pi u \in \mathbb{B}(\partial K)$, see (3.4), is defined in the following way. Assume for the time being that $K \notin L_1$. Let $\widehat{I} = [-1, 1]$. Given an edge $s \subseteq \partial K$, πu is defined as the push-forward of a function $\widehat{\pi u} \in \mathbb{P}_{p_s}(\widehat{I})$ which we fix as follows. Given $\widehat{u}$ be the pull-back of $u|_s$ on $\widehat{I}$, $\widehat{\pi u}'$ is the Legendre expansion of $\widehat{u}$ up to order $p_s - 1$. In particular, we write:

$$\widehat{u}'(\xi) = \sum_{i=0}^{\infty} c_i L_i(\xi), \qquad \widehat{\pi u}'(\xi) = \sum_{i=0}^{p_s - 1} c_i L_i(\xi). \tag{3.37}$$

Here $\{L_i(\xi)\}_{i=0}^{\infty}$ is the $L^2(\widehat{I})$ orthogonal basis of Legendre polynomials, defined at the endpoints of $\widehat{I}$ as $L_i(-1) = (-1)^i$ and $L_i(1) = 1$. Next, we define $\widehat{\pi u}$ as:

$$\widehat{\pi u}(\xi) = \int_{-1}^{\xi} \widehat{\pi u}'(\eta) d\eta + \widehat{u}(-1).$$

It is possible to prove, by using the definition of $\widehat{\pi u}$ and the fundamental theorem of calculus, that $\widehat{\pi u}$ interpolates $\widehat{u}$ at the endpoints of $\widehat{I}$.

Recalling [96, Theorem 3.14] and using simple algebra, the following holds true:

$$\|\widehat{u} - \widehat{\pi u}\|_{\ell,\widehat{I}} \lesssim e^{s_K} p_s^{-s_K - 1 + \ell} |u|_{s_K+1,\widehat{I}}, \quad \ell = 0,\, 1, \quad \forall\, 1 \le s_K \le p_K. \tag{3.38}$$

Applying a scaling argument, interpolation theory [101, 102] and summing over all the edges, we get:

$$\|u-\pi u\|^2_{\frac{1}{2},\partial K} \lesssim \sum_{s\in\mathcal{E}^K} e^{2s_K+1}\left(\frac{h_s}{p_s}\right)^{2s_K+1}|u|^2_{s_K+1,s} \quad \forall\, 1\le s_K\le p_K. \tag{3.39}$$

If now $K\in L_1$, we define $\pi u|_s$ as above assuming s does not belong to the interface between L_0 and L_1, otherwise u_I is defined as the linear interpolant of u at the two endpoints of s. We point out that (3.39) remains valid also if $K\in L_1$ paying an additional constant c^{2s_K+1}, since $p_K\approx 2$ whenever $K\in L_1$. We also note that (3.39) implies, recalling from assumption (**P1**) that $p_s\approx p_K$ if $s\subseteq\partial K$ and following the ideas of [96, Lemma 3.39]:

$$\|u-u_I\|^2_{\frac{1}{2},\partial K}=\|u-\pi u\|^2_{\frac{1}{2},\partial K}\lesssim \sigma^{(n-j)(3-2\beta)}p_K^{-2s_K-1}\left(\frac{\rho\, e}{2}\right)^{2s_K+1}\sum_{s\in\mathcal{E}^K}|u|^2_{H^{s_K+1,2}_\beta(s)}, \tag{3.40}$$

where we recall that j denotes the number of the layer to which K belongs.

We are now ready to prove the error estimate. Recalling that $f-\Pi^0_{p_K-2}f$ has zero average over K, one has that (3.33) is valid. Choosing c_2 in (3.33) to be the average of $u-\pi u$ on ∂K and applying a Poincaré inequality yield:

$$\begin{aligned}|u-u_I|^2_{1,K}&\lesssim \left(|u-u_I|_{1,K}+\|f-\Pi^0_{p_K-2}f\|_{0,K}\right)\|u-\pi u-c_1\|_{\frac{1}{2},\partial K}+\|f-\Pi^0_{p_K-2}f\|_{0,K}|u-u_I|_{1,K}\\ &\lesssim |u-u_I|_{1,K}\left\{\|f-\Pi^0_{p_K-2}f\|_{0,K}+\|u-\pi u-c_1\|_{\frac{1}{2},\partial K}\right\}+\|f-\Pi^0_{p_K-2}f\|_{0,K}\|u-\pi u-c_1\|_{\frac{1}{2},\partial K}.\end{aligned}$$

where the hidden constant depends on the parameters ρ_0 and c introduced in assumptions (**G1**)-(**G2**)-(**G3**).

We deduce, picking c_1 to be the average of $u-u_I$ on ∂K and applying a Poincaré inequality:

$$|u-u_I|^2_{1,K}\lesssim \|f-\Pi^0_{p_K-2}f\|^2_{0,K}+\|u-\pi u\|^2_{\frac{1}{2},\partial K}.$$

In order to conclude, it suffices to apply (3.40). □

We turn now our attention to the approximation on the polygons abutting the singularity.

Lemma 3.2.5. *Let assumptions (**G0**)-(**G1**)-(**G2**)-(**G4**)-(**G5**)-(**G7**)-(**P1**) hold. Let f, the right-hand side of* (1.27)*, belong to space $\mathcal{B}^0_\beta(\Omega,\mathbf{0})$ and consequently u, the solution to problem* (1.27)*, belongs to $\mathcal{B}^2_\beta(\Omega,\mathbf{0})$, where we recall that the Babuška spaces under consideration are defined in* (1.36)*, with $1-\alpha_{1,1}<\beta$, $\alpha_{1,1}$ being the first singular exponent* (A.4) *associated with vertex* **0**. *Assume that $p_K=2$ if $K\in L_0$. Then there exists $u_I\in V(K)$ such that:*

$$|u-u_I|^2_{1,K}\lesssim \sigma^{2(1-\beta)n}\||\mathbf{x}|^\beta D^2u\|^2_{0,K}+\|f-\Pi^0_{p_K-2}f\|^2_{0,K}.$$

where we recall that $\Pi^0_{p_K-2}$ is the $L^2(K)$ orthogonal projection from $V(K)$ into $\mathbb{P}_{p_K-2}(K)$ defined in (2.18)*, σ is the grading parameter of the mesh introduced in* (1.39) *and $n+1$ is the number of layers.*

Proof. We consider u_I defined as in (3.36); in particular, we fix πu, the trace of u_I on ∂K to be the piecewise affine interpolant of u at the vertices of K. Arguing as in Lemma 3.2.4, we have:

$$|u-u_I|^2_{1,K}\lesssim \|f-\Pi^0_{p_K-2}f\|^2_{0,K}+\|u-u_I-c_1\|^2_{\frac{1}{2},\partial K}, \tag{3.41}$$

where c_1 is the average of $u-u_I$ on $\partial K$and where the hidden constant in (3.41) depends solely on the parameters ρ_0 and c introduced in assumptions (**G1**)-(**G2**)-(**G3**).

In order to get the claim, it suffices to bound the second term. As in Lemma 3.2.2, we consider the subtriangulation $\widetilde{\mathcal{T}}_n=\widetilde{\mathcal{T}}_n(K)$ of K obtained by connecting all the vertices of K to **0**, see assumption (**G7**). In particular, every triangle $T\in\widetilde{\mathcal{T}}_n$ is star-shaped with respect to a ball of radius $\ge\widetilde{\gamma}h_T$, where $\widetilde{\gamma}$ is a positive universal constant. We define $\widetilde{u}_K$ as the piecewise linear interpolant polynomials over the triangular subtriangulation, interpolating u at the vertices of T,

for every $T \in \widetilde{\mathcal{T}}_n$. Using [96, Lemma 4.16], arguing similarly to what done in Lemma 3.2.3 and applying a Poincaré inequality, yield:

$$\begin{aligned}&\|u - u_I - c_1\|^2_{\frac{1}{2},\partial K}\\ &\lesssim \|u - \widetilde{u}_K - c_1\|^2_{1,K} \lesssim \sum_{T\in\widetilde{\mathcal{T}}_n} |u - \widetilde{u}_K|^2_{1,T} \lesssim \sum_{T\in\widetilde{\mathcal{T}}_n} h_T^{2(1-\beta)} \||\mathbf{x}|^\beta D^2 u\|^2_{0,T} \lesssim \sigma^{2(1-\beta)} \||\mathbf{x}|^\beta D^2 u\|^2_{0,K},\end{aligned} \tag{3.42}$$

where, again, the hidden constant in (3.42) depends solely on the parameters ρ_0 and c introduced in assumptions (**G1**)-(**G2**)-(**G3**). We stress that the third inequality in (3.42) holds since $\widetilde{u}_K|_T$ is a linear polynomial and therefore $D^2\widetilde{u}_K = 0$ on all $T \in \widetilde{\mathcal{T}}_n$. □

We note that in Lemmata 3.2.4 and 3.2.5 the error between f and its L^2 projection can be bounded using Lemmata 3.2.6 and 3.2.7 in the next section.

We also point out that the hypothesis concerning the distribution of the local degrees of accuracy, i.e. the fact that $p_K = 2$ if $K \in L_0$ and assumption (**P1**), are in accordance with the forthcoming definition (3.45) that we will introduce for the proof of Theorem 3.2.8. Finally, we point out in Lemmata 3.2.4 and 3.2.5 we introduced a function u_I which is locally in $V(K)$ and globally continuous; thus, u_I is a function in the global Virtual Element Space V_n introduced in (3.7).

3.2.3 Local approximation of the oscillation of the right-hand side

Here, we deal with the approximation of the third local terms on the right-hand side of (3.20).

Since we are approximating it with piecewise polynomials of local degree p_K-2, we set $\overline{\mathbf{p}} = \mathbf{p}-2$, i.e. for all $K \in \mathcal{T}_n$, $\overline{p}_K = p_K - 2$. where we recall that we are assuming for the sake of simplicity $p_K \geq 2$ for all $K \in \mathcal{T}_n$, see (3.3).

As in Section 3.2.1, we develop a different analysis for polygons near and far from the singularity. We start with the "far" case.

Lemma 3.2.6. *Under assumptions (**G0**)-(**G1**)-(**G2**)-(**G4**)-(**G5**)-(**G7**), let $K \in L_j$, $j = 1, \dots, n$. Let $Q(K)$ be defined in (**G7**) and let $f \in H^{\overline{s}_K+3,2}_\beta(Q(K))$, $0 \leq \overline{s}_K \leq \overline{p}_K$, with $\overline{p}_K = p_K - 2$. Then, for all $v_n \in V(K)$ defined in* (3.5)*:*

$$F_K(v_n) \leq |v_n|_{1,K} \left\{ \sigma^{(n-j)(2-\beta)} \left(\frac{\Gamma(\overline{p}_K - \overline{s}_K + 1)}{\Gamma(\overline{p}_K + \overline{s}_K + 1)} \right)^{\frac{1}{2}} \left(\frac{\rho}{2}\right)^{\overline{s}_K} |f|_{H^{\overline{s}_K+3,2}_\beta(Q(K))} \right\},$$

where we are employing the same notation of Lemma 3.2.1.

Proof. It suffices to use a Cauchy-Schwarz inequality in (3.18), standard bounds for the projection errors and analogous estimate to those in Lemma 3.2.1. □

Assume now that K is an element in the finest level L_0. We work here a bit differently from what we did in Lemma 3.2.2. In particular we get the following.

Lemma 3.2.7. *Under assumptions (**G0**)-(**G1**)-(**G2**)-(**G4**)-(**G5**)-(**G7**), let $K \in L_0$. Assume $f \in L^2(K)$. Let $\beta \in [0, 1)$. Then:*

$$F_K(v_n) \leq h_K^{1-\beta} |v_n|_{1,K} \|f\|_{0,K} \lesssim \sigma^{n(1-\beta)} |v_n|_{1,K}, \quad \forall\, v_n \in V(K),$$

where σ is the grading parameter of the mesh introduced in (1.39) *and where $FE(v_n)$ is defined in* (3.18)*.*

Proof. Using a Cauchy-Schwarz inequality and Bramble-Hilbert lemma we obtain:

$$F_K(v_n) \lesssim h_K |v_n|_{1,K} \|f\|_{0,K} \leq h_K^{1-\beta} |v_n|_{1,K} \|f\|_{0,K} \lesssim \sigma^{n(1-\beta)} |v_n|_{1,K} \qquad \forall\, v_n \in V(K).$$

□

We point out that for the proof of Lemmata 3.2.2 and 3.2.7 we work directly on the polygon without the need of using the covering squares technique of assumption (**G7**), like in Lemmata 3.2.1 and 3.2.6. This justifies the fact that in assumption (**G7**) we did not require the existence of a collection of squares $\mathcal{C}_n^0$ associated with the finest layer L_0 but only the existence of collection $\mathcal{C}_1^n$ associated with all the other layers.

3.2.4 Exponential convergence

We set:

$$\Omega^{ext} = \cup_{n\in\mathbb{N}}\Omega_n^{ext} = \Omega_1^{ext}, \tag{3.43}$$

where the extended domains Ω_n^{ext} are introduced in (**G7**). We recall that we are assuming that $\mathbf{0} \in \partial\Omega^{ext}$.

We observe that our error analysis needs regularity on f and subsequently on u, the right-hand side and the solution to problem (1.27), respectively. In particular, we will require:

$$f \text{ can be extended to a function in } \mathcal{B}_\beta^0\left(\Omega^{ext}, \mathbf{0}\right), \quad u \text{ can be extended to a function in } \mathcal{B}_\beta^2\left(\Omega^{ext}, \mathbf{0}\right), \tag{3.44}$$

where the modified Babuška spaces are defined in (1.36).

With a little abuse of notation we will call this two functions f and u. In the classical *hp* finite element method, this regularity leads to exponential convergence of the energy error, see e.g. [96]. In order to prove the same exponential convergence with *hp* VEM, we need (3.44) since the approximation by means of polynomials on the polygons not abutting the singularity needs regularity of the target function on a square containing the polygon, see Lemmata 3.2.1 and 3.2.6.

We recall the enlarged domain Ω^{ext} has been built in such a way that the singularity at $\mathbf{0}$ is never at the interior of Ω^{ext}, see assumption (**G7**). We highlight also the fact that (3.44) can be easily generalized to the case of multiple singularities, see e.g. [96].

In order to obtain exponential convergence of the energy error in terms of the number of degrees of freedom, we will henceforth assume that the vector $\mathbf{p}$ of the degrees of accuracy associated with $\mathcal{T}_n$ is given by:

$$\mathbf{p}_K = \begin{cases} 2 & \text{if } K \in L_0, \\ \max\left(2, \lceil \mu \cdot (j+1) \rceil\right) & \text{if } K \in L_j,\ j \geq 1, \end{cases} \tag{3.45}$$

where μ is a positive constant which will be determined in the proof of Theorem 3.2.8 and where $\lceil\cdot\rceil$ is the ceiling function. This is in accordance with previous Lemmata 3.2.4 and 3.2.5. For instance, if we pick in (3.45) $\mu = 1$, we have a distribution of local degree of accuracy as in Figure 3.4.

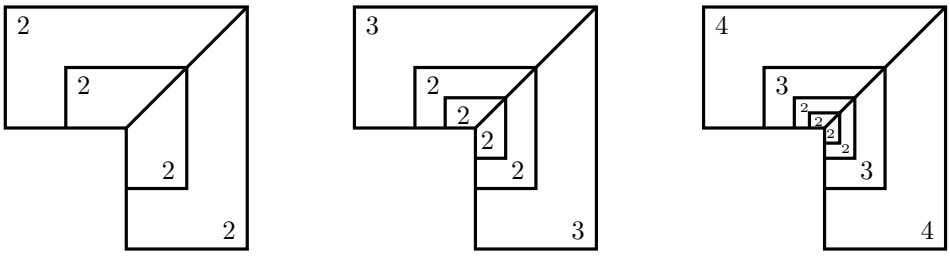

Figure 3.4: Example of distribution of local degrees of accuracy, picking $\mu = 1$ in (3.45).

It is clear from (3.45) that if K_1 and K_2 belong to the j-th and the $(j+1)$-th layers respectively, for some $j = 1, \ldots, n-1$, then $p_{K_1} \approx p_{K_2}$, independently of all the other discretization parameters. Thus, owing to requirement (3.12), we also have $\alpha(p_{K_1}) \approx \alpha(p_{K_2})$, independently of all the other discretization parameters. Besides, $p_s \approx p_K$ whenever $s \subseteq \partial K$.

We are now ready to prove the main result of the chapter, namely exponential convergence of the method in terms of the number of the number of degrees of freedom.

Theorem 3.2.8. *Under assumptions (**A_n1**)-(**A_n2**)-(**G0**)-(**G1**)-(**G2**)-(**G4**)-(**G5**)-(**G7**)-(**P1**), let u and u_n be the solutions to problems* (1.27) *and* (3.17) *respectively and let f be the right-hand*

side of problem (1.27). *Assume that* u *and* f *satisfy* (3.44). *Given* $N = N(n) = \dim(V_n)$, *there exists* $\mu > 0$ *such that* $\mathbf{p}$, *defined in* (3.45), *guarantees the following exponential convergence of the* H^1 *error of the method in terms of the number of degrees of freedom:*

$$\|u - u_n\|_{1,\Omega} \lesssim \exp(-b\sqrt[3]{N}), \tag{3.46}$$

with b *a constant independent of the discretization parameters.*

Proof. It suffices to combine Lemma 3.1.1, Lemmata from 3.2.1 to 3.2.7, assumption (3.12) and to use the same arguments of [96, Theorem 4.51], properly choosing the parameter μ.

The basic idea behind the proof is that around the singularity, geometric mesh refinement are employed, since p approximation leads only to an algebraic decay of the error; on the other hand, on polygons far from the singularity, it suffices to increase the degree of accuracy, since on such polygons both the loading term and the exact solution to (1.27) are assumed to belong to the Babuška spaces $\mathcal{B}^2_{\boldsymbol{\beta}}(\Omega^{ext}, \mathbf{0})$ and $\mathcal{B}^2_{\boldsymbol{\beta}}(\Omega^{ext}, \mathbf{0})$ defined in (1.22) respectively and therefore p approximation leads to exponential convergence of the local errors, see Theorem 2.3.6.

Following [96, Theorem 4.51] and using Lemma 3.1.1 yield:

$$|u - u_n|_{1,\Omega} \leq c \max_{K' \in \mathcal{T}_n} \alpha(K') \sigma^{2(1-\beta)(n+1)}, \tag{3.47}$$

where c is a constant independent of both the discretizations parameters and the number of layers. Applying (3.12), we obtain:

$$\alpha(K) \lesssim p_K^{r_1} \max_{K' \in \mathcal{T}_n} p_{K'}^{r_2} \lesssim (n+1)^{r_1 + r_2}, \quad \forall K \in \mathcal{T}_n, \tag{3.48}$$

where we recall $n+1$ denotes the number of layers and r_1 and r_2 are the two positive universal constants introduced in (3.12). Plugging (3.48) in (3.47), we get:

$$|u - u_n|_{1,\Omega} \leq (n+1)^{r_1 + r_2} \sigma^{2(1-\beta)(n+1)}.$$

We infer:

$$|u - u_n|_{1,\Omega} \lesssim \exp(-b(n+1)), \quad \text{for some } b > 0.$$

Now, we prove that $N \lesssim (n+1)^3$. To this purpose, we proceed as follows. In each layer there exists a fixed maximum number of elements; this follows from the geometric assumptions (**G1**)-(**G3**), applying for instance the arguments in [72, Section 4]. Using geometric assumption (**G2**), which guarantees a maximum number of edges per each element, the definition of the local VE space $V(K)$ in (3.5) and the distribution of the local degrees of accuracy (3.45), it is straightforward to note that $\forall\, K \in \mathcal{T}_n$ the dimension of each local space $V(K)$ is proportional to p_K^2, with $p_K^2 \approx \ell^2$ for $K \in L_\ell$.

Recalling again (3.45), we can now compute a bound for the dimension of the local space, viz. the number of the degrees of freedom:

$$N \lesssim \sum_{\ell=0}^{n} \ell^2 \leq L \max_{\ell=0}^{n} \ell^2 = n^3,$$

where we stress that we are using that in each layer there is a fixed maximum number of elements.

The result follows from Poincaré inequality. □

In order to conclude this chapter, we highlight two issues:

- the assumption (3.12), which plays a fundamental role in the proof of Theorem 3.2.8, is in fact valid choosing the stabilization (6.8);
- Theorem 3.2.8 is validated by numerical tests in Section 7.2.

Chapter 4

The harmonic virtual element method and its hp version on geometrically graded meshes

In this chapter, we do not consider any more Poisson problem (1.27), but rather a Laplace problem (1.29) with *nonhomogeneous* Dirichlet boundary condition g.

The reason for considering this problem is twofold. The first reason is that we provide a method which is extremely efficient in approximating Laplace problems; to the best of our knowledge, this is the first H^1 conforming Trefftz method for Laplace equation available in the literature and guaranteeing convergence faster than the one in Theorem 3.2.8. The second is that the approach that we show here paves the way for building novel methods approximating more appealing problems, e.g. Helmholtz equation.

This is not of course the first attempt to approximate efficiently a Laplace problem with methods based on approximation spaces having small dimension. Among the other methods available, we limit ourselves to recall only two of them.

The first one is the boundary element method (BEM), see e.g. [93]. BE spaces consist of functions defined *only* on the boundary of the computational domain. Clearly, the BE space on a boundary mesh of characteristic meshsize h contains many less degrees of freedom than the corresponding FE space on a volume mesh having the same characteristic meshsize h. This comes at a price of a fully populated matrix in the resulting system of linear equations, expensive quadrature rules needed for evaluation of matrix entries, and expensive numerical reconstruction of the solution in the interior of the computational domain. These difficulties can be partially alleviated by using advanced *fast boundary element methods* (see e.g. [93] and references therein), that usually results in complex algorithms that are not easy to implement.

A second (and more recent) approach is given by the so-called Trefftz Discontinuous Galerkin FEM (TDG-FEM), which was introduced in [75, 76] and was generalized to its hp version in [72]. TDG-FEM spaces consist of piecewise harmonic polynomials over a decomposition of the computational domain into triangles and quadrilaterals. As a consequence, the resulting method has a DG structure, since the dimension of harmonic polynomial spaces is not large enough for enforcing global continuity of the discretization space. We also point out that in [72] it was provided a result concerning hp approximation of harmonic functions by means of harmonic polynomials, following the ideas of the pioneering works [81, 85].

The advantage of TDG-FEM with respect to standard FEM is that the dimension of local spaces considerably reduces still keeping the optimal rate of convergence of the error. More precisely, for a fixed local polynomial degree p, the dimension of the local TDG-FEM space is equal to $2p+1 \approx 2p$, whereas the dimension of local FEM spaces is $\frac{(p+1)(p+2)}{2} \approx \frac{p^2}{2}$. This advantage is possible since the degrees of freedom that are removed in TDG-FEM are superfluous for the approximation of a Laplace equation. We emphasize that employing piecewise harmonic polynomials leads inevitably to a discontinuous method, which is therefore not anymore H^1-conforming, even on triangular meshes. The approach in [72] can be generalized easily to polygonal TDG-FEM, following e.g. [8].

In this chapter, we focus on the numerical approximation of the Laplace problem following the VEM approach employed for the approximation of Poisson problem introduced in Chapters 2 and 3, mimicking at the same time to mimic the "harmonic" approach of TDG-FEM.

The arising method, which goes by the name of Harmonic VEM, makes use only of local *boundary* degrees of freedom (the internal degrees of freedom of the standard VEM can be ommitted). More precisely, functions in the Harmonic VEM space are harmonic reconstructions of piecewise continuous polynomial traces over the boundary of the polygons in the polygonal decomposition of the computational domain. It is immediate to check that the associated space contains (globally discontinuous) piecewise harmonic polynomials.

We underline that, differently from what done in Chapter 3, we define a space with uniform local degrees of accuracy. This choice allows to avoid additional technicalities in the approximation estimates. It is worth to stress that adopting properly-chosen nonuniform degree of accuracy distributions gives actually numerical results that are comparable with those performed using uniform distributions, see numerical tests in Section 7.3.

As typically done in standard VEM, the stiffness matrix is not computed exactly on the Harmonic VEM space. Its construction is based on two ingredients: a local energy projector on the space of harmonic polynomials and a stabilizing bilinear form, which only approximates the continuous one but which is computable on the complete space.

The main result of this chapter states that, similarly to the *hp* version of TDG-FEM, the asymptotic convergence rate for the energy error is proportional to $\exp(-b\sqrt[2]{N})$, where N is the dimension of the global discretization space. This result is an improvement of the analogous statement in the framework of the *hp* FEM, see [96], and *hp* VEM, see Theorem 3.2.8, where the rate of decay of the error is proportional to $\exp(-b\sqrt[3]{N})$.

We state the difference between the two approaches, namely the TDG-FEM [72] and the Harmonic VEM. The *hp* TDG-FEM is a nonH^1-conforming method, but local spaces are made of explicitly known functions, i.e. (harmonic) polynomials; besides, only *internal* degrees of freedom on each element are considered. The *hp* Harmonic VEM is a H^1-conforming method which only employs *boundary* degrees of freedom; the basis functions are not known explicitly, but the stiffness matrix can be built efficiently employing only the degrees of freedom. Importantly, both methods are characterized by the fact that harmonic polynomials are locally contained in both the approximation spaces; in fact, the TDG-FEM space *is* the space of (globally discontinuous) piecewise harmonic polynomials.

Throughout the chapter, we *only* investigate the *hp* version of Harmonic VEM, that is the method of choice for an efficient approximation of corner singularities. A modification of Section 4.2, along with the arguments in [85], leads to h approximation results. For the p version of Harmonic VEM (when the mesh is kept fixed), instead, one has to deal with some issues that lie outside the scope of the present thesis; just to mention one of them, the p approximation estimates by harmonic functions depend on the shape of the domain of approximation via the so called "*exterior cone condition*", see [19, Theorem 2]. These matters introduce additional technicalities which will not be addressed in this chapter.

We assume that the Dirichlet datum g of problem (1.29) belongs to space $\mathcal{B}^{\frac{3}{2}}_{\boldsymbol{\beta}}(\partial\Omega)$, with $1-\alpha_{i,1}<\beta_i$ for all $i=1,\dots,N_\Omega$ where the singular exponents $\alpha_{i,j}$ ($i=1,\dots,N_\Omega$, $j\in\mathbb{N}$) are defined in (A.4). As a consequence, Theorem A.0.4 guarantees that u, the solution to problem (1.27), belongs to space $\mathcal{B}^2_{\boldsymbol{\beta}}(\Omega)$.

Besides, we assume that the sequences of polygonal decompositions $\{\mathcal{T}_n\}_{n\in\mathbb{N}}$ satisfy assumptions (**G0**)-(**G1**)-(**G2**)-(**G4**)-(**G5**), that is we consider geometric meshes refined towards a single vertex only, namely $\mathbf{0}$.

In addition, we also assume that u and g, the solution and the Dirichlet datum of problem (1.29) respectively, belong to modified Babuška spaces $\mathcal{B}^2_\beta(\Omega,\mathbf{0})$ and $\mathcal{B}^{\frac{3}{2}}_\beta(\partial\Omega,\mathbf{0})$ where $\mathcal{B}^2_\beta(\Omega,\mathbf{0})$ is defined in (1.36) whereas $\mathcal{B}^{\frac{3}{2}}_\beta(\partial\Omega,\mathbf{0})$ is the set of traces of functions in $\mathcal{B}^2_\beta(\Omega,\mathbf{0})$. Here, we assume that $1-\alpha_{1,1}<\beta$, with $\alpha_{1,1}$ being the first singular exponent (A.4) associated with vertex $\mathbf{0}$.

As observed already in Chapter 3, all what is going to be proven in this chapter holds true also in the case of "multiple" singularities, but we prefer to stick for simplicity to the case of a single singularity.

The outline of the chapter follows. In Section 4.1, we build the Harmonic VEM, whereas, in Section 4.2, we prove exponential convergence in terms of the total number of degrees of freedom and, under proper assumptions on the stabilization of the method, we prove that at the theoretical level there is no pollution effect due to this stabilization.

The topics covered in this chapter are contained in [58].

4.1 Harmonic Virtual Elements with nonuniform degree of accuracy

In this section, we introduce the Harmonic VEM for the approximation of Laplace problem (1.29).

Recall that we are given sequences of polygonal decompositions $\{\mathcal{T}_n\}_{n\in\mathbb{N}}$ satisfying assumptions (**G0**)-(**G1**)-(**G2**)-(**G4**)-(**G5**).

As usual, we begin by defining the local Harmonic VE spaces. Given $p \in \mathbb{N}$ and given the space of piecewise continuous polynomials of degree p over the boundary of K:

$$\mathbb{B}_p(\partial K) := \left\{ v_n \in \mathcal{C}^0(\partial K) \mid v_n|_s \in \mathbb{P}_p(s) \text{ for all } s \text{ edge of } K \right\}, \tag{4.1}$$

we set the local Harmonic VE spaces as:

$$V^{\Delta}(K) := \left\{ v_n \in H^1(K) \mid \Delta v_n = 0,\, v_n|_{\partial K} \in \mathbb{B}(\partial K) \right\}. \tag{4.2}$$

The functions in $V^{\Delta}(K)$ are then the solutions to Laplace problems with piecewise polynomial Dirichlet data; therefore, they are not known explicitly in a closed-form.

Let us consider the following set of linear functionals on $V^{\Delta}(K)$. Given $v_n \in V^{\Delta}(K)$:

- the values of v_n at the vertices of K;
- the values of v_n at $p-1$ internal Gauß-Lobatto nodes on each s, edge of K.

This is a set of degrees of freedom, since (i) the dimension of $V^{\Delta}(K)$ is equal to the number of functionals defined above and (ii) such functionals are uninsolvent, owing to the fact that weak harmonic functions that vanish on ∂K, vanish also in the interior of K. Thus, the dimension of space $V^{\Delta}(K)$ is finite and is equal to

$$\dim(V^{\Delta}(K)) = p\, N_K, \tag{4.3}$$

where we recall that N_K is the number of vertices (and therefore edges) of K.

We define the global Harmonic Virtual Element space:

$$V_n^{\Delta} := \left\{ v_n \in \mathcal{C}^0(\overline{\Omega}) \mid v_n|_K \in V^{\Delta}(K),\, \forall\, K \in \mathcal{T}_n \right\}, \tag{4.4}$$

its subspace having vanishing boundary trace:

$$V_{n,0}^{\Delta} := \{ v_n \in V_n \mid v_n|_{\partial\Omega} = 0 \} \tag{4.5}$$

and its affine subspace containing interpolated essential boundary conditions:

$$V_{n,g}^{\Delta} := \{ v_n \in V_n \mid v_n|_s = g_{GL}^s \text{ for all } s \text{ edge on the } \partial\Omega \}. \tag{4.6}$$

Here, g_{GL}^s is the Gauß-Lobatto interpolant of degree p of g on edge s. We remark that g_{GL}^s is well defined, since $g \in \mathcal{B}_{\beta}^{\frac{3}{2}}(\Omega)$, which implies $g \in \mathcal{C}^0(\overline{\Omega})$, see [96, Proposition 4.3].

The choice of Gauß-Lobatto interpolation on the boundary of the computational domain is not a matter of taste, but will play a role in approximation estimates by functions in the Harmonic VE space, see Section 4.2.3

For what concerns the construction of the global bilinear form, we follow the guidelines of Chapters 2 and 3, and we decompose it into a sum of local contributions:

$$a_{\Delta}(u_n, v_n) = \sum_{K\in\mathcal{T}_n} a_{\Delta}^K(u_n, v_n) \qquad \forall\, u_n,\, v_n \in V_n^{\Delta}, \tag{4.7}$$

where we split the local discrete bilinear forms as usual:

$$a_\Delta^K(u_n, v_n) = a^K(\Pi_p^{\nabla,\Delta,K} u_n, \Pi_p^{\nabla,\Delta,K} v_n) + S_\Delta^K((I - \Pi_p^{\nabla,\Delta,K})u_n, (I - \Pi_p^{\nabla,\Delta,K})v_n) \quad \forall\, u_n,\, v_n \in V^\Delta(K) \tag{4.8}$$

Here, we have employed a computable stabilizing bilinear form

$$S_\Delta^K : \ker(\Pi_p^{\nabla,\Delta,K}) \times \ker(\Pi_p^{\nabla,\Delta,K}) \to \mathbb{R}$$

and an energy projector

$$\Pi_p^{\nabla,\Delta,K} : V^\Delta(K) \to \mathbb{H}_p(K),$$

defined by:

$$\begin{cases} a^K(q_{p,\Delta}, v_n - \Pi_p^{\nabla,\Delta,K} v_n) = 0 \\ \int_{\partial K} v_n - \Pi_p^{\nabla,\Delta,K} v_n = 0 \end{cases} \qquad \forall\, q_{p,\Delta} \in \mathbb{H}_p(K), \quad \forall\, v_n \in V^\Delta(K), \tag{4.9}$$

where we recall that $\mathbb{H}_p(K)$ is the space of harmonic polynomials over K. When no confusion occurs, we write $\Pi_p^{\nabla,\Delta}$ in lieu of $\Pi_p^{\nabla,\Delta,K}$.

We observe that projection $\Pi_p^{\nabla,\Delta}$ can be computed by means of the dofs of space $V^\Delta(K)$. In fact, it suffices to apply an integration by parts to get:

$$\int_K \nabla q_{p,\Delta} \cdot \nabla v_n = \int_{\partial K} (\partial_{\mathbf{n}} q_{p,\Delta})\, v_n \qquad \forall\, q_{p,\Delta} \in \mathbb{H}_p(K), \quad \forall\, v_n \in V^\Delta(K),$$

where we used that $q_{p,\Delta}$ is a harmonic polynomial and therefore the bulk term obtained by the integration by parts disappears. In order to conclude, it suffices to note that both v_n and $\partial_{\mathbf{n}} q_{p,\Delta}$ are explicitly known on ∂K.

As done in Chapter 3, we demand the following property on the stabilization S_Δ^K:

$$c_*(p)|v_n|_{1,K}^2 \le S_\Delta^K(v_n, v_n) \le c^*(p)|v_n|_{1,K}^2 \qquad \forall\, v_n \in V^\Delta(K), \tag{4.10}$$

with:

$$c_*(p) = c\, p^{-r_3}, \qquad c^*(p) = c\, p^{r_4} \tag{4.11}$$

for some universal positive constants c, r_3 and r_4.

In Section 6.3, we exhibit explicit choices for S^K satisfying (4.11) with explicit expressions for r_3 and r_4. Having such behaviour of the stability constants gives us the possibility of showing exponential convergence of the method in Theorem 4.2.6.

It can be proven that the local discrete bilinear forms a_Δ^K satisfy the two following properties:

($\mathbf{A}^\Delta\mathbf{1}$) **local harmonic polynomial consistency**: for all $K \in \mathcal{T}_n$, it must hold:

$$a^K(q_{p,\Delta}, v_n) = a_\Delta^K(q_{p,\Delta}, v_n) \qquad \forall\, q_{p,\Delta} \in \mathbb{H}_p(K),\ \forall\, v_n \in V^\Delta(K), \tag{4.12}$$

where we recall that $\mathbb{H}_p(K)$ is the space of harmonic polynomials of degree p over K;

($\mathbf{A}^\Delta\mathbf{2}$) **local stability**: for all $K \in \mathcal{T}_n$, it must hold:

$$\alpha_*(p)|v_n|_{1,K}^2 \le a_\Delta^K(v_n, v_n) \le \alpha^*(p)|v_n|_{1,K}^2 \quad \forall\, v_n \in V^\Delta(K), \tag{4.13}$$

where $\alpha_*(p) = \min(1, c\, p^{-r_3})$ and $\alpha^*(p) = \max(1, c\, p^{r_4})$.

We are now able to introduce the Harmonic VEM:

$$\begin{cases} \text{find } u_n \in V_{n,g}^\Delta \text{ such that} \\ a_\Delta(u_n, v_n) = 0 \quad \forall\, v_n \in V_{n,0}^\Delta \end{cases}. \tag{4.14}$$

Having set:

$$\alpha_\Delta(p) := \frac{\alpha^*(p)}{\alpha_*(p)}, \tag{4.15}$$

where $\alpha_*(p)$ and $\alpha^*(p)$ are introduced in (4.13), we prove the following abstract error analysis result which traces Lemmata 2.1.1 and 3.1.1.

Lemma 4.1.1. *Under assumptions (**A**$^{\Delta}$**1**) and (**A**$^{\Delta}$**2**), let u and u_n be the solutions to problems* (1.29) *and* (4.14) *respectively. Then, there holds:*

$$|u-u_n|_{1,\Omega} \leq \alpha_{\Delta}(p)\{|u-u_\pi|_{1,\mathcal{T}_n} + |u-u_I|_{1,\Omega}\} \qquad \forall\, u_\pi \in \mathcal{S}_{\Delta}^{p,-1}(\Omega,\mathcal{T}_n), \quad \forall\, u_I \in V_{n,g}^{\Delta}, \quad (4.16)$$

where we recall that $\mathcal{S}_{\Delta}^{p,-1}(\Omega,\mathcal{T}_n)$ is defined in (1.44)*, whereas $\alpha_{\Delta}(p)$ is defined in* (4.15)*.*

Proof. For any $u_\pi \in \mathcal{S}_{\Delta}^{p,-1}(\Omega,\mathcal{T}_n)$ and $u_I \in V_{n,g}^{\Delta}$ we have, owing to assumptions (**A**$^{\Delta}$**1**) and (**A**$^{\Delta}$**2**) and formulations (1.29) and (4.14):

$$\begin{aligned}
|u_I-u_n|_{1,\Omega}^2 &= \sum_{K\in\mathcal{T}_n} |u_I-u_n|_{1,K}^2 \leq \sum_{K\in\mathcal{T}_n} \alpha_*^{-1}(p)\left\{a_{\Delta}^K(u_I,u_I-u_n) - a_{\Delta}^K(u_n,u_I-u_n)\right\}\\
&= \alpha_*^{-1}(p)\sum_{K\in\mathcal{T}_n}\left\{a_{\Delta}^K(u_I-u_\pi,u_I-u_n) + a_{\Delta}^K(u_\pi,u_I-u_n)\right\}\\
&= \alpha_*^{-1}(p)\sum_{K\in\mathcal{T}_n}\left\{a_{\Delta}^K(u_I-u_\pi,u_I-u_n) + a^K(u_\pi-u,u_I-u_n)\right\}\\
&\leq \alpha_*^{-1}(p)\sum_{K\in\mathcal{T}_n}\left\{(1+\alpha^*(p))|u-u_\pi|_{1,K}|u_I-u_n|_{1,K} + \alpha^*(p)|u-u_I|_{1,K}|u_I-u_n|_{1,K}\right\}.
\end{aligned}$$

The claim follows from simple algebra. □

Lemma 4.1.1 states that, up to the pollution factor $\alpha_{\Delta}(p)$ defined in (4.15) due to the presence of the stabilization, the error of the method is bounded by the sum of two terms:

- a best error term with respect to piecewise discontinuous *harmonic* polynomials of degree p;
- a best error term with respect to functions in the global VE spaces $V_{n,g}^{\Delta}$ defined in (4.6). Importantly, this term is the one which take into account the approximation of the boundary datum.

The forthcoming section, is devoted to estimate these two terms. Thanks to (4.11), we prove exponential convergence of the method in terms of the total number of degrees of freedom without the pollution effect due to the stabilization.

4.2 Exponential convergence with *hp* Harmonic VEM

In this section, we study the convergence of method (4.14) assuming that u, the solution to problem (1.29) belongs to space $\mathcal{B}_{\beta}^2(\Omega,\mathbf{0})$ defined in (1.36), with $1-\alpha_{1,1}<\beta$, $\alpha_{1,1}$ being the first singular exponent (A.4) associated with vertex $\mathbf{0}$. In particular, u has the natural regularity that one would expect when solving a Poisson problem on a polygonal domain, see Theorem A.0.4.

Here, we do not demand additional regularity on the sequences of meshes $\{\mathcal{T}_n\}_{n\in\mathbb{N}}$ as done instead in Section 4.1 for standard *hp* VEM, see assumption (**G7**). We limit ourselves to recall that we are employing sequences of meshes geometrically refined toward vertex $\mathbf{0}$. We only ask here the following:

(**G8**) the shape regularity constant ρ_0 introduced in assumptions (**G1**)-(**G2**) is such that $\rho_0 \in \left(0,\frac{1}{2}\right)$; moreover, for all $K\in\mathcal{T}_n$ abutting $\mathbf{0}$, it is possible to construct a subtriangulation $\widetilde{\mathcal{T}}_n = \widetilde{\mathcal{T}}_n(K)$ by joining the vertices of K to $\mathbf{0}$ is made of triangles that are star-shaped with respect to a ball of radius greater than or equal to $\rho_0 h_T$, h_T being $\mathrm{diam}(T)$ for all $T\in\widetilde{\mathcal{T}}_n$. For all $T\in\widetilde{\mathcal{T}}_n(K)$, it holds $h_K \approx h_T$.

The remainder of this section is organized as follows. In Section 4.2.1, we state some regularity results concerning functions in Babuška spaces. In Sections 4.2.2 and 4.2.3, we estimate the local contributions of the two terms appearing on the right-hand side of (4.16). Finally, in Section 4.2.4, we prove exponential convergence of the method in terms of the total number of degrees of freedom; here, thanks to (4.11), it is possible to get rid of the pollution effect of the stabilization.

4.2.1 Issues concerning the regularity of the solution

Assume that $u \in \mathcal{B}^2_\beta(\Omega)$ defined in (1.36). Then, owing to [17, Theorem 2.2], one also has $u \in \mathcal{O}^2_\beta(\Omega)$. In particular, it holds that for every $\boldsymbol{\alpha} \in \mathbb{N}^2$, $|\boldsymbol{\alpha}| = k \geq 1$, $k \in \mathbb{N}$, it holds that:

$$|D^{\boldsymbol{\alpha}} u(\mathbf{x}_0)| \leq \left|D^k u(\mathbf{x}_0)\right| \leq c_u \frac{d_u^{|\boldsymbol{\alpha}|}}{\Phi_k(\mathbf{x}_0)} |\boldsymbol{\alpha}|! \qquad \forall\, \mathbf{x}_0 \in \overline{\Omega}, \tag{4.17}$$

since $\beta - 1 \in [-1, 0)$.

As a consequence, any function in $\mathcal{O}^2_\beta(\Omega)$ admits an analytic continuation on:

$$\mathcal{N}(u) := \bigcup_{\mathbf{x}_0 \in \overline{\Omega};\, \mathbf{x}_0 \neq \mathbf{0}} \left\{ \mathbf{x} \in \mathbb{R}^2 \,\middle|\, |\mathbf{x} - \mathbf{x}_0| < c \frac{\Phi(\mathbf{x}_0)}{d_u},\ \forall\, c \in \left(0, \frac{1}{2}\right) \right\}. \tag{4.18}$$

In order to see this, it suffices to show that the Taylor series:

$$\sum_{\boldsymbol{\alpha} \in \mathbb{N}^2} \frac{D^{\boldsymbol{\alpha}} u(\mathbf{x}_0)}{\boldsymbol{\alpha}!} (\mathbf{x} - \mathbf{x}_0)^{\boldsymbol{\alpha}}, \quad \mathbf{x}_0 \in \overline{\Omega}, \quad \mathbf{x}_0 \neq \mathbf{0}, \tag{4.19}$$

converges uniformly in $\mathcal{N}(u)$.

In particular, we prove that it converges uniformly in the ball $B\left(\mathbf{x}_0, c\frac{\Phi(\mathbf{x}_0)}{d_u}\right)$ for all $c \in \left(0, \frac{1}{2}\right)$, where $\mathbf{x}_0 \in \overline{\Omega}$, $\mathbf{x}_0 \neq \mathbf{0}$. In other words, we have to prove:

$$\sum_{k \in \mathbb{N}} \sum_{|\boldsymbol{\alpha}| = k} \frac{|D^{\boldsymbol{\alpha}} u(\mathbf{x}_0)|}{\boldsymbol{\alpha}!} |\mathbf{x} - \mathbf{x}_0|^{|\boldsymbol{\alpha}|} \leq \overline{c} < \infty \qquad \forall\, \mathbf{x} \in B\left(\mathbf{x}_0, c\frac{\Phi(\mathbf{x}_0)}{d_u}\right), \quad c \in \left(0, \frac{1}{2}\right),$$

where $\overline{c}$ is a positive constant depending only on function u.

Using (4.17) and the fact that $\mathbf{x}$ belongs to $B\left(\mathbf{x}_0, c\frac{\Phi(\mathbf{x}_0)}{d_u}\right)$, we obtain:

$$\begin{aligned} &\sum_{k \in \mathbb{N}} \sum_{|\boldsymbol{\alpha}| = k} \frac{|D^{\boldsymbol{\alpha}} u(\mathbf{x}_0)}{\boldsymbol{\alpha}!} |\mathbf{x} - \mathbf{x}_0|^k \leq \sum_{k \in \mathbb{N}} \sum_{|\boldsymbol{\alpha}| = k} \frac{1}{\boldsymbol{\alpha}!} c_u \frac{d_u^k}{\Phi_k(\mathbf{x}_0)} |\boldsymbol{\alpha}|! c^k \frac{\Phi_k(\mathbf{x}_0)}{d_u^k(\mathbf{x}_0)} \\ &= c_u \sum_{k \in \mathbb{N}} \sum_{|\boldsymbol{\alpha}| = k} \frac{|\boldsymbol{\alpha}|!}{\boldsymbol{\alpha}!} c^k = c_u \sum_{k \in \mathbb{N}} \sum_{\ell = 0}^{k} \binom{k}{\ell} c^k = c_u \sum_{k \in \mathbb{N}} (2c)^k \leq \overline{c} < +\infty, \end{aligned} \tag{4.20}$$

since we are assuming that $c \in \left(0, \frac{1}{2}\right)$.

We proved that u, the solution to problem (1.29), has a singular behaviour at vertex $\mathbf{0}$ but is analytic elsewhere, and in fact can be extended to an analytic function on $\mathcal{N}(u)$ defined in (4.18).

The regularity argument here discussed can be straightforwardly extended to the "natural" case of multiple singularities.

4.2.2 Local approximation by harmonic polynomials

In this section, we discuss approximation estimates by means of harmonic polynomials. Such results will be used for the approximation of the first term on the right-hand side of (4.16), that is the best approximation in the H^1 seminorm of the solution to (1.29) by (piecewise discontinuous) harmonic polynomials.

We will firstly deal with approximation by harmonic polynomials on the polygons that are far from the singularity, see Lemma 4.2.2. Secondly, we will discuss approximation estimates by harmonic polynomials on the polygons abutting the singularity, see Lemma 4.2.3.

Before that, we recall a (technical) auxiliary result, involving approximation on a polygon K with $h_K = 1$ by means of harmonic polynomials. The proof of this theorem can be found in [72, Theorem 4.10] and relies on some results contained in the pioneering works [81, 85].

Theorem 4.2.1. *Let $\widehat{K}$ be a polygon with $h_{\widehat{K}} = 1$. In particular, meas$(\widehat{K}) < 1$. Assume that the following parameters are given:*

$$\begin{aligned} &\delta \in \left(0, \frac{1}{2}\right]; \qquad \xi = \begin{cases} 1 & \text{if } \widehat{K} \text{ is convex} \\ \frac{2}{\pi}\arcsin\left(\frac{\rho_0}{1-\rho_0}\right) & \text{otherwise} \end{cases}; \qquad c_{\widehat{K}} = \frac{27}{\xi}; \\ &\overline{r} < \min\left(\frac{1}{3}\left(\frac{\delta}{c_{\widehat{K}}}\right)^{\frac{1}{\xi}}, \frac{\rho_0}{4}\right); \qquad c_I = \frac{\rho_0}{4}; \qquad c_{approx} \leq \frac{7}{\rho_0^2}; \qquad \gamma \leq \frac{72}{\rho_0^4}, \end{aligned} \tag{4.21}$$

*where we recall that ρ_0 is the radius of the ball with respect to which $\widehat{K}$ is star shaped, see assumption (**G1**). Let also:*

$$\widehat{K}_\delta := \left\{\widehat{\mathbf{x}} \in \mathbb{R}^2 \mid dist(\widehat{K}, \widehat{\mathbf{x}}) < \delta\right\}. \tag{4.22}$$

Then, there exists a sequence $\{\widehat{q}_{p,\Delta}\}_{p=1}^{\infty}$ of harmonic polynomials of degree p such that, for any $\widehat{u} \in W^{1,\infty}(\widehat{K}_\delta)$:

$$|\widehat{u} - \widehat{q}_{p,\Delta}|_{1,\widehat{K}} \leq \sqrt{2} c_{appr} \frac{2}{c_I \overline{r}^2} \overline{r}^{-\gamma} (1+\overline{r})^{-p_K} \|\widehat{u}\|_{W^{1,\infty}(\widehat{K}_\delta)}. \tag{4.23}$$

We do not discuss the proof of Thorem 4.2.1, but we point out that in order to have this result we are using the fact that ρ_0 introduced in assumption (**G1**) is such that $\rho_0 \in (0, \frac{1}{2})$, see assumption (**G8**), since [72, Theorem 4.10] holds under this hypothesis.

As a consequence of Theorem 4.2.1, for all the regular (in the sense of assumptions (**G1**)-(**G2**)) polygons $\widehat{K}$ with diameter 1 it holds that there exists an harmonic polynomial $\widehat{q}_{p,\Delta}$ of degree p such that:

$$|\widehat{u} - \widehat{q}_{p,\Delta}|_{1,\widehat{K}} \leq c \exp(-b\,p) \|\widehat{u}\|_{W^{1,\infty}(\widehat{K}_\delta)}, \tag{4.24}$$

where c and b are two positive constants depending uniquely on ρ_0 introduced in assumption (**D1**) and the "enlargement factor" δ introduced in (4.21). Since both ρ_0 and δ are for the time being fixed, then c and b are two positive universal constants.

Assume now that polygon K belongs to layer L_j, $j = 1, \ldots, n$, i.e. does not abut $\mathbf{0}$, and consequently has diameter unequal to 1 in general. Then, having set u and $q_{p,\Delta}$ the push-forward of $\widehat{u}$ and $\widehat{q}_{p,\Delta}$ respectively, a scaling argument immediately yields:

$$|u - q_{p,\Delta}|_{1,K} \approx |\widehat{u} - \widehat{q}_{p,\Delta}|_{1,\widehat{K}} \lesssim \exp(-b\,p) \|\widehat{u}\|_{W^{1,\infty}(\widehat{K}_\delta)} \lesssim \exp(-bp) \|u\|_{W^{1,\infty}(K_\varepsilon)}, \tag{4.25}$$

where $\widehat{K}$, the polygon obtained by scaling K, is such that $h_{\widehat{K}} = 1$, where $\{\widehat{q}_{p,\Delta}\}_{p=1}^{\infty}$ is the sequence validating (4.24), where K_ε is defined as in (4.22) and where the "enlargement" factor ε must be chosen in such a way that when we scale K to $\widehat{K}$, then K_ε is mapped in $\widehat{K}_\delta$, δ being *exactly* the parameter fixed in (4.21).

We note that sequence $\{q_{p,\Delta}\}_{p=1}^{\infty}$ is made of harmonic polynomials since it is the composition of a sequence of harmonic polynomials with a dilatation.

What we have to check is that the size of K_ε is not too large. In particular, we want that K_ε is kept separated from the singularity at $\mathbf{0}$, for all L_j, $j = 1, \ldots, n$.

Let u be the solution to problem (1.29). Henceforth, we assume that $\text{dist}(K, \mathbf{0}) < 1$ (which is always valid if one takes Ω, the domain of problem (1.29), small enough). From Section 1.3, we know that u, the solution to problem (1.29), is analytic on the set $\mathcal{N}(u)$ defined in (4.18). In particular, u is analytic on the following domain depending on K:

$$\mathcal{N}_K(u) = \left\{\mathbf{x} \in \mathbb{R}^2 \mid \text{dist}(K, \mathbf{x}) < c \frac{\text{dist}(K, \mathbf{0})}{d_u}\right\} \quad \forall\, c \in \left(0, \frac{1}{2}\right). \tag{4.26}$$

since $\mathcal{N}_K(u) \subset \mathcal{N}(u)$. This fact has an extreme relevance in the proof of the forthcoming Lemma 4.2.2. The important issue is that more the polygon is near the singularity, the smaller is the extended domain $\mathcal{N}_K(u)$, see Figure 4.1. In any case, $\mathcal{N}_K(u)$ remains contained in the global analiticity domain $\mathcal{N}(u)$, which is fixed once and for all.

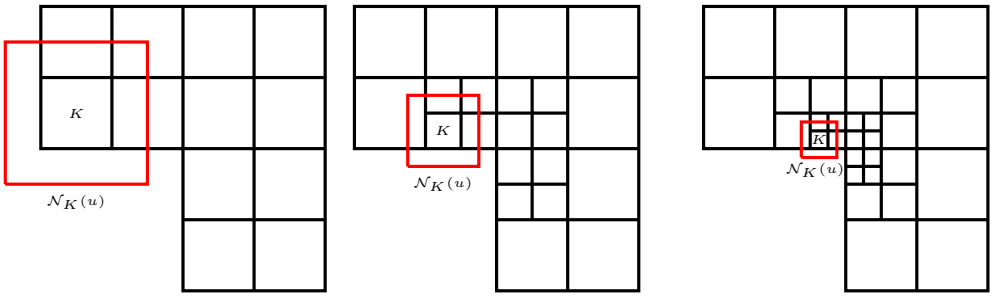

Figure 4.1: Given K polygon in $\mathcal{T}_n$, its extension keeps separated from the singularity, since the smaller is the polygon the smaller can be taken the extension.

We choose $c = \frac{1}{4}$ in (4.26). Owing to (1.39) and recalling that $K \notin L_0$, there exist two positive constants $\alpha_1 \leq 1 \leq \alpha_2$ independent of K such that $\alpha_1 h_K \leq \mathrm{dist}(K, \mathbf{0}) \leq \alpha_2 h_K$. Thus:

$$\frac{1}{4}\frac{\mathrm{dist}(K,\mathbf{0})}{d_u} = \frac{1}{4}\alpha_1 \frac{\alpha_1^{-1}\mathrm{dist}(K,\mathbf{0})}{d_u} \geq \frac{1}{4}\frac{\alpha_1}{d_u} h_K.$$

This implies that u is analytic on the following domain too:

$$\widetilde{\mathcal{N}}_K(u) = \left\{ \mathbf{x} \in \mathbb{R}^2 \mid \mathrm{dist}(K, \mathbf{x}) < \frac{1}{4}\frac{\alpha_1}{d_u} h_K \right\} \subseteq \mathcal{N}_K(u), \quad K \in L_j,\ j = 1, \ldots, n. \tag{4.27}$$

Therefore, we fix for instance $\varepsilon = \frac{1}{8}\frac{\alpha_1}{d_u} h_K$. In this way, we have built $K_\varepsilon = \widetilde{\mathcal{N}}_K(u)$, neighbourhood of K not covering $\mathbf{0}$.

It is straightforward to note that scaling K to $\widehat{K}$ with $h_{\widehat{K}} = 1$, we also scale K_ε to $\widehat{K}_\delta$ (see (4.22) for the definition of $\widehat{K}_\delta$), where $\delta = \frac{1}{8}\frac{\alpha_1}{d_u}$ is now independent of K and only depends on u. Fixing such a δ in Theorem 4.2.1, we have that (4.25) holds with $\mathbf{0} \notin \overline{K_\varepsilon}$; in particular, the norm appearing on the right-hand side of (4.25) is finite for all $K \in L_j$, $j = 1, \ldots, n$.

We are now ready to state the bound on the best error with respect to harmonic polynomials on the polygons not abutting the singularity.

Lemma 4.2.2. *Under assumptions **(G0)-(G1)-(G2)-(G4)-(G5)-(G8)**, let $K \in L_j$, $j = 1, \ldots, n$, u be the solution to problem (1.29) and $\widetilde{\mathcal{N}}_K(u)$ be defined in (4.27). Then, there exists a sequence $\{q_{p,\Delta}\}_{p=1}^{\infty}$ of harmonic polynomials of degree p_K such that:*

$$|u - q_{p,\Delta}|_{1,K} \lesssim h_{\widetilde{\mathcal{N}}_K(u)} \exp(-b\,p) \|u\|_{W^{1,\infty}(\widetilde{\mathcal{N}}_K(u))} \lesssim \exp(-b\,p), \tag{4.28}$$

where b is a constant independent of K.

Proof. The proof follows from Theorem 4.2.1 and the subsequent discussion. □

Remark 7. The first inequality in (4.28) follows from a scaling argument. The second inequality, instead, is a consequence of computations similar to those in (4.20) and the definition of $\widetilde{\mathcal{N}}_K(u)$) in (4.27).

It is clear from the above discussion that we must follow a different strategy for the elements in the first layer; in fact, here, the $W^{1,\infty}$ of u is not finite in principle.

It holds in particular the following result.

Lemma 4.2.3. *Under assumptions **(G0)-(G1)-(G2)-(G4)-(G5)-(G8)**, let $K \in L_0$ and let $u \in H^{2,2}_\beta(\Omega)$, where $H^{2,2}_\beta$ is defined in (1.35), where $1 - \alpha_{1,1} < \beta$, $\alpha_{1,1}$ being the first singular exponent (A.4) associated with vertex $\mathbf{0}$. Then, there exists $q_1 \in \mathbb{P}_1(K)$ such that:*

$$|u - q_1|_{1,K} \lesssim h_K^{2(1-\beta)} \| |\mathbf{x}^\beta| |D^2 u| \|^2_{0,K} \lesssim \sigma^{2(1-\beta)n}.$$

In particular, q_1 is a harmonic polynomial.

Proof. The polynomial q_1 is given by the linear interpolant of u at, for instance, three nonaligned vertices of K. The proof follows the lines of Lemma 3.2.2. □

Remark 8. Lemma 4.2.3 suggests that one could also consider Harmonic VE spaces with nonuniform degrees of accuracy, still guaranteeing optimal approximation estimates. In particular, one could consider degrees of accuracy equal to a generic $p \in \mathbb{N}$ on all the layers not abutting $\mathbf{0}$ and equal to 1 in L_0, as depicted in Figure 4.2. At the interface s of two nondisjoint elements K_0

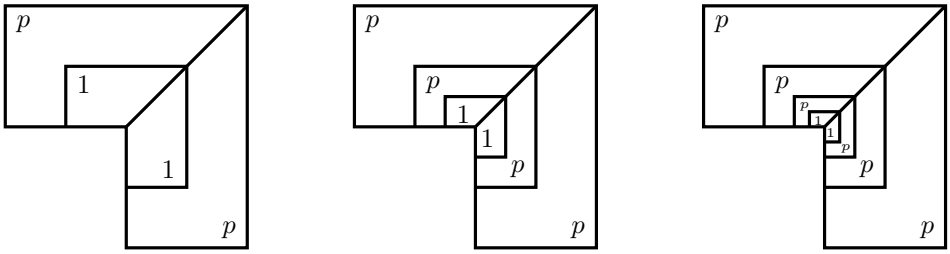

Figure 4.2: Nonuniform distribution of degrees of accuracy. In layer L_0 $p = 1$. In layers L_j, $j = 1, \dots, n$, $p \in \mathbb{N}$.

and K_1 in layers L_0 and L_1 one associates $p_s = \max(1, p) = p$ (*maximum rule*) in order to define nonuniform boundary spaces $\mathbb{B}(\partial K)$ similarly to (3.4), as depicted in Figure 4.3.

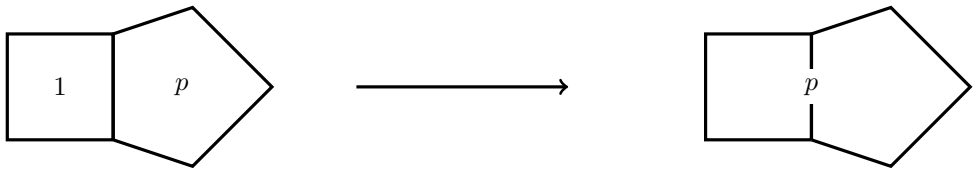

Figure 4.3: If one considers nonuniform degrees of accuracy, then the largest polynomial degree at the interface can be taken (*maximum rule*).

4.2.3 Local approximation by functions in the Harmonic VE space

Here, we discuss approximation estimates by functions in the Harmonic Virtual Element Space which will be used for the approximation of the second term on the right-hand side of (4.16). As in Section 4.2.2, we firstly investigate approximation estimates on polygons not abutting the singularity, see Lemma 4.2.4; secondly, we discuss approximation estimates of polygons in the finest layer L_0, see Lemma 4.2.5.

Lemma 4.2.4. *Under assumptions (**G0**)-(**G1**)-(**G2**)–(**G3**)-(**G5**)-(**G8**), let $K \in L_j$, $j = 1, \dots, n$ and let $\beta \in [0, 1)$. Let g, the Dirichlet datum of problem* (1.29)*, belong to space $\mathcal{B}^{\frac{3}{2}}_{\beta}(\partial\Omega, \mathbf{0})$ and let u, the solution to problem* (1.29)*, belong to space $\mathcal{B}^2_{\beta}(\Omega, \mathbf{0})$, where the Babuška spaces under consideration are defined in* (1.36)*, where $1 - \alpha_{1,1} < \beta$, $\alpha_{1,1}$ being the first singular exponent associated with vertex $\mathbf{0}$. Then, there exists $u_I \in V^{\Delta}(K)$ such that:*

$$
\begin{aligned}
|u - u_I|_{1,K} &\lesssim e^{s_K+\frac{1}{2}} \left(\frac{h_K}{p_K}\right)^{s_K+\frac{1}{2}} |u|_{s_K+1,\partial K} \\
&\lesssim e^{s_K+\frac{1}{2}} p^{-s_K-\frac{1}{2}} \sigma^{(n-j)(1-\beta)} \left\{ |u|_{H^{s_K+1,2}_{\beta}(K)} + |u|_{H^{s+2,2}_{\beta}(K)} \right\} \quad \forall\, s_K \in \mathbb{N},
\end{aligned}
$$

where we recall that σ is the grading parameter of the mesh introduced in (1.39).

Proof. Before proving the result, we observe that the $H^{s_K+1}(\partial K)$ seminorm exists, since $u \in \mathcal{B}^2_{\beta}(\Omega, \mathbf{0})$ implies that u is analytic far from the singularity.

Let us consider $u_I \in V^{\Delta}(K)$ defined as the weak solution to the following local Laplace problem:

$$\begin{cases} -\Delta u_I = 0 & \text{in } K, \\ u_I = u_{GL} & \text{on } \partial K, \end{cases} \tag{4.29}$$

where u_{GL} is the Gauß-Lobatto interpolant of degree p of u on each edge s. Then, using the fact that $u - u_I$ is harmonic and using (3.33):

$$|u - u_I|^2_{1,K} \lesssim |u - u_I|_{1,K} \|u - u_{GL} - c\|_{\frac{1}{2},\partial K}, \tag{4.30}$$

for every $c \in \mathbb{R}$, where the hidden constant depends solely on the parameters ρ_0 and c introduced in assumptions (**G1**)-(**G2**)-(**G3**).

We deduce that we must deal with the boundary error term only. We fix $c = 0$ in (4.30) (the case $c \neq 0$ will become important in the following). Since u is analytic far from the singularity, as discussed in Section 4.2.1, we inherit the two following results from [43, Theorems 4.2 and 4.5]:

$$\|u - u_{GL}\|_{0,s} \lesssim e^{s_K+1} \left(\frac{h_s}{p}\right)^{s_K+1} \sum_{s \text{ edge of } K} |u|_{s_K+1,s}, \quad \forall\, s \text{ edge of } K, \forall s_K \in \mathbb{N},$$

$$|u - u_{GL}|_{1,s} \lesssim e^{s_K} \left(\frac{h_s}{p}\right)^{s_K} \sum_{s \text{ edge of } K} |u|_{s_K+1,s}, \quad \forall\, s \text{ edge of } K, \forall s_K \in \mathbb{N}.$$

Using interpolation theory [101, 102], recalling from assumption (**G2**) that $h_s \approx h_K$ and that the number of edges of each $K \in \mathcal{T}_n$ is uniformly bounded, yield:

$$\|u - u_I\|^2_{\frac{1}{2},\partial K} = \|u - u_{GL}\|^2_{\frac{1}{2},\partial K} \lesssim e^{2\,s_K+1} \left(\frac{h_K}{p}\right)^{2\,s_K+1} \sum_{s \text{ edge of } K} |u|^2_{s_K+1,s}, \tag{4.31}$$

where j denotes the layer to which polygon K belongs and $n+1$ denotes the number of layers in the decomposition.

We apply a multiplicative trace inequality [83, Theorem 4.8], assumption (**G2**) and the trivial bound $|a||b| \leq a^2 + b^2$, a, $b \in \mathbb{R}$, getting:

$$\sum_{s \text{ edge of } K} |u|^2_{s_K+1,s} \lesssim h_K^{-1} |u|^2_{s_K+1,K} + h_K |u|^2_{s_K+2,K}. \tag{4.32}$$

Recalling the definition of weighted Sobolev seminorms (1.19), one obtains:

$$|u|^2_{H^{s_K+\ell,2}_{\beta}(K)} \geq \|\Phi_{\beta+s_K+\ell-2}\, |D^{(s_K+\ell)} u|\, \|^2_{0,K} \gtrsim \operatorname{dist}(K, \mathbf{0})^{2(\beta+s_K+\ell-2)} |u|^2_{s_K+\ell,K}, \quad \ell = 1, 2. \tag{4.33}$$

Combining (1.39), (4.32) and (4.33), we deduce:

$$|u|^2_{s_K+1,\partial K} \lesssim h_K^{-2(\beta+s_K-\frac{1}{2})} \left\{ |u|^2_{H^{s_K+1,2}_{\beta}(K)} + |u|^2_{H^{s_K+2,2}_{\beta}(K)} \right\}. \tag{4.34}$$

Finally, recalling from assumption (**G5**) that $h_K \approx \sigma^{n-j}$, we get the claim by inserting (4.34) in (4.31). □

Next, we turn our attention to the approximation in the polygons belonging to the first layer.

Lemma 4.2.5. *Under assumptions (**G0**)-(**G1**)-(**G2**)-(**G3**)-(**G5**)-(**G8**), let $K \in L_0$. Let g, the Dirichlet datum of problem* (1.29)*, belong to space $\mathcal{B}^{\frac{3}{2}}_{\beta}(\partial\Omega, \mathbf{0})$ and let and let u, the solution to problem* (1.29)*, belong to space $\mathcal{B}^2_{\beta}(\Omega, \mathbf{0})$, where the Babuška spaces under consideration are defined in* (1.36)*, where $1 - \alpha_{1,1} < \beta$, $\alpha_{1,1}$ being the first singular exponent associated with vertex $\mathbf{0}$. Then, there exists $u_I \in V^{\Delta}(K)$ such that:*

$$|u - u_I|^2_{1,K} \lesssim \sigma^{2n(1-\beta)},$$

where we recall that σ is the geometric grading parameter of assumption of the mesh introduced in (1.39)*.*

Proof. Let u_I be defined as in (4.29), with u_{GL} being now the linear interpolant of u on each edge s of K. Let $\widetilde{\mathcal{T}}_n(K)$ be the subtriangulation of K obtained by joining $\mathbf{0}$ with the other vertices of K. Such a subtriangulation is regular, see assumption (**G8**).

As in (4.30), we have:

$$|u - u_I|_{1,K} \lesssim \|u - u_{GL} - c\|_{\frac{1}{2},\partial K} \quad \forall\, c \in \mathbb{R}, \tag{4.35}$$

where the hidden constant in (4.35) depends solely on the parameters ρ_0 and c introduced in assumptions (**G1**)-(**G2**)-(**G3**). We denote by $\widetilde{u}_{GL}$ the linear interpolant of u over every $T \in \widetilde{\mathcal{T}}_n(K)$ at the three vertices of T. One obviously has $\widetilde{u}_{GL} = u_{GL}$ on ∂K. Applying a trace inequality and using argument similar to those of Lemma 3.2.3, we get:

$$|u - u_I|_{1,K} \lesssim \|u - \widetilde{u}_{GL} - c\|_{1,K}, \tag{4.36}$$

where, once again, the hidden constant in (4.36) depends solely on the parameters ρ_0 and c introduced in assumptions (**G1**)-(**G2**)-(**G3**). By picking c the average of $u - \widetilde{u}_{GL}$ over K, applying a Poincarè inequality and recalling that $\mathrm{card}(\widetilde{\mathcal{T}}_n)$ is uniformly bounded, we get:

$$|u - u_I|^2_{1,K} \lesssim \sum_{K \in \widetilde{\mathcal{T}}_n(K)} |u - \widetilde{u}_{GL}|^2_{1,T}.$$

In order to conclude, we apply [96, Lemma 4.16] and (1.39) obtaining:

$$|u - u_I|^2_{1,K} \lesssim \sum_{K \in \widetilde{\mathcal{T}}_n(K)} h_T^{2(1-\beta)} \||\mathbf{x}|^\beta |D^2 u|\|^2_{0,T} \lesssim \sigma^{2n(2-\beta)} \||\mathbf{x}|^\beta |D^2 u|\|^2_{0,T} \lesssim \sigma^{2n(1-\beta)},$$

which holds since $u \in \mathcal{B}^2_\beta(\Omega, \mathbf{0})$. □

Again, for the proof of Lemma 4.2.5, one could have used nonuniform degrees of accuracy as discussed in Remark 8.

In order to conclude this section, we highlight that we built in Lemmata 4.2.4 and 4.2.5 a continuous approximant of u, which belongs to space $V^\Delta_{n,g}$ defined in (4.6).

4.2.4 Exponential convergence

Here, we discuss the main result of the work, namely the exponential convergence of the energy error in terms of the number of degrees of freedom. In order to achieve such a result, we fix as a degree of accuracy:

$$p = n + 1, \qquad n + 1 \text{ being the number of layers of } \mathcal{T}_n. \tag{4.37}$$

The main result of the chapter follows.

Theorem 4.2.6. *Let $\{\mathcal{T}_n\}_{n\in\mathbb{N}}$ be a sequence of polygonal decomposition satisfying assumptions (**A$^\Delta$1**)-(**A$^\Delta$2**)-(**G0**)-(**G1**)-(**G2**)-(**G3**)-(**G5**)-(**G8**). Let u and u_n be the solutions to problems* (1.29) *and* (4.14) *respectively. Let g, the Dirichlet datum of problem* (1.29)*, belong to $\mathcal{B}^{\frac{3}{2}}_\beta(\partial\Omega, \mathbf{0})$, where the Babuška spaces under consideration are defined in* (1.36)*, where $q - \alpha_{1,1} < \beta$, $\alpha_{1,1}$ being the first singular exponent associated with vertex $\mathbf{0}$. Then, the following holds true:*

$$|u - u_n|_{1,\Omega} \lesssim \exp\left(-b\sqrt[2]{N}\right), \tag{4.38}$$

where b is a constant independent of the discretization parameters and N is the number of degrees of freedom of V^Δ_n defined in (4.6)*.*

Proof. We only give the sketch of the proof. Applying Lemma 4.1.1, bound (6.43), Lemmata 4.2.4 to 4.2.5 to the first term on the right-hand side of (4.16) along with standard *hp* approximation strategies [96] and Lemmata 4.2.2 and 4.2.3 to the second term of the right-hand side of (4.16) along with [72, Theorem 5.5], we have:

$$|u - u_n|_{1,K} \lesssim \exp\left(-\widetilde{b}\,(n+1)\right), \tag{4.39}$$

for some $\widetilde{b}$ independent of the disctretization parameters, $n+1$ being the number of layers in $\mathcal{T}_n$, but depending on the universal constants r_3 and r_4 introduced in (4.11).

In order to conclude, it suffices to find out the relation between n and N, the number of degrees of freedom of space V_n^{Δ}. For thi purpose, we recall from [72, (5.6)] that in each layer L_j there exists a fixed maximum number of elements, see assumption (**G5**). Moreover, thanks to assumption (**G2**), there exists a fixed maximum number of edges per element.

If we set N_{edge} the maximum number of edges per element and N_{element} the maximum number of elements per layer, we conclude that:

$$N = \dim(V_n) \lesssim N_{\text{edge}} N_{\text{element}} \sum_{\ell=0}^{n} (n+1) \lesssim (n+1)^2,$$

where c is a positive constant depending on N_{edge} and N_{element}. In particular, $\sqrt{N} \lesssim n$. This, along with (4.39), implies the assertion. □

In order to conclude this chapter, we highlight two issues:

- the assumption (4.11), which plays a fundamental role in the proof of Theorem 4.2.6, is valid choosing the stabilization presented in (6.25);
- Theorem 4.2.6 is validated by numerical tests in Section 7.3; the performances of *hp* Harmonic VEM are also compared with those of *hp* VEM, see Theorem 3.2.8.

Chapter 5

Residual-based a-posteriori error analysis of *hp* VEM

In this chapter, we deal with residual-based a-posteriori error analysis of *hp* VEM.

We emphasize that what we are going to present in the following is only an *initial* step in the theory of *hp* a-posteriori error analysis of VEM. In particular, there are some issues that we do not fully address in this thesis and that are currently in progress, namely:

- no numerical tests, validating numerical experiments, are presented;
- local optimal L^2 error estimates in terms of p by means of functions in the VE space are not proven;
- the "reliability" and "efficiency" bounds, typical of residual-based a-posteriori analysis, depend on the choice of the stabilization of the method.

The a-posteriori h version of VEM has been investigated in [38, 46, 54], when dealing with general elliptic problems and Steklov eigenvalue problem, but the issue of presenting bounds explicit in terms of the "polynomial degree" is therein never taken into account. Instead, the literature regarding a-posteriori *hp* VEM is more lavish; therefore, in order to avoid to get lost in a tangle of technical works, we decide here to partially follow the approach of a milestone of *hp* a-posteriori error analysis, namely [84].

It is worth to mention at least one of the reasons for which a-posteriori *hp* VEM is a riveting topic. On the one hand, VEM allows for a very efficient handing of the geometry of a domain both in the local *refining* process (allowing in fact for the employment of hanging nodes without additional technicalities), see Figure 5.1, and in the *derefining* process, see Figure 5.2 On the other

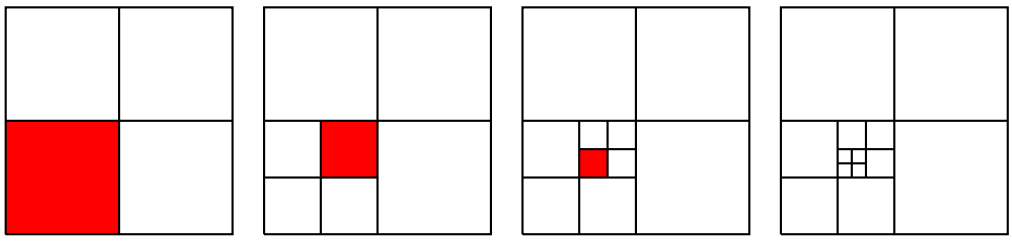

Figure 5.1: The refinement process in VEM is extremely flexible, since hanging nodes are treated as "standard" nodes. No modifications in the VEM linear system or employment of (possibly bad-shaped) subtriangulations are required. In red, we depict the "to-be-refined" polygon.

hand, *hp* adaptivity consists in both locally refining a mesh and increasing the dimension of local spaces. This is an issue of extreme interest since we know, for instance from Section 2.3, that the p version of VEM (as well as of FEM), provides better approximation estimates than those of the h version whenever the target solution is regular enough.

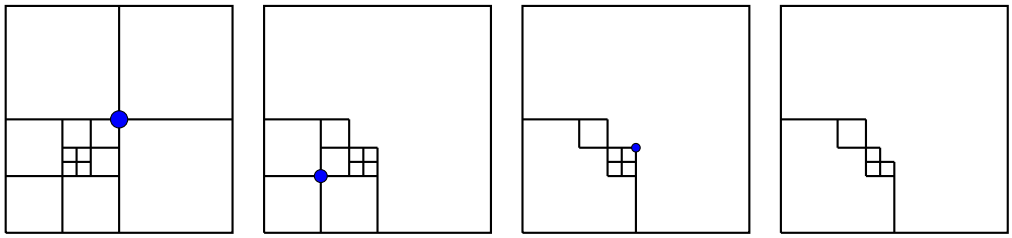

Figure 5.2: Sometimes, within the adaptive scheme, it is useful to *derefine* the mesh, e.g. whenever the error indicator is small. In the figure, we *derefine* the patch of polygons around the blue vertex, obtaining meshes with very weird-shaped polygons.

A possible combination of h and p adaptivity leads therefore to refinement of the mesh where the solution is possibly "irregular" and to increase the dimension of local spaces if the solution is "regular". A heuristic rule for choosing between h and p refinement can be found in [84, Section 4.2].

We emphasize in addition that the VEM technology allows for an easy handling of approximation spaces with degrees of accuracy varying elementwise.

The outline of the chapter follows. In Section 5.1, we recall some notations from the previous chapters and we introduce and discuss a set of technical tools needed for the analysis of the a-posteriori *hp* VEM. In Section 5.2 we deal with the a-posteriori error analysis; in particular, we introduce an error estimator and we discuss the "reliability" and the "efficiency" of such an estimator.

5.1 Notation and technical tools

In the following, our target problem is Poisson problem with Dirichlet homogeneous boundary conditions (1.27); furthermore, we employ VE spaces with nonuniform degree of accuracy as those presented in Chapter 3. The only difference here is that we will employ the *minimum rule* instead of the *maximum rule* described in Figure 3.1 when assigning the degree to the edges in the skeleton of a polygonal mesh; the reason for this change is that we want to follow as much as possible the approach of [84], but we stress that it is not mandatory.

The sequence of meshes $\{\mathcal{T}_n\}_{n\in\mathbb{N}}$ that we employ throughout this chapter satisfies assumptions (**G0**)-(**G1**)-(**G2**); as emphasized in Remark 2, it is possible to construct a regular subtriangulation $\widetilde{\mathcal{T}}_n(K)$ on each polygon K. By $\widetilde{\mathcal{T}}_n$, we denote the global subtriangulation obtained by collecting the local ones.

Let $\mathcal{V}_n$ ($\widetilde{\mathcal{V}}_n$) and $\mathcal{E}_n$ ($\widetilde{\mathcal{E}}_n$) be the sets of vertices and edges of $\mathcal{T}_n$ ($\widetilde{\mathcal{T}}_n$) respectively. We denote by $\mathbf{p}$ a vector of degrees of accuracy associated with polygonal mesh $\mathcal{T}_n$, see (3.1). To each $T \in \widetilde{\mathcal{T}}_n$ we associate p_T equal to p_K and we denote by $\widetilde{\mathbf{p}}$ the vector of degrees of accuracy associated with subtriangulation $\widetilde{\mathcal{T}}_n$.

Besides, to each edge $\widetilde{s}$ of T we associate $p_{\widetilde{s}}$ equal to p_s whenever $s = \overline{T} \cap \overline{K} = \widetilde{s}$, i.e. whenever $\widetilde{s}$ is also an edge of K. To the other edges $\widetilde{s}$ of T, i.e. whenever $\widetilde{s}$ is internal to K, we associate $p_{\widetilde{s}}$ equal to p_K.

We also associate with each vertex $\mathbf{V} \in \widetilde{\mathcal{V}}_n$ ($\mathbf{V} \in \mathcal{V}_n$):

$$p_{\mathbf{V}} = \min(p_T \mid \mathbf{V} \in \overline{T},\, T \in \widetilde{\mathcal{T}}_n). \tag{5.1}$$

We refer to Figure 5.3 for a graphical idea regarding the distribution of the degrees over $\mathcal{T}_n$ and $\widetilde{\mathcal{T}}_n$.

We also demand that the vector p of the degrees of accuracy satisfies assumption (**P1**). This means that the degrees of accuracy of two neighbouring elements must be comparable.

The outline of the remainder of this section follows. In Section 5.1.1, we discuss *hp* approximation properties of local VE spaces. Instead, in Subsection 5.1.2, we recall from [84] the existence of a lifting operator of a polynomial from any edge of a triangle into its interior with good stability properties.

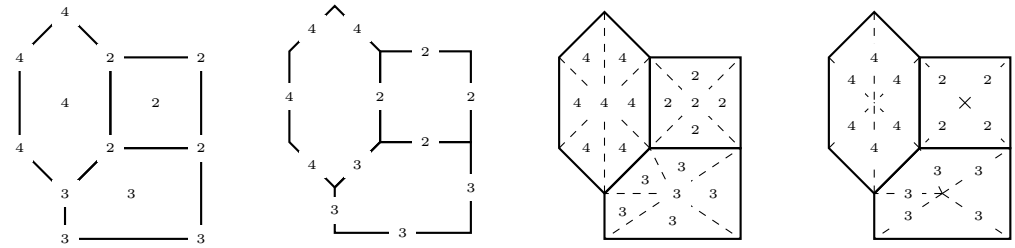

Figure 5.3: Nonuniform degree of accuracy distribution on the polygonal decomposition $\mathcal{T}_n$, on the associated subtriangulation $\widetilde{\mathcal{T}}_n$ and related skeleton $\mathcal{E}_n$ and $\widetilde{\mathcal{E}}_n$ and related set of vertices $\mathcal{V}_n$ and $\widetilde{\mathcal{V}}_n$.

We adopt the following notation concerning spaces of piecewise continuous and discontinuous polynomials which takes into account both polygonal decomposition $\mathcal{T}_n$ and the related subtriangulation $\widetilde{\mathcal{T}}_n$. Let $\overline{\mathcal{T}}_n$ be either $\mathcal{T}_n$ or $\widetilde{\mathcal{T}}_n$; then, we write:

$$\begin{aligned}\mathcal{S}^{\overline{\mathbf{p}},0}(\Omega,\overline{\mathcal{T}}_n) &= \left\{q\in\mathcal{C}^0(\Omega)\mid q|_D\in\mathbb{P}_{\overline{p}_D}(D),\,\forall D\in\overline{\mathcal{T}}_n,\ q|_s\in\mathbb{P}_{\overline{p}_s}(s)\right\},\\ \mathcal{S}^{\overline{\mathbf{p}},-1}(\Omega,\overline{\mathcal{T}}_n) &= \left\{q\in L^2(\Omega)\mid q|_D\in\mathbb{P}_{\overline{p}_D}(D),\,\forall D\in\overline{\mathcal{T}}_n,\ q|_s\in\mathbb{P}_{\overline{p}_s}(s)\right\},\end{aligned} \tag{5.2}$$

where the choice of the polynomial degrees $\overline{p}_s$ on the edges is made following the minimum rule presented in Figure 5.3.

5.1.1 Approximation estimates by means of function in the VE Space

In this section, we discuss approximation properties of the local VE spaces $V(K)$ defined in (3.5). In particular, we prove local approximation estimates in the L^2 and H^1 (semi)norms and also in the L^2 norm on the boundary.

To this purpose, we need to recall a technical tool from [82, 84] which is based on the concept of triangular and polygonal patches around a vertex.

In particular, given vertex $\mathbf{V}\in\widetilde{\mathcal{V}}_n$ of subtriangulation $\widetilde{\mathcal{T}}_n$, we set the triangular patch around vertex $\mathbf{V}$ as:

$$\omega(\mathbf{V})=\bigcup\left\{T\in\widetilde{\mathcal{T}}_n\mid\mathbf{V}\text{ is a vertex of }T\right\},\quad \overline{\omega}(\mathbf{V})=\bigcup\left\{K\in\mathcal{T}_n\mid\mathbf{V}\text{ is a vertex of }K\right\}. \tag{5.3}$$

Given D either a polygon of $\mathcal{T}_n$ or a triangle of $\widetilde{\mathcal{T}}_n$, we define the *triangular* patch around D as:

$$\omega(D):=\bigcup\left\{\omega(\mathbf{V})\mid\mathbf{V}\text{ is a vertex of }D\right\}. \tag{5.4}$$

Besides, given an edge $s\in\mathcal{E}_n$, we also define the *triangular* patch around s as follows:

$$\omega(s):=\bigcup\left\{\omega(\mathbf{V})\mid\mathbf{V}\text{ is an endpoint of }s\right\}. \tag{5.5}$$

In Figures 5.4, 5.5, 5.6 and 5.7 we provide graphical examples of patches around a vertex, a polygon, a triangle and an edge.

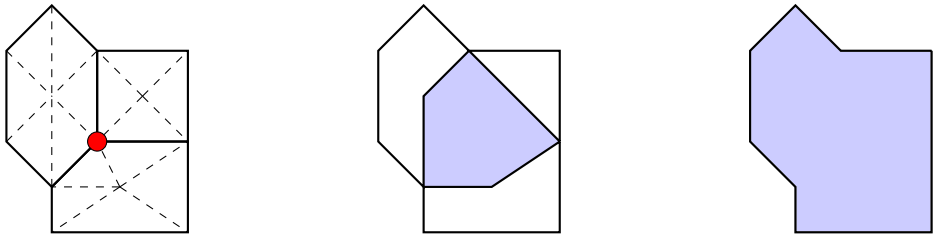

Figure 5.4: Left: polygonal mesh $\mathcal{T}_n$ and subtriangulation $\widetilde{\mathcal{T}}_n$, in red a vertex $\mathbf{V}$. Center: in light blue, $\omega(\mathbf{V})$, triangular patch around vertex $\mathbf{V}$, defined in (5.3). Right: in light blue, $\overline{\omega}(\mathbf{V})$, polygonal patch around vertex $\mathbf{V}$, defined in (5.3).

We now recall the following Clément -type approximation result.

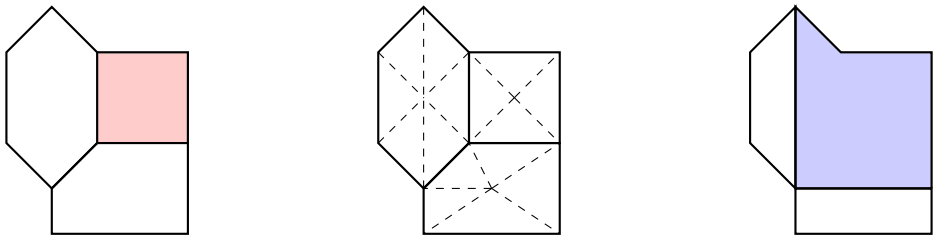

Figure 5.5: Left: polygonal mesh $\mathcal{T}_n$, in light red a polygon K. Center: regular subtriangulation $\widetilde{\mathcal{T}}_n$, see Remark 2. Right: in light blue, $\omega(K)$, triangular patch around K, defined in (5.4).

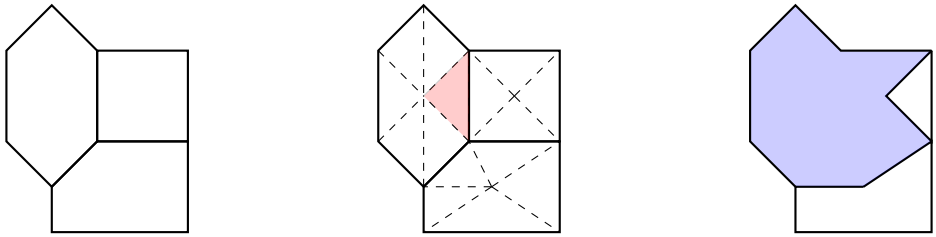

Figure 5.6: Left: polygonal mesh $\mathcal{T}_n$. Center: regular subtriangulation $\widetilde{\mathcal{T}}_n$, see Remark 2, in light red a triangle T. Right: in light blue, $\omega(T)$, triangular patch around T, defined in (5.4).

Lemma 5.1.1. *Given $u \in H_0^1(\Omega)$, there exists $u_M \in \mathcal{S}^{\widetilde{\mathbf{p}},0}(\Omega, \widetilde{\mathcal{T}}_n)$, see (5.2), such that, for each T triangle in $\widetilde{\mathcal{T}}_n$ and for each s edge of $\widetilde{\mathcal{E}}_n$, the following estimates hold true:*

$$\|u - u_M\|_{0,T} + \frac{h_T}{p_T}|u - u_M|_{1,T} \leq c_M \frac{h_T}{p_T}|u|_{1,\omega(T)}, \tag{5.6a}$$

$$\|u - u_M\|_{0,s} \leq c_M \left(\frac{h_T}{p_T}\right)^{\frac{1}{2}} |u|_{1,\omega(s)}, \tag{5.6b}$$

where c_M is a positive constant independent of u, h_T and p_T and where $\omega(T)$ and $\omega(s)$ are the triangular patch around triangle T and the triangular patch around edge s defined in (5.4) and (5.5) respectively.

Proof. This result was firstly shown in [82, Theorem 2.3] and [84, Theorem 2.1]. Here, we only give a sketch of the proof, which mainly bases on two ingredients. We recall that we are assuming that assumptions (**G0**)-(**G1**)-(**G2**)-(**P1**) hold true.

The first one is a local approximation result. Given $\mathbf{V}$ a vertex of the subtriangulation $\widetilde{\mathcal{T}}_n$, $\omega(\mathbf{V})$ the triangular patch around $\mathbf{V}$ defined in (5.3) and $p_{\mathbf{V}}$ the polynomial degree associated with vertex $\mathbf{V}$ defined in (5.1), the following result holds true, see [82, Lemma 2.7]: there exists a bounded linear operator $I_{\mathbf{V}} : L^1(\omega_{\mathbf{V}}) \to \mathcal{S}^{\widetilde{\mathbf{p}}_{\mathbf{V}}-1,0}(\omega(\mathbf{V}), \widetilde{\mathcal{T}}_n|_{\omega(\mathbf{V})}), \mathcal{S}^{\widetilde{\mathbf{p}}_{\mathbf{V}}-1,0}(\omega(\mathbf{V}), \widetilde{\mathcal{T}}_n|_{\omega(\mathbf{V})})$ being defined in (5.2), such that, for all $T \in \widetilde{\mathcal{T}}_n|_{\omega(\mathbf{V})}$ and each edge in $\widetilde{\mathcal{T}}_n|_{\omega(\mathbf{V})}$:

$$\begin{aligned} &\|u - I_{\mathbf{V}}u\|_{0,T} + \frac{h_T}{p_T}|u - I_{\mathbf{V}}u|_{1,T} \leq c\frac{h_T}{p_T}|u|_{1,\omega(\mathbf{V})}, \\ &\|u - I_{\mathbf{V}}u\|_{0,s} \leq c\left(\frac{h_T}{p_T}\right)^{\frac{1}{2}} |u|_{1,\omega(\mathbf{V})}, \end{aligned} \tag{5.7}$$

where c is a positive constant independent of u, h_K and p_K.

The second ingredient is the following construction, typical of the partition of unity method [18, 85]. We associate with every vertex $\mathbf{V}$ of $\widetilde{\mathcal{T}}_n$ the standard hat function given by the (unique) piecewise continuous affine polynomial over $\widetilde{\mathcal{T}}_n$ which is 1 at vertex $\mathbf{V}$ and 0 at all the other vertices.

It is possible to check, see [82, Lemma 2.6], that the function u_M satisfying (5.6a) and (5.6b) is given by:

$$u_M = \sum_{\mathbf{V} \text{ vertex of } \widetilde{\mathcal{T}}_n} \varphi_{\mathbf{V}}\, I_{\mathbf{V}}u. \tag{5.8}$$

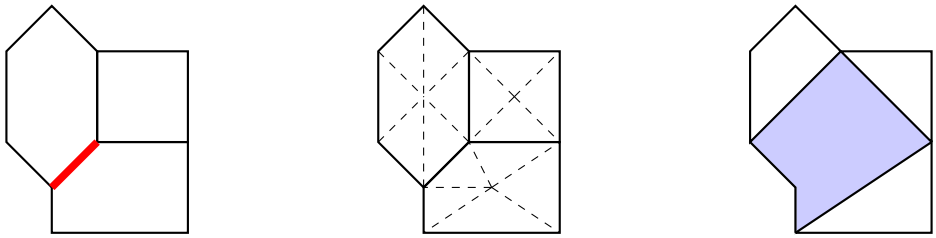

Figure 5.7: Left: polygonal mesh $\mathcal{T}_n$, in red an edge s. Center: regular subtriangulation $\widetilde{\mathcal{T}}_n$, see Remark 2. Right: in light blue, $\omega(s)$, triangular patch around edge s, defined in (5.5).

□

Lemma 5.1.1 is a key ingredient for the following result which deals with local approximation properties of functions in the VE space. Such result and its proof differs from their counterparts in Lemmata 2.2.3, 2.3.3 and 3.2.4, since we are here assuming only $u \in H^1(K)$.

Lemma 5.1.2. *Let u be the solution to (1.27). Let $K \in \mathcal{T}_n$ and let s one of its edges. Then, there exists a function $u_I \in V_n$, such that its restriction to K satisfies the following estimates:*

$$\|u - u_I\|_{0,K} + h_K |u - u_I|_{1,K} \leq c h_K |u|_{1,\omega(K)}, \tag{5.9a}$$

$$\|u - u_I\|_{0,s} \leq c \left(\frac{h_T}{p_T}\right)^{\frac{1}{2}} |u|_{1,\omega(s)}, \tag{5.9b}$$

where c is a positive constant independent of u, h_K and p_K and where $\omega(K)$ and $\omega(s)$ are the triangular patch around polygon K and the triangular patch around edge s defined in (5.4) and (5.5) respectively.

Proof. We define u_I on polygon K as the solution to the following problem:

$$\begin{cases} -\Delta u_I = -\Delta \Pi^\nabla_{p_K} u & \text{in } K, \\ u_I = u_M & \text{on } \partial K, \end{cases} \tag{5.10}$$

where $\Pi^\nabla_{p_K}$ is the energy projector defined in (2.8), while the Melenk quasi-interpolant u_M is introduced in Lemma 5.1.1.

The L^2 estimates on edge s (5.9b) is a straightforward consequence of (5.6b).

Proceeding as in Lemma 2.2.3, the H^1 error bound in (5.9a) is a consequence of a minimum energy argument. In fact, we deduce from (5.10) that:

$$\begin{cases} -\Delta(u_I - \Pi^\nabla_{p_K} u) = 0 & \text{in } K, \\ u_I - \Pi^\nabla_{p_K} u = u_M - \Pi^\nabla_{p_K} u & \text{on } \partial K, \end{cases}$$

which implies:

$$\begin{aligned} |u - \Pi^\nabla_{p_K} u|_{1,K} &\leq \inf \left\{ |v|_{1,K} \mid v \in H^1(K) \text{ and } v = u_M - \Pi^\nabla_{p_K} u \text{ on } \partial K \right\} \\ &\leq |u_M - \Pi^\nabla_{p_K} u|_{1,K} \leq |u - \Pi^\nabla_{p_K} u_M|_{1,K} + |u - \Pi^\nabla_{p_K} u|_{1,K}. \end{aligned}$$

Therefore:

$$|u - u_I|_{1,K} \leq 2|u - \Pi^\nabla_{p_K} u|_{1,K} + |u - u_M|_{1,K}$$

and the desired inequality follows from standard error estimates, see e.g. [49], and from Lemma 5.1.1.

Regarding the L^2 estimates in (5.9a), we note that:

$$\|u - u_I\|_{0,K} \leq \|u - u_M\|_{0,K} + \|u_I - u_M\|_{0,K}.$$

The assertion of the theorem is then a consequence of Lemma 5.1.1, a Poincaré inequality, a triangular inequality and the estimate on the H^1 seminorm in (5.9a). □

Remark 9. Comparing the error estimates of Lemmata 5.1.1 and 5.1.2, it is possible to observe that local estimates stated in (5.9a) by functions in the VE space are suboptimal of one power of p.

Optimal L^2 approximation estimates by means of functions in the VE space are currently under investigation and are going to appear in future publications.

5.1.2 A lifting operator

In this section, we recall the existence of a lifting operator from an edge of a triangle to its interior.

Theorem 5.1.3. *Given $T \in \widetilde{\mathcal{T}}_n$ a triangle and s any of its edges, let b_s be the quadratic bubble function associated with edge s. Moreover, assume that $h_T \approx h_s$ for all edges s of T. Given $q_{p_s} \in \mathbb{P}_{p_s}(s)$ and $\alpha \in \left(\frac{1}{2}, 1\right]$, there exist a function $E(q_{p_s}) \in H^1(T)$ such that, for every $\varepsilon > 0$:*

$$E(q_{p_s})|_s = q_{p_s} b_s^{\alpha}, \qquad E(q_{p_s})|_{\partial T \setminus s} = 0, \tag{5.11}$$

$$\|E(q_{p_s})\|_{0,T}^2 \leq c_\alpha \, h_T \, \varepsilon \|q_{p_s} b_s^{\frac{\alpha}{2}}\|_{0,s}^2, \tag{5.12}$$

$$|E(q_{p_s})|_{1,T}^2 \leq c_\alpha \, h_T^{-1} \, (\varepsilon p_T^{2(2-\alpha)} + \varepsilon^{-1}) \|q_{p_s} b_s^{\frac{\alpha}{2}}\|_{0,s}^2, \tag{5.13}$$

where c_α is a positive constant depending only on α.

Proof. The assertion follows from [84, Lemma 2.6] along with a scaling argument. □

Note that, since $E(q_{p_s})$ annihilates on $\partial T \setminus s$, then it can be extended to 0 on the remaining part of the polygon containing T as part of its subtriangulation. As a consequence, Theorem 5.1.3 can be "generalized" in a straightforward way, putting on the left-hand side (semi)norms on the complete polygon containing T in lieu of the same (semi)norms on T.

5.2 A posteriori error analysis

In this section, we build an error estimator and we prove upper and lower bounds with respect to the H^1 error of the method.

The remainder of the the section is structured as follows. In Section 5.2.1, we write the residual equation basing mainly on the results presented in [54]. In Section 5.2.2, we construct an error estimator and we show that the H^1 seminorm of the error can be bounded in terms of such an estimator. In Section 5.2.3, we show that the *local* estimator can be bounded by the H^1 seminorm of the *quasi-local* error plus a couple of terms involving the oscillation on the right-hand side of (1.27) and the stabilization of the virtual element method. Finally, in Section 5.2.4, we summarize the results presented in the foregoing sections.

In order to avoid unnecessary technicalities in dealing with the discrete right-hand side (3.15), we assume that (3.3) holds true, i.e. we demand that $p_K \geq 2$ for all $K \in \mathcal{T}_n$.

5.2.1 The residual equation

We begin by introducing the residual equation. Let $e := u - u_n$ be the difference between the solution to the continuous (1.27) and discrete (3.17) problems respectively. In order to avoid a heavy notation regarding the oscillation of the right-hand side we denote with an abuse of notation $\langle f_n, v_n \rangle_n$ by $(f_n, v_n)_{0,\Omega}$ where here f_n denotes $\Pi^0_{p_K-2} f$, $\Pi^0_{p_K-2}$ being the L^2 projector defined in (2.18). Given $v \in H^1_0(\Omega)$ and $\chi_n \in V_n$, one has:

$$\begin{aligned} a(e, v) &= (f, v)_{0,\Omega} - a(u_n, v) = (f, v)_{0,\Omega} - a(u_n, \chi_n) - a(u_n, v - \chi_n) \\ &= (f, v)_{0,\Omega} - (f_n, \chi_n)_{0,\Omega} + a_n(u_n, \chi_n) - a(u_n, \chi_n) - a(u_n, v - \chi_n) \\ &= (f - f_n, \chi_n)_{0,\Omega} + (f, v - \chi_n)_{0,\Omega} + a_n(u_n, \chi_n) - a(u_n, \chi_n) - a(u_n, v - \chi_n). \end{aligned} \tag{5.14}$$

We rewrite the last term of the right-hand side of (5.14) by observing that, given $w \in H_0^1(\Omega)$, the following holds true:

$$\begin{aligned} a(u_n, w) &= \sum_{K\in\mathcal{T}_n} a^K(u_n, w) = \sum_{K\in\mathcal{T}_n} \left\{a^K(\Pi^\nabla_{p_K} u_n, w) + a^K((I - \Pi^\nabla_{p_K})u_n, w)\right\} \\ &= \sum_{K\in\mathcal{T}_n} \left\{-(\Delta\Pi^\nabla_{p_K} u_n, w)_{0,K} + a^K((I - \Pi^\nabla_{p_K})u_n, w)\right\} + \sum_{s\in\mathcal{E}_n} \left(\left[\!\left[\partial_{\mathbf{n}}\Pi^\nabla_{p_K} u_n\right]\!\right]_s, w\right)_{0,s}, \end{aligned} \tag{5.15}$$

where $[\![\cdot]\!]_s$ denotes the jump across edge s.

We highlight that the key point in (5.15) is the presence of a polynomial projector; without such a projector we would not be able to compute exactly the jump across the edges of normal derivatives of functions in the VE space.

Plugging (5.15) in (5.14) with $w = v - \chi_n$, we deduce:

$$\begin{aligned} a(e, v) = &\sum_{K\in\mathcal{T}_n} \left\{(\Delta\Pi^\nabla_{p_K} u_n + f_n, v - \chi_n)_{0,K} - a^K((I - \Pi^\nabla_{p_K})u_n, v - \chi_n) + (f - f_n, v - \chi_n)_{0,K}\right\} \\ &+ (f - f_n, \chi_n)_{0,\Omega} + a_n(u_n, \chi_n) - a(u_n, \chi_n) - \sum_{s\in\mathcal{E}_n} \left(\left[\!\left[\partial_{\mathbf{n}}\Pi^\nabla_{p_K} u_n\right]\!\right], v - \chi_n\right)_{0,s} \\ = &\sum_{K\in\mathcal{T}_n} \left\{(\Delta\Pi^\nabla_{p_K} u_n + f_n, v - \chi_n)_{0,K} + (f - f_n, v)_{0,K} - a^K((I - \Pi^\nabla_{p_K})u_n, v - \chi_n)\right. \\ &\left. + a^K_n(u_n, \chi_n) - a^K(u_n, \chi_n)\right\} - \sum_{s\in\mathcal{E}_n} \left(\left[\!\left[\partial_{\mathbf{n}}\Pi^\nabla_{p_K} u_n\right]\!\right]_s, v - \chi_n\right)_{0,s}. \end{aligned} \tag{5.16}$$

The first two internal terms and the edge term are analogous to the terms appearing in the *hp* FEM counterpart of the residual equation, see [84, Lemma 3.1]. The only difference here, is that we need a term containing the polynomial projection $\Pi^\nabla_{p_K}$, since in the following we use *hp* polynomial inverse estimates employing weighted bubble functions. In the case of FEM such a projection applied to the solution coincides with the solution itself (since the solution is a piecewise polynomial). The other terms are instead typical of the VEM framework and they take into account the fact that the VEM bilinear form an approximation of the exact one.

5.2.2 Upper bound

In this section, we both discuss the construction of an error estimator and the bound of the energy error with respect to such an estimator.

To this purpose, we use (5.16) with $v = e := u - u_n$ and $\chi_n = e_I = (u - u_n)_I$, where the approximation properties of the virtual interpolant e_I of e are described in Lemma 5.1.2. We obtain:

$$\begin{aligned} |e|^2_{1,\Omega} = &\sum_{K\in\mathcal{T}_n} \left\{(\Delta\Pi^\nabla_{p_K} u_n + f_n, e - e_I)_{0,K} + (f - f_n, e)_{0,K}\right. \\ &\left. - a^K((I - \Pi^\nabla_{p_K})u_n, e - e_I) + a^K_n(u_n, e_I) - a^K(u_n, e_I)\right\} \\ &- \sum_{s\in K_i} \left(\left[\!\left[\partial_{\mathbf{n}}\Pi^\nabla_{p_K} u_n\right]\!\right]_s, e - e_I\right)_{0,s} \\ =: &\sum_{K\in\mathcal{T}_n} \{I + II + III + IV\} + \sum_{s\in K_i} V. \end{aligned} \tag{5.17}$$

We estimate the five local terms separately. We start with the first one, i.e. the bound on the projected internal residual. Applying Lemma 5.1.2, we get:

$$I := (\Delta\Pi^\nabla_{p_K} u_n + f_n, e - e_I)_{0,K} \le \|\Delta\Pi^\nabla_{p_K} u_n + f_n\|_{0,K}\|e - e_I\|_{0,K} \lesssim h_K\|\Delta\Pi^\nabla_{p_K} u_n + f_n\|_{0,K}|e|_{1,\omega(K)}. \tag{5.18}$$

Importantly, we observe that if we had optimal approximation estimates in Lemma 5.1.1, then we would gain here a factor p^{-1} (currently a work in progress).

Secondly, we investigate the term involving the oscillation on the right-hand side. Owing to L^2 orthogonality and approximation properties of such projector, see Lemma 2.3.4, we can write:

$$II := (f - f_n, e)_{0,K} = (f - f_n, e - \Pi^0_{p_K-2} e)_{0,K} \leq \|f - f_n\|_{0,K} \frac{h_K}{p_K} |e|_{1,K},$$

where we recall that the L^2 projector $\Pi^0_{p_K-2}$ is defined in (2.18).

Next, we deal with the projected edge residual term:

$$\begin{aligned} V &:= -\left(\left[\!\left[\partial_{\mathbf{n}} \Pi^\nabla_{p_K} u_n \right]\!\right]_s, e - e_I \right)_{0,s} \leq \left\| \left[\!\left[\partial_{\mathbf{n}} \Pi^\nabla_{p_K} u_n \right]\!\right]_s \right\|_{0,s} \|e - e_I\|_{0,s} \\ &\lesssim \left(\frac{h_s}{p_s} \right)^{\frac{1}{2}} \left\| \left[\!\left[\partial_{\mathbf{n}} \Pi^\nabla_{p_K} u_n \right]\!\right]_s \right\|_{0,s} |e|_{1,\omega(s)} \leq \left(\frac{h_s}{p_s} \right)^{\frac{1}{2}} \left\| \left[\!\left[\partial_{\mathbf{n}} \Pi^\nabla_{p_K} u_n \right]\!\right]_s \right\|_{0,s} |e|_{1,\omega(K)}, \end{aligned}$$

where in the last but one inequality we employed Lemma 5.1.2.

The inconsistency VEM term can be bounded as follows:

$$\begin{aligned} III &:= -a^K((I - \Pi^\nabla_{p_K}) u_n, e - e_I) \leq |(I - \Pi^\nabla_{p_K}) u_n|_{1,K} |e - e_I|_{1,K} \\ &\lesssim |(I - \Pi^\nabla_{p_K}) u_n|_{1,K} |e|_{1,\omega(K)} \lesssim \alpha_*(p_K)^{-\frac{1}{2}} S^K((I - \Pi^\nabla_{p_K}) u_n, (I - \Pi^\nabla_{p_K}) u_n)^{\frac{1}{2}} |e|_{1,\omega(K)}, \end{aligned}$$

where we applied again Lemma 5.1.2 (in the last but one inequality) and the stability property of VEM (3.14) (in the last inequality). We emphasize that we make appear the stabilization term since in the definition of the error residual we need computable quantities only.

Finally, we study the error related to the approximation of the bilinear form:

$$\begin{aligned} IV &:= a^K_n(u_n, e_I) - a^K(u_n, e_I) = a^K(\Pi^\nabla_{p_K} u_n, \Pi^\nabla_{p_K} e_I) + S^K((I - \Pi^\nabla_{p_K}) u_n, (I - \Pi^\nabla_{p_K}) e_I) - a^K(u_n, e_I) \\ &= a^K(\Pi^\nabla_{p_K} u_n - u_n, e_I) + S^K((I - \Pi^\nabla_{p_K}) u_n, (I - \Pi^\nabla_{p_K}) e_I) \\ &\leq |u_n - \Pi^\nabla_{p_K} u_n|_{1,K} |e_I|_{1,K} + S^K((I - \Pi^\nabla_{p_K}) u_n, (I - \Pi^\nabla_{p_K}) e_I) \\ &\lesssim \alpha_*(p_K)^{-\frac{1}{2}} S^K((I - \Pi^\nabla_{p_K}) u_n, (I - \Pi^\nabla_{p_K}) u_n)^{\frac{1}{2}} |e|_{1,\omega(K)} \\ &\quad + S^K((I - \Pi^\nabla_{p_K}) u_n, (I - \Pi^\nabla_{p_K}) u_n)^{\frac{1}{2}} \alpha^*(p_K)^{\frac{1}{2}} |(I - \Pi^\nabla_{p_K}) e_I|_{1,K} \\ &\lesssim \left(\frac{\alpha^*(p_K)}{\alpha_*(p_K)} \right)^{\frac{1}{2}} S^K((I - \Pi^\nabla_{p_K}) u_n, (I - \Pi^\nabla_{p_K}) u_n)^{\frac{1}{2}} |e|_{1,\omega(K)}, \end{aligned}$$

where we applied several times Lemma 5.1.2 and the stability property (3.14).

In order to simplify the notation, we henceforth write:

$$R_K := (\Delta \Pi^\nabla_{p_K} u_n + f_n)|_K \qquad \forall\, K \in \mathcal{T}_n, \qquad\qquad R_s := \left[\!\left[\partial_{\mathbf{n}} \Pi^\nabla_{p_K} u_n \right]\!\right]_s \quad \forall\, s \text{ edge of } K. \tag{5.19}$$

Plugging the estimates on the five terms in (5.17), we get:

$$\begin{aligned} |e|^2_{1,\Omega} &\lesssim \sum_{K \in \mathcal{T}_n} \left\{ h_K^2 \|R_K\|^2_{0,K} + \frac{h_K^2}{p_K^2} \|f - f_n\|^2_{0,K} + \frac{\alpha^*(p_K)}{\alpha_*(p_K)} S^K((I - \Pi^\nabla_{p_K}) u_n, (I - \Pi^\nabla_{p_K}) u_n) \right\} \\ &\quad + \sum_{s \in K_i} \frac{h_s}{p_s} \|R_s\|^2_{0,s} \\ &= \sum_{K \in \mathcal{T}_n} \left\{ p_K^2 \eta_K^2 + \frac{h_K^2}{p_K^2} \|f - f_n\|^2_{0,K} + \frac{\alpha^*(p_K)}{\alpha_*(p_K)} S^K((I - \Pi^\nabla_{p_K}) u_n, (I - \Pi^\nabla_{p_K}) u_n) \right\} \\ &\quad + \sum_{s \in \mathcal{E}_n} \eta_s^2 =: \eta, \end{aligned} \tag{5.20}$$

where we have set the local error estimators as:

$$\eta_K = \frac{h_K}{p_K} \|R_K\|_{0,K}, \quad \eta_s = \left(\frac{h_s}{p_s} \right)^{\frac{1}{2}} \|R_s\|_{0,s}. \tag{5.21}$$

In (5.20), we have presented a possible choice η for the global error estimator. In particular, we have bounded the H^1 seminorm of the error of the method with such a global estimator. We note once more that the term involving the internal residual is suboptimal in terms of p. In fact, the hp FEM counterpart, see [84, Lemma 3.1], has not the factor p_K^2 in front of it. The suboptimality in terms of p is due to the suboptimality of the L^2 estimates by functions in the VE space, presented in Lemma 5.1.2 and consequently when bounding term I in (5.18), see also Remark 9. A better L^2 estimate in terms of p is currently work in progress.

5.2.3 Lower bound

In this section, we bound the error estimator η introduced in (5.20) with the H^1 seminorm of the error of the method plus an oscillation term for the right-hand side and a term related to the stabilization of the method. In particular, we only need to bound the local error estimators in (5.21).

The remainder of the section is organized as follows. In Section 5.2.3.1, we bound the bulk term appearing in the definition of the global error residual (5.20) with the H^1 seminorm of the error plus a term involving the oscillation of the right-hand side and a term related to the nonexactness of the VEM bilinear form, whereas in Section 5.2.3.2, we prove analogous bounds for the boundary term appearing in (5.20).

5.2.3.1 Bounding the internal residual

We begin with the term involving R_K, namely the local internal residual. To this purpose, we note that plugging $\chi_n = 0$ in (5.16), we have:

$$a(e,v) = \sum_{K\in\mathcal{T}_n} \left\{ (R_K, v)_{0,K} + (f - f_n, v)_{0,K} - a^K((I - \Pi^\nabla_{p_K})u_n, v) \right\} - \sum_{s\in K_i} (R_s, v)_{0,s}. \tag{5.22}$$

Let us focus our attention on a single element K. Given b_K the piecewise bubble function associated with element K defined as the piecewise bubble function over the subtriangulation of K, see also (B.37), we plug $v = b_K^\alpha R_K$ in (5.22) with $\alpha > \frac{1}{2}$, obtaining:

$$\begin{aligned} a(e, b_K^\alpha R_K) &= \sum_{K'\in\mathcal{T}_n} \left\{ (R_{K'}, b_K^\alpha R_K)_{0,K'} + (f - f_n, b_K^\alpha R_K)_{0,K'} - a^{K'}((I - \Pi^\nabla_{p_{K'}})u_n, b_K^\alpha R_K) \right\} \\ &= (R_K, b_K^\alpha R_K)_{0,K} + (f - f_n, b_K^\alpha R_K)_{0,K} - a^K((I - \Pi^\nabla_{p_K})u_n, b_K^\alpha R_K), \end{aligned} \tag{5.23}$$

since b_K is null on ∂K and can be trivially extended to 0 outside.

From (5.23), we get:

$$\begin{aligned} \|b_K^{\frac{\alpha}{2}} R_K\|_{0,K}^2 = (R_K, b_K^\alpha R_K)_{0,K} &= a^K(e, b_K^\alpha R_K) - (f - f_n, b_K^\alpha R_K)_{0,K} + a^K((I - \Pi^\nabla_{p_K})u_n, b_K^\alpha R_K) \\ &\lesssim |b_K^\alpha R_K|_{1,K}|e|_{1,K} + \|(f - f_n)b_K^{\frac{\alpha}{2}}\|_{0,K}\|b_K^{\frac{\alpha}{2}} R_K\|_{0,K} + |(I - \Pi^\nabla_{p_K})u_n|_{1,K}|b_K^\alpha R_K|_{1,K}. \end{aligned}$$

As a consequence, applying the stability bounds (3.14) and the hp polynomial inverse estimate on polygons (B.47), one has:

$$\|b_K^{\frac{\alpha}{2}} R_K\|_{0,K} \lesssim \frac{p_K^{2-\alpha}}{h_K} \left\{ |e|_{1,K} + \alpha_*(p_K)^{-\frac{1}{2}} S^K((I - \Pi^\nabla_{p_K})u_n, (I - \Pi^\nabla_{p_K})u_n)^{\frac{1}{2}} \right\} + \|f - f_n\|_{0,K},$$

or equivalently:

$$\frac{h_K}{p_K}\|b_K^{\frac{\alpha}{2}} R_K\|_{0,K} \lesssim p_K^{1-\alpha} \left\{ |e|_{1,K} + \alpha_*(p_K)^{-\frac{1}{2}} S^K((I - \Pi^\nabla_{p_K})u_n, (I - \Pi^\nabla_{p_K})u_n)^{\frac{1}{2}} \right\} + \frac{h_K}{p_K}\|f - f_n\|_{0,K}.$$

We are now ready to prove the bound on the internal residual. Recalling that $\alpha > \frac{1}{2}$, the hp polynomial inverse estimate on polygons (B.45) implies:

$$\|R_K\|_{0,K} \lesssim p_K^\alpha \|b_K^{\frac{\alpha}{2}} R_K\|_{0,K}.$$

Hence:

$$\frac{h_K}{p_K}\|R_K\|_{0,K} \lesssim p_K \left\{ |e|_{1,K} + \alpha_*(p_K)^{-\frac{1}{2}} S^K((I-\Pi^\nabla_{p_K})u_n, (I-\Pi^\nabla_{p_K})u_n)^{\frac{1}{2}} \right\} + h_K p_K^{\alpha-1}\|f-f_n\|_{0,K}.$$

Since α is arbitrarily bigger than $\frac{1}{2}$ and appears only in front of the oscillation of the right-hand side, we minimize the loss in terms of p by requiring $\alpha = \frac{1}{2}+\varepsilon$, with ε positive and arbitrarily small.

This gives us, for every $\varepsilon > 0$ arbitrarily small:

$$\frac{h_K^2}{p_K^2}\|R_K\|^2_{0,K} \lesssim p_K^2 \left(|e|^2_{1,K} + \alpha_*(p_K)^{-1} S^K((I-\Pi^\nabla_{p_K})u_n, (I-\Pi^\nabla_{p_K})u_n) \right) + \frac{h_K^2}{p_K^{1-2\varepsilon}}\|f-f_n\|^2_{0,K}. \tag{5.24}$$

5.2.3.2 Bounding the edge residual

Next, we investigate the bound on the edge residual. Without loss of generality s is an internal edge; the general case straightforwardly follows.

Let R_s be the edge residual on edge s. We henceforth consider a function $\overline{R}_s$ defined as $E(R_s)$, where R_s is defined in (5.19) while the "extension" operator E is defined in Theorem 5.1.3. We recall that the restriction of $\overline{R}_s$ on s is equal to $b_s^\alpha R_s$, where b_s is the quadratic edge bubble function on s and where $\alpha > \frac{1}{2}$.

We note that $\overline{R}_s$, which is defined on the two triangles T_1 and T_2 abutting edge s, can be extended to 0 outside $\overline{T}_1 \cup \overline{T}_2$, see (5.5). Let us denote by K_1 and K_2 the two polygons containing triangles T_1 and T_2.

We plug $v = \overline{R}_s$ and $\chi_n = 0$ in (5.16), obtaining:

$$a(e, \overline{R}_s) = \sum_{i=1}^{2} \left\{ (R_{K_i}, \overline{R}_s)_{0,K_i} + (f-f_n, \overline{R}_s)_{0,s} - a^{K_i}((I-\Pi^\nabla_{p_{K_i}})u_n, \overline{R}_s) \right\} - (R_s, \overline{R}_s)_{0,s}. \tag{5.25}$$

We observe that the following bound on the third term on the right-hand side of (5.25) holds true:

$$\begin{aligned}\sum_{i=1}^{2} a^{K_i}((I-\Pi^\nabla_{p_{K_i}})u_n, \overline{R}_s) &\leq \sum_{i=1}^{2} |(I-\Pi^\nabla_{p_{K_i}})u_n|_{1,K_i} |\overline{R}_s|_{1,K_i} \\ &\lesssim \sum_{i=1}^{2} \left\{ \alpha_*(p_{K_i})^{-\frac{1}{2}} S^{K_i}((I-\Pi^\nabla_{p_{K_i}})u_n, (I-\Pi^\nabla_{p_{K_i}})u_n)^{\frac{1}{2}} \right\} |\overline{R}_s|_{1,K_i}.\end{aligned} \tag{5.26}$$

We deduce from (5.25):

$$\begin{aligned}&\|b_s^{\frac{\alpha}{2}} R_s\|^2_{0,s} = (R_s, \overline{R}_s)_{0,s} \\ &= a(e, \overline{R}_s) - \sum_{i=1}^{2} \left\{ (R_{K_i}, \overline{R}_s)_{0,K_i} + (f-f_n, \overline{R}_s)_{0,K_i} - a^{K_i}((I-\Pi^\nabla_{p_{K_i}})u_n, \overline{R}_s) \right\}.\end{aligned}$$

and thus, by (5.26):

$$\begin{aligned}&\|b_s^{\frac{\alpha}{2}} R_s\|^2_{0,s} \\ &\lesssim \sum_{i=1}^{2} \left\{ \left(|e|_{1,K_i} + \alpha_*(p_{K_i})^{-\frac{1}{2}} S^{K_i}((I-\Pi^\nabla_{p_{K_i}})u_n, (I-\Pi^\nabla_{p_{K_i}})u_n)^{\frac{1}{2}} \right) |\overline{R}_s|_{1,K_i} \right. \\ &\qquad \left. + \left(\|R_{K_i}\|_{0,K_i} + \|f-f_n\|_{0,K_i} \right) \|\overline{R}_s\|_{0,K_i} \right\}.\end{aligned}$$

We can now apply Theorem 5.1.3 with $\alpha = 1$ on $|\overline{R}_s|_{1,K_i}$ and $\|\overline{R}_s\|_{0,K_i}$, obtaining for every

$\varepsilon > 0$:

$$\begin{aligned}
&\|b_s^{\frac{\alpha}{2}} R_s\|_{0,s}^2 \\
&\lesssim \sum_{i=1}^{2} \left\{ \left(|e|_{1,K_i} + \alpha_*(p_{K_i})^{-\frac{1}{2}} S^{K_i}((I-\Pi^{\nabla}_{p_{K_i}})u_n, (I-\Pi^{\nabla}_{p_{K_i}})u_n)^{\frac{1}{2}} \right) h_s^{-\frac{1}{2}} \left(\varepsilon p_{K_i}^{2(2-\alpha)} + \varepsilon^{-1} \right)^{\frac{1}{2}} \|b_s^{\frac{1}{2}} R_s\|_{0,s} \right. \\
&\qquad \left. + \left(\|R_{K_i}\|_{0,K_i} + \|f - f_n\|_{0,K_i} \right) h_s^{\frac{1}{2}} \varepsilon^{\frac{1}{2}} \|b_s^{\frac{1}{2}} R_s\|_{0,s} \right\}.
\end{aligned}$$

Therefore, we can write:

$$\begin{aligned}
&\left(\frac{h_s}{p_s}\right)^{\frac{1}{2}} \|b_s^{\frac{\alpha}{2}} R_s\|_{0,s} \\
&\lesssim \sum_{i=1}^{2} \left\{ \left(|e|_{1,K_i} + \alpha_*(p_K)^{-\frac{1}{2}} S^{K_i}((I-\Pi^{\nabla}_{p_{K_i}})u_n, (I-\Pi^{\nabla}_{p_{K_i}})u_n)^{\frac{1}{2}} \right) \left(\varepsilon p_{K_i}^{2(2-\alpha)} + \varepsilon^{-1} \right)^{\frac{1}{2}} p_s^{-\frac{1}{2}} \right. \\
&\qquad \left. + \varepsilon^{\frac{1}{2}} \frac{h_s}{p_s^{\frac{1}{2}}} \left(\|R_{K_i}\|_{0,K_i} + \|f - f_n\|_{0,K_i} \right) \right\}.
\end{aligned}$$

Hence, elevating to the square both sides, one deduces:

$$\begin{aligned}
\frac{h_s}{p_s} \|b_s^{\frac{\alpha}{2}} R_s\|_{0,s}^2 \lesssim \sum_{i=1}^{2} &\left\{ \left(|e|_{1,K_i}^2 + \alpha_*(p_{K_i})^{-1} S^{K_i}((I-\Pi^{\nabla}_{p_{K_i}})u_n, (I-\Pi^{\nabla}_{p_{K_i}})u_n) \right) \left(\varepsilon p_{K_i}^{2(2-\alpha)} + \varepsilon^{-1} \right) p_s^{-1} \right. \\
&\left. + \varepsilon \frac{h_s^2}{p_s} \left(\|R_{K_i}\|_{0,K_i}^2 + \|f - f_n\|_{0,K_i}^2 \right) \right\}.
\end{aligned}$$

Applying the bound on the internal residual (5.24) and assumption (**P1**), we deduce:

$$\begin{aligned}
&\frac{h_s}{p_s} \|b_s^{\frac{\alpha}{2}} R_s\|_{0,s}^2 \\
&\lesssim \sum_{i=1}^{2} \left\{ \left(|e|_{1,K_i}^2 + \alpha_*(p_{K_i})^{-1} S^{K_i}((I-\Pi^{\nabla}_{p_{K_i}})u_n, (I-\Pi^{\nabla}_{p_{K_i}})u_n) \right) \left(\varepsilon p_{K_i}^{2(2-\alpha)} + \varepsilon^{-1} \right) p_s^{-1} \right. \\
&\qquad \left. + \varepsilon p_s \left(p_K^2 \left(|e|_{1,K}^2 + \alpha_*(p_K)^{-1} S^K((I-\Pi^{\nabla}_{p_K})u_n, (I-\Pi^{\nabla}_{p_K})u_n) \right) + \frac{h_K^2}{p_K^{1-2\varepsilon}} \|f - f_n\|_{0,K}^2 \right) \right\},
\end{aligned}$$

whence:

$$\begin{aligned}
&\frac{h_s}{p_s} \|b_s^{\frac{\alpha}{2}} R_s\|_{0,s}^2 \\
&\lesssim \sum_{i=1}^{2} \left\{ \left(|e|_{1,K_i}^2 + \alpha_*(p_{K_i})^{-1} S^{K_i}((I-\Pi^{\nabla}_{p_{K_i}})u_n, (I-\Pi^{\nabla}_{p_{K_i}})u_n) \right) \left[p_s^{-1} \left(\varepsilon p_{K_i}^{2(2-\alpha)} + \varepsilon^{-1} \right) + p_{K_i}^3 \varepsilon \right] \right. \\
&\qquad \left. \varepsilon p_{K_i}^{2(\varepsilon+1)} \left(\frac{h_{K_i}}{p_{K_i}} \right)^2 \|f - f_n\|_{0,K_i}^2 \right\},
\end{aligned}$$

Selecting $\varepsilon = p_s^{-2}$ and using once more assumption (**P1**), one obtains:

$$\begin{aligned}
&\frac{h_s}{p_s} \|b_s^{\frac{\alpha}{2}} R_s\|_{0,s}^2 \\
&\lesssim \sum_{i=1}^{2} \left\{ p_{K_i} \left(|e|_{1,K_i}^2 + \alpha_*(p_{K_i})^{-1} S^{K_i}((I-\Pi^{\nabla}_{p_{K_i}})u_n, (I-\Pi^{\nabla}_{p_{K_i}})u_n) \right) + p_{K_i}^{\frac{2}{p_K^2}} \left(\frac{h_{K_i}}{p_{K_i}} \right)^2 \|f - f_n\|_{0,K_i}^2 \right\}.
\end{aligned}$$

So far, we have assumed that $\alpha > \frac{1}{2}$. In order to get the desired bound on the edge residual, i.e. the one with $\alpha = 0$, we apply the 1D *hp* polynomial inverse estimate (B.6) with weights 0 and

$\frac{1}{2}+\varepsilon$, respectively, getting:

$$\begin{aligned}\frac{h_s}{p_s}\|R_s\|_{0,s}^2 &\lesssim p_s^{1+2\varepsilon}\frac{h_s}{p_s}\|b_s^{\frac{1}{2}}R_s\|_{0,s}^2\\ &\lesssim \sum_{i=1}^{2} p_{K_i}^{1+2\,\varepsilon}\left\{p_{K_i}\left(|e|_{1,K_i}^2+\alpha_*(p_{K_i})^{-1}S^{K_i}((I-\Pi_{p_{K_i}}^{\nabla})u_n,(I-\Pi_{p_{K_i}}^{\nabla})u_n)\right)\right.\\ &\qquad\left.+p_{K_i}^{\frac{2}{p_K^2}}\left(\frac{h_{K_i}}{p_{K_i}}\right)^2\|f-f_n\|_{0,K_i}^2\right\}.\end{aligned}$$

5.2.4 Summary

In this section, we collect in a single result the lower and upper bounds presented in Sections 5.2.2 and 5.2.3.

Theorem 5.2.1. *Assume that assumptions **(G0)-(G1)-(G2)-(P1)** hold true. Let u and u_n be the solutions to* (1.27) *and* (3.17) *respectively and let $e=u-u_n$. For all $K\in\mathcal{T}_n$ and $s\in\mathcal{E}_n$ internal edge, let η_K and η_s be the internal and edge residuals defined in* (5.21) *respectively. Then, the following upper bound for the energy of e holds true:*

$$\begin{aligned}|e|_{1,\Omega}^2 \lesssim &\sum_{K\in\mathcal{T}_n}\left\{p_K^2\eta_K^2+\frac{h_K^2}{p_K^2}\|f-f_n\|_{0,K}^2+\frac{\alpha^*(p_K)}{\alpha_*(p_K)}S^K((I-\Pi_{p_K}^{\nabla})u_n,(I-\Pi_{p_K}^{\nabla})u_n)\right\}\\ &+\sum_{s\in\mathcal{E}_n}\eta_s^2.\end{aligned}\tag{5.27}$$

Further, for every $K\in\mathcal{T}_n$, $s\in\mathcal{E}_n$ and for all $\varepsilon>0$, the following local lower bounds on the local internal and edge residuals hold true:

$$\begin{aligned}\eta_K^2 &\lesssim p_K^2\left(|e|_{1,K}^2+\alpha_*(p_K)^{-1}S^K((I-\Pi_{p_{K_i}}^{\nabla})u_n,(I-\Pi_{p_{K_i}}^{\nabla})u_n)\right)+\frac{h_K^2}{p_K^{1-2\varepsilon}}\|f-f_n\|_{0,K}^2,\\ \eta_s^2 &\lesssim \sum_{i=1}^{2} p_{K_i}^{1+2\,\varepsilon}\left\{p_{K_i}\left(|e|_{1,K_i}^2+\alpha_*(p_{K_i})^{-1}S^{K_i}((I-\Pi_{p_{K_i}}^{\nabla})u_n,(I-\Pi_{p_{K_i}}^{\nabla})u_n)\right)\right.\\ &\qquad\left.+p_{K_i}^{\frac{2}{p_K^2}}\left(\frac{h_{K_i}}{p_{K_i}}\right)^2\|f-f_n\|_{0,K_i}^2\right\},\end{aligned}\tag{5.28}$$

where the polygons K_i, $i=1,2$, in the second equation of (5.28) *are such that $\overline{K}_1\cap\overline{K}_2=s$. If s is a boundary edge, then the sum in the bound on the edge residual* (5.28) *reduces to a single term with all the quantities defined on element K, where $s=K\cap\partial\Omega$.*

We emphasize that the suboptimality of the L^2 approximation estimates by functions in the VE space presented in Lemma 5.1.2 implies an additional term p_K^2 in front of the internal residual η_K in (5.27).We deem that having an "optimal" version of Lemma 5.1.2 would mitigate the bounds in terms of p in Theorem 5.2.1; as already stated in Remark 9, such an optimal version of Theorem 5.2.1 is currently under investigation and is going to appear in future works.

It is moreover important to stress that, apart from the term involving the stabilization, the bounds of both the internal and edge residuals mimic their FEM counterparts, see [84, Lemmata 3.4, 3.5].

Finally, we highlight that in the upper and lower bounds one has to take into account the effect of the stabilization, which plays a role through the ratio $\frac{\alpha^*(p)}{\alpha_*(p)}$ in (5.27) and through $\alpha_*(p)^{-1}$ in (5.28). The effect in terms of p on these two terms is investigated in Chapter 6.

Chapter 6

The role of the stabilization in p and hp VEM

In Chapters 2, 3 and 4, we investigated the h and p, hp and Harmonic hp version of VEM respectively.

In all the three cases, we described how the discrete bilinear form is split into local bilinear forms which consist of the combination of two terms, see (2.13), (3.9) and (4.8): the first one is the standard local H^1 bilinear form applied to a energy projection defined on local virtual space into polynomial spaces, the second one is a stabilizing bilinear form defined on the product of kernel of the aforementioned projection.

We have not addressed yet the issue of introducing such local stabilizations, which we recall have to be properly chosen in order to avoid (or more likely to mitigate) the pollution effect on the convergence of the method, see Lemmata 2.1.1, 3.1.1 and 4.1.1.

The aim of the present chapter is to present various choices for the local stabilization, both recalling standard choices that can be found in VEM literature and introducing novel choices for the p and hp VEM framework.

The outline of the chapter follows. In Section 6.1, we recall the original choice of VEM stabilization, tailored for the h case, and we discuss numerically the associated stability bounds in terms of p (such a stabilization was also used in the first work dealing with p VEM namely [31]); moreover, we also mention other stabilizations available in the literature. In Section 6.2, we present instead some stabilizations for the hp version of VEM, that were introduced in [32]; such stabilizations are characterized by quite pessimistic bounds in terms of p, nonetheless we give numerical evidence that the actual behaviour of these bounds is in fact much milder than the theory asserts; throughout the section, hp polynomial inverse estimates on polygons proven in Appendix B are spreadly employed. In Section 6.3, some stabilizations for the hp version of Harmonic VEM are discussed. Explicit bounds in terms of p that are much better than those shown in hp VEM are proven; further, we also provide a recipe for constructing a provably p independent stabilization; we follow here [58]. Finally, in Section 6.4, we supply further comments regarding the issue of the stabilization and we rapidly summarize the results discussed in the chapter.

Before proceeding, we need additional notation. Given N_{V_K} the dimension of a local VE space defined on polygon K we define:

$$\left\{\mathrm{dof}_i^K\right\}_{i=1}^{N_{V_K}} = \{\mathrm{dof}_i\}_{i=1}^{N_{V_K}} \tag{6.1}$$

the set of degrees of freedom described in Section 2.1 and:

$$\left\{\varphi_i^K\right\}_{i=1}^{N_{V_K}} = \{\varphi_i\}_{i=1}^{N_{V_K}} \tag{6.2}$$

the local canonical VE basis, i.e. the set of functions satisfying:

$$\mathrm{dof}_i(\varphi_j) = \delta_{i,j} \qquad \forall\, i,\, j = 1, \dots, N_{V_K},$$

where $\delta_{i,j}$ it the Kronecker delta.

6.1 The original VEM stabilization

In this section, we recall the original VEM stabilization introduced firstly in [25,30] and we numerically investigate the behaviour in terms of p of the stability constants involved in bound (2.15).

We stress that in the first work concerning p VEM, namely [31], this stabilization was employed. We anticipate that the pollution effect described in Lemma 2.1.1 has a very mild impact in numerical tests in Section 7.1 also for finite Sobolev regularity as one would expect, cf. Theorem 2.2.6.

The original VEM stabilization reads:

$$S_1^K(u_{hp}, v_{hp}) = \sum_{i=1}^{N_{V_K}} \mathrm{dof}_i(u_{hp})\,\mathrm{dof}_i(v_{hp}) \qquad \forall\, u_{hp},\, v_{hp} \in V_{hp}(K), \tag{6.3}$$

where we recall that $V_{hp}(K)$ is defined in (2.3), N_{V_K} is the dimension of $V_{hp}(K)$ and dof_i is the i-th degree of freedom introduced in (6.1).

It is not clear how to prove explicit stabilization bounds (2.12) and (2.15) using S_1^K. What instead is clear is that choice S_1^K has the proper scaling in terms of h_K with respect to the local H^1 seminorm $|\cdot|_{1,K}$, whenever p is fixed. In fact, if we are given φ_i element of the canonical basis (6.2), we have:

$$S_1^K(\varphi_i, \varphi_i) = 1, \qquad |\varphi_i|_{1,K}^2 \approx 1.$$

We highlight that there exist variants of (6.3). We limit ourselves to recall two of them. The first one was introduced in [33]. While we have defined:

$$S_1^K(\varphi_i, \varphi_j) = \delta_{i,j},$$

where $\delta_{i,j}$ is the Kronecker delta, we define a variant S_3^K of S_1^K by requiring:

$$S_3^K(\varphi_i, \varphi_j) = \delta_{i,j}\, \max(1, a^K(\Pi_p^\nabla \varphi_i, \Pi_p^\nabla \varphi_j)), \tag{6.4}$$

where Π_p^∇ is defined in (2.8).

Another possible stabilization reads:

$$S_4^K(u_{hp}, v_{hp}) = \sum_{i=1}^{N_K^{bndr}} \mathrm{dof}_i^{bndr}(u_{hp})\,\mathrm{dof}_i^{bndr}(v_{hp}), \tag{6.5}$$

where N_K^{bndr} is the number of boundary dofs of space $V_{hp}(K)$ and $\left\{\mathrm{dof}_i^{bndr}\right\}_{i=1}^{N_K^{bndr}}$ denotes the set of boundary degrees of freedom.

We are now ready to discuss the dependence on p of the stability bounds in the complete local bilinear form (2.13). More precisely, given $K \in \mathcal{T}_n$, we want to investigate the behaviour in terms of p of the constants $\alpha_*(p)$ and $\alpha^*(p)$ introduced in (2.15).

We note that finding $\alpha_*(p)$ and $\alpha^*(p)$ in (2.15) is equivalent to find the minimum and the maximum eigenvalue, say λ_{min} and λ_{max}, of the generalized eigenvalue problem:

$$\mathbf{A}_{hp}^K \mathbf{v}_{hp} = \lambda \mathbf{A}^K \mathbf{v}_{hp}, \tag{6.6}$$

where $\mathbf{A}_{hp}^K$, $\mathbf{A}^K \in \mathbb{R}^{\dim(V_{hp}(K))\times\dim(V_{hp}(K))}$ are the local discrete and continuous stiffness matrices respectively:

$$(\mathbf{A}_{hp}^K)_{i,j} = a_{hp}^K(\varphi_i, \varphi_j), \qquad (\mathbf{A}^K)_{i,j} = a^K(\varphi_i, \varphi_j),$$

$\{\varphi_i\}_{i=1}^{\dim(V_{hp}(K))}$ being the local canonical virtual basis defined in (6.2). Since both matrixes (that are symmetric and positive semi-definite) have a kernel given by the vectors representing constant functions, without loss of generality we restrict the analysis to the zero-average functions in $V_h(K)$. Besides, since matrix $\mathbf{A}^K$ is not computable exactly, we approximate its entries by solving numerically the associated diffusion problem, using a very fine triangular mesh on the polygon and hp FEM.

We stress that we are in particular interested in the behaviour in terms of p of:

$$\frac{\alpha^*(p)}{\alpha_*(p)} \qquad \text{i.e.} \qquad \frac{\lambda_{max}}{\lambda_{min}}, \tag{6.7}$$

since this is the quantity that is involved in the pollution effect of which method (2.1) suffers, see Lemma 2.1.1.

In Table 6.1 we present tests on three regular sample polygons: a triangle, a square and a hexagon. In all three cases we assume that the polygons are equilateral.

Table 6.1 Minimum and maximum eigenvalues of the generalized eigenvalue problem (6.6) on: tr= a triangle; sq= a square; he= a hexagon. Stabilization employed: S_1^K.

p	tr. λ_{min}	tr. λ_{max}	sq. λ_{min}	sq. λ_{max}	he. λ_{min}	he. λ_{max}
2	1.0000e+00	1.0825e+00	1.0000e+00	1.1225e+00	4.6394e-01	1.2079e+00
3	6.1649e-01	1.0000e+00	3.7333e-01	1.1978e+00	4.4218e-01	1.2234e+00
4	2.7391e-01	1.0000e+00	3.0515e-01	1.0365e+00	4.5071e-01	1.3473e+00
5	6.1234e-02	1.0000e+00	3.0203e-01	1.2361e+00	4.2189e-01	1.3208e+00
6	4.4998e-02	1.0000e+00	2.0408e-01	1.0580e+00	4.2771e-01	1.2256e+00
7	2.3220e-02	1.0000e+00	2.0026e-01	1.1509e+00	4.0537e-01	1.2696e+00
8	7.9998e-03	1.0000e+00	1.3968e-01	1.0433e+00	4.0755e-01	1.2439e+00
9	5.2406e-03	1.0000e+00	1.3176e-01	1.1310e+00	4.0183e-01	1.2364e+00
10	2.6406e-03	1.0000e+00	8.9375e-02	1.0390e+00	3.8648e-01	1.2514e+00

First of all, we note that that $\lambda = 1$ is always an eigenvalue since, due to the consistency condition (2.14), for all vectors $\mathbf{v}_{hp}$ associated to polynomial functions the two operators above give the same result. Therefore λ_{max} is always bigger than or equal to 1 and λ_{min} always smaller than or equal to 1. We moreover observe that the maximum eigenvalue is almost constant in all the three cases. On the other hand, the minimum eigenvalue behaves differently, and depends on the polygon. In the case of the hexagon, it is still almost constant. For the square, we notice a very slow decay. Finally, for the triangle we have instead a considerable decay in terms of p.

The nonmonotonicity of the eigenvalues in Table 6.1 is due to the fact that the matrices $\mathbf{A}_{hp}^K$ are associated with bilinear forms which vary in p, see (2.13), since their definition also depend on the choice of the stabilization.

6.2 Stabilizations for hp VEM

In this section, we present two explicit choices for the stabilizing bilinear form S^K introduced in (3.10) and we discuss the associated stability bounds (3.11) in terms of the local degree of accuracy. The first choice for the stabilization is the following. For all u_n and v_n in space $V(K)$ defined in (3.5) and given p_K the local degree of accuracy on K, we set:

$$S_2^K(u_n, v_n) = \frac{p_K}{h_K}(u_n, v_n)_{0,\partial K} + \frac{p_K^2}{h_K^2}(\Pi^0_{p_K-2}u_n, \Pi^0_{p_K-2}v_n)_{0,K}. \tag{6.8}$$

We note that this local stabilization term is explicitly computable by means of the local degrees of freedom, since on the boundary virtual functions are known polynomials and the L^2 projectors defined in (2.18) are computable using only the internal degrees of freedom defined in (2.4).

In order to prove the desired stability bounds, we need a technical result.

Lemma 6.2.1. *Under assumptions **(G1)-(G2)-(G3)**, let $K \in \mathcal{T}_n$ be any* convex *polygon and let $\Pi^\nabla_{p_K}$ be defined in* (2.8)*. Then, for any $v_n \in V(K)$ defined in* (3.5)*, the following holds true:*

$$\|v_n - \Pi^\nabla_{p_K} v_n\|_{0,K} \leq c\frac{h_K}{p_K}|v_n - \Pi^\nabla_{p_K} v_n|_{1,K} \qquad \forall\, v_n \in V(K), \tag{6.9}$$

where c is a positive constant independent of h_K, p_K and v_n.

Proof. We consider the auxiliary problem:

$$\begin{cases} -\Delta\eta = v_n - \Pi^{\nabla}_{p_K} v_n & \text{in } K \\ \partial_{\mathbf{n}}\eta = 0 & \text{on } \partial K \\ \int_K \eta = 0 \end{cases}. \tag{6.10}$$

We observe that the compatibility condition:

$$\int_K v_n - \Pi^{\nabla}_{p_K} v_n = 0$$

is valid owing to (3.2) and definition (2.8).

Thanks to [96, Section 4.2], we have the following regularity bound for Neumann problems on convex polygonal domain:

$$\|\eta\|_{2,K} \lesssim \|v_n - \Pi^{\nabla}_{p_K} v_n\|_{0,K}. \tag{6.11}$$

As a consequence, applying (6.10) and Lemma 2.2.2, we obtain:

$$\begin{aligned} \|v_n - \Pi^{\nabla}_{p_K} v_n\|^2_{0,K} &= (v_n - \Pi^{\nabla}_{p_K} v_n, -\Delta\eta)_{0,K} = (\nabla(v_n - \Pi^{\nabla}_{p_K} v_n), \nabla\eta)_{0,K} \\ &\leq |v_n - \Pi^{\nabla}_{p_K} v_n|_{1,K} |\eta - \Pi^{\nabla}_{p_K}\eta|_{1,K} \lesssim |v_n - \Pi^{\nabla}_{p_K} v_n|_{1,K} \frac{h_K}{p_K} \|\eta\|_{2,K}. \end{aligned} \tag{6.12}$$

In order to conclude it suffices to plug (6.11) on the right-hand side of (6.12). □

It is possible to generalize Lemma 6.2.1 to nonconvex K. Given $\pi < \omega_K < 2\pi$ the largest angle of K, the Aubin-Nitsche analysis in addition to interpolation theory, see [101, 102], can be refined giving:

$$\|v_n - \Pi^{\nabla}_{p_K} v_n\|_{0,K} \lesssim \left(\frac{h_K}{p_K}\right)^{\frac{\pi}{\omega_K} - \varepsilon} |v_n - \Pi^{\nabla}_{p_K} v_n|_{1,K}, \qquad \forall\, v_n \in V(K), \quad \forall \varepsilon > 0 \text{ small}, \tag{6.13}$$

More precisely, it suffices in the proof of Lemma 6.2.1 to use regularity bounds for Neumann problems analogous to (6.11) on nonconvex polygons and modify accordingly the computation in (6.12).

We now prove the following result.

Theorem 6.2.2. *Under assumptions (**G1**)-(**G2**)-(**G3**), assume that p_K, the degree of accuracy of the method on the element K, coincides with the polynomial degrees p_s, for all edges s of polygon K. Then, using definition* (6.8)*, the bounds in* (3.11) *hold with:*

$$c_*(p_K) \gtrsim p_K^{-5}, \qquad c^*(p_K) \lesssim \begin{cases} 1 & \text{if } K \text{ is convex} \\ p_K^{2\left(1 - \frac{\pi}{\omega_K} + \varepsilon\right)} & \text{otherwise} \end{cases} \qquad \forall \varepsilon > 0, \tag{6.14}$$

where ω_K denotes the largest angle of K.

Proof. We assume without loss of generality that the size of polygon K is 1. The general result follows from a scaling argument.

We start by proving the estimate on $c_*(p_K)$. For the purpose, we need a technical result, namely the following *hp* polynomial inverse estimate on polygons, see Theorem B.2.6, which can be applied thanks to Remark 2:

$$\|q_{p_K-2}\|_{0,K} \lesssim (p_K - 1)^2 \|q_{p_K-2}\|_{-1,K} \leq p_K^2 \|q_{p_K-2}\|_{-1,K}, \quad \forall q_{p_K-2} \in \mathbb{P}_{p_K-2}(K), \tag{6.15}$$

where we denote by $\|\cdot\|_{-1,K}$ the negative norm defined in (1.15) and where the hidden constant in (4.35) depends solely on the parameters ρ_0 and c introduced in assumptions (**G1**)-(**G2**)-(**G3**). We apply now (3.34) to get:

$$|v_n|^2_{1,K} \lesssim \left\{ (\|\Delta v_n\|_{0,K} + |v_n|_{1,K}) \|v_n\|_{\frac{1}{2},\partial K} + \|\Delta v_n\|_{0,K} \|\Pi^0_{p-2} v_n\|_{0,K} \right\}, \tag{6.16}$$

where the hidden constant depends once more on the parameters ρ_0 and c introduced in assumptions (**G1**)-(**G2**)-(**G3**).

For what concerns the term $\|\Delta v_n\|_{0,K}$, we note that, owing to (6.15), we have:

$$\begin{aligned}\|\Delta v_n\|_{0,K} \lesssim p_K^2 \|\Delta v_n\|_{-1,K} &= p_K^2 \sup_{\Phi\in H_0^1(K)\setminus\{0\}} \frac{(\Delta v_n,\Phi)_{0,K}}{|\Phi|_{1,K}} \\ &= p_K^2 \sup_{\Phi\in H_0^1(K)\setminus\{0\}} \frac{(\nabla\Phi,\nabla v_n)_{0,K}}{|\Phi|_{1,K}} \le p_K^2 |v_n|_{1,K}.\end{aligned} \tag{6.17}$$

For what concerns instead the term $\|v_n\|_{\frac{1}{2},\partial K}$, we apply a one dimensional hp inverse estimate in addition to interpolation theory [101, 102], thus obtaining:

$$\|v_n\|_{\frac{1}{2},\partial K} \lesssim p \|v_n\|_{0,\partial K} \tag{6.18}$$

Plugging (6.17) and (6.18) in (6.16), we deduce:

$$|v_n|_{1,K}^2 \lesssim |v_n|_{1,K} \left\{ p_K^2 \|\Pi^0_{p_K-2} v_n\|_{0,K} + p_K^3 \|v_n\|_{0,\partial K} \right\},$$

whence:

$$|v_n|_{1,K}^2 \lesssim p_K^2 \left(p_K^2 \|\Pi^0_{p_K-2} v_n\|_{0,K}^2 \right) + p_K^5 \left(p_K \|v_n\|_{0,\partial K}^2 \right) \le p_K^5 S_2^K(v_n, v_n).$$

Note that the bound on $c_*(p)$ is valid for function in $V(K)$ and not only in $\ker(\Pi^\nabla_{p_K})$.

Next, we estimate $c^*(p_K)$. Let $v_n \in \ker(\Pi^\nabla_{p_K})$, then:

$$\begin{aligned} S^K(v_n, v_n) &= p_K \|v_n\|_{0,\partial K}^2 + p_K^2 \|\Pi^0_{p_K-2} v_n\|_{0,K}^2 \\ &\lesssim p_K \|v_n\|_{0,\partial K}^2 + p_K^2 \|v_n - \Pi^0_{p_K-2} v_n\|_{0,K}^2 + p_K^2 \|v_n - \Pi^\nabla_{p_K} v_n\|_{0,K}^2, \end{aligned}$$

having used that $\Pi^\nabla_{p_K} v_n = 0$.

We estimate the three terms separately. We begin with the first one. Applying the multiplicative trace inequality, see e.g. [83, Lemma 4.3], the Aubin-Nitsche Neumann-based duality arguments (6.9) for convex K and (6.13) for nonconvex K:

$$\begin{aligned} p_K \|v_n\|_{0,\partial K}^2 &\lesssim p_K \left(\|v_n\|_{0,K} |v_n|_{1,K} + \|v_n\|_{0,K}^2 \right) = p_K \left(\|v_n - \Pi^\nabla_{p_K} v_n\|_{0,K} |v_n|_{1,K} + \|v_n - \Pi^\nabla_{p_K} v_n\|_{0,K}^2 \right) \\ &\lesssim \begin{cases} p_K \left(p_K^{-1} |v_n|_{1,K}^2 + p_K^{-2} |v_n|_{1,K}^2 \right) \le |v_n|_{1,K}^2, & \text{if } K \text{ is convex} \\ p_K \left(p_K^{-\frac{\pi}{\omega_K}} |v_n|_{1,K}^2 + p_K^{-2\frac{\pi}{\omega_K}} |v_n|_{1,K}^2 \right) \le p_K^{1-\frac{\pi}{\omega_K}+\varepsilon} |v_n|_{1,K}^2, & \text{otherwise} \end{cases}, \end{aligned} \tag{6.19}$$

for all $\varepsilon > 0$ small, where we recall ω_K is the largest angle in K.

We now deal with the second term; thanks to Lemma 2.2.1, one writes:

$$p_K^2 \|v_n - \Pi^0_{p_K-2} v_n\|_{0,K}^2 \lesssim p_K^2 p_K^{-2} \|v_n\|_{1,K}^2 = \|v_n - \Pi^\nabla_{p_K} v_n\|_{1,K}^2 \lesssim |v_n|_{1,K}^2, \tag{6.20}$$

where in the last inequality we used that $v_n - \Pi_p^{\nabla,K} v_n$ has zero average over K.

Finally, we treat the third term; using Aubin-Nitsche argument (6.9) and its modified version for nonconvex polygon (6.13):

$$p_K^2 \|v_n - \Pi^\nabla_{p_K} v_n\|_{0,K}^2 \lesssim \begin{cases} p_K^2 p_K^{-2} |v_n - \Pi^\nabla_{p_K} v_n|_{1,K}^2 = |v_n|_{1,K}^2 & \text{if } K \text{ is convex} \\ p_K^2 p_K^{-2\frac{\pi}{\omega_K}} |v_n - \Pi^\nabla_{p_K} v_n|_{1,K}^2 = p_K^{2\left(1-\frac{\pi}{\omega_K}+\varepsilon\right)} |v_n|_{1,K}^2 & \text{otherwise} \end{cases}, \tag{6.21}$$

for all $\varepsilon > 0$ small.

The hidden constants in (6.19), (6.20) and (6.21) depend solely on the parameters ρ_0 and c introduced in assumptions (**G1**)-(**G2**)-(**G3**).

Collecting the three bounds, we obtain the claim. □

Remark 10. In order to keep the notation simpler, we proved Theorem 6.2.2 assuming that the polynomial degrees p_s on each edge s of K coincide with the degree of accuracy p_K of the local space $V(K)$ defined in (3.5); the same result remains valid if $p_K \approx p_s$, for all $s \in \mathcal{E}^K$. This is in fact the case of interest, see the assumption on the distribution of the local degrees of accuracy (3.45).

As a consequence of Theorem 6.2.2, the quantity $\alpha(p_K)$ defined in (3.19) can be bounded in terms of p_K as follows:

$$\begin{aligned}\alpha(p_K) = \frac{\alpha^*(p_K)}{\min_{K'\in\mathcal{T}_n}\alpha_*(p_{K'})} &= \frac{\max(1, c^*(p_K))}{\min_{K'\in\mathcal{T}_n}(\min(1, c_*(p_{K'})))} \\ &\lesssim \begin{cases} \max_{K\in\mathcal{T}_n} p_K^5 & \text{if all } K \text{ are convex} \\ p_K^{2\left(1-\frac{\pi}{\omega}+\varepsilon\right)} \max_{K\in\mathcal{T}_n} p_K^5 & \text{otherwise} \end{cases},\end{aligned} \tag{6.22}$$

for all $\varepsilon > 0$ small.

In particular the important assumption made in (3.12) is valid with an explicit representation of the two constants r_1 and r_2.

Let us recall the following result, concerning quadrature formulas.

Lemma 6.2.3. *Let $\widehat{I} = [-1, 1]$ and let $\{\rho_j^{p_{\hat{I}}+1}\}_{j=0}^{p_{\hat{I}}}$ and $\{\xi_j^{p_{\hat{I}}+1}\}_{j=0}^{p_{\hat{I}}}$ be the Gauß-Lobatto nodes and weights on $\widehat{I}$ respectively. Then:*

$$c\sum_{j=0}^{p_{\hat{I}}} q_{p_{\hat{I}}}^2(\xi_j^{p_{\hat{I}}+1})\rho_j^{p_{\hat{I}}+1} \le \|q_{p_{\hat{I}}}\|_{0,\widehat{I}}^2 \le \sum_{j=0}^{p_{\hat{I}}} q_{p_{\hat{I}}}^2(\xi_j^{p_{\hat{I}}+1})\rho_j^{p_{\hat{I}}+1} \qquad \forall\, q_{p_{\hat{I}}} \in \mathbb{P}_{p_{\hat{I}}}(\widehat{I}), \tag{6.23}$$

where c is a positive universal constant.

Proof. See [43, formula (2.14)]. □

Remark 11. Owing to Lemma 6.2.3, we could replace the boundary term of S_2^K, defined in (6.8), with a spectrally equivalent algebraic expression employing Gauß-Lobatto nodes.

In particular, we could replace in (6.8) the L^2 integral on the boundary with a piecewise Gauß-Lobatto combination, mapping each edge on the reference interval $\widehat{I}$ and using (6.23); the advantage of such a choice is that we can automatically use the *nodal* degrees of freedom on the skeleton, assuming that they have a Gauß-Lobatto distribution on each edge.

The boundary term of the new stabilization is now very close to the original stabilization S_1^K defined in (6.3) and its implementation is much easier than the implementation of (6.8), where one should reconstruct polynomials on each edge; in fact, it suffices to take instead of the Euclidean inner product of *all* the degrees of freedom only the boundary one with some Gauß-Lobatto weights.

6.2.1 Numerical tests for the stability bounds of S_2^K

In Theorem 6.2.2, we proved the stability bounds (3.11) for the stabilization S_2^K defined in (6.8). Such bounds, which also reflect on $\alpha_*(p_K)$ and $\alpha^*(p_K)$ introduced in (3.14), are rigorously proven but have a quite strong dependence on p_K. In the following, we check numerically whether the dependence on p of the above-mentioned constants is sharp.

In order to do that, we note that finding $\alpha_*(p_K)$ and $\alpha^*(p_K)$ in (3.14) is equivalent to find the minimum and maximum eigenvalues λ_{min} and λ_{max} of the generalized eigenvalue problem:

$$\mathbf{A}_n^K \mathbf{v}_n = \lambda \mathbf{A}^K \mathbf{v}_n, \tag{6.24}$$

where $\mathbf{A}_n^K$, $\mathbf{A}^K \in \mathbb{R}^{\dim(V(K))\times\dim(V(K))}$ are the local discrete and continuous stiffness matrices respectively:

$$(\mathbf{A}_n^K)_{i,j} = a_n^K(\varphi_i, \varphi_j); \qquad (\mathbf{A}^K)_{i,j} = a^K(\varphi_i, \varphi_j),$$

$\{\varphi_i\}_{i=1}^{\dim(V(K))}$ being the local canonical virtual basis being defined in (6.2).

We note that we restrict our analysis on functions having zero average over K, since both $\mathbf{A}_n^K$ and $\mathbf{A}^K$ have constant functions in their kernel; this strategy allows to avoid the problems

related to solving the generalized eigenvalue problem for singular matrices. Moreover, the entries of matrix $\mathbf{A}^K$ are not computable exactly, since virtual functions are not known explicitly; therefore, we approximate them by solving numerically the associated diffusion problem, by means of a *fine* and high-order finite element approximation.

In Table 6.2, we present the results on three different types of polygon: a square, a nonconvex decagon, like any of the polygons in the outer layer of Figure 1.4 (right), a nonconvex hexagon, like any of the polygons in the outer layer of Figure 1.4 (center).

Table 6.2 Minimum and maximum eigenvalues of the generalized eigenvalue problem (6.6) on: sq.= a square; dec.= a nonconvex decagon; hex.= a nonconvex hexagon. Stabilization employed: S_2^K.

p	sq. λ_{min}	sq. λ_{max}	dec. λ_{min}	dec. λ_{max}	hex. λ_{min}	hex. λ_{max}
2	7.8559e-01	1.0000e+00	7.9262e-02	5.5516e+00	1.6168e-01	1.1183e+00
3	4.6667e-01	1.0000e+00	1.0306e-01	8.6605e+00	1.3342e-01	1.4751e+00
4	3.3195e-01	1.0000e+00	4.5039e-02	1.0852e+01	1.0321e-01	1.6253e+00
5	2.7547e-01	1.0000e+00	3.4944e-02	1.0513e+01	7.4247e-02	1.8672e+00
6	2.1557e-01	1.0000e+00	2.3463e-02	1.1835e+01	5.5556e-02	1.6707e+00
7	1.8994e-01	1.0000e+00	2.0730e-02	9.7514e+00	3.5664e-02	1.9013e+00
8	1.4136e-01	1.0000e+00	1.6122e-02	1.0447e+01	2.7559e-02	1.8801e+00
9	1.2446e-01	1.0000e+00	1.8555e-02	7.9781e+00	2.1313e-02	1.8337e+00
10	9.2933e-02	1.0000e+00	1.3736e-02	3.9577e+01	1.7991e-02	5.6544e+00

As theoretically expected, the maximum generalized eigenvalue always scales like 1. On the contrary, the minimum eigenvalue behaves in all the three cases like p^{-1}. This means that in fact the bounds of Theorem 6.2.2 are pessimistic, whereas the *actual* behaviour of the stability bounds may be much milder.

Finally, we stress that the nonmonotonicity of the eigenvalues can be justified as done for the eigenvalues of Table 6.1.

6.3 Stabilizations for *hp* Harmonic VEM

In this section, we present a stabilization that was firstly introduced in the framework of Harmonic VEM of Chapter 4, see [58]. We anticipate that the stability bounds here proven are better than those for the *hp* VEM presented in Section 6.2.

The outline of this section is the following. In Section 6.3.1, we present a stabilization based on L^2-norm on the skeleton of polygonal mesh $\mathcal{T}_n$, whereas in Section 6.3.2 we exhibit an optimal (i.e. spectrally equivalent to local H^1 seminorm $|\cdot|_{1,K}$ on each element $K \in \mathcal{T}_n$) stabilization based on $H^{\frac{1}{2}}$ norm on the skeleton.

We recall that in the context of *hp* Harmonic VEM we assumed for the sake of simplicity uniform degree of accuracy p.

6.3.1 A stabilization with the L^2-norm on the skeleton

In this section we introduce a computable local stabilizing bilinear form S_Δ^K satisfying (4.10) with explicit bounds in terms of the degree of accuracy p of the corresponding stabilization constants $c_*(p)$ and $c^*(p)$.

Our first candidate is:

$$S_\Delta^K(u_n, v_n) = \frac{p}{h_K}(u_n, v_n)_{0,\partial K} = \frac{p}{h_K} \sum_{s \text{ edges of } K} (u_n, v_n)_{0,s} \quad \forall\, u_n,\, v_n \in V(K). \tag{6.25}$$

Since functions in $V(K)$, defined in (4.2), are piecewise polynomials on the boundary of the element, then it is clear that the local stabilization introduced in (6.25) is explicitly computable.

For computational purposes, we substitute the edge integrals on the right-hand side of (6.25) with Gauß-Lobatto quadrature formulas using, as done in Lemma 6.2.3.

Thus, we emphasize our choice of S_Δ^K by writing explicitly its definition. To each s edge of K we associate the set of Gauß-Lobatto nodes and weights $\{\eta_j^{p_s,s}\}_{j=0}^{p_s}$ and $\{\xi_j^{p_s,s}\}_{j=0}^{p_s}$ respectively. Our second candidate for being local stabilizing bilinear form associated with method (4.14) reads:

$$\widetilde{S}_\Delta^K(u_n, v_n) = \frac{p}{h_K} \sum_{s \text{ edge of } K} \left(\sum_{j=0}^{p_s} \eta_j^{p_s,s} u_n(\xi_j^{p_s,s}) v_n(\xi_j^{p_s,s}) \right). \tag{6.26}$$

Next, we discuss the issue of showing explicit stability bounds (4.10) in terms of the local degree of accuracy. We begin with an auxiliary lemma.

Let us denote by:

$$\overline{v} := \frac{1}{|K|} \int_K v \tag{6.27}$$

the domain average of some $v \in H^1(K)$, $K \in \mathcal{T}_n$. Then, the Poincaré inequality implies:

$$\|v - \overline{v}\|_{0,K} \lesssim h_K |v|_{1,K} \qquad \forall v \in H^1(K). \tag{6.28}$$

When, moreover, $v \in \ker(\Pi_p^{\nabla,\Delta})$ the following improved estimate is valid.

Lemma 6.3.1. *Under assumptions (**G1**)-(**G2**)-(**G3**), let $K \in \mathcal{T}_n$ and let $\Pi_p^{\nabla,\Delta}$ be defined in* (4.9). *For any $v_n \in \ker(\Pi_p^{\nabla,\Delta})$, the following holds true:*

$$\|v_n - \overline{v_n}\|_{0,K} \lesssim \begin{cases} h_K \left(\frac{\log(p)}{p}\right)^{\frac{\lambda_K}{\pi}} |v_n|_{1,K} & \text{if } K \text{ is convex} \\ h_K \left(\frac{\log(p)}{p}\right)^{\frac{\lambda_K}{\omega_K} - \varepsilon} |v_n|_{1,K} & \text{otherwise} \end{cases}, \quad \forall\, \varepsilon > 0, \tag{6.29}$$

where λ_K and ω_K denote the smallest exterior and largest interior angles of K, respectively.

Proof. We prove the assertion only for K convex, i.e. $0 < \omega_K < \pi$, since the nonconvex case can be treated analogously. Moreover, we assume without loss of generality that $h_K = 1$. The general form of the assertion (6.29) follows then by the scaling argument.

The proof is based on an Aubin-Nitsche-type argument, slightly different from the one presented in Lemma 6.2.1. For a fixed $v_n \in \ker(\Pi_p^{\nabla,\Delta})$ consider an auxiliary problem of finding η such that:

$$\begin{cases} -\Delta \eta = v_n - \overline{v_n} & \text{in } K \\ \partial_{\mathbf{n}} \eta = 0 & \text{on } \partial K \\ \int_K \eta = 0 \end{cases}, \tag{6.30}$$

where $\overline{v}$ is defined in (6.27).

Observe that by construction the right-hand side in (6.30) has vanishing mean and thus by the Lax-Milgram lemma the solution $\eta \in H^1(K)$ is well-defined. The additional regularity of η depends on the size of interior angles of K. In particular, if K is convex there holds $\eta \in H^2(K)$; more precisely:

$$\|\eta\|_{2,K} \lesssim \|v_n - \overline{v_n}\|_{0,K}, \tag{6.31}$$

see e.g. [96, Section 4.2].

In the following, we also make usage of the splitting $\eta = \eta_1 + \eta_2$, where:

$$\begin{cases} -\Delta \eta_1 = v_n - \overline{v_n} & \text{in } K \\ \eta_1 = 0 & \text{on } \partial K \end{cases}, \qquad \begin{cases} -\Delta \eta_2 = 0 & \text{in } K \\ \eta_2 = \eta & \text{on } \partial K \end{cases}. \tag{6.32}$$

Again, standard a priori regularity theory entails:

$$\|\eta_1\|_{2,K} \lesssim \|v_n - \overline{v_n}\|_{0,K}. \tag{6.33}$$

Therefore, combining (6.31), (6.33) and using triangular inequality, yields:

$$\|\eta_2\|_{0,K} \leq \|\eta\|_{0,K} + \|\eta_1\|_{0,K} \lesssim \|v_n - \overline{v_n}\|_{0,K}. \tag{6.34}$$

Moreover, for each harmonic function $w \in H^1(K)$:

$$(\nabla\eta_1, \nabla w)_{0,K} = (\eta_1, \partial_{\mathbf{n}} w)_{0,\partial K} - (\eta_1, \Delta w)_{0,K} = 0. \tag{6.35}$$

Recalling that $v_n \in \ker(\Pi_p^{\nabla,\Delta})$ and applying sequentially (6.30), integration by parts, (6.35), orthogonality of $\Pi_p^{\nabla,\Delta}$, Cauchy-Schwarz inequality and [19, Theorem 2], we deduce:

$$\begin{aligned} \|v_n - \overline{v_n}\|_{0,K}^2 &= (-\Delta\eta, v_n - \overline{v_n})_{0,K} = (\nabla\eta, \nabla(v_n - \overline{v_n}))_{0,K} = \left(\nabla\eta_2, \nabla(v_n - \Pi_p^{\nabla,\Delta} v_n)\right)_{0,K} \\ &= \left(\nabla(\eta_2 - \Pi_p^{\nabla,\Delta}\eta_2), \nabla v_n\right)_{0,K} \leq |\eta_2 - \Pi_p^{\nabla,\Delta}\eta_2|_{1,K} |v_n|_{1,K} \lesssim \left(\frac{\log(p)}{p}\right)^{\frac{\lambda_K}{\pi}} \|\eta_2\|_{2,K} |v_n|_{1,K}, \end{aligned} \tag{6.36}$$

where λ_K denotes the smallest exterior angle of K.

Plugging (6.34) in (6.36), we get the assertion (6.29).

□

We emphasize that Lemma 6.3.1 is a modification of Lemma 6.2.1. The difference is that without the presence of $\overline{v_n}$, the compatibility condition in (6.30) would not hold; in fact, we recall that it is not possible to fix constants with the average over the interior of the polygon in the definition of $\Pi_p^{\nabla,\Delta}$ defined in (4.9) since no internal moments are available in local Harmonic VE spaces (4.2).

Now we are ready to prove stability estimates for the L^2-norm stabilization.

Theorem 6.3.2. *Under assumptions (**G1**)-(**G2**)-(**G3**), the bilinear forms S_Δ^K defined in* (6.25) *and* (6.26) *fulfill the two-sided estimate* (4.10) *with constants satisfying:*

$$c_*(p) \gtrsim p^{-1}, \qquad c^*(p) \lesssim \begin{cases} p\left(\frac{\log(p)}{p}\right)^{2\frac{\lambda_K}{\pi}} & \text{if } K \text{ is convex} \\ p\left(\frac{\log(p)}{p}\right)^{2\left(\frac{\lambda_K}{\omega_K} - \varepsilon\right)} & \text{otherwise} \end{cases} \qquad \forall\, \varepsilon > 0 \text{ small}, \tag{6.37}$$

where λ_K and ω_K denote the smallest exterior and the largest interior angles of K, respectively.

Proof. In view of Lemma 6.2.3, it suffices to consider the bilinear form S_Δ^K defined in (6.25). Moreover, we assume h_K=1 since the assertion will follow by the scaling argument. Moreover, we also assume K convex, since the nonconvex case can be dealt with similarly.

We start by proving the lower bound for $c_*(p)$. Given $v_n \in \ker(\Pi_p^{\nabla,\Delta})$, we write:

$$|v_n|_{1,K}^2 = \int_K \nabla v_n \cdot \nabla v_n = \int_{\partial K} (\partial_{\mathbf{n}} v_n)\, v_n, \tag{6.38}$$

where we used an integration by parts and the fact that v_n is harmonic in K.

We apply now (3.34) and the fact that v_n is harmonic, in order to show that:

$$\int_{\partial K} (\partial_{\mathbf{n}} v_n)\, v_n \leq \|\partial_{\mathbf{n}} v_n\|_{-\frac{1}{2},\partial K} \|v_n\|_{\frac{1}{2},\partial K} \lesssim |v_n|_{1,K} \|v_n\|_{\frac{1}{2},\partial K}, \tag{6.39}$$

where the hidden constant in (6.39) depends on the parameters ρ_0 and c introduced in assumptions (**G1**)-(**G2**)-(**G3**).

Plugging (6.38) in (6.39) and using the inverse inequality for polynomials on an interval [96, Theorem 3.91] and interpolation theory [101, 102] we obtain:

$$|v_n|_{1,K}^2 \lesssim \|v_n\|_{\frac{1}{2},\partial K}^2 \lesssim p^2 \|v_n\|_{0,\partial K}^2 = p \cdot S_\Delta^K(v_n, v_n),$$

which is the asserted bound on $c_*(p)$.

Next, we investigate the behaviour of $c^*(p)$. Let $v_n \in \ker(\Pi_p^{\nabla,\Delta})$ and $\overline{v_n}$ be defined as in (6.27), then:

$$S_\Delta^K(v_n, v_n) = p\|v_n\|_{0,\partial K}^2 \lesssim p(\|v_n - \overline{v_n}\|_{0,\partial K}^2 + |\partial K| \cdot |\overline{v_n}|^2). \tag{6.40}$$

Observe that by (4.9) v_n has zero boundary mean and therefore by the Cauchy-Schwarz inequality:

$$|\partial K| \cdot |\overline{v_n}|^2 = \frac{1}{|\partial K|} \cdot \left| \int_{\partial K} (v_n - \overline{v_n}) \right|^2 \leq \|v_n - \overline{v_n}\|^2_{0,\partial K} \tag{6.41}$$

Hence, by (6.40), (6.41), the multiplicative trace inequality, see [83, Lemma 4.3], and (6.29):

$$\begin{aligned} S^K_\Delta(v_n, v_n) &\lesssim p\|v_n - \overline{v_n}\|^2_{0,\partial K} \lesssim p\left(\|v_n - \overline{v_n}\|_{0,K}|v_n|_{1,K} + \|v_n - \overline{v_n}\|^2_{0,K}\right) \\ &\lesssim p\left(\frac{\log(p)}{p}\right)^{2\frac{\lambda_K}{\pi}} |v_n|^2_{1,K}, \end{aligned} \tag{6.42}$$

where λ_K denotes the smallest exterior angle of K and where the hidden constant in (6.42) depends on the parameters ρ_0 and c introduced in assumptions (**G1**)-(**G2**)-(**G3**). □

Lemma 6.3.2 and (4.13) imply that $\alpha_\Delta(p)$ introduced in (4.15) admits the upper bound:

$$\alpha_\Delta(p) := \frac{\alpha^*(p)}{\alpha_*(p)} \lesssim \begin{cases} p^2\left(\frac{\log(p)}{p}\right)^{2\frac{\lambda_K}{\pi}} & \text{if } K \text{ is convex} \\ p^2\left(\frac{\log(p)}{p}\right)^{2\left(\frac{\lambda_K}{\omega_K}-\varepsilon\right)} & \text{otherwise} \end{cases} \qquad \forall \varepsilon > 0, \tag{6.43}$$

where we recall that λ_K and ω_K denote the smallest exterior and the largest interior angles of K, respectively.

We conclude this section by noting that the stabilization introduced in (6.25) is basically, up to a p scaling, stabilization (6.5).

6.3.2 A stabilization with the $H^{\frac{1}{2}}$-norm on the skeleton

In view of Theorem 4.2.6, which guarantees exponential convergence of the Harmonic VEM in terms of the number of degrees of freedom, the mild blow-up behaviour of the stability constants $c_*(p)$ and $c^*(p)$ described in Lemma 6.3.2 in terms of p has no effect on the asymptotic convergence rate of the method that remains exponential.

However, it is worth mentioning that there exists an optimal stabilization bilinear form S^K_Δ with uniformly bounded stability constants $c_*(p)$ and $c^*(p)$. In particular, we introduce the stabilization:

$$S^K_{\Delta,1}(u_n, v_n) = (u_n, v_n)_{\frac{1}{2},\partial K} \quad \forall\, u_n,\, v_n \in \ker(\Pi^{\nabla,\Delta}_p), \tag{6.44}$$

where inner product $(\cdot,\cdot)_{\frac{1}{2},\partial K}$ is defined through Aronszajn-Slobodeckij seminorm (1.11).

Theorem 6.3.3. *Under assumptions (**G1**)-(**G2**)-(**G3**), let S^K_Δ be defined as in* (6.44)*. Then, for all $v_n \in \ker(\Pi^{\nabla,\Delta}_p)$, $\Pi^{\nabla,\Delta}_p$ being defined in* (4.9)*, the following holds true:*

$$S^K_\Delta(v_n, v_n) \approx |v_n|^2_{1,K}.$$

Proof. It is a straightforward consequence of the proof of Lemma 6.3.1 and a scaling argument. □

It can be expected that the evaluation of (6.44) is more involved than the evaluation of the other variants of stabilization presented in Section 6.3.1, namely those in (6.25) and (6.26). In the following we briefly discuss evaluation of the local stabilization (6.44).

We firstly recall the definition of the Aronszajn-Slobodeckij $H^{\frac{1}{2}}$ inner product:

$$\begin{aligned} (u_n, v_n)_{\frac{1}{2},\partial K} &= (u_n, v_n)_{0,\partial K} + \int_{\partial K}\int_{\partial K} \frac{(u_n(\xi) - u_n(\eta))(v_n(\xi) - v_n(\eta))}{|\xi - \eta|^2}\, d\xi\, d\eta \\ &= (u_n, v_n)_{0,\partial K} + \sum_{s_i=1}^{N_K}\sum_{s_j=1}^{N_K} I_{ij}, \qquad I_{ij} = \int_{s_i}\int_{s_j} \frac{(u_n(\xi) - u_n(\eta))(v_n(\xi) - v_n(\eta))}{|\xi - \eta|^2}\, d\xi\, d\eta, \end{aligned} \tag{6.45}$$

where we recall that N_K denotes the number of edges of K and $\{s_i\}_{i=1}^{N_K}$ denotes its set of edges. Observe that, owing to the fact that the stabilization is defined on $\ker(\Pi_p^{\nabla,\Delta})$, it is possible to drop in (6.45) the contribution of the L^2 inner product.

We discuss now the evaluation of the double integral I_{ij} in (6.45). We distinguish three different variants of the mutual locations of two edges s_i and s_j.

1. s_i and s_j are identical ($s_i \equiv s_j$). In this case the integrand in (6.45) has a removable singularity and is, in fact, a polynomial of degree $2p-2$. Such an integral is computed *exactly* by means of a Gauß-Lobatto quadrature formula with $p+1$ points.

2. s_i and s_j are distant ($\overline{s}_i \cap \overline{s}_j = \emptyset$). In this case the integrand in (6.45) is an analytic function and can be efficiently approximated e.g. by a Gauß-Lobatto quadrature rule, see e.g. [59, Theorem 5.4].

3. s_i and s_j share a vertex $\vec{v}$ and make an interior angle $0 < \varphi < 2\pi$. Then s_i and s_j admit local parametrizations:

$$s_i = \{\xi = \vec{v} + \vec{a}s \mid 0 < s < 1\}, \qquad s_j = \{\eta = \vec{v} + \vec{b}t \mid 0 < t < 1\}, \tag{6.46}$$

for some $\vec{a}$ and $\vec{b} \in \mathbb{R}^2$. Since the functions $u_n, v_n \in V^{\Delta}(K)$ are polynomials of degree p along s_i and s_j and are continuous in $\vec{v}$ there holds:

$$u_n(\xi) - u_n(\eta) = s\,f(s) - t\,g(t), \qquad v_n(\xi) - v_n(\eta) = s\,q(s) - t\,r(t), \tag{6.47}$$

where f, g, q and r are polynomials of degree $p-1$ and one has, using a change of coordinate:

$$I_{ij} = |\vec{a}| \cdot |\vec{b}| \int_0^1 \int_0^1 F(s,t)\,dsdt, \quad \text{where} \quad F(s,t) = \frac{\big(s\,f(s) - t\,g(t)\big)\big(s\,q(s) - t\,r(t)\big)}{|\vec{a}s - \vec{b}t|^2}. \tag{6.48}$$

The integrand $F(s,t)$ is not smooth in $(0,1)^2$ (its derivatives blow up near the origin) and is not even defined in the origin, but it becomes regular after a coordinate transformation [64]. Having split the integral over the square $(0,1)^2$ into a sum of integrals over the two triagles obtained by bisecting such square with the segment of endpoints $(0,0)$ and $(1,1)$, simple algebra yields:

$$\begin{aligned} I_{ij} &= |\vec{a}| \cdot |\vec{b}| \int_0^1 \int_0^t \big(F(s,t) + F(t,s)\big)\,dsdt \\ &= |\vec{a}| \cdot |\vec{b}| \int_0^1 \int_0^1 t \cdot \big(F(tz,t) + F(t,tz)\big)\,dzdt, \end{aligned} \tag{6.49}$$

after the transformation $s = tz$ in the inner integral. The integrand admits the representation:

$$F(tz,t) = \frac{\big(z\,f(tz) - g(t)\big)\big(z\,q(tz) - r(t)\big)}{|\vec{a}z - \vec{b}|^2}, \tag{6.50}$$

which is a rational function with uniformly positive denominator:

$$|\vec{a}z - \vec{b}|^2 \geq \left\{ \begin{array}{ll} |\vec{b}|^2 \sin^2\varphi, & \text{for } \cos\varphi > 0 \\ |\vec{b}|^2, & \text{for } \cos\varphi \leq 0 \end{array} \right\} > 0. \tag{6.51}$$

Hence, the integrand (6.49) is an analytic function and can be efficiently approximated by Gauß quadrature.

6.4 Comments and conclusions

In this chapter, we discussed various stabilizations available in the literature along with their properties. In Chapter 7, we show numerical tests employing stabilizations S_1^K defined in (6.3) for the h and p VEM (see Chapter 2), S_2^K defined in (6.8) for hp VEM (defined in Chapter 3) and S_Δ^K defined in (6.25) for hp Harmonic VEM (see Chapter 4).

Moreover, in Chapter 8, we compare the numerical performances of stabilizations S_i^K, $i = 1,2,3,4$, defined respectively in (6.3), (6.8), (6.4) and (6.5); we anticipate that, although the stabilizations look different, the associated approximation results are comparable.

Chapter 7

Numerical results: a priori analysis

In this chapter, we present a number of numerical tests validating the approximation results of h and p VEM on quasi-uniform meshes (see Chapter 2), hp VEM on geometrically refined meshes (see Chapter 3) and Harmonic hp VEM on geometrically refined meshes (see Chapter 4), namely Theorems 2.2.6, 2.3.6, 3.2.8 and 4.2.6; such numerical tests are performed respectively in Sections 7.1, 7.2 and 7.3.

An interesting issue regards how to compute the error of the method, since a fully explicit representation of a function in a VE space is not available on the complete domain but only on the skeleton of the mesh.

A possible way to overcome this problem is the following. Let Π^∇ denote generically one of the energy projectors from local VE spaces into spaces of (possibly harmonic) polynomials defined either in (2.8) or (4.9). We recall that such projectors are computable via the local degrees of accuracy on each VE space.

Then, instead of computing the exact relative L^2 and H^1 errors of the method:

$$\frac{\|u - u_{\mathrm{VEM}}\|_{0,\Omega}}{\|u\|_{0,K}}, \qquad \frac{|u - u_{\mathrm{VEM}}|_{1,\Omega}}{|u|_{1,K}}, \tag{7.1}$$

one computes:

$$\begin{aligned} \frac{\|u - \Pi^\nabla u_{\mathrm{VEM}}\|_{0,K}}{\|u\|_{0,K}} &= \frac{\sqrt{\sum_{K\in\mathcal{T}_n} \|u - \Pi^\nabla u_{\mathrm{VEM}}\|^2_{0,K}}}{\|u\|_{0,K}}, \\ \frac{|u - \Pi^\nabla u_{\mathrm{VEM}}|_{1,\mathcal{T}_n}}{|u|_{1,K}} &= \frac{\sqrt{\sum_{K\in\mathcal{T}_n} |u - \Pi^\nabla u_{\mathrm{VEM}}|^2_{0,K}},}{|u|_{1,K}} \end{aligned} \tag{7.2}$$

where u_{VEM} generically denotes the VEM solution in any of the methods (2.1), (3.17) and (4.14).

Henceforth, with an abuse of notation, we denote the relative error avoiding to explicitly write the denominator.

The reason for which we consider (7.2) in lieu of (7.1) is therefore twofold. Clearly, doing so, we take into account the "virtuality" of the functions in VE spaces and we provide fully computable errors; moreover, focusing e.g. on the H^1 broken error in (7.2), we note that:

$$|u - \Pi^\nabla u_{\mathrm{VEM}}|_{1,\mathcal{T}_n} \leq |u - u_{\mathrm{VEM}}|_{1,\Omega} + |u_{\mathrm{VEM}} - \Pi^\nabla u_{\mathrm{VEM}}|_{1,\mathcal{T}_n}$$

and thus, owing to hp approximation properties of energy projector, see Sections 2.2.1, 2.3.2 and 4.2.2, one recovers, employing errors (7.2), the same rate of convergence of the original errors (7.1) of the method. Nonetheless, one should not forget that VEM provides also an explicit continuous discrete solution on the mesh skeleton; in Sections 7.2 and 7.3, we consider in fact also the L^2 error on the skeleton of the grid.

It is worth to underline that, in the two first sections, the local internal dofs (2.4) are defined taking as a dual polynomial basis the one of monomials defined in (8.4); as will be clear from Chapter 8, this choice is not particularly shrewd but has the merit of providing an easily implementable method. In Chapter 8, we address the issue of selecting more clever and "reliable" polynomial bases dual to the internal dofs (2.4).

We emphasize that, depending on the method under consideration, we use different stabilizations that will be explicated in the following.

Finally, we underline that the implementation details of *hp* VEM can be found in [30]; we present a rapid overview on such details in Section 8.2.

The implementation of Harmonic VEM strictly follows the lines of its VEM counterpart; the only nontrivial issue here is the choice of the basis of $\mathbb{H}_p(K)$, the space of Harmonic polynomials over polygon K, with respect to which we expand the energy projector (4.9).

Such basis can be clearly chosen in many different ways; we present here one possibility which can be found e.g. in [13, Theorem 5.24].

The first element is simply given by $m_1 = 1$. At each additional degree, we add two elements of the following sort. For every $\ell = 1, \dots, p$:

$$\begin{aligned} m_{2\,\ell} &= \sum_{k=1,\,k\ \text{odd}}^{\ell} (-1)^{\frac{k-1}{2}} \binom{\ell}{k} \left(\frac{x - x_K}{h_K}\right)^{\ell-k} \left(\frac{y - y_K}{h_K}\right)^{k}, \\ m_{2\,\ell+1} &= \sum_{k=0,\,k\ \text{even}}^{\ell} (-1)^{\frac{k}{2}} \binom{\ell}{k} \left(\frac{x - x_K}{h_K}\right)^{\ell-k} \left(\frac{y - y_K}{h_K}\right)^{k}, \end{aligned} \tag{7.3}$$

where we recall that (x_K, y_K) and h_K denote the barycenter and the diameter of element K respectively.

We observe that the two harmonic polynomials in (7.3) are nothing but the real and the imaginary (hence harmonic) parts of the complex polynomial $(x + i\,y)^{\ell}$. Importantly, one has $\dim(\mathbb{H}_p(K)) = 2p + 1$.

7.1 Numerical tests for h and p VEM on quasi-uniform meshes

In this section, we present a number of numerical experiments regarding the h and p version of VEM on quasi-uniform meshes discussed in Chapter 2.

We employ as a local stabilization S_1^K defined in (6.3), i.e. we consider here the original VEM stabilization which was introduced in the pioneering work [25]. We recall that in Section 6.1, we numerically investigated the possible influence in terms of p of the pollution factor $\frac{\alpha^*(p)}{\alpha_*(p)}$, see Lemma 2.1.1, in the convergence of the method, see Theorems 2.2.6 and 2.3.6.

We split this section into two parts. In Section 7.1.1, we validate the algebraic convergence in terms of h and p of the method, assuming that the exact solution has finite Sobolev regularity; here the pollution effect due to the stabilization has actually a mild impact on the convergence of the error. Instead, in Section 7.1.2 we validate the exponential convergence in terms of p, assuming that the exact solution is analytic on enlarged domain (2.40).

7.1.1 h and p algebraic convergence for finite Sobolev regularity solutions

In this section, we verify numerical the algebraic convergence of the h and p version of VEM assuming that the exact solution has finite Sobolev regularity. In particular, we set:

$$u(r, \theta) = r^{2.5} \sin(2.5\,\theta) \qquad \text{on } \Omega = [0, 1]^2, \tag{7.4}$$

where (ρ, θ) are the polar coordinates with respect to the origin $\mathbf{0}$. Since the function u is harmonic, the loading term $f = 0$ and the Dirichlet boundary conditions are set in accordance with $u|_{\partial\Omega}$. We note that $u \in H^{3.5-\varepsilon}(\Omega)$, for $\varepsilon > 0$ arbitrarily small.

We firstly investigate convergence in terms of h. For the purpose, we consider sequences of hexagonal and Voronoi-Lloyd meshes as those in Figure 1.3 (down-left) and (down-right) and we fix as (uniform) degree of accuracy $p = 3$ and $p = 5$ in Figures 7.1 and 7.2.

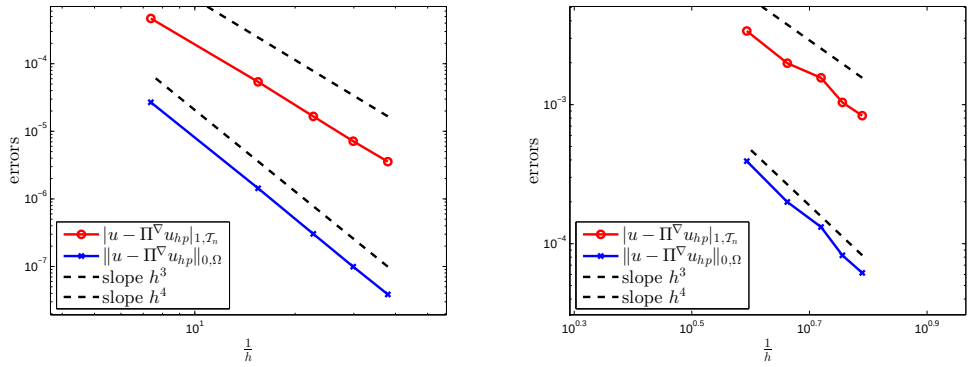

Figure 7.1: $u(r, \theta) = r^{2.5} \sin(2.5\,\theta)$. Convergence of the h version of VEM on quasi-uniform meshes. Left: regular hexagonal mesh. Right: Voronoi-Lloyd mesh. Degree of accuracy $p = 3$.

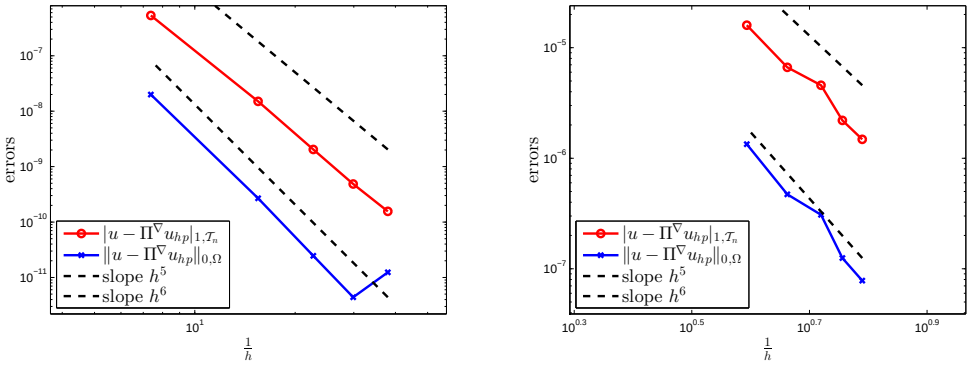

Figure 7.2: $u(r, \theta) = r^{2.5} \sin(2.5\,\theta)$. Convergence of the h version of VEM on quasi-uniform meshes. Left: regular hexagonal mesh. Right: Voronoi-Lloyd mesh. Degree of accuracy $p = 5$.

We observe that the slope of the errors are in accordance with Theorem 2.2.6 and with estimate (2.39).

Next, we investigate convergence in terms of p. Owing to the arguments of Section 2.4 and recalling that the test case u defined in (7.4) has the same structure of (2.56), one recovers a double rate of convergence $p^{-5+\varepsilon}$ for $\varepsilon > 0$ arbitrarily small.

In Figures 7.3 and 7.4, we depict the H^1 broken error defined in (7.2) for the p VEM based on the four meshes in Figure 1.3. We observe that the slope of the H^1 error, which should be almost of type $p^{-5+\varepsilon}$ for $\varepsilon > 0$ small, is slightly suboptimal, probably due to the pollution factor of the stabilization.

7.1.2 p exponential convergence for analytic solutions

In this section, we verify exponential convergence of the p version of VEM on quasi-uniform meshes assuming that the exact solution is analytic on enlarged domain (2.40). In particular, we choose as an exact solution:

$$u(x, y) = \sin(\pi\, x)\, \sin(\pi, y) \qquad \text{on } \Omega = [0, 1]^2. \tag{7.5}$$

Such u is clearly analytic on $\mathbb{R}^2$ and therefore is analytic on any enlarged domain of Ω.

In Figures 7.5 and 7.6, we show exponential convergence in terms of the two norms defined in (7.2). We observe that the method loses convergence when p is (moderately) high. We do not

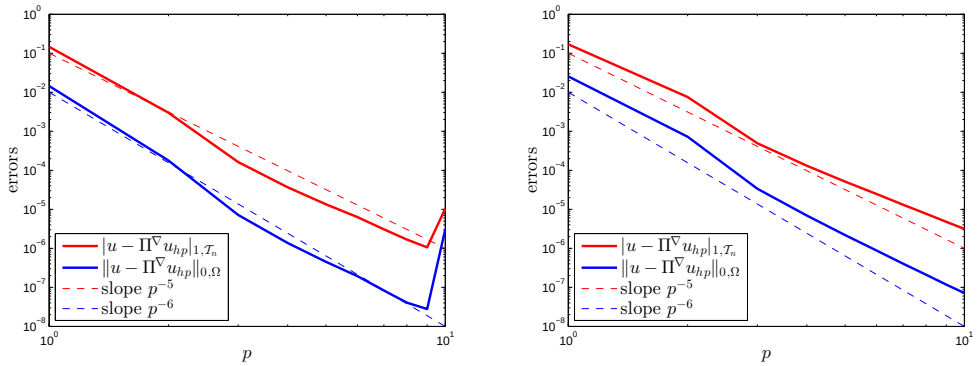

Figure 7.3: $u = r^{2.5}\sin(2.5\,\theta)$. Convergence of the p version of VEM on quasi-uniform meshes. Left: unstructured triangle mesh. Right: square mesh.

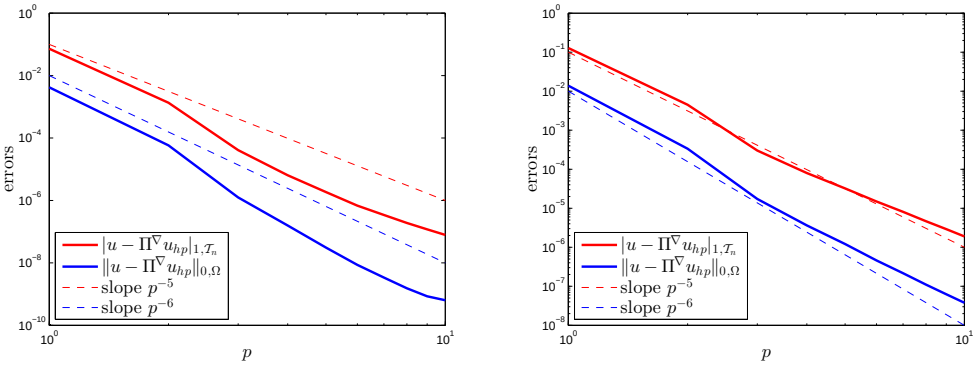

Figure 7.4: $u = r^{2.5}\sin(2.5\,\theta)$. Convergence of the p version of VEM on quasi-uniform meshes. Left: regular hexagonal mesh. Right: Voronoi-Lloyd mesh.

tackle this issue here but we postpone (and suggest remedies for) it to Chapter 8.

7.2 Numerical tests for *hp* VEM on geometrically graded meshes

In this section, we present a number of numerical experiments regarding the *hp* version of VEM on geometrically refined meshes discussed in Chapter 3.

We employ here as a local stabilization S_2^K defined in (6.8) on which we are to prove explicit stability bounds in terms of p, see Theorem 6.2.2, which guarantee exponential convergence of the method, employing sequences of meshes refined geometrically towards the singular vertices.

We consider as a test case the following function:

$$u(r,\theta) = r^{\frac{2}{3}}\sin\left(\frac{2}{3}\left(\theta+\frac{\pi}{2}\right)\right) \qquad \text{on } \Omega, \tag{7.6}$$

where (r,θ) are the polar coordinates centered at the origin $\mathbf{0}$ and where Ω, the domain of u, is defined as the L-shaped domain:

$$\Omega = [-1,1]^2 \setminus [-1,0]^2. \tag{7.7}$$

We observe that:

- u, defined in (7.6), belongs to $H^{\frac{5}{3}-\varepsilon}(\Omega)$ for $\varepsilon > 0$ arbitrarily small; in fact, u belongs also to $H^{\frac{5}{3}-\varepsilon}(\Omega^{ext})$ for $\varepsilon > 0$ arbitrarily small, Ω^{ext} being defined in (3.43);
- u, defined in (7.6), is a "natural-singular" function associated with Poisson problem (1.26), cf. Theorem A.0.1.

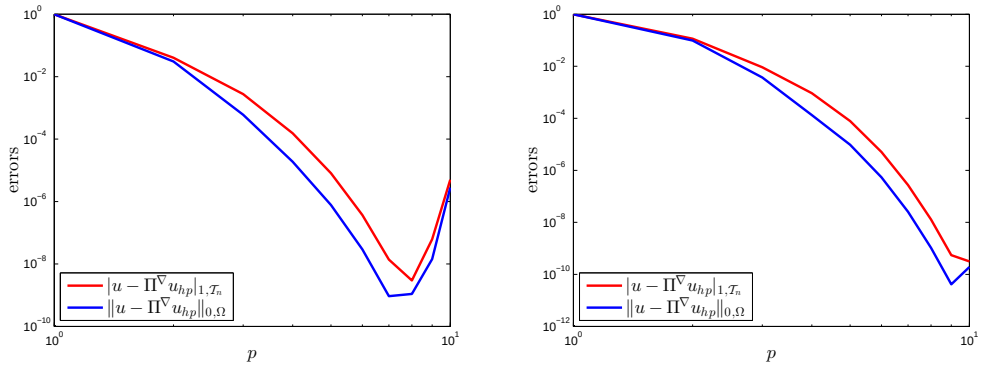

Figure 7.5: $u(x, y) = \sin(\pi\, x)\, \sin(\pi, y)$. Convergence of the p version of VEM on quasi-uniform meshes. Left: unstructured triangle mesh. Right: square mesh.

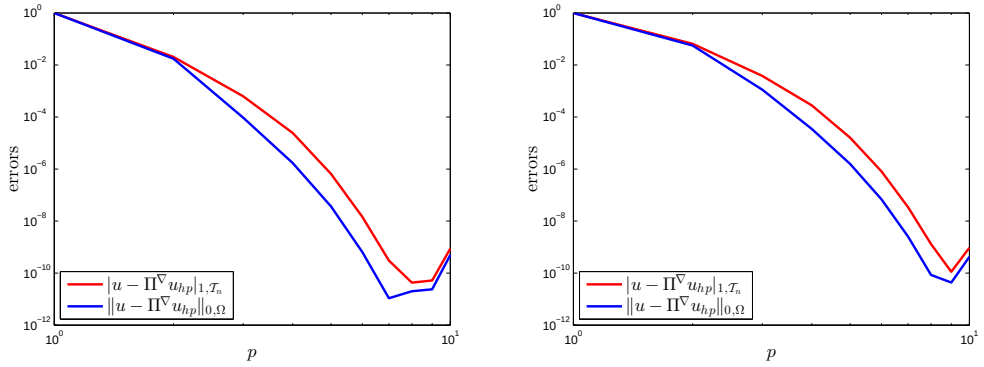

Figure 7.6: $u(x, y) = \sin(\pi\, x)\, \sin(\pi, y)$. Convergence of the p version of VEM on quasi-uniform meshes. Left: regular hexagonal mesh. Right: Voronoi-Lloyd mesh.

We consider the sequences of the three meshes that are refined geometrically towards $\mathbf{0}$ as those depicted in Figure 1.4.

We investigate the convergence assuming that $\mathbf{p}$ the vector of local degrees of accuracy, is defined either as in (3.45), i.e. we consider graded distributions of local degree of accuracy with low p near $\mathbf{0}$ and higher p when moving to the "regular" part of the domain, or we consider uniform degrees of accuracy, by picking:

$$\mathbf{p} = (n + 1,\, n + 1, \ldots, n + 1), \tag{7.8}$$

when employing meshes with $n + 1$ layers.

Such a choice clearly still guarantees the validity of Theorem 3.2.8, since we are enriching the approximation space while keeping asymptotically the same dimension as the space obtained by choosing $\mathbf{p}$ distributed as in (3.45).

We consider the behaviour of the error with three different σ grading parameters, namely $\sigma = \frac{1}{2}$, $\sqrt{2} - 1$ and $(\sqrt{2} - 1)^2$, cf. (1.39).

We denote by mesh a), mesh b) and mesh c), the sequence of meshes in Figure 1.4 (left), (center) and (right) respectively.

In Figure 7.7, we compare the broken H^1 error in (7.2) employing sequences of meshes as in Figure 1.4 and choosing $\mathbf{p}$ distributed as in (7.8) (left) and (3.45) (right) respectively; the grading parameter σ is equal to $\frac{1}{2}$.

We do exactly the same thing in Figures 7.8 and 7.9, picking $\sigma = \sqrt{2} - 1$ and $\sigma = (\sqrt{2} - 1)^2$ respectively.

In all cases, the expected exponential convergence is achieved.

We want now to show a comparison between the performances of *hp* (quadrilateral and triangular) FEM and *hp* VEM. We stress that an analogous of Theorem 3.2.8 holds for *hp* FEM,

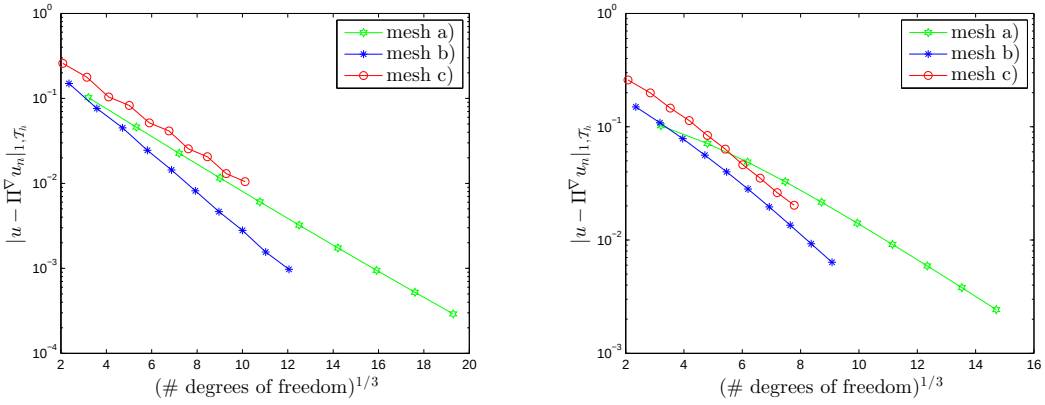

Figure 7.7: $u(r,\theta) = r^{\frac{2}{3}}\sin(\frac{2}{3}(\theta+\frac{\pi}{2}))$. Convergence of the *hp* version of VEM on geometrically graded meshes. Error $|u-\Pi^\nabla_{\mathbf{p}}u_n|_{1,n,\Omega}$ for the meshes in Figure 1.4, $\sigma=\frac{1}{2}$. Left: the degree of accuracy is uniform and equal to the number of layers. Right: the degree of accuracy is varying over the mesh layers, $\mu=1$ in (3.45).

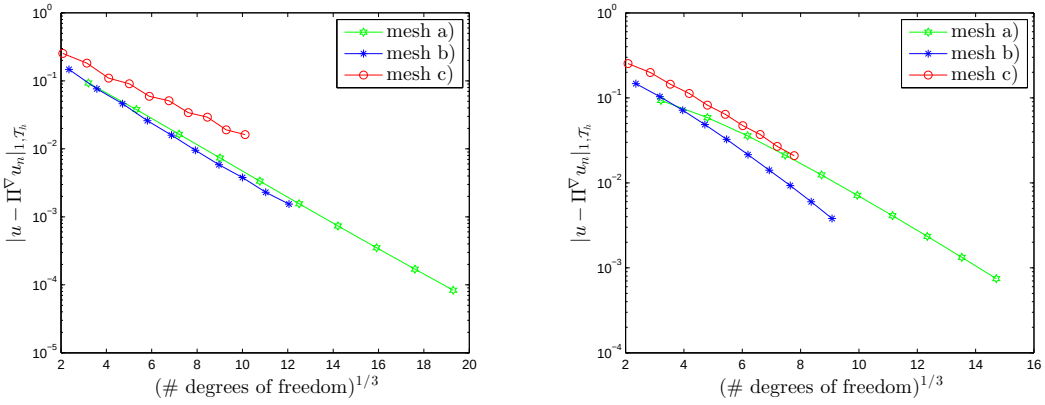

Figure 7.8: $u(r,\theta) = r^{\frac{2}{3}}\sin(\frac{2}{3}(\theta+\frac{\pi}{2}))$. Convergence of the *hp* version of VEM on geometrically graded meshes. Error $|u-\Pi^\nabla_{\mathbf{p}}u_n|_{1,n,\Omega}$ for the meshes in Figure 1.4, $\sigma=\sqrt{2}-1$. Left: the degree of accuracy is uniform and equal to the number of layers. Right: the degree of accuracy is varying over the mesh layers, $\mu=1$ in (3.45).

see e.g. [96]. We consider again the benchmark with known solution (7.6) and we consider the quadrilateral mesh in Figure 7.10. In the following we will denote such mesh by mesh d) whereas we recall that we denote by mesh a), b) and c) the meshes depicted in Figure 1.4 (left), (center) and (right) respectively. In particular, we pick in both cases $\mathbf{p_K}$ as in (3.45) for all K$\in\mathcal{T}_n$, with $\mu=1$. We discuss the case of sequences of meshes with grading parameter σ equal to $\frac{1}{2}$, $\sqrt{2}-1$ and $(\sqrt{2}-1)^2$.

Since we cannot compute the "*true*" energy error with the virtual element method (it is not computable since functions in the virtual space are not known explicitly), in order to compare the two methods, we investigate the L^2 error on $\mathcal{E}_n$, the skeleton of mesh $\mathcal{T}_n$ (it is computable in all cases a), ..., d), since also the virtual functions are piecewise continuous polynomials on such skeleton), i.e.:

$$\|u-u_n\|_{0,\mathcal{E}_n}.$$

and we postpone the comparison between H^1 errors later. The results are shown in Figure 7.11.

It is possible to see that there is not a preferential choice; for instance, *hp* VEM performs better than *hp* FEM when $\sigma=\frac{1}{2}$, they perform almost the same when $\sigma=\sqrt{2}-1$, performs much worse when $\sigma=(\sqrt{2}-1)^2$.

In this sense, we can say that the two methods are comparable; nonetheless, the virtual element methods leads to a huge flexibility in the choice of the domain meshing, thus implying the possibility

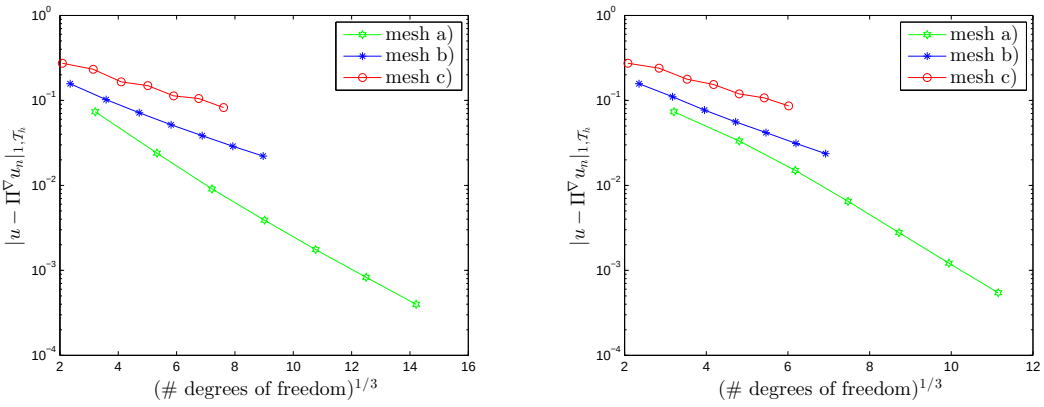

Figure 7.9: $u(r,\theta) = r^{\frac{2}{3}} \sin(\frac{2}{3}(\theta + \frac{\pi}{2}))$. Convergence of the *hp* version of VEM on geometrically graded meshes. Error $|u - \Pi^{\nabla}_{\mathbf{p}} u_n|_{1,n,\Omega}$ for the meshes in Figure 1.4, $\sigma = (\sqrt{2}-1)^2$. Left: the degree of accuracy is uniform and equal to the number of layers. Right: the degree of accuracy is varying over the mesh layers, $\mu = 1$ in (3.45).

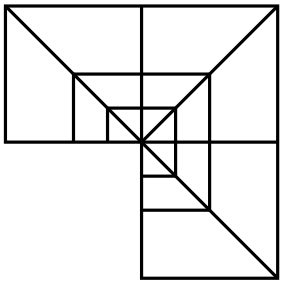

Figure 7.10: Quad-tri mesh used for the *hp* FEM.

of constructing spaces with a smalller number of degrees of freedom.

We believe that, in order to really see a marked advantage of *hp*-VEM over *hp*-FEM, more complex situations need to be addressed. This may involve, for instance, complex geometries (where polyhedral meshes can do a better job), hp-adaptivity (where again there is more refinement freedom) or more involved problems (Discrete Fracture Network, crack propagation, Fluid Structure Interaction, ...). At the present stage, on the Laplace problem on academic examples, what we can display is the flexibility in refining near corners. Note that *hp*-adaptivity is currently under investigation.

Next, in Figure 7.12, we compare the H^1 error of VEM defined in (7.2) with the standard H^1 error of *hp* FEM employing the same meshes and discretization parameters discussed for the comparison of L^2 errors on the skeleton.

The results are comparable to those related to the L^2 error on the skeleton and more precisely the two method display similar behaviours.

7.3 Numerical tests for Harmonic *hp* VEM on geometrically graded meshes

In this section, we present a number of numerical experiments regarding Harmonic *hp* VEM on geometrically refined meshes discussed in Chapter 4.

We employ as a local stabilization S^K_Δ defined in (6.25) on which we are able to prove stability bounds explicit in terms of p, see Theorem 6.3.2, which guarantees exponential convergence of the method employing sequences of meshes that are geometrically refined towards the singular vertices.

The exact solution that we consider is u defined in (7.6) on the domain Ω introduced in (7.7).

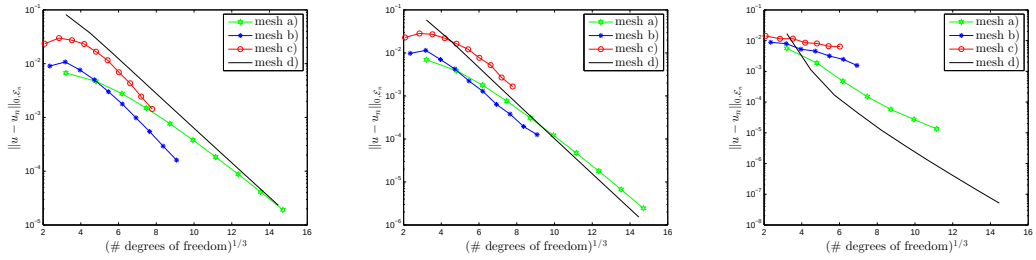

Figure 7.11: *hp* FEM vs *hp* VEM on geometrically refined meshes. L^2 error on the skeleton $\mathcal{E}_n$ of mesh $\mathcal{T}_n$: $\|u - u_n\|_{0,\mathcal{E}_n}$ for different sequence of meshes and different parameters σ. Left: $\sigma = \frac{1}{2}$, center: $\sigma = \sqrt{2} - 1$, right: $\sigma = (\sqrt{2} - 1)^2$, linearly varying over the mesh layers degrees of accuracy ($\mu = 1$ in (3.45)).

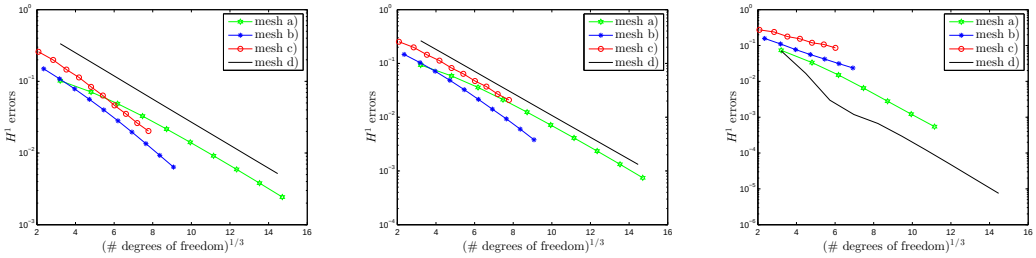

Figure 7.12: *hp* FEM vs *hp* VEM. Broken H^1 error for *hp* VEM defined in (7.2) and standard H^1 error for *hp* FEM, employing different sequence of meshes and different parameters σ. Left: $\sigma = \frac{1}{2}$, middle: $\sigma = \sqrt{2} - 1$, right: $\sigma = (\sqrt{2} - 1)^2$, linearly varying over the mesh layers degrees of accuracy $\mu = 1$ defined in (3.45).

We consider sequences of meshes that are refined geometrically towards $\mathbf{0}$ as those depicted in Figure 1.4.

We firstly investigate in Figure 7.13 the performances of Harmonic *hp* VEM choosing a distribution of degrees of accuracy $\mathbf{p}$ as in (4.37). With this choice, we know that Theorem 4.2.6 holds true.

Secondly, we investigate in Figure 7.14 the performances of the Harmonic *hp* VEM by taking a nonuniform distribution of degrees of accuracy. In particular, we consider a (graded) distribution given by:

$$p_K = j + 1, \qquad \text{where} \qquad K \in L_j, \quad j = 0, \dots, n. \tag{7.9}$$

At the interface of two polygons in different layers one associates a polynomial degree p_s via the *maximum rule* as in Figure 4.3, thus modifying straightforwardly the definition of space $\mathbb{B}(\partial K)$ defined in (4.1) as in (3.4).

In both figures, we consider sequences of meshes with different geometric refinement parameters σ; we recall that the properties fulfilled by σ are discussed in assumption (**G5**). We fix in particular $\sigma = \frac{1}{2}$, $\sigma = \sqrt{2} - 1$ and $\sigma = (\sqrt{2} - 1)^2$.

Importantly, exponential convergence is still observed also under choice (7.9) of the local degrees of accuracy. Our conjecture is that Theorem 4.2.6 still holds under (7.9). Nonetheless, we avoid to investigate this issue on the one hand in order to avoid additional technicalities, on the other because the dimension of space V_n^Δ under choices (4.37) and (7.9) behaves like n^2 and $\frac{1}{2}n^2$ respectively. This implies that the exponential decay is still valid with the same exponential rate in both cases.

We also perform a numerical comparison between Harmonic *hp* VEM and *hp* VEM described in Chapter 3.

In both cases, we consider a distribution of local degrees of accuracy as in (4.37).

From Figure 7.15, it is possible to observe the faster decay of the broken H^1 error (7.2) when employing Harmonic *hp* VEM, when compared to the same error employing *hp* VEM, which is what we expect from Theorems 3.2.8 and 4.2.6.

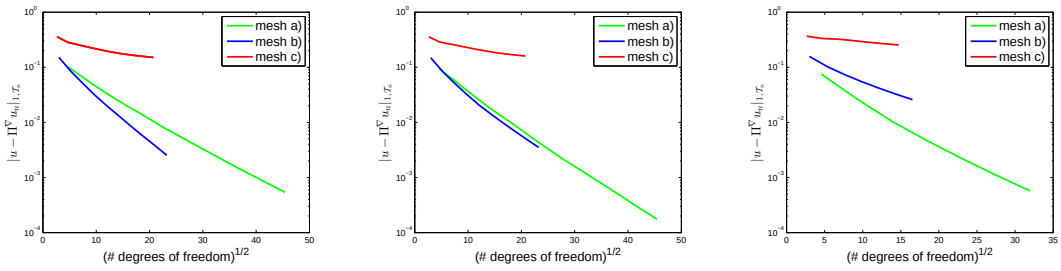

Figure 7.13: $u(r,\theta) = r^{\frac{2}{3}} \sin(\frac{2}{3}(\theta+\frac{\pi}{2}))$. Convergence of the *hp* version of Harmonic VEM employing geometrically graded meshes. Error $|u-\Pi^{\nabla}_{\mathbf{p}} u_n|_{1,\mathcal{T}_n}$ on the three meshes in Figure 1.4. We denote with a), b) and c) the meshes in Figure 1.4 (left), (center) and (right) respectively. The geometric refinement parameters are different. Left: $\sigma = \frac{1}{2}$, center: $\sigma = \sqrt{2}-1$, right: $\sigma = (\sqrt{2}-1)^2$. On each element, the local degree of accuracy is equal to the number of layers.

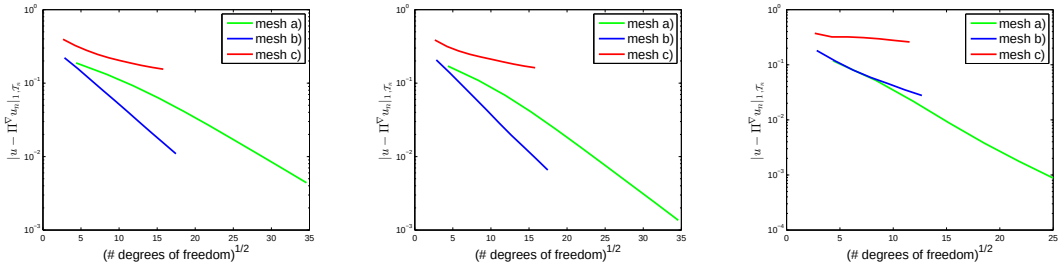

Figure 7.14: $u(r,\theta) = r^{\frac{2}{3}} \sin(\frac{2}{3}(\theta+\frac{\pi}{2}))$. Convergence of the *hp* version of Harmonic VEM employing geometrically graded meshes. Error $|u-\Pi^{\nabla}_{\mathbf{p}} u_n|_{1,\mathcal{T}_n}$ on the three meshes in Figure 1.4. We denote with a), b) and c) the meshes in Figure 1.4 (left), (center) and (right) respectively. The geometric refinement parameters are different. Left: $\sigma = \frac{1}{2}$, center: $\sigma = \sqrt{2}-1$, right: $\sigma = (\sqrt{2}-1)^2$. The vector of local degrees of accuracy is given by $p_K = j+1$. $j = 0,\ldots,n$, $n+1$ being the number of layers in $\mathcal{T}_n$.

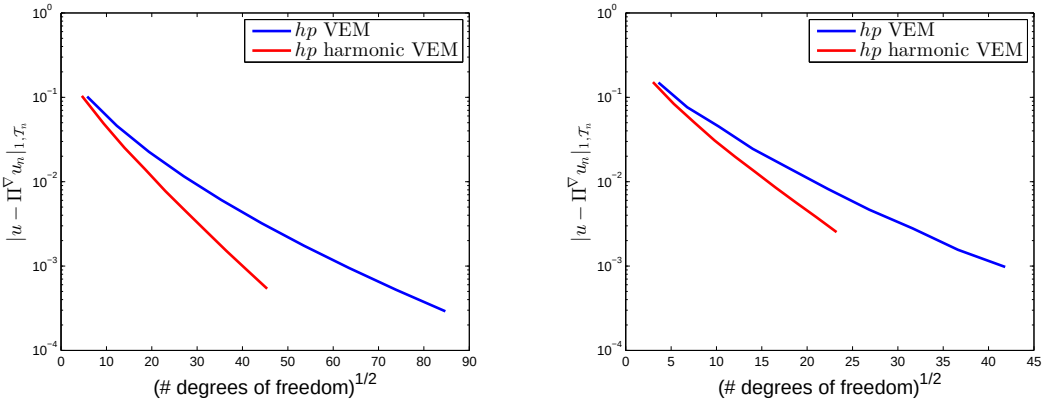

Figure 7.15: *hp* Harmonic VEM vs *hp* VEM employing geometrically graded meshes. Uniform degree of accuracy $p = n+1$, $n+1$ being the number of layers. $u(r,\theta) = r^{\frac{2}{3}} \sin(\frac{2}{3}(\theta+\frac{\pi}{2}))$. Error $|u-\Pi^{\nabla}_{\mathbf{p}} u_n|_{1,\mathcal{T}_n}$. The geometric refinement parameters is $\sigma = \frac{1}{2}$. Left: mesh in Figure 1.4 (left). Right: mesh in Figure 1.4 (center).

Chapter 8

Ill-conditioning in the p version of VEM: bases and stabilizations

In Chapter 7, we observed that the computable errors of VEM defined in (7.2) start to grow when employing (moderately) high degrees of accuracy p, see Figures 7.5 and 7.6. This growth is due to the ill-conditioning of the VEM stiffness matrix; it is well-known in fact that both direct and iterative methods for solving linear systems typically suffer high condition numbers of the system matrix.

Another situation where the method is haunted by high condition number was investigated in [45]; there, the problem is not the employment of high degree of accuracy but rather the employment of sequences of meshes that do not fulfill enough regularity assumptions (small edges, loss of star-shapedness, ...).

A first attempt to mitigate such ill-conditioning was presented in [31, Appendix A.2]. At any rate, we present in this chapter a more recent approach to tackle this issue, which can be found in [79].

Among the possible reasons of this ill-conditioning we highlight two of them. The first one is related to the fact that in the VEM framework one does not employ the exact bilinear form but an approximated one; the choice of the discrete bilinear form, and, in particular, of the stabilization, may have an impact on the 3D version of VEM as observed in [33]. The second one is the choice of the basis. This is also the case for FEM, where the choice of the basis has an important role on the ill-conditioning of the system, see [2, 63, 96] and the references therein.

The aim of the present chapter is to discuss various choices for both the discrete bilinear forms and the VE bases and check numerically that particular choices can cure the ill-conditioning which arises in high-order (or in presence of bad-shaped polygons) VEM.

In particular, we show that, while the choice of the stabilization has not a deep impact on the ill-conditioning (at least for the 2D case, which is our focus here), a proper choice of the basis can actually improve the condition number of the stiffness matrix. However, it is worth to mention that in various situations, i.e. low-to-moderate order VEM and VEM applied to shape-regular polygonal decompositions, it is preferable to employ the "standard" choice of the basis (e.g. the one described in [25]) rather than those we are going to present in this chapter, since the implementation aspects of the former choice turn out to be much simpler.

The outline of the chapter follows. In Section 8.1, we fix some notations and we present various choices both for the stabilization of the method and for the canonical basis bubble functions, i.e. those associated with (2.4). In Section 8.2, we give a hint on the implementation details employing the new bases introduced in the foregoing section. Finally, in Section 8.3, we present a number of numerical experiments comparing the behaviour of the method when changing various stabilizations and VE bases.

We stress that an analogous numerical analysis for the 3D version of VEM was performed in [61], but such analysis lies beyond the scope of the present thesis.

8.1 Stabilizations and bases

Throughout the chapter, we focus on the h and the p version of VEM on quasi-uniform meshes introduced in Chapter 2; nonetheless, trivial modifications allow for an extension to hp VEM on geometrically refined meshes discussed in Chapter 3.

We split this section into two parts. In Section 8.1.1, we recall some possible VEM stabilizations from Chapter 6; on the other hand, in Section 8.1.2,we introduce three possible polynomial bases instrumental in the definition of the internal dofs defined in (2.4). Finally, in Section 8.1.3, we highlight the influence of the choices of the stabilizations and of the local basis elements on the performances of the method.

We fix some notations. All the VE spaces, virtual VE functions, discrete bilinear forms, discrete right-hand sides ..., are going to be denoted with subscript p instead of hp; everything is defined as in Chapter 2. We believe that this choice simplifies the notation.

Furthermore, we observe that the local VE spaces $V_p(K)$ defined as in (2.3), can be split as follows:

$$\begin{aligned} V_p(K) &= \{v_p \in V_p(K) \mid v_p \in \mathbb{P}_p(K)\} \oplus \left\{v_p \in V(K) \mid \Pi_p^\nabla v_p = 0\right\} \\ &= \mathbb{P}_p(K) \oplus \ker(\Pi_p^\nabla) =: V_{p,1}(K) \oplus V_{p,2}(K), \end{aligned} \tag{8.1}$$

where we recall that the projector Π_p^∇ is defined in (2.8).

We point out that, given N_K the number of vertices of K, one has:

$$\begin{aligned} \dim(V_{p,1}(K)) &= \dim(\mathbb{P}_p(K)) = \frac{(p+1)(p+2)}{2}, \\ \dim(V_{p,2}(K)) &= \dim(V_p(K)) - \dim(V_{p,1}(K)) \\ &= N_K \cdot p + \frac{(p-1)p}{2} - \frac{(p+1)(p+2)}{2} = (N_K - 2)p - 1. \end{aligned} \tag{8.2}$$

This entails that the actual "pure virtual" part of space $V_p(K)$, i.e. $\ker(\Pi_p^\nabla)$, is asymptotically smaller than its polynomial counterpart, if the number of vertices of K remains uniformly bounded. More precisely, $\dim(V_{p,2}(K)) \approx p$ whereas $\dim(V_{p,1}(K)) \approx p^2$.

8.1.1 Stabilizations

In this section, we briefly recall various stabilizations from Chapter 6 on which, in Section 8.3, we perform some numerical experiments concerning the impact of the ill-conditioning of the solver associated with the VEM system.

The (local) stabilizations that we take into account are:

- S_1^K defined in (6.3), which we recall is the original VEM stabilization, see [25];
- S_2^K defined in (6.8), which is the original p VEM stabilization, firstly introduced in [32];
- S_3^K defined in (6.4), which was introduced firstly for the 3D version of VEM in [33];
- S_4^K defined in (6.5), which is a modification of the original VEM stabilization S_1^K.

8.1.2 Polynomial bases dual to internal dofs (2.4)

In this section, we discuss three possible choices of the local VE basis. More precisely, we consider internal moments (2.4) taken with respect to three different polynomial bases $\{q_\alpha^i\}_{\alpha=1}^{\dim(\mathbb{P}_{p-2}(K))}$, $i = 1, 2, 3$, of $\mathbb{P}_{p-2}(K)$, thus modifying the definition of the VE bubble functions.

The hope is that a proper choice of the polynomial basis dual to internal moments (2.4), and therefore of internal VEM basis elements, entails a better conditioning of the stiffness matrix.

Henceforth, we will employ, with an abuse of notation, the natural bijection between couples of natural numbers and positive natural numbers given by:

$$(0,0) \leftrightarrow 1, \quad (1,0) \leftrightarrow 2, \quad (0,1) \leftrightarrow 3, \quad (2,0) \leftrightarrow 4, \quad (1,1) \leftrightarrow 5, \quad (0,2) \leftrightarrow 6, \quad \dots \tag{8.3}$$

We also occasionally write, with another abuse of notation:

$$\{q^i_{\boldsymbol{\alpha}}\}^{p-2}_{|\boldsymbol{\alpha}|=0} \quad \text{instead of } \{q^i_{\alpha}\}^{\dim(\mathbb{P}_{p-2}(K))}_{\alpha=1} \qquad \text{for } i=1,2,3.$$

The first choice of the polynomial basis is the "standard" one, i.e. the one which is used in the majority of VEM literature, since, at the implementation level, is the most convenient and is given by the monomial basis which is defined as follows:

$$q^1_{\boldsymbol{\alpha}}(\mathbf{x}) = \left(\frac{\mathbf{x}-\mathbf{x}_K}{h_K}\right)^{\boldsymbol{\alpha}} = \left(\frac{x-x_K}{h_K}\right)^{\alpha_1}\left(\frac{y-y_K}{h_K}\right)^{\alpha_2} \quad \forall\, \boldsymbol{\alpha}=(\alpha_1,\alpha_2)\in\mathbb{N}^2, \quad |\boldsymbol{\alpha}|=0,\dots,p-2, \tag{8.4}$$

where we recall that x_K and h_K are the barycenter and the diameter of K respectively.

Although choice (8.4) is very suitable from the computational point of view, it turns out that has bad effects on the condition number of the stiffness matrix for (moderately) high local degrees of accuracy p, see Section 7.1.2, and in presence of bad-shaped polygons, see [45] and the references therein.

For this reason, we suggest two possible modifications which rely on orthogonalization processes of $\{q^1_{\boldsymbol{\alpha}}\}^{p-2}_{|\boldsymbol{\alpha}|=0}$ with respect to the L^2 norm on polygon K.

The first modification, which allows to construct an $L^2(K)$ orthonormal basis $\{q^2_{\boldsymbol{\alpha}}\}^{p-2}_{|\boldsymbol{\alpha}|=0}$, is based on the stable Gram-Schmidt orthonormalization process presented in [23]. We point out that basis $\{q^2_{\boldsymbol{\alpha}}\}^{p-2}_{|\boldsymbol{\alpha}|=0}$ was firstly introduced in the context of p-VEM multigrid algorithm for the construction of the multrigrid scheme, see Chapter 9.

The third choice of the polynomial basis is inspired by an orthonormalization procedure used in [45]. In order to present the third basis $\{q^3_{\boldsymbol{\alpha}}\}^{p-2}_{|\boldsymbol{\alpha}|=0}$, we set matrix:

$$\mathbf{H}_{\boldsymbol{\alpha},\boldsymbol{\beta}} = (q^1_{\boldsymbol{\alpha}}, q^1_{\boldsymbol{\beta}})_{0,K} \quad \forall\, \boldsymbol{\alpha},\ \boldsymbol{\beta}\in\mathbb{N}^2, \quad |\boldsymbol{\alpha}|,\,|\boldsymbol{\beta}|=0,\dots,p-2.$$

Given $n_\ell = \dim(\mathbb{P}_\ell(K))$, we fix $q^3_{\boldsymbol{\alpha}} = q^1_{\boldsymbol{\alpha}}$ if $\alpha = 1$ and we decompose matrix $\mathbf{H}$ into blocks as:

$$\mathbf{H} = \begin{matrix} \\ 1 \\ n_{p-2}-1 \end{matrix} \begin{matrix} \begin{matrix} 1 & \quad n_{p-2}-1 \end{matrix} \\ \begin{pmatrix} \mathbf{H}_{1,1} & \mathbf{H}_{1,2} \\ \mathbf{H}_{2,1} & \mathbf{H}_{2,2} \end{pmatrix} \end{matrix},$$

we diagonalize matrix $\mathbf{H}_{2,2}$ and we get:

$$\mathbf{V}^T\cdot\mathbf{H}_{2,2}\cdot\mathbf{V} = \mathbf{D} \Longrightarrow (\mathbf{V}\cdot\mathbf{D}^{-\frac{1}{2}})^T\cdot\mathbf{H}_{2,2}\cdot(\mathbf{V}\cdot\mathbf{D}^{-\frac{1}{2}}) = \mathbf{Id}. \tag{8.5}$$

This entails that matrix $\mathbf{V}\cdot\mathbf{D}^{-\frac{1}{2}}$ contains the coefficients which orthonormalize $\{q^1_{\boldsymbol{\alpha}}\}^{p-2}_{|\boldsymbol{\alpha}|=1}$, the monomial basis of $\mathbb{P}_{p-2}(K)/\mathbb{R}$. Therefore, one has:

$$q^3_{\boldsymbol{\alpha}}(\mathbf{x}) = \begin{cases} q^1_{\boldsymbol{\alpha}} & \text{if } |\boldsymbol{\alpha}|=0 \\ \sum_{|\boldsymbol{\beta}|=1}^{p-2}(\mathbf{V}\cdot\mathbf{D}^{-\frac{1}{2}})^T_{\boldsymbol{\alpha},\boldsymbol{\beta}}\, q^1_{\boldsymbol{\beta}}(\mathbf{x}) & \text{if } |\boldsymbol{\alpha}|=1,\dots,p-2 \end{cases}. \tag{8.6}$$

It is worth to stress that here the orthonormalization process is performed with a different target with respect to what was done in [45]; in fact, there, the method is built employing the canonical bases computed taking moments with respect to scaled monomials $\{q^1_{\boldsymbol{\alpha}}\}^{p-2}_{|\boldsymbol{\alpha}|=0}$; however, the projectors onto polynomial spaces, i.e. Π^0_{p-2} and Π^∇_p defined in (2.18) and (2.8), respectively, are computed expanding with respect to polynomial basis $\{q^3_{\boldsymbol{\alpha}}\}^{p-2}_{|\boldsymbol{\alpha}|=0}$ defined in (8.6). Here, we define in addition internal moments with respect to basis $\{q^3_{\boldsymbol{\alpha}}\}^{p-2}_{|\boldsymbol{\alpha}|=0}$.

The implementation issues regarding this new basis are discussed in Section 8.2.2.

The implementation of VEM with basis $\{q^1_{\boldsymbol{\alpha}}\}^{p-2}_{|\boldsymbol{\alpha}|=0}$ is well-known, see [30]. For what concerns the implementation when employing the two novel bases $\{q^2_{\boldsymbol{\alpha}}\}^{p-2}_{|\boldsymbol{\alpha}|=0}$ and $\{q^3_{\boldsymbol{\alpha}}\}^{p-2}_{|\boldsymbol{\alpha}|=0}$, we refer to Section 8.2.

In summary, we presented three choices for the polynomial basis dual to internal moments (2.4). One is of easy implementation, but it may be the cause of a high condition number of

the stiffness matrix when using high-order methods or in presence of "bad-shaped" polygons. The other two bases are obtained by two distinct orthonormalization processes; their performances with respect to the condition number are investigated in Section 8.3. What we can anticipate is that they outclass the performances of their counterpart using the standard basis $\{q^1_{\boldsymbol{\alpha}}\}^{p-2}_{|\boldsymbol{\alpha}|=0}$ in the two situations above mentioned.

A *heuristic* reason for this fact is the following. If, for each element K, the local Virtual Element Space $V(K)$ were a space consisting of polynomials only, then picking internal moments (2.4) with respect to an $L^2(K)$ orthonormal polynomial basis would automatically entail that the local canonical basis is made of polynomials and contain a subset of $L^2(K)$ orthonormal polynomials spanning $\mathbb{P}_{p-2}(K)$; it is well-known in the theory of Spectral Elements, see e.g. [57, 90], that employing L^2 orthonormal canonical basis damp the condition number of the stiffness matrix when increasing the polynomial degree.

Nonetheless, local Virtual Element Spaces does not contain polynomials only, but also other functions needed for prescribing H^1 conformity. As stated in (8.2), the dimension of the subspace of nonpolynomial functions is, in terms of the degree of accuracy, asymptotically smaller than the dimension of the subspace of polynomial functions. Therefore, *in a very rough sense*, employing L^2 orthonormal polynomials in the definition of internal moments entails a sort of *partial "orthonormalization"* of the local canonical basis.

Before concluding this section, we associate to bases $\{q^i_{\boldsymbol{\alpha}}\}^{p-2}_{|\boldsymbol{\alpha}|=0}$ the sets of dofs $\{\mathrm{dof}^i_j\}^{N_{V_K}}_{j=1}$ and the canonical bases $\{\varphi^i_j\}^{N_{V_K}}_{j=1}$, for all $i = 1, 2, 3$, where we recall that the canonical basis is defined in (6.2) and N_{V_K} is the dimension of space $V_p(K)$. This notation will be instrumental in the forthcoming section.

8.1.3 Stabilizations and bases: the effects on the method

Having presented in the two foregoing sections various choices of stabilizations and canonical bases, we want here to highlight the effects of such choices on the method and on the ill-conditioning of the stiffness matrix.

Stabilization. The choice of the stabilization has two effects. The first one is related to the convergence of the method since nonproperly tailored choices of the stabilization automatically entail higher pollution factor $\frac{\alpha^*(p)}{\alpha_*(p)}$, see (2.52) and especially (2.37). Secondly, since the stabilization appears in the discrete bilinear form of the method, see (2.13), there is also an effect on the condition number of the stiffness matrix.

Canonical basis. The choice of the canonical basis has also two effects. Firstly, it has an impact on the condition number of the global stiffness matrix, simply because by changing the basis automatically the entries of the stiffness matrix modify. Secondly, by picking different canonical bases, one also changes the definition of the stabilization; as an example, if we fix stabilization S^K_1 defined in (6.3) and we apply it to functions in the Virtual Element space, then we get in general different values, since the definition of the internal degrees of freedom vary depending on the choice of the basis; in particular, one also modify the behaviour of the pollution factor $\frac{\alpha^*(p)}{\alpha_*(p)}$.

8.2 Hitchhikers guide for VEM based on the new bases $\{q^2_{\boldsymbol{\alpha}}\}^{p-2}_{|\boldsymbol{\alpha}|=0}$ and $\{q^3_{\boldsymbol{\alpha}}\}^{p-2}_{|\boldsymbol{\alpha}|=0}$

In this section, we deal with the computational aspects employing the two (nonmonomial) bases discussed in Section 8.1.2.

We split this section into two parts. In Section 8.2.1, we discuss the implementation details by employing basis $\{q^2_{\boldsymbol{\alpha}}\}^{p-2}_{|\boldsymbol{\alpha}|=0}$, whereas, in Section 8.2.2, we do the same thing for basis $\{q^3_{\boldsymbol{\alpha}}\}^{p-2}_{|\boldsymbol{\alpha}|=0}$.

We fix preliminarily some notations. In [30], the implementation details employing basis $\{q^1_{\boldsymbol{\alpha}}\}^{p-2}_{|\boldsymbol{\alpha}|=0}$ defined in (8.4) were discussed. In particular, it was proven that the local stiffness

matrix can be built with the aid of some auxiliary matrices which we recall here:

$$\begin{aligned}
&\mathbf{G}_{\alpha,\beta} = \begin{cases} P_0(q^1_{\boldsymbol{\beta}}) & \text{if } \alpha = 1 \\ (\nabla q^1_{\boldsymbol{\alpha}}, \nabla q^1_{\boldsymbol{\beta}})_{0,K} & \text{if } \alpha \geq 2 \end{cases}, \qquad \widetilde{\mathbf{G}}_{\alpha,\beta} = (\nabla q^1_{\boldsymbol{\alpha}}, \nabla q^1_{\boldsymbol{\beta}})_{0,K}, \\
&\mathbf{D}_{j,\alpha} = \mathrm{dof}^1_j(q^1_{\boldsymbol{\alpha}}), \qquad \mathbf{B}_{\alpha,j} = \begin{cases} P_0\varphi^1_j & \text{if } \alpha = 1 \\ (\nabla q^1_{\boldsymbol{\alpha}}, \nabla \varphi^1_j)_{0,K} & \text{if } \alpha \geq 2 \end{cases}, \\
&\forall\, \boldsymbol{\alpha},\, \boldsymbol{\beta} \in \mathbb{N}^2 \quad \text{with} \quad |\boldsymbol{\alpha}|,\, |\boldsymbol{\beta}| = 0, \ldots, p, \quad i = 0, \ldots, N_{V_K},
\end{aligned} \tag{8.7}$$

where we recall that P_0 is defined in (2.9) and (2.10), that N_{V_K} is the dimension of local space $V_p(K)$ defined in (2.3) and that we are employing with an abuse of notation bijection (8.3).

The local stiffness matrix reads:

$$\mathbf{K}^K_p = (\mathbf{\Pi}^\nabla_*)^T \cdot \widetilde{\mathbf{G}} \cdot (\mathbf{\Pi}^\nabla_*) + (\mathbf{Id} - \mathbf{\Pi}^\nabla)^T \cdot \mathbf{S}^{\mathbf{K}} \cdot (\mathbf{Id} - \mathbf{\Pi}^\nabla), \tag{8.8}$$

where $\mathbf{S}^{\mathbf{K}}$ denotes the matrix associated with any of the bilinear forms S^K introduced in Section 8.1.1, where $\mathbf{\Pi}^\nabla_*$ denotes the matrix associated with operator Π^∇_p introduced in (2.8) acting from the local VE space $V(K)$ to $\mathbb{P}_p(K)$ with respect to basis $\{q^1_{\boldsymbol{\alpha}}\}^{p-2}_{|\boldsymbol{\alpha}|=0}$ and where $\mathbf{\Pi}^\nabla$ denotes the matrix associated with the operator Π^∇_p introduced in (2.8) acting from the local VE space $V(K)$ to $\mathbb{P}_p(K)$ with respect to canonical basis $\{\varphi^1_j\}^{N_{V_K}}_{j=1}$ defined in (6.2).

In [30], it was shown that:

$$\mathbf{\Pi}^\nabla_* = \mathbf{G}^{-1} \cdot \mathbf{B}, \qquad \mathbf{\Pi}^\nabla = \mathbf{D} \cdot \mathbf{G}^{-1} \cdot \mathbf{B}. \tag{8.9}$$

The aim of the two forthcoming sections is to give a hint on how to construct the counterparts of the matrices in (8.7) and therefore also in (8.9), by employing the polynomial and canonical bases $\{q^i_{\boldsymbol{\alpha}}\}^{p-2}_{|\boldsymbol{\alpha}|=0}$ and $\{\varphi^i_j\}^{N_{V_K}}_{i=1}$ for $i = 2$, 3 respectively.

8.2.1 A hitchhiker's guide to VEM based on basis $\{q^2_{\boldsymbol{\alpha}}\}^{p-2}_{|\boldsymbol{\alpha}|=0}$

The aim of the present section is to write the local stiffness matrix employing the new canonical basis $\{\varphi^2_j\}^{N_{V_K}}_{j=1}$ associated with polynomial basis $\{q^2_{\boldsymbol{\alpha}}\}^{p-2}_{|\boldsymbol{\alpha}|=0}$ and expanding all the projectors with respect to the polynomial spaces on polynomial basis $\{q^2_{\boldsymbol{\alpha}}\}^{p}_{|\boldsymbol{\alpha}|=0}$ of $\mathbb{P}_p(K)$ introduced in Section 8.1.2, which is obtained by an L^2 ortonormalization of the monomial basis $\{q^1_{\boldsymbol{\alpha}}\}^{p-2}_{|\boldsymbol{\alpha}|=0}$ defined in (8.4) using the stable Gram-Schmidt process presented in [23]. In particular, we can write, always using with a little abuse of notation the bijection (8.3):

$$q^2_{\boldsymbol{\alpha}}(\mathbf{x}) = \sum_{\beta=1}^{\alpha} \mathbf{GS}_{\alpha,\beta}\, q^1_{\boldsymbol{\alpha}}(\mathbf{x}) \qquad \forall\, \boldsymbol{\alpha} \in \mathbb{N}^2, \quad |\boldsymbol{\alpha}| = 0, \ldots, p, \tag{8.10}$$

where $\mathbf{GS}$ is the lower triangular matrix containing the orthonormalization coefficients.

Importantly, the polynomials involved in the construction of the VEM stiffness matrix associated with basis $\{q^2_{\boldsymbol{\alpha}}\}^{p-2}_{|\boldsymbol{\alpha}|=0}$ are expanded in terms of basis $\{q^1_{\boldsymbol{\alpha}}\}^{p-2}_{|\boldsymbol{\alpha}|=0}$.

For the sake of simplicity, we denote the counterpart of the VEM matrices in (8.7) and (8.9) associated with bases $\{q^2_{\boldsymbol{\alpha}}\}^{p}_{|\boldsymbol{\alpha}|=0}$ and $\{\varphi^2_j\}^{N_{V_K}}_{j=1}$ with a bar at the top of each one of them. We explain how to compute in the new setting such new matrices.

We start with matrix $\overline{\widetilde{\mathbf{G}}}$, which is defined as:

$$\overline{\widetilde{\mathbf{G}}}_{\alpha,\beta} = (\nabla q^2_{\boldsymbol{\alpha}}, \nabla q^2_{\boldsymbol{\beta}})_{0,K} \qquad \forall\, \boldsymbol{\alpha},\, \boldsymbol{\beta} \in \mathbb{N}^2, \quad |\boldsymbol{\alpha}|,\, |\boldsymbol{\beta}| = 0, \ldots, p.$$

One simply has to compute:

$$\overline{\widetilde{\mathbf{G}}} = \mathbf{GS} \cdot \widetilde{\mathbf{G}} \cdot \mathbf{GS}^T.$$

Now, we consider matrix $\overline{\mathbf{G}}$ defined as:

$$\overline{\mathbf{G}}_{\alpha,\beta} = \begin{cases} P_0(q^2_{\boldsymbol{\beta}}) & \text{if } \alpha = 1 \\ (\nabla q^2_{\boldsymbol{\alpha}}, \nabla q^2_{\boldsymbol{\beta}})_{0,K} & \text{if } \alpha \geq 2 \end{cases} \qquad \forall\, \boldsymbol{\alpha},\, \boldsymbol{\beta} \in \mathbb{N}^2, \quad |\boldsymbol{\alpha}|,\, |\boldsymbol{\beta}| = 0, \ldots, p.$$

We obviously have to take care only of the first line of the matrix since the remainder is inherited from $\widetilde{\overline{\mathbf{G}}}$, where we recall that P_0 is defined in (2.9) when $p = 1$ and in (2.10) when $p \geq 2$.

We distinguish two cases.

($p = 1$) $P_0(q^2_{\boldsymbol{\beta}}) = \frac{1}{N_K} \sum_{\ell=1}^{N_K} q^2_{\boldsymbol{\beta}}(\nu_\ell)$, where we recall that $\{\nu_\ell\}_{\ell=1}^{N_K}$ denotes the set of vertices of K. We shall then write:

$$\begin{aligned} P_0(q^2_{\boldsymbol{\beta}}) &= \frac{1}{N_K} \sum_{\ell=1}^{N_K} \left(\sum_{\gamma=1}^{\beta} \mathbf{GS}_{\beta,\gamma} q^1_{\boldsymbol{\gamma}}(\nu_\ell) \right) = \sum_{\gamma=1}^{\beta} \mathbf{GS}_{\beta,\gamma} \left(\frac{1}{N_K} \sum_{\ell=1}^{N_K} q^1_{\boldsymbol{\gamma}}(\nu_\ell) \right) \\ &= \sum_{\gamma=1}^{\beta} \mathbf{GS}_{\beta,\gamma} \mathbf{G}_{1,\gamma} = \mathbf{GS}(\beta, 1:\beta) \cdot \mathbf{G}(1, 1:\beta)^T. \end{aligned}$$

($p \geq 2$) In this case, we have:

$$P_0(q^2_{\boldsymbol{\beta}}) = \frac{1}{|K|} \int_K q^2_{\boldsymbol{\beta}} = \mathbf{GS}^{-1}_{1,1} \frac{1}{|K|} \int_K q^2_{\boldsymbol{\beta}} \mathbf{GS}_{1,1} = \mathbf{GS}^{-1}_{1,1} \frac{1}{|K|} \int_K q^2_1 q^2_{\boldsymbol{\beta}} = \begin{cases} \frac{1}{\mathbf{GS}_{1,1}|K|} & \text{if } \beta = 1 \\ 0 & \text{else} \end{cases},$$

since basis $\{q^2_{\boldsymbol{\alpha}}\}_{\alpha=1}^{n_p}$ is $L^2(K)$ orthonormal by construction.

Next, we turn our attention to the matrix $\overline{\mathbf{D}}$ which is defined as:

$$\overline{\mathbf{D}}_{j,\alpha} = \mathrm{dof}^2_j(q^2_{\boldsymbol{\alpha}}) \qquad \forall\, \boldsymbol{\alpha} \in \mathbb{N}^2, \quad |\boldsymbol{\alpha}| = 0, \ldots, p, \quad j = 1, \ldots, N_{V_K}$$

and we distinguish two situations.

- Let us consider firstly the boundary dofs:

$$\overline{\mathbf{D}}_{j,\alpha} = \mathrm{dof}^2_j(q^2_{\boldsymbol{\alpha}}) = q^2_{\boldsymbol{\alpha}}(\xi_j) = \sum_{\beta=1}^{\alpha} \mathbf{GS}_{\alpha,\beta} q^1_{\boldsymbol{\beta}}(\xi_j) = \sum_{\beta=1}^{\alpha} \mathbf{GS}_{\alpha,\beta} \mathbf{D}_{j,\beta} = \mathbf{GS}(\alpha, 1:\alpha) \cdot \mathbf{D}(j, 1:\alpha)^T.$$

  where ξ_j is a proper node on the boundary.

- Next, we deal with the internal dofs. One simply has, if $q^2_{\boldsymbol{\gamma}}$ is the polynomial associated with dof^2_j:

$$\mathrm{dof}^2_j(q^2_{\boldsymbol{\alpha}}) = \frac{1}{|K|} \int_K q^2_{\boldsymbol{\alpha}}\, q^2_{\boldsymbol{\gamma}} = \frac{1}{|K|} \delta_{\alpha,j} \qquad \forall\, j = 1, \ldots, n_{p-2},$$

  owing again to the L^2 orthonormality of basis $\{q^2_{\boldsymbol{\alpha}}\}_{|\boldsymbol{\alpha}|=0}^{p}$.

Finally, we discuss the construction of matrix $\overline{\mathbf{B}}$ which is defined as:

$$\overline{\mathbf{B}}_{\alpha,j} = \begin{cases} P_0(\varphi^2_j) & \text{if } \alpha = 1 \\ (\nabla q^2_{\boldsymbol{\alpha}}, \nabla \varphi^2_j)_{0,K} & \text{if } \alpha \geq 2 \end{cases} \qquad \forall\, \boldsymbol{\alpha} \in \mathbb{N}^2, \quad |\boldsymbol{\alpha}| = 0, \ldots, p, \quad \forall\, j = 1, \ldots, N_{V_K},$$

where we recall that P_0 is defined in (2.9) when $p = 1$ and in (2.10) when $p \geq 2$.

We firstly deal with the first line and we consider separately the two cases $p = 1$ and $p \geq 2$.

($p = 1$) $P_0(\varphi^2_j) = \frac{1}{N_K} \sum_{\ell=1}^{N_K} \varphi^2_j(\nu_\ell) = \frac{1}{N_K} \sum_{\ell=1}^{N_K} \varphi^1_j(\nu_\ell)$, where we recall that $\{\nu_\ell\}_{\ell=1}^{N_K}$ is the set of vertices of polygon K. Thus $\overline{\mathbf{B}}_{1,j} = \mathbf{B}_{1,j}$, since $\varphi^2_j = \varphi^1_j$ on ∂K for all $j = 1, \ldots, N_{V_K}$.

($p \geq 2$) In this case, we can write:

$$P_0(\varphi_j^2) = \frac{1}{|K|}\int_K \varphi_j^2 = \mathbf{GS}_{1,1}^{-1}\frac{1}{|K|}\int_K \varphi_j^2\,\mathbf{GS}_{1,1} = \mathbf{GS}_{1,1}^{-1}\frac{1}{|K|}\int_K \varphi_j^2\, q_1^2$$
$$= \begin{cases} \mathbf{GS}_{1,1}^{-1} & \text{if } \varphi_j \text{ is the first internal element,} \\ 0 & \text{else,} \end{cases}$$

since $q_1^2 = \mathbf{GS}_{1,1}q_1^1 = \mathbf{GS}_{1,1}$. Thus $\overline{\mathbf{B}}_{1,j} = \mathbf{GS}_{1,1}^{-1}\mathbf{B}_{1,j}$ for all $j = 1, \ldots, N_{V_K}$.

Next, we treat all the other lines. We must compute $(\nabla q_{\boldsymbol{\alpha}}^2, \nabla\varphi_j^2)_{0,K}$. Again, we consider two different situations.

- If φ_j^2 is a boundary basis function, i.e. $j = 1, \ldots, pN_K$, where we recall that N_K is the number of edges (and vertices) of K, then:

$$(\nabla q_{\boldsymbol{\alpha}}^2, \nabla\varphi_j^2)_{0,K} = \int_{\partial K}(\partial_{\mathbf{n}} q_{\boldsymbol{\alpha}}^2)\,\varphi_j^2 = \sum_{\beta=1}^{\alpha}\mathbf{GS}_{\alpha,\beta}\int_{\partial K}(\partial_{\mathbf{n}} q_{\boldsymbol{\beta}}^1)\,\varphi_j^2$$
$$= \sum_{\beta=1}^{\alpha}\mathbf{GS}_{\alpha,\beta}\int_{\partial K}(\partial_{\mathbf{n}} q_{\boldsymbol{\beta}}^1)\,\varphi_j^1 = \sum_{\beta=1}^{\alpha}\mathbf{GS}_{\alpha,\beta}\mathbf{B}_{\beta,j} = \mathbf{GS}(\alpha, 1:\alpha)\cdot\mathbf{B}(1:\alpha, j),$$

  where we used that $\varphi_j^1 = \varphi_j^2$ on ∂K for all $j = 1, \ldots, N_{V_K}$.

- Assume now φ_j^2 is an internal basis function. This case is a bit more involved. We write:

$$(\nabla q_{\boldsymbol{\alpha}}^2, \nabla\varphi_j^2)_{0,K} = -\int_K (\Delta q_{\boldsymbol{\alpha}}^2)\varphi_j^2. \tag{8.11}$$

  We are able to expand $\Delta q_{\boldsymbol{\alpha}}^2$ into a combination of elements of the basis $\{q_{\boldsymbol{\beta}}^2\}_{\beta=0}^{n_{p-2}}$ since the Laplace operator eliminates the high ($p-1$ and p) polynomial degree contributions. We get:

$$\Delta q_{\boldsymbol{\alpha}}^2 = \sum_{|\boldsymbol{\beta}|=0}^{p-2}\overline{\mathbf{F}}_{\alpha,\beta}\, q_{\boldsymbol{\beta}}^2. \tag{8.12}$$

  We only need to compute the entries of matrix $\overline{\mathbf{F}}$. To this purpose, we test (8.12) with $q_{\boldsymbol{\gamma}}^2$ and we obtain, owing to L^2 orthogonality of basis $\{q_{\boldsymbol{\alpha}}^2\}_{|\boldsymbol{\alpha}|=0}^{p-2}$:

$$\overline{\mathbf{F}}_{\alpha,\gamma} = (\Delta q_{\boldsymbol{\alpha}}^2, q_{\boldsymbol{\gamma}}^2)_{0,K} = -(\nabla q_{\boldsymbol{\alpha}}^2, \nabla q_{\boldsymbol{\gamma}}^2)_{0,K} + \left(\partial_{\mathbf{n}} q_{\boldsymbol{\alpha}}^2, q_{\boldsymbol{\gamma}}^2\right)_{0,\partial K}.$$

  The first term is nothing but $-\overline{\widetilde{\mathbf{G}}}_{\alpha,\gamma}$. We wonder how to compute the second term. We note that matrix $\mathbf{L}$ defined as:

$$\mathbf{L}_{\alpha,\beta} = \int_{\partial K}(\partial_{\mathbf{n}} q_{\boldsymbol{\alpha}}^1)\, q_{\boldsymbol{\beta}}^1 \qquad \forall\,\boldsymbol{\alpha},\,\boldsymbol{\beta}\in\mathbb{N}^2, \quad |\boldsymbol{\alpha}|, |\boldsymbol{\beta}| = 0, \ldots, p, \tag{8.13}$$

  can be computed exactly. For the sake of completeness, we explicitly write how. Given $\mathcal{E}(K)$ the set of edges of K:

$$\mathbf{L}_{\alpha,\beta} = \sum_{s\in\mathcal{E}(K)}\int_s (\partial_{\mathbf{n}} q_{\boldsymbol{\alpha}}^1)\, q_{\boldsymbol{\beta}}^1 = \sum_{s\in\mathcal{E}(K)}\left\{\sum_{k=0}^{p}\omega_k^e\left(\partial_{\mathbf{n}} q_{\boldsymbol{\alpha}}^1, q_{\boldsymbol{\beta}}^1\right)_{0,\partial K}(\nu_k^s)\right\},$$

  where ω_k^e and ν_k^e, $k = 0, \ldots, p$, are the k-th weight and node of the Gauß-Lobatto quadrature over edge s. It is easy to check that if we set:

$$\overline{\mathbf{L}}_{\alpha,\beta} = \int_{\partial K}(\partial_{\mathbf{n}} q_{\boldsymbol{\alpha}}^2)\, q_{\boldsymbol{\beta}}^2,$$

then:

$$\overline{\mathbf{L}} = \mathbf{GS} \cdot \mathbf{L} \cdot \mathbf{GS}^T.$$

As a consequence:

$$\overline{\mathbf{F}} = \overline{\mathbf{L}} - \overline{\widetilde{\mathbf{G}}}.$$

Now, we plug (8.12) in (8.11) obtaining:

$$\begin{aligned}\overline{\mathbf{B}}_{\alpha,j} =& (\nabla q^2_{\boldsymbol{\alpha}}, \nabla \varphi^2_j)_{0,K} = -\sum_{|\boldsymbol{\beta}|=0}^{p-2} \overline{\mathbf{F}}_{\alpha,\beta} (q^2_{\boldsymbol{\beta}}, \varphi^2_j)_{0,K} \\ =& -\sum_{|\boldsymbol{\beta}|=0}^{p-2} \overline{\mathbf{F}}_{\alpha,\beta} \overline{\mathbf{C}}_{\beta,j} = -\overline{\mathbf{F}}(\alpha, 1:n_{p-2}) \cdot \overline{\mathbf{C}}(1:n_{p-2}, j),\end{aligned}$$

where $\overline{\mathbf{C}}$ is a matrix defined as follows:

$$\overline{\mathbf{C}}_{\alpha,j} = (q^2_{\boldsymbol{\alpha}}, \varphi^2_j)_{0,K} \qquad \forall\, \boldsymbol{\alpha} \in \mathbb{N}^2, \quad |\boldsymbol{\alpha}| = 0, \dots, p-2, \quad \forall j = 1, \dots N_{V_K}.$$

One concludes by noting that for all $\boldsymbol{\alpha} \in \mathbb{N}^2$ with $|\boldsymbol{\alpha}| = 0, \dots, p-2$:

$$\overline{\mathbf{C}}_{\alpha,j} = (q^2_{\boldsymbol{\alpha}}, \varphi^2_j)_{0,K} = \begin{cases} 0 & \text{if } \varphi^2_j \text{ is a boundary basis element} \\ |K| \frac{1}{|K|} \int_K q^2_{\boldsymbol{\alpha}}\, \varphi^2_j = \delta_{\alpha,j}|K| & \text{otherwise} \end{cases}.$$

8.2.2 A hitchhiker's guide to VEM based on basis $\{q^3_{\boldsymbol{\alpha}}\}^{p-2}_{|\boldsymbol{\alpha}|=0}$

The aim of the present section is to write the local stiffness matrix employing the new canonical basis $\left\{\varphi^3_j\right\}_{j=1}^{N_{V_K}}$ associated with polynomial basis $\{q^3_{\boldsymbol{\alpha}}\}^{p-2}_{|\boldsymbol{\alpha}|=0}$ and expanding all the projectors with respect to the polynomial spaces on polynomial basis $\{q^3_{\boldsymbol{\alpha}}\}^{p}_{|\boldsymbol{\alpha}|=0}$, which is obtained by a partial orthogonalization of $\{q^1_{\boldsymbol{\alpha}}\}^{p}_{|\boldsymbol{\alpha}|=0}$.More precisely, we write, always using with a little abuse of notation the bijection (8.3):

$$\begin{cases} q^3_{\boldsymbol{\alpha}} = q^1_{\boldsymbol{\alpha}} & \forall\, \boldsymbol{\alpha} \in \mathbb{N}^2, \quad |\boldsymbol{\alpha}| = 0,\, p-1,\, p \\ q^3_{\boldsymbol{\alpha}}(\mathbf{x}) = \sum_{\beta=1}^{\alpha} \mathbf{GS}_{\alpha,\beta}\, q^1_{\boldsymbol{\alpha}}(\mathbf{x}) & \forall\, \boldsymbol{\alpha} \in \mathbb{N}^2, \quad |\boldsymbol{\alpha}| = 1, \dots, p-2 \end{cases},$$

where $\mathbf{GS}$ is the matrix containing the orthonormalization coefficients described in (8.6). In particular, we have here $\mathbf{GS} \in \mathbb{R}^{n_{p-2}-1 \times n_{p-2}-1}$. We note that we are using, with an abuse of notation, the same name of the (lower triangular) matrix containing the orthonormalization coefficients described in (8.10).

For the sake of simplicity, we denote again the counterpart of the VEM matrices in (8.7) and (8.8) associated with bases $\{q^3_{\boldsymbol{\alpha}}\}^{p}_{|\boldsymbol{\alpha}|=0}$ and $\{\varphi^3_j\}_{j=1}^{N_{V_K}}$ with a bar at the top of each one of them. We explain how to compute in the new setting such new matrices.

We firstly observe that if $p = 1, 2$, then the two bases $\{q^1_{\boldsymbol{\alpha}}\}^{p}_{|\boldsymbol{\alpha}|=0}$ and $\{q^3_{\boldsymbol{\alpha}}\}^{p}_{|\boldsymbol{\alpha}|=0}$ coincide. For this reason, we assume without loss of generality that $p \geq 3$.

Matrix $\overline{\widetilde{\mathbf{G}}}$ can be computed as in Section 8.2.1. Therefore, for the computation of $\overline{\mathbf{G}}$, we only need to treat the first row. We have:

$$\overline{\mathbf{G}}_{1,\boldsymbol{\beta}} = P_0(q^3_{\boldsymbol{\beta}}) = \frac{1}{|K|} \int_K q^3_{\boldsymbol{\beta}} \qquad \forall\, \boldsymbol{\beta} \in \mathbb{N}^2 \text{ such that } |\boldsymbol{\beta}| = 0, \dots, p.$$

Therefore:

$$\begin{aligned}\overline{\mathbf{G}}_{1,\boldsymbol{\beta}} &= \begin{cases} \mathbf{G}_{1,\boldsymbol{\beta}} & \text{if } |\boldsymbol{\beta}| = 0, p-1, p \\ \frac{1}{|K|} \sum_{|\boldsymbol{\alpha}|=1}^{p-2} \mathbf{GS}_{\beta-1,\alpha} \int_K q^1_{\boldsymbol{\alpha}} & \text{otherwise} \end{cases} \\ &= \begin{cases} \mathbf{G}_{1,\boldsymbol{\beta}} & \text{if } |\boldsymbol{\beta}| = 0, p-1, p \\ \mathbf{GS}(\beta-1, 2:n_{p-2}) \cdot \mathbf{G}(1, 2:n_{p-2})^T & \text{otherwise} \end{cases}.\end{aligned}$$

Matrix $\overline{\mathbf{D}}$ is defined instead by:

$$\overline{\mathbf{D}}_{i,\alpha} = \mathrm{dof}_i^3(q_{\boldsymbol{\alpha}}^3).$$

We start by assuming that dof_i^3 is a vertex/edge dof. We have given ξ_i a vertex or a Gauß-Lobatto node:

$$\overline{\mathbf{D}}_{i,\boldsymbol{\alpha}} = q_{\boldsymbol{\alpha}}^3(\xi_i) = \begin{cases} q_{\boldsymbol{\alpha}}(\xi_i) & \text{if } |\boldsymbol{\alpha}| = 0, p-1, p \\ \mathbf{GS}(\alpha - 1, 2 : n_{p-2}) \cdot \mathbf{D}(i, 2 : n_{p-2})' & \text{otherwise} \end{cases}.$$

Next, we assume that dof_i^3 is an internal dof. We distinguish two subcases. Firstly, let $q_{\boldsymbol{\alpha}}^3$ be such that $|\boldsymbol{\alpha}| = 1, \ldots, p-2$. Then, given $q_{\boldsymbol{\beta}}^3$, $|\boldsymbol{\beta}| = 0, \ldots, p-2$, the polynomial associated with degree of freedom dof_i^3:

$$\begin{aligned} \mathrm{dof}_i^3(q_{\boldsymbol{\beta}}^3) &= \frac{1}{|K|} \int_K q_{\boldsymbol{\beta}}^3 q_{\boldsymbol{\alpha}}^3 \\ &= \begin{cases} |K|^{-1} \delta_{\alpha,\beta} & \text{if } |\boldsymbol{\beta}| = 0 \\ \frac{1}{|K|} \sum_{|\boldsymbol{\gamma}|=1}^{p-2} \mathbf{GS}_{\boldsymbol{\beta}-1,\boldsymbol{\gamma}} \int_K q_{\boldsymbol{\gamma}}^1 = \mathbf{GS}(\beta - 1, 2 : n_{p-2}) \cdot \mathbf{D}(1, 2 : n_{p-2})^T & \text{if } |\boldsymbol{\beta}| = 1, \ldots, p-2 \end{cases}. \end{aligned}$$

If now $q_{\boldsymbol{\alpha}}^3$ is such that $|\boldsymbol{\alpha}| = 0, p, p-1$, then:

$$\begin{aligned} \mathrm{dof}_i^3(q_{\boldsymbol{\alpha}}^3) = \mathrm{dof}_i^3(q_{\boldsymbol{\alpha}}^1) &= \frac{1}{|K|} \int_K q_{\boldsymbol{\beta}}^3 q_{\boldsymbol{\alpha}}^1 \\ &= \begin{cases} \frac{1}{|K|} \int_K q_{\boldsymbol{\beta}}^1 q_{\boldsymbol{\alpha}}^1 & \text{if } |\boldsymbol{\beta}| = 0 \\ \sum_{|\gamma|=1}^{p-2} \mathbf{GS}_{\beta-1,\gamma} \frac{1}{|K|} \int_K q_{\boldsymbol{\gamma}}^1 q_{\boldsymbol{\alpha}}^1 & \text{otherwise} \end{cases} \\ &= \begin{cases} \mathbf{D}_{i,\boldsymbol{\alpha}} & \text{if } |\boldsymbol{\beta}| = 0 \\ \mathbf{GS}(\beta - 1, 2 : n_{p-2}) \cdot \mathbf{D}(\mathrm{end} - n_{p-2} + 2 : \mathrm{end}, \alpha) & \text{otherwise} \end{cases}. \end{aligned}$$

The construction of matrix $\overline{\mathbf{B}}$ is the most complicated. We set:

$$\overline{\mathbf{B}}_{\boldsymbol{\alpha},i} = (\nabla q_{\boldsymbol{\alpha}}^3, \nabla \varphi_i^3)_{0,K} = (\partial_{\mathbf{n}} q_{\boldsymbol{\alpha}}^3, \varphi_i^3)_{0,\partial K} - (\Delta q_{\boldsymbol{\alpha}}^3, \varphi_i^3)_{0,K}. \tag{8.14}$$

We firstly assume φ_i^3 vertex/edge basis element. We distinguish two subcases. If $q_{\boldsymbol{\alpha}}^3$ is such that $|\boldsymbol{\alpha}| = 1, \ldots, p-2$, we deduce:

$$\overline{\mathbf{B}}_{\boldsymbol{\alpha},i} = (\partial_{\mathbf{n}} q_{\boldsymbol{\alpha}}^3, \varphi_i^3)_{0,\partial K} = \sum_{|\boldsymbol{\beta}|=1}^{p-2} \mathbf{GS}_{\alpha-1,\beta} (\partial_{\mathbf{n}} q_{\boldsymbol{\beta}}^1, \varphi_i^3)_{0,\partial K} = \mathbf{GS}(\alpha - 1, 1 : n_{p-2}) \cdot \mathbf{B}(1 : n_{p-2}, i).$$

If $q_{\boldsymbol{\alpha}}^3$ is such that $|\boldsymbol{\alpha}| = 0, p-1, p$, we simply have:

$$\overline{\mathbf{B}}_{\boldsymbol{\alpha},i} = (\partial_{\mathbf{n}} q_{\boldsymbol{\alpha}}^3, \varphi_i^3)_{0,\partial K} = (\partial_{\mathbf{n}} q_{\boldsymbol{\alpha}}^1, \varphi_i^1)_{0,\partial K} = \mathbf{B}_{\boldsymbol{\alpha},i}.$$

Next, we assume φ_i^3 internal basis element. We distinguish again two subcases. We begin by assuming that $q_{\boldsymbol{\alpha}}^3$ is such that $|\boldsymbol{\alpha}| = 1, \ldots, p-2$:

$$\overline{\mathbf{B}}_{\boldsymbol{\alpha},i} = (-\Delta q_{\boldsymbol{\alpha}}^3, \varphi_i^3)_{0,K}.$$

We want to expand $-\Delta q_{\boldsymbol{\alpha}}^3$ in terms of the basis $\{q_{\boldsymbol{\alpha}}^3\}_{|\boldsymbol{\alpha}|=0}^{p-2}$, which we recall is not completely orthonormal due to the presence of q_1^3:

$$-\Delta q_{\boldsymbol{\alpha}}^3 = \sum_{|\boldsymbol{\beta}|=0}^{p-2} \mu_{\boldsymbol{\alpha},\boldsymbol{\beta}} q_{\boldsymbol{\beta}}^3.$$

Using L^2 orthogonality, if $|\boldsymbol{\beta}| = 1, \dots, p-2$:

$$\mu_{\boldsymbol{\alpha},\boldsymbol{\beta}} = (-\Delta q^3_{\boldsymbol{\alpha}}, q^3_{\boldsymbol{\beta}})_{0,K} = (\nabla q^3_{\boldsymbol{\alpha}}, \nabla q^3_{\boldsymbol{\beta}})_{0,K} - (\partial_{\mathbf{n}} q^3_{\boldsymbol{\alpha}}, q^3_{\boldsymbol{\beta}})_{0,\partial K} = I - II. \tag{8.15}$$

The first term on the right-hand side of (8.15) is nothing but $\overline{\widetilde{\mathbf{G}}}_{\alpha,\beta}$, while the second term is $\overline{\mathbf{L}}_{\alpha,\beta}$, where matrix $\overline{\mathbf{L}}$ is computed as in Section 8.2.1.

Finally, we investigate what happens if $q^3_{\boldsymbol{\alpha}}$ is such that $|\boldsymbol{\alpha}| = 0, p-1, p$. If $|\boldsymbol{\alpha}| = 0$, then one simply has $\overline{\mathbf{B}}_{\alpha,i} = 0$. Otherwise:

$$-\Delta q^1_{\boldsymbol{\alpha}} = -\Delta q^1_{(\alpha_1,\alpha_2)} = -\alpha_1(\alpha_1-1) q^1_{(\alpha_1-2,\alpha_2)} - \alpha_2(\alpha_2-1) q^1_{(\alpha_1,\alpha_2-2)} =: c_1 q^1_{\widetilde{\boldsymbol{\alpha}}_1} + c_2 q^1_{\widetilde{\boldsymbol{\alpha}}_2}, \tag{8.16}$$

with $|\widetilde{\boldsymbol{\alpha}}_1|$, $|\widetilde{\boldsymbol{\alpha}}_2| = 0, \dots, p-2$. This implies that we have to compute, for $j = 1, 2$:

$$(q^1_{\widetilde{\boldsymbol{\alpha}}_j}, \varphi^3_i)_{0,K}.$$

We expand $q^1_{\widetilde{\boldsymbol{\alpha}}_j}$ with respect to basis $\{q^3_{\boldsymbol{\alpha}}\}^{p-2}_{|\boldsymbol{\alpha}|=0}$:

$$(q^1_{\widetilde{\boldsymbol{\alpha}}}, \varphi^3_i)_{0,K} = (q^3_1, \varphi^3_i)_{0,K} + \sum_{|\boldsymbol{\beta}|=1}^{p-2} \mathbf{GS}^{-1}_{\widetilde{\alpha}_j - 1, \beta} (q^3_{\boldsymbol{\beta}}, \varphi^3_i)_{0,K} = |K| \mathbf{GS}^{-1}_{\widetilde{\alpha}_j - 1, i}. \tag{8.17}$$

In order to conclude, one uses (8.14), (8.16) and (8.17).

8.3 Numerical results

In this section, we present some numerical experiments in which we compare the performances of the stabilizations and polynomial bases introduced in Sections 8.1.1 and 8.1.2 respectively.

More precisely, we investigate the behaviour and the related effects of the condition number in two critical situations.

In Section 8.3.1, we investigate the behaviour of the condition number of the p version of VEM and the effects on the linear solver used for the solution to the associated linear system. We are also interested in the behaviour of the condition number when varying the stabilization and the polynomial basis dual to internal moments (2.4) in presence ofa sequence of "badly shaped" polygons (collapsing bulks, collapsing edges...) this is probed in Sections 8.3.2 and 8.3.3. The condition number is computed as the ratio between the maximum and minimum (nonzero) eigenvalue of the stiffness matrix.

Finally, in Section 8.3.4, we state some conclusions.

8.3.1 Numerical results: the p version of VEM

Let us consider the three meshes depicted in Figure 1.3 (up-right), (down-left) and (down-right), i.e. a square mesh, a regular hexagonal mesh and a Voronoi-Lloyd mesh.

We investigate in this section the behaviour of the condition number of the stiffness matrix associated with method (2.1) by keeping fixed the meshes under consideration and by increasing p. To this purpose, we modify both the choice of the stabilization and the choice of the polynomial basis dual to internal moments (2.4).

In Figure 8.1, we depict the behaviour of the condition number by fixing the stabilization to be S^K_1 defined in (6.3) and we consider the three polynomial bases introduced in Section 8.1.2. For all the three sequences of meshes, basis $\{q^2_{\boldsymbol{\alpha}}\}^{p-2}_{|\boldsymbol{\alpha}|=0}$ shows the best performances, whereas the standard monomial basis $\{q^1_{\boldsymbol{\alpha}}\}^{p-2}_{|\boldsymbol{\alpha}|=0}$ shows the worst results.

From Figure 8.1, it is also clear that using basis $\{q^1_{\boldsymbol{\alpha}}\}^{p-2}_{|\boldsymbol{\alpha}|=0}$ entails an *exponential* growth of the condition number in terms of p.

Furthermore, employing $\{q^i_{\boldsymbol{\alpha}}\}^{p-2}_{|\boldsymbol{\alpha}|=0}$ with $i = 2, 3$, suggests instead an algebraic growth of the condition number in terms of p. A polynomial fitting yields:

$$\mathrm{cond}(\mathbf{K}_p) \approx a\, p^b \qquad \text{with } a = \begin{cases} 130.4 & \text{if } i = 2 \\ 131.7 & \text{if } i = 3 \end{cases}, \quad b = \begin{cases} 3.344 & \text{if } i = 2 \\ 3.371 & \text{if } i = 3 \end{cases}. \tag{8.18}$$

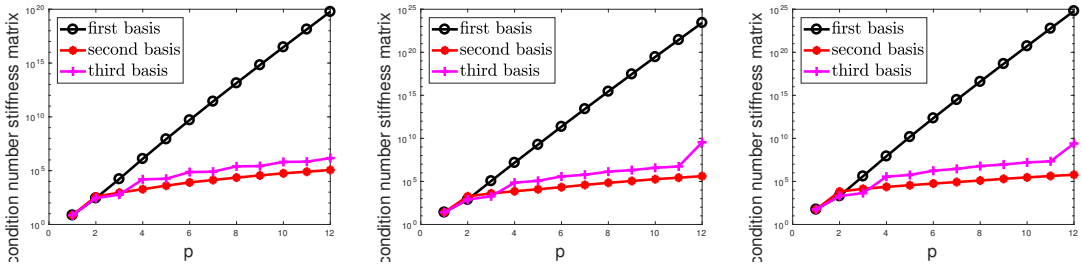

Figure 8.1: Condition number of the VEM stiffness matrix in terms of p. The stabilization is fixed and equal to S_1^K defined in (6.3). We compare the behaviour in terms of the three polynomial bases presented in Section 8.1.2. Left: square mesh. Center: Voronoi-Lloyd mesh. Right: regular-hexagonal mesh.

This behaviour is extremely interesting since it is well-known, see e.g. [90], that the growth in terms of p of the condition number in triangular Spectral Elements with nodal bases is of the following sort:

$$\text{cond}(\mathbf{K}_p) \approx a\, p^b \qquad \text{with } b = 4, \quad \text{for some } a > 0. \tag{8.19}$$

We also point out that when employing hexagonal and Voronoi mesh and a rather high degree of accuracy, namely $p = 12$, the condition number when employing basis $\{q^3_{\boldsymbol{\alpha}}\}^{p-2}_{|\boldsymbol{\alpha}|=0}$ seems to have a stray behaviour.

We want now to understand how much the ill-conditioning pollutes the convergence of the broken H^1 error defined in (7.2).

To this purpose, we consider a test case with analytic solution (7.5), for which we know that the method converges exponentially, see (2.52), as numerically shown in Figures 7.3 and 7.4. In Figure 8.2, we compare the broken H^1 error defined in (7.2) using the three meshes above mentioned (always using S_1^K defined in (6.3) as a stabilization) and comparing the three bases $\{q^i_{\boldsymbol{\alpha}}\}^{p-2}_{|\boldsymbol{\alpha}|=0}$, $i = 1, 2, 3$. We observe that, due to the ill-conditioning of the stiffness matrix computed with basis

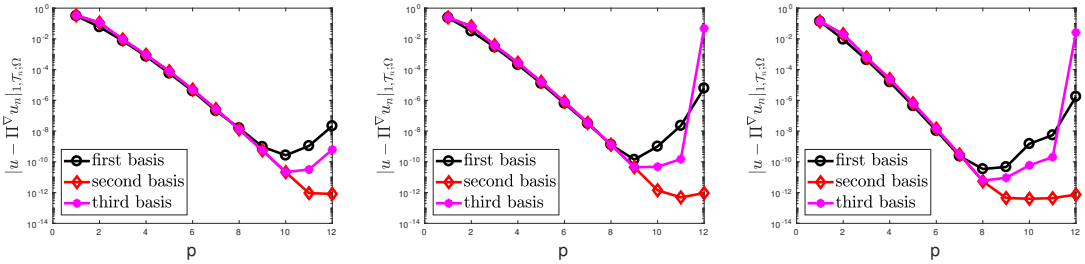

Figure 8.2: Error $|u - \Pi^\nabla_p u_n|_{1,\mathcal{T}_n}$ with exact solution given in (7.5). The stabilization is fixed and equal to S_1^K defined in (6.3). We compare the behaviour in terms of the three polynomial bases presented in Section 8.1.2. Left: square mesh. Center: Voronoi-Lloyd mesh. Right: regular-hexagonal mesh.

$\{q^1_{\boldsymbol{\alpha}}\}^{p-2}_{|\boldsymbol{\alpha}|=0}$ for high values of p, the linear solver of the system (namely the one associated with the \ command of MATLAB) does not work properly. For this reason, we highly recommend to use basis $\{q^2_{\boldsymbol{\alpha}}\}^{p-2}_{|\boldsymbol{\alpha}|=0}$ in lieu of basis $\{q^1_{\boldsymbol{\alpha}}\}^{p-2}_{|\boldsymbol{\alpha}|=0}$ when approximating with high-order VEM. It is also worth to underline that employing basis $\{q^3_{\boldsymbol{\alpha}}\}^{p-2}_{|\boldsymbol{\alpha}|=0}$ is not a wise choice on hexagonal and Voronoi meshes since for rather high degree of accuracy, namely $p = 12$, the errors have a blow up. This is probably due to the numerical instability appearing when diagonalizing the monomial mass matrix in (8.5).

In order to understand better "how much the (linear) solver fails" when solving the system arising from (2.1), we consider as an exact solution:

$$u(x, y) = 1 - x - y, \tag{8.20}$$

which, owing to polynomial consistency assumption (2.14), is approximated exactly by the VEM up to machine precision.

In exact-arithmetic one expects the broken H^1 error defined in (7.2) to vanish, while in floating-point arithmetic the error is not zero but grows along with the condition number of the stiffness matrix.

In Figure 8.3, we compare the broken H^1 error defined in (7.2) using the three meshes above discussed, using S_1^K (6.3) as a stabilization and the three bases $\{q_{\boldsymbol{\alpha}}^i\}_{|\boldsymbol{\alpha}|=0}^{p-2}$, $i = 1, 2, 3$. The be-

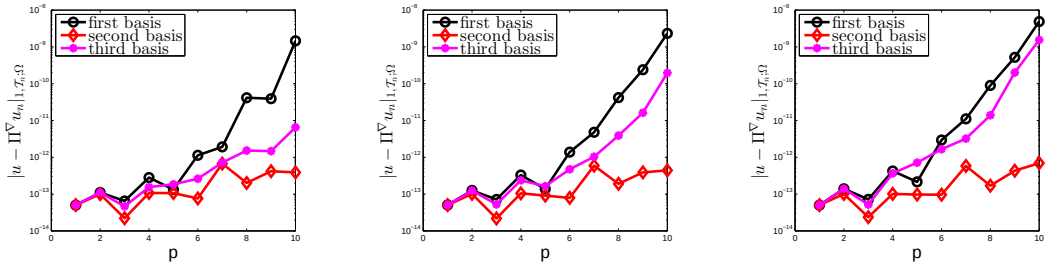

Figure 8.3: Error $|u - \Pi_p^\nabla u_n|_{1,\mathcal{T}_n}$ with exact solution given in (8.20). The stabilization is fixed and equal to S_1^K defined in (6.3). We compare the behaviour in terms of the three polynomial bases presented in Section 8.1.2. Left: square mesh. Center: Voronoi-Lloyd mesh. Right: regular-hexagonal mesh.

haviour of basis $\{q_{\boldsymbol{\alpha}}^2\}_{|\boldsymbol{\alpha}|=0}^{p-2}$ is again superior to the other two bases. More precisely, employing basis $\{q_{\boldsymbol{\alpha}}^1\}_{|\boldsymbol{\alpha}|=0}^{p-2}$ has a large effect on the error for high degrees of accuracy p.

In order to conclude this section, we present in Figure 8.4 a numerical test where we fix the polynomial basis dual to the internal moments (2.4) to be $\{q_{\boldsymbol{\alpha}}^2\}_{|\boldsymbol{\alpha}|=0}^{p-2}$ and we consider the four different stabilizations presented in Section 8.1.1. The four stabilizations have almost the same

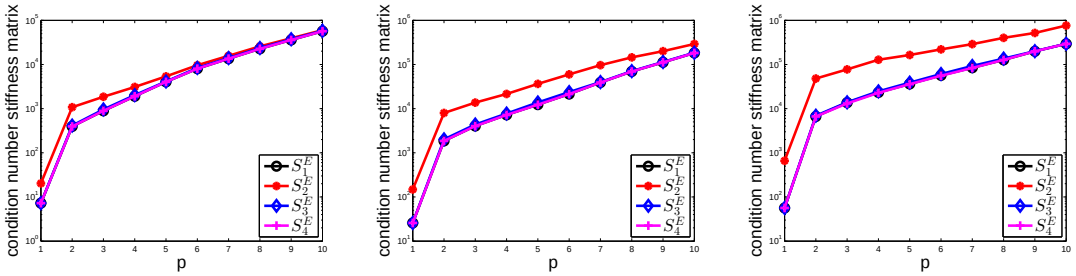

Figure 8.4: Condition numbers of the VEM stiffness matrix in terms of p on a square mesh, a Voronoi-Lloyd mesh and a regular-hexagonal mesh. The polynomial basis dual to internal moments (2.4) is $\{q_{\boldsymbol{\alpha}}^2\}_{|\boldsymbol{\alpha}|=0}^{p-2}$. We compare the behaviour in terms of the four stabilizations presented in Section 8.1.1. Left: square mesh. Center: Voronoi-Lloyd mesh. Right: regular-hexagonal mesh.

impact on the condition number (stabilization S_2^K seems to perform slightly worse than the other stabilizations).

8.3.2 Numerical results: collapsing polygons

It is also interesting to understand the impact of the choice of the stabilization and of the polynomial basis dual to internal moments (2.4) in presence of a sequence of "badly shaped" polygons (i.e. with collapsing bulk) on the condition number of the local stiffness matrix. In this way, we also test the robustness of the method when assumption (**G1**) is not valid.

To this purpose, we here present a quite limited and preliminary study. More precisely, we consider $\{K_i\}_{i\in\mathbb{N}}$, sequence of "collapsing" hexagons, as those depicted in Figure 8.5. In particular, the coordinates of K_i, the i-th element, are:

$$\mathbf{A}_i = (1, 0), \quad \mathbf{B}_i = (2, 2^{-i+1}), \quad \mathbf{C}_i = (1, 2^{-i+2}), \quad \mathbf{D}_i = (0, 2^{-i+1}), \quad \mathbf{E}_i = (-1, 2^{-i+1}), \quad \mathbf{F}_i = (0, 0). \tag{8.21}$$

Needless to say, sequence $\{K_i\}_{i\in\mathbb{N}}$ does not satisfy the star-shapedeness assumption (**G1**).

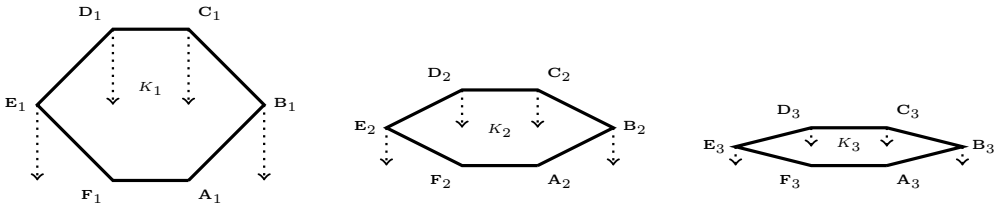

Figure 8.5: First three elements of sequence $\{K_i\}_{i\in\mathbb{N}}$.

In Figure 8.6, we depict the behaviour of the condition number of the local stiffness matrix in terms of i, parameter used in the definition of the coordinates (8.21) of the pentagons K_i. In particular, we compare such behaviour employing the three bases $\{q^i_{\boldsymbol{\alpha}}\}^{p-2}_{|\boldsymbol{\alpha}|=0}$, $i = 1, 2, 3$, discussed in Section 8.1.2 and choosing $p = 3$ and $p = 6$ respectively. The stabilization is fixed to be S^K_1 defined in (6.3). From Figure 8.6, we deduce that the standard choice for the polynomial basis

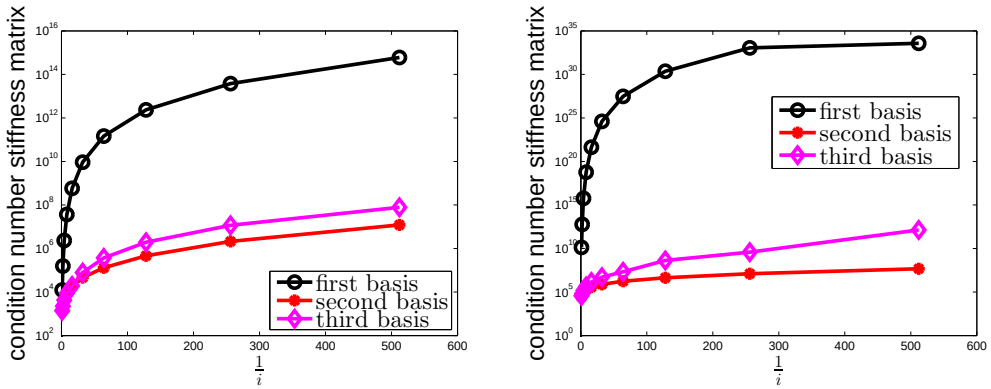

Figure 8.6: Condition numbers of the local VEM stiffness matrix on the sequence of hexagons depicted in Figure 8.5 in dependence of i, parameter used in the definition of the coordinates (8.21) of the pentagons K_i. The stabilization is fixed and equal to S^K_1 defined in (6.3). We compare the behaviour in terms of the three polynomial bases presented in Section 8.1.2. Left p=3. Right: p=6.

(8.4) leads to a dramatic growth of the condition number. It turns out that the safest choice, in terms of ill-conditioning, is the one associated with basis $\{q^2_{\boldsymbol{\alpha}}\}^{p-2}_{|\boldsymbol{\alpha}|=0}$, which we recall is obtained by an orthonormalization of the standard monomial basis $\{q^1_{\boldsymbol{\alpha}}\}^{p-2}_{|\boldsymbol{\alpha}|=0}$ via a stable Gram-Schmidt process. Basis $\{q^3_{\boldsymbol{\alpha}}\}^{p-2}_{|\boldsymbol{\alpha}|=0}$, although behaves much better than the monomial basis, is not as good as $\{q^2_{\boldsymbol{\alpha}}\}^{p-2}_{|\boldsymbol{\alpha}|=0}$.

Next, in Figure 8.7, we compare the condition number of the stiffness matrix by fixing $p = 6$ and the polynomial basis $\{q^2_{\boldsymbol{\alpha}}\}^{p-2}_{|\boldsymbol{\alpha}|=0}$, which, from the previous tests, seems to be the best for the conditioning of VEM, and by modifying the choice of the stabilizations; more precisely, we consider again the four stabilization discussed in Section 8.1.1. We deduce from Figure 8.7 that the choice of the stabilization does not have evident effects on the condition number, at least in the set of experiments here shown.

As a byproduct, in Figure 8.8 we consider a comparison between the four stabilizations by employing the standard monomial basis $\{q^1_{\boldsymbol{\alpha}}\}^{p-2}_{|\boldsymbol{\alpha}|=0}$ as dual basis for internal moments (2.4) with degree of accuracy $p = 6$ and we note again the practical independence of the condition number with respect to the choice of the stabilization.

8.3.3 Numerical results: hanging nodes

As a final set of numerical results, we study the behaviour of the condition number of the stiffness matrix employing various bases and stabilizations in presence of hanging nodes collapsing on a

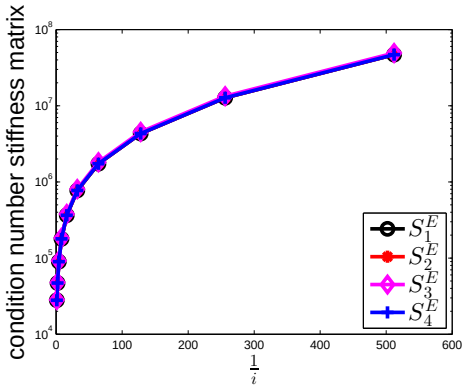

Figure 8.7: Condition numbers of the local VEM stiffness matrix on the sequence of hexagons depicted in Figure 8.5 in dependence of i, parameter used in the definition of the coordinates (8.21) of sequence $\{K_i\}_{i\in\mathbb{N}}$. The polynomial basis, dual to the internal moments (2.4) is fixed to be $\{q^2_{\boldsymbol{\alpha}}\}^{p-2}_{|\boldsymbol{\alpha}|=0}$. We compare the behaviour in terms of the four stabilizations presented in Section 8.1.1. The degree of accuracy is p=6.

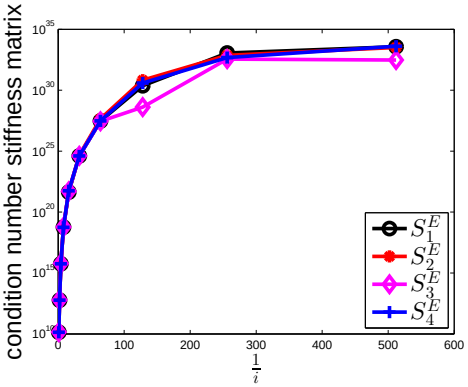

Figure 8.8: Condition numbers of the local VEM stiffness matrix on the sequence of hexagons depicted in Figure 8.5 in dependence of i, parameter used in the definition of the coordinates (8.21) of sequence $\{K_i\}_{i\in\mathbb{N}}$. The polynomial basis, dual to the internal moments (2.4) is fixed to be $\{q^1_{\boldsymbol{\alpha}}\}^{p-2}_{|\boldsymbol{\alpha}|=0}$. We compare the behaviour in terms of the four stabilizations presented in Section 8.1.1. The degree of accuracy is p=6.

vertex, checking thus the robustness of the method when assumption (**G2**) is not fulfilled.

Again, we present here only a quite limited and preliminary study. In particular, we present a sequence of "squared pentagons", that is a sequence of squares with a hanging node on a prescribed edge. More precisely, see Figure 8.9, we consider a sequence $\{K_i\}_{i\in\mathbb{N}}$ such that each K_i, $i \in \mathbb{N}$, has the following set of coordinates:

$$\mathbf{A}_i = (1,0), \quad \mathbf{B}_i = (1,1), \quad \mathbf{C}_i = (2^{-i},1), \quad \mathbf{D}_i = (0,1), \quad \mathbf{E}_i = (0,0),\ i \in \mathbb{N}. \tag{8.22}$$

In Figure 8.10, we depict the behaviour of the condition number of the local stiffness matrix in terms of i, parameter used in the definition of the coordinates (8.22) of the pentagons K_i. In particular, we compare such behaviour employing the three bases $\{q^i_{\boldsymbol{\alpha}}\}^{p-2}_{|\boldsymbol{\alpha}|=0}$, $i = 1, 2, 3$, discussed in Section 8.1.2 and choosing $p = 3$ and $p = 6$, respectively. The stabilization is fixed to be S_1^K defined in (6.3). The condition number is almost independent of parameter i for all choices of the canonical basis. This is not surprising since the bulk of the elements in the sequence remains the same for all i. However, when employing basis $\{q^1_{\boldsymbol{\alpha}}\}^{p-2}_{|\boldsymbol{\alpha}|=0}$, the condition number is higher.

Mimicking what was done in Section 8.3.2, we compare in Figures 8.11 and 8.12 the condition number of the stiffness matrix by fixing $p = 6$ and the polynomial bases $\{q^2_{\boldsymbol{\alpha}}\}^{p-2}_{|\boldsymbol{\alpha}|=0}$ and $\{q^1_{\boldsymbol{\alpha}}\}^{p-2}_{|\boldsymbol{\alpha}|=0}$, respectively, and by considering the four stabilization discussed in Section 8.1.1.

We deduce from Figures 8.11 and 8.12 again that the behaviour of the method employing different stabilizations is basically the same.

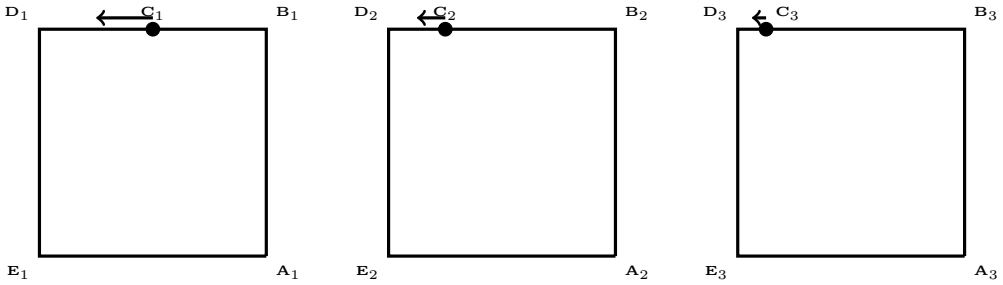

Figure 8.9: First three elements of sequence $\{K_i\}_{i\in\mathbb{N}}$ with hanging node collapsing on a vertex.

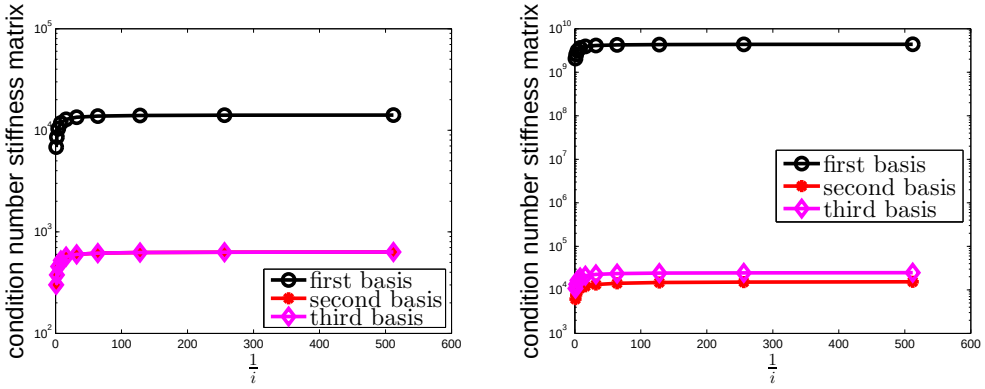

Figure 8.10: Condition numbers of the local VEM stiffness matrix on the sequence of pentagons (squares with a hanging node) depicted in Figure 8.9 in dependence of i, parameter used in the definition of the coordinates (8.21) of the pentagons K_i. The stabilization is fixed and equal to S_1^K (6.3). We compare the behaviour in terms of the three polynomial bases presented in Section 8.1.2. Left p=3. Right: p=6.

8.3.4 Conclusions

We now state some conclusions concerning what we have discussed so far.

We addressed and suggested possible cures to the problem of the ill-conditioning of the virtual element method, arising from high values of the polynomial degree p and in presence of highly anisotropic elements. In particular, we focused our attention on the effects of the stabilization of the method and the choice of internal degrees of freedom. It turned out that, whereas various stabilizations presented in literature have almost the same effect on the condition number of the stiffness matrix, the choice of the internal degrees of freedom has a deep impact.

We suggested two practical modifications of such internal degrees of freedom which greatly improve the behaviour of high-order VEM and VEM in presence of bad-shaped polygons.

It is worth to mention that we focused our attention to a simple 2D Poisson problem only. If one turns for instance to 3D problems, then the choice of the stabilization plays a major role, as shown in [33, 61].

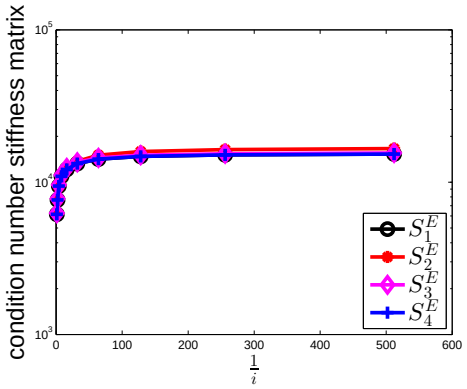

Figure 8.11: Condition numbers of the local VEM stiffness matrix on the sequence of pentagons (squares with a hanging node) depicted in Figure 8.9 in dependence of i, parameter used in the definition of the coordinates (8.21) of sequence $\{K_i\}_{i\in\mathbb{N}}$. The polynomial basis, dual to the internal moments (2.4) is fixed to be $\{q_{\boldsymbol{\alpha}}^2\}_{|\boldsymbol{\alpha}|=0}^{p-2}$. We compare the behaviour in terms of the four stabilizations presented in Section 8.1.1. The degree of accuracy is p=6.

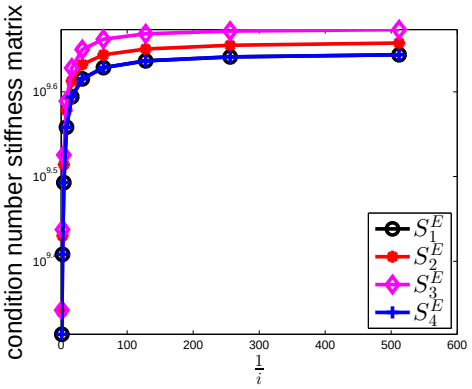

Figure 8.12: Condition numbers of the local VEM stiffness matrix on the sequence of pentagons (squares with a hanging node) depicted in Figure 8.9 in dependence of i, parameter used in the definition of the coordinates (8.21) of sequence $\{K_i\}_{i\in\mathbb{N}}$. The polynomial basis, dual to the internal moments (2.4) is fixed to be $\{q_{\boldsymbol{\alpha}}^1\}_{|\boldsymbol{\alpha}|=0}^{p-2}$. We compare the behaviour in terms of the four stabilizations presented in Section 8.1.1. The degree of accuracy is p=6.

Chapter 9

A multigrid algorithm for p VEM

So far, the issue of developing efficient solution techniques for the linear systems of equations stemming from both the h, p and hp-versions of the VEM has not been addressed yet. The main difficulty in the development of optimal (multilevel) solution techniques relies on the construction of consistent coarse solvers which are non-trivial on grids formed by general polyhedra. Recently, using the techniques of [11, 12] a multigrid algorithm for the hp-version Discontinuous Galerkin methods on agglomerated polygonal/polyhedral meshes has been analyzed in [9].

The aim of this chapter, which traces the work [10], is to develop efficient iterative solvers for the solution to the linear systems of equations stemming from the p version of the Virtual Element discretization of a two-dimensional Poisson problem with (for simplicity) homogeneous Dirichlet boundary conditions. We propose to employ a W-cycle p VEM algorithm, i.e. coarse levels are obtained by decreasing progressively the polynomial approximation degree up to the coarsest level which corresponds to the lowest (linear) VE space. The key point is the construction of suitable prolongation operators between the hierarchy of VE spaces. With the standard VE space such prolongation operators cannot be constructed employing only the degrees of freedom. For such a reason we introduce a suitable auxiliary VE space, which is identical to the standard VE space from the algebraic point of view and which allows to construct computable interspace operators but results into non-inherited sublevel solvers.

This in turn complicates the analysis of the multigrid algorithms, since we need to account for non-inherited sublevel solvers. Employing a Richardson smoother and following the classical framework, see e.g. [49], we prove that the W- cycle algorithm converges uniformly provided the number of smoothing steps is chosen sufficiently large. We also demonstrate that the resulting multigrid algorithm provides a uniform preconditioner for the Preconditioned Conjugate Gradient method (PCG), i.e., the number of PCG iterations needed to reduce the (relative) residual up to a (user-defined) tolerance is uniformly bounded independently of the number of degrees of freedom. Further, employing the Gauss-Seidel smoother in place of the Richardson one can improve the performance of our iterative scheme.

The extension of the present setting to h multigrid methods, i.e. where the coarse levels are formed by geometric agglomeration of the underlying grid is currently under investigation.

Importantly, the use of iterative solvers for the solution to linear systems associated with 2D Galerkin methods in general are not needed, since the size of such systems is often small; nevertheless, we deem that the construction of the 2D multigrid algorithm here presented paves the way for an extension to the 3D case, where instead iterative solvers are typically needed.

The remaining part of the paper is organized as follows. In Section 9.1, we recall some notations from the foregoing chapters and we introduce an auxiliary VE space instrumental for the construction of the algorithm. In Section 9.2, we present the W-cycle p VEM multigrid algorithm; its convergence analysis is the topic of Section 9.3. Finally, in Section 9.4, numerical results are shown.

9.1 Notations and an auxiliary VE space

We want to apply the multigrid algorithm to a VEM approximating Poisson problem with homogeneous Dirichlet boundary conditions (1.27).

More precisely, the VEM that we consider is the one defined in (2.1). As done in Chapter 8, we use subscript p instead of subscript hp, stressing in this way the fact that here we are only interested in the p version of VEM. Throughout this chapter, in particular, we do not make particular assumptions on the mesh, since it is fixed.

Importantly, in the definition of the internal dofs (2.4), we use as a dual polynomial basis, the one defined by $\{q^2_{\boldsymbol{\alpha}}\}^{p-2}_{|\boldsymbol{\alpha}|=0}$ in Section 8.1.2; we recall that such a basis is L^2 orthonormal over polygon K. This choice is not a matter of taste, but will play a fundamental role in the construction of the multigrid algorithm.

Furthermore, we employ as a stabilization the bilinear form S^K_1 defined in (6.3). We denote henceforth such stabilization by S^K. We are able to provide explicit bounds in terms of p of the stability constants $c_*(p)$ and $c^*(p)$ defined in (2.12) when using basis $\{q^2_{\boldsymbol{\alpha}}\}^{p-2}_{|\boldsymbol{\alpha}|=0}$ and stabilization S^K. More precisely, the following result, holds true.

Theorem 9.1.1. *Let $K \in \mathcal{T}_n$ and let $S^K(\cdot,\cdot)$ be the stabilizing bilinear form defined in* (6.3)*. Then, the following bound on the stability constants $c_*(p)$ and $c^*(p)$ introduced in* (2.12) *holds true:*

$$c_*(p)|v_p|^2_{1,K} \lesssim S^K(v_p,v_p) \lesssim c^*(p)|v_p|^2_{1,K} \qquad \forall\, v_p \in \ker(\Pi^\nabla_p),$$

where $c_*(p) \geq p^{-6}$ and $c^*(p) \leq p^3$.

Proof. The assertion follows by combining the two forthcoming technical Lemmata 9.1.2 and 9.1.3. □

An immediate consequence of Theorem 9.1.1 and (2.16) is that it holds:

$$\alpha_*(p) \gtrsim p^{-6}, \quad \alpha^*(p) \lesssim p^3, \tag{9.1}$$

where $\alpha_*(p)$ and $\alpha^*(p)$ are defined in (2.15).

Lemma 9.1.2. *Let $\widetilde{S}^K(\cdot,\cdot)$ be the local* auxiliary *stabilization defined as in* (6.8)*. Then, it holds:*

$$c_*(p)|v_p|^2_{1,K} \lesssim \widetilde{S}^K(v_p,v_p) \lesssim c^*(p)|v_p|^2_{1,K} \qquad \forall\, v_p \in \ker(\Pi^\nabla_p), \tag{9.2}$$

where $c_*(p) \gtrsim p^{-5}$, $c^*(p) \lesssim p^2$, and where Π^∇_p is the energy projector defined in (2.8)*.*

Proof. It is a straightforward consequence of Theorem 6.2.2. □

We observe that bounds on $c_*(p)$ and $c^*(p)$ sharper than those in Lemma 9.1.2 are available from Theorem 6.2.2 and from the numerical study of Section 6.2.1, nonetheless we prefer here to avoid the technical dependence on the largest angle of polygon K.

We are now ready for proving a second technical result.

Lemma 9.1.3. *Let $K \in \mathcal{T}_n$ and let S^K and $\widetilde{S}^K$ be defined as in* (6.3) *and* (6.8) *respectively. Then, the following spectral relations between the two stabilizations holds true:*

$$p^{-1}S^K(v_p,v_p) \leq \widetilde{S}^K(v_p,v_p) \lesssim p^2 S^K(v_p,v_p) \quad \forall\, v_p \in V_p(K).$$

Before showing the proof of Lemma 9.1.3, we recall from Lemma 6.2.3 that given $\{\rho^{p+1}_j\}^p_{j=0}$ and $\{\xi_j\}^p_{j=0}$ the $p+1$ Gauß-Lobatto nodes and weights on $\widehat{I} = [-1,1]$ respectively, one has:

$$\sum_{j=0}^{p} q_p^2(\xi^{p+1}_j)\rho^{p+1}_j \lesssim \|q_p\|^2_{0,\widehat{I}} \leq \sum_{j=0}^{p} q_p^2(\xi^{p+1}_j)\rho^{p+1}_j \quad \forall\, q_p \in \mathbb{P}_p(\widehat{I}). \tag{9.3}$$

Moreover, one also has the following behaviour of the Gauß-Lobatto weights:

$$p^{-2} \lesssim \rho^{p+1}_j \lesssim p^{-1} \quad \forall\, j = 0,\dots,p+1, \tag{9.4}$$

where the hidden constants are positive and independent of p, see [43, Corollary 2.8].

Proof. By using (9.3) and (9.4), we obtain:

$$\frac{1}{h_K}p^{-1}\sum_{j=1}^{p(\#\text{ of edge of }K)}\text{dof}_{b,j}^2(v_p)\lesssim\frac{p}{h_K}\|v_p\|_{0,\partial K}^2\lesssim\frac{1}{h_K}\sum_{j=1}^{p(\#\text{ of edge of }K)}\text{dof}_{b,j}^2(v_p),\tag{9.5}$$

where $\text{dof}_{b,j}$ denotes the j-th boundary (either vertex or edge) degree of freedom. This concludes the discussion concerning the boundary term.

Next, we study the bulk term in (6.8) and consider the expansion of $\Pi^0_{p-2}v_p$ into the $L^2(K)$ orthonormal basis $\{q^2_{\boldsymbol{\alpha}}\}^{p-2}_{|\boldsymbol{\alpha}|=0}$ introduced in Section 8.1.2:

$$\Pi^0_{p-2}v_p=\sum_{|\boldsymbol{\alpha}|\leq p-2}c_{\boldsymbol{\alpha}}q^2_{\boldsymbol{\alpha}}.\tag{9.6}$$

Testing (9.6) with $q^2_{\boldsymbol{\beta}}$, $|\boldsymbol{\beta}|\leq p-2$, we obtain:

$$|K|\text{dof}_{\boldsymbol{\beta}}(v_p)=\int_K v_pq^2_{\boldsymbol{\beta}}=\int_K\Pi^0_{p-2}v_pq^2_{\boldsymbol{\beta}}=c_{\boldsymbol{\beta}},$$

where $\text{dof}_{\boldsymbol{\beta}}(\cdot)$ denotes the internal degrees of freedom associated with polynomial $m_{\boldsymbol{\beta}}$. As a consequence:

$$\Pi^0_{p-2}v_p=\sum_{|\boldsymbol{\alpha}|\leq p-2}|K|\text{dof}_{\boldsymbol{\alpha}}(v_p)q^2_{\boldsymbol{\alpha}}.\tag{9.7}$$

The Parseval identity implies:

$$\frac{p^2}{h_K^2}(\Pi^0_{p-2}v_p,\Pi^0_{p-2}v_p)_{0,K}=\frac{p^2}{h_K^2}\sum_{|\boldsymbol{\alpha}|\leq p-2}|K|^2\text{dof}^2_{i,\boldsymbol{\alpha}}(v_p),\tag{9.8}$$

where $\text{dof}_{i,|\boldsymbol{\alpha}|}(\cdot)$ denotes the internal degree of freedom associated with polynomial $q^2_{\boldsymbol{\alpha}}$. The assertion follows from (9.5) and (9.8). □

Finally, we focus on the construction of the linear system of equations stemming from (2.1). By expanding the trial function u_p as a combination of the elements in the global canonical basis, which is obtained by a combination of local canonical bases defined in (6.2):

$$u_p=\sum_{i=1}^{\dim(V_p)}\text{dof}_i(u_p)\varphi_i=:\sum_{i=1}^{\dim(V_p)}(\mathbf{u}_p)_i\varphi_i,$$

where $\mathbf{u}_p\in\mathbb{R}^{\dim(V_p)}$ is the set of dofs of u_p, and selecting v_p as φ_j, $j=1,\dots,\dim(V_p)$, we obtain:

$$\mathbf{A}_p\cdot\mathbf{u}_p=\mathbf{f}_p,\tag{9.9}$$

where:

$$(\mathbf{A}_p)_{i,j}=a_p(\varphi_j,\varphi_i),\quad(\mathbf{f}_p)_i=\langle f_p,\varphi_i\rangle_p,\quad i,\,j=1,\dots,\dim(V_p).\tag{9.10}$$

Next, we introduce an auxiliary VE space which will be crucial for the construction of the multigrid algorithm in Section 9.2. In the spirit of [4], we consider a modification of $V_p(K)$ into a *diverse* space on which we are able to compute a higher order L^2 projector. In particular, we set:

$$\begin{aligned}\widetilde{V}_p(K)=\{v_p\in H^1(K)\mid v_p|_{\partial K}\in\mathbb{B}_p(\partial K),\,\Delta v_p\in\mathbb{P}_{p-1}(K),\\ \int_K(\Pi^0_{p-2}v_p-v_p)q^2_{\boldsymbol{\alpha}}=0,\,\forall\,\boldsymbol{\alpha}\in\mathbb{N}^2\text{ with }|\boldsymbol{\alpha}|=p-1\Big\},\end{aligned}\tag{9.11}$$

where we recall that $\{q^2_{\boldsymbol{\alpha}}\}^{p-1}_{|\boldsymbol{\alpha}|=0}$ is a basis of $\mathbb{P}_{p-1}(K)$ obtained by an $L^2(K)$ orthonormalization of the monomial basis $\{q^1_{\boldsymbol{\alpha}}\}^{p-1}_{|\boldsymbol{\alpha}|=0}$ defined in (8.4).

Henceforth, we denote with the expression *enhancing constraints* the following set of constraints employed in the definition of modified space $\widetilde{V}_p(K)$:

$$\int_K (\Pi^0_{p-2} v_p - v_p)\, q_{\boldsymbol{\alpha}} = 0, \qquad \forall\, \boldsymbol{\alpha} \in \mathbb{N}^2 \text{ with } |\boldsymbol{\alpha}| = p-1, \quad \forall\, v_p \in \widetilde{V}_p(K). \tag{9.12}$$

The definition of the enhanced local space $\widetilde{V}_p(K)$ is different from the one presented in [4]. Moreover, we observe that $\mathbb{P}_p(K) \nsubseteq \widetilde{V}_p(K)$, but $\mathbb{P}_{p-2}(K) \subseteq \widetilde{V}_p(K)$. To be more precise, owing to the $L^2(K)$ orthonormality of the $\{q^1_{\boldsymbol{\alpha}}\}^{p-1}_{|\boldsymbol{\alpha}|=0}$ basis, it holds in fact:

$$\mathbb{P}_{p-2}(K) \oplus (\mathbb{P}_p(K)/\mathbb{P}_{p-2}(K))^{\perp_{\mathbb{P}_{p-1}(K)}} \subseteq \widetilde{V}_p(K),$$

where $(\mathbb{P}_p(K)/\mathbb{P}_{p-2}(K))^{\perp_{\mathbb{P}_{p-1}(K)}}$ denotes the space of polynomials of degree p, not in the space of polynomials of degree $p-2$, orthogonal to $\{q^2_{\boldsymbol{\alpha}}\}^{p-2}_{|\boldsymbol{\alpha}|=0}$.

We endow the local space $\widetilde{V}_p(K)$ with the same degrees of freedom of the space V_p introduced in (2.3). Using the *auxiliary* local virtual space $\widetilde{V}_p(K)$ introduced in (9.11), it is clear that we are able to compute the following operator:

$$\Pi^0_{p-1} : \widetilde{V}_p(K) \to \mathbb{P}_{p-1}(K) \quad \text{s. t.} \quad (q_{p-1}, v_p - \Pi^0_{p-1} v_p)_{0,K} \quad \forall\, q_{p-1} \in \mathbb{P}_{p-1}(K), \forall\, v_p \in \widetilde{V}_p(K).$$

We stress that there is no chance to be able to compute explicitly Π^0_{p-1} as a map defined on $V_p(K)$, since the internal degrees of freedom are up to order $p-2$, whereas this is possible in the new space $\widetilde{V}_p(K)$ since the enhancing constraints in (9.12) allows to compute internal moments up to order $p-1$.

The global *auxiliary* VE space is obtained again by gluing continuously the local spaces as done in (2.7):

$$\widetilde{V}_p = \left\{ v_p \in H^1_0(\Omega) \cap \mathcal{C}^0(\overline{\Omega}) \mid v_p|_K \in \widetilde{V}_p(K), \forall\, K \in \mathcal{T}_n \right\}. \tag{9.13}$$

The choice of the discrete bilinear form a_p and of the right-hand side f_p in (2.1) are exactly the same as those in Section 2.1 associated with space V_p.

Importantly, we emphasize that the choice of the stabilization when employing the new spaces $V_p(K)$ reads as in (6.3), although functions in local enhanced spaces $\widetilde{V}_p(K)$ defined in (9.11) are different with respect to their counterparts in standard VE spaces defined in (2.3). In particular, the following spectral bounds for the stability are valid.

Theorem 9.1.4. *Given $K \in \mathcal{T}_h$ and S^K the stabilization defined in* (6.3)*, the following holds true:*

$$c_*(p)|v_p|^2_{1,K} \lesssim S^K(v_p, v_p) \lesssim c^*(p)|v_p|^2_{1,K} \quad \forall v_p \in \ker(\Pi^\nabla_p) \subset V_p(K),$$

where $c_*(p)$ and $c^*(p)$ satisfy the same bounds of Theorem 9.1.1 and where Π^∇_p is the energy projector defined in (2.8) *applied to functions in $V_p(K)$.*

Proof. It suffices to show that the counterparts of Lemmata 9.1.2 and 9.1.3 are valid for functions in $\ker(\Pi^\nabla_p) \subset V_p(K)$.

For what concerns Lemma 9.1.2, following [32, Theorem 2], it is immediate to prove analogous bounds to those in (9.2) employing the auxiliary stabilization:

$$\widetilde{S}^K_{p,\mathrm{aux}}(u_p, v_p) = \frac{p}{h_K}(u_p, v_p)_{0,\partial K} + \frac{p^2}{h^2_K}(\Pi^0_{p-1} u_p, \Pi^0_{p-1} v_p)_{0,\partial K}.$$

However, we note that the definition of the enhancing constraints (9.12) entails that:

$$\Pi^0_{p-1} v_p = \Pi^0_{p-2} v_p \quad \forall v_p \in V_p(K),$$

whence the counterpart of Lemma 9.1.2 for functions in $\ker(\Pi^\nabla_p) \subset V_p(K)$. In view of this, the counterpart of Lemma 9.1.3 for functions in $\ker(\Pi^\nabla_p) \subset V_p(K)$ immediately follows. □

As a consequence of Theorem 9.1.4, we have:

$$\alpha_*(p)|v_p|^2_{1,K} \leq a_p^K(v_p, v_p) \leq \alpha^*(p)|v_p|^2_{1,K} \quad \forall v_p \in V_p(K), \forall K \in \mathcal{T}_h, \tag{9.14}$$

where $\alpha_*(p)$ and $\alpha^*(p)$ satisfy the same bounds as in (9.1).

It is crucial to remark that the linear systems stemming from the use of V_p and $\widetilde{V}_p$ are the same. In fact, it is clear from (2.13) that the construction of the local discrete bilinear forms depends uniquely on the choice of the set of the degrees of freedom (which we recall are the same for the two spaces) and the energy projector Π_p^∇ defined in (2.8), which is computed without the need of (9.12).

Also the construction of the discrete right-hand side (2.19) does not depend on the choice of the space since the L^2 projector Π_{p-2} defined in (2.18) is built using the internal degrees of freedom only, while the enhancing constraints (9.12) are neglected.

Remark 12. The aforementioned equivalence between the two linear systems associated with spaces V_p and $\widetilde{V}_p$ is of great importance in order to design and analyse the multigrid algorithm in Section 9.2. However, V_p and $\widetilde{V}_p$ have significant differences.

The first issue we want to highlight is that the method associated with space $\widetilde{V}_p$ defined in (9.13) is not, at least in principle, a "good" method from the point of view of the approximation property. It is possible to show p approximation results on the first and the third term on the right hand side of (2.22) following what was done e.g. in Section 2.2. The problematic term is the second one, i.e. the best error term with respect to functions in the virtual space. The approach used in Section 2.2.2, which is nothing but the p version of [87, Proposition 4.2], does not hold anymore in the enhanced version of VEM. To the best of our knowledge, the p approximation of the "best virtual" error term in enhanced space is still an open problem. On the other hand, the error analysis in terms of p employing as an approximation space V_p is available from Chapter 2.

The second issue we underline, is that the space $\widetilde{V}_p$ defined in (9.13) is more suited for the construction of the multigrid algorithm than the space V_p defined in (2.7), as will be clear from Section 9.2.

Let us summarize the strategy we will follow. We consider a discretization of problem (1.27) by means of the virtual element method (2.1) employing as an approximation space V_p defined in (2.7). The associated linear system (9.9) coincides algebraically with the one arising by employing the VE space $\widetilde{V}_p$ defined in (9.13). For this reason, we can solve system (9.9) by means of a multigrid algorithm based on the sequences of spaces $\widetilde{V}_p$ defined in (9.13).

Having the vector of degrees of freedom $\mathbf{u}_p$, one can reconstruct functions in two different spaces: either in the space V_p defined in (2.7), or in the space $\widetilde{V}_p$ defined in (9.13). The discrete solution in the former space is the one to be taken into account, since it has the proper p approximation properties, see Figure 9.1.

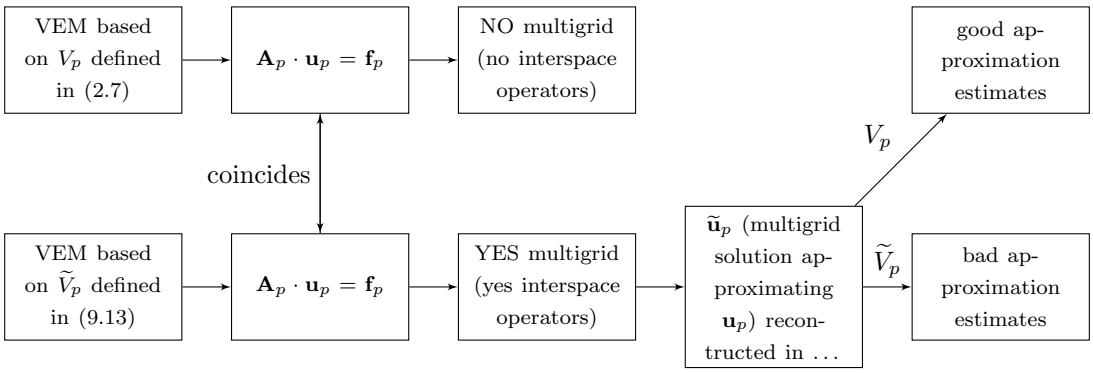

Figure 9.1: Strategy that we follow for the construction of the multigrid algorithm.

9.2 Multigrid methods with non inherited sublevel solvers

In this section, we present a p-VEM multigrid algorithm and the key ingredients for its formulation.

In the construction of our multigrid algorithm, we will make use of two key ingredients. The first one are suitable (computable) interspace operators, i.e. prolongation/restriction operators between two VE spaces. These operators will be constructed by employing the properties of the following space-dependent inner product:

$$(w_p, v_p)_p = \sum_{i=1}^{\dim(V_p)} \mathrm{dof}_i(w_p)\mathrm{dof}_i(v_p) \qquad \forall\, w_p, v_p \in V_p. \tag{9.15}$$

The second ingredient is a suitable smoothing scheme B_p, which aims at reducing the high frequency components of the error.

We aim at introducing a multigrid iterative method for the solution to the linear system in (9.9), which we recall is given by:

$$\mathbf{A}_p \cdot \mathbf{u}_p = \mathbf{f}_p, \tag{9.16}$$

where the coefficient matrix $\mathbf{A}_p$ and the right-hand side $\mathbf{f}_p$ are the matrix representations with respect to the their expansion in the canonical basis of space $\widetilde{V}_p$ (but also V_p, as discussed in the foregoing section), defined in (9.13), of the operators A_p and f_p defined by:

$$(A_p w_p, v_p)_p = a_p(w_p, v_p), \qquad (\mathrm{f}_p, v_p)_p = \langle f_p, v_p \rangle_p, \qquad \forall\, w_p,\, v_p \in V_p, \tag{9.17}$$

cf. (2.13) and (2.19) respectively.

In order to introduce our p-multigrid method, we assume $p \geq 2$ and we consider a sequence of VE spaces given by $\widetilde{V}_p, \widetilde{V}_{p-1}, \ldots, \widetilde{V}_1$, where the ℓ-th level is given by $\widetilde{V}_{p-\ell}$, $\ell = 0, \ldots, p-1$. Let now consider the linear system of equations on level ℓ: $\boldsymbol{A}_\ell \cdot \mathbf{z}_\ell = \mathbf{g}_\ell$. We denote by $\mathtt{MG}(\ell, \mathbf{g}_\ell, \mathbf{z}_\ell^{(0)}, m_2)$ one iteration obtained by applying the ℓ-th level iteration of our MG scheme to the above linear system, with initial guess $\mathbf{z}_\ell^{(0)}$ and using m_2 post-smoothing steps, respectively. For $\ell = 1$, (coarsest level) the solution is computed up to machine precision with a direct method, that is $\mathtt{MG}(1, \mathbf{g}_1, \mathbf{z}_1^{(0)}, m_2) = \boldsymbol{A}_1^{-1}\mathbf{g}_1$, while for $\ell > 1$ we adopt the recursive procedure described in Algorithm 1.

Algorithm 1 ℓ-th level of the p-multigrid algorithm

Coarse grid correction:
$\mathbf{r}_{\ell-1} = \mathbf{I}_\ell^{\ell-1} \cdot (\mathbf{g}_\ell - \boldsymbol{A}_\ell \cdot \mathbf{z}_\ell^{(0)})$; (restriction of the residual)
$\overline{\mathbf{e}}_{\ell-1} = \mathtt{MG}(\ell-1, \mathbf{r}_{\ell-1}, \mathbf{0}_{\ell-1}, m_2)$; (approximation of the residual equation ...)
$\mathbf{e}_{\ell-1} = \mathtt{MG}(\ell-1, \mathbf{r}_{\ell-1}, \overline{\mathbf{e}}_{\ell-1}, m_2)$; ($\ldots \boldsymbol{A}_{p-1} \cdot \mathbf{z}_{p-1} = \mathbf{r}_{p-1}$)
$\mathbf{z}_\ell^{(1)} = \mathbf{z}_\ell^{(0)} + \mathbf{I}_{\ell-1}^{\ell} \cdot \mathbf{e}_{\ell-1}$; (error correction step)
Post-smoothing:
for $i = 2 : m_2 + 1$ **do**
  $\mathbf{z}_\ell^{(i)} = \mathbf{z}_\ell^{(i-1)} + \mathbf{B}_\ell^{-1} \cdot (\mathbf{g}_\ell - \boldsymbol{A}_\ell \cdot \mathbf{z}_\ell^{(i-1)})$;
end for

$\mathtt{MG}(\ell, \mathbf{g}_\ell, \mathbf{z}_\ell^{(0)}, m_2) = \mathbf{z}_\ell^{(m_2+1)}$.

In presenting Algorithm 1, we used some objects that are not defined so far. In particular, $\mathbf{I}_{\ell-1}^{\ell}$ and $\mathbf{I}_\ell^{\ell-1}$ denote the matrix representation of the interspace operators defined in Section 9.2.2, while $\mathbf{B}_p$ denotes the matrix representation of the smoothing operator defined in Section 9.2.3.

For a given user defined tolerance `tol` and a given initial guess $\mathbf{u}_p^{(0)}$, the full p-multigrid algorithm employed to solve (9.16) is summarized in Algorithm 2; its analysis is presented in Section 9.3.

Remark 13. As a byproduct, we underline that it is possible to employ multigrid algorithms where two "adjacent" levels, associated to spaces $\widetilde{V}_{p_1}$ and $\widetilde{V}_{p_2}$, respectively, satisfy $|p_1 - p_2| \geq 2$. In such cases, to build the interspace operators, it suffices to modify the definition (9.11) by using

Algorithm 2 p-multigrid algorithm: $\widetilde{\mathbf{u}}_p = \texttt{MG}(p, \mathbf{f}_p, \widetilde{\mathbf{u}}_p^{(0)}, m_2)$.

$\mathbf{r}_p^{(0)} = \mathbf{f}_p - \mathbf{A}_p \cdot \widetilde{\mathbf{u}}_p^{(0)}$;
while $\|\mathbf{r}_p^{(i)}\| \leq \texttt{tol}\|\boldsymbol{f}_p\|$ **do**
  $\widetilde{\mathbf{u}}_p^{(i+1)} = \texttt{MG}(p, \mathbf{f}_p, \widetilde{\mathbf{u}}_p^{(i)}, m_2)$;
  $\mathbf{r}_p^{(i+1)} = \mathbf{f}_p - \mathbf{A}_p \cdot \widetilde{\mathbf{u}}_p^{(i+1)}$;
  $i \longrightarrow i+1$;
end while

a "larger" enhancing technique and imposing that the laplacian of functions in the virtual space is a polynomial of higher degree, and then reduce the space with additional constraints on the L^2-projectors.

9.2.1 Space-dependent inner products

The aim of this section is to prove the following result on the space-dependent inner product (9.15), which will be useful for the forthcoming analysis.

Theorem 9.2.1. *Let $(\cdot,\cdot)_p$ be defined as in* (9.15)*. Then, the following holds true:*

$$\beta_*(p)|v_p|^2_{1,\Omega} \lesssim (v_p, v_p)_p \lesssim \beta^*(p)|v_p|^2_{1,\Omega} \qquad \forall\, v_p \in \widetilde{V}_p, \tag{9.18}$$

where $\beta_*(p) \gtrsim p^{-8}$ and $\beta^*(p) \lesssim 1$.

In order to prove Theorem 9.2.1, it suffices to combine the forthcoming technical results. The first one makes use of the following *auxiliary* space-dependent inner product defined as:

$$(u_p, v_p)_{p,\text{aux}} = \sum_{K\in\mathcal{T}_h} (u_p, v_p)_{p,\text{aux};K} \qquad \forall\, u_p, v_p \in \widetilde{V}_p, \tag{9.19}$$

where the local contributions read:

$$(u_p, v_p)_{p,\text{aux};K} = h_K^{-1}(u_p, v_p)_{0,\partial K} + h_K^{-2}(\Pi^0_{p-1}u_p, \Pi^0_{p-1}v_p)_{0,K} \;\; u_p, v_p \in \widetilde{V}_p(K),\; \forall K \in \mathcal{T}_n. \tag{9.20}$$

Lemma 9.2.2. *Let $(\cdot,\cdot)_{p,aux}$ be defined in* (9.19)*. Then, it holds:*

$$\widetilde{\beta}_*(p)|v_p|^2_{1,\Omega} \lesssim (v_p, v_p)_{p,aux} \lesssim \widetilde{\beta}^*(p)|v_p|^2_{1,\Omega} \qquad \forall\, v_p \in V_p, \tag{9.21}$$

where $\widetilde{\beta}_*(p) \gtrsim p^{-6}$ and $\widetilde{\beta}^*(p) \lesssim 1$.

Proof. The proof is slightly different from the one for the stability bounds (9.2); in fact, here we work on the complete virtual space and not only on $\ker(\Pi_p^\nabla)$, being Π_p^∇ defined in (2.8). In the following, we neglect the dependence on the size of the elements since we are assuming that the mesh is fixed; the general case follows from a scaling argument.

The upper bound follows from a trace inequality, arguments analogous to those in Lemma 3.2.3 and the stability of orthogonal projection:

$$(v_p, v_p)_{p,\text{aux};K} = \|v_p\|^2_{0,\partial K} + \|\Pi^0_{p-1}v_p\|^2_{0,K} \lesssim \|v_p\|_{1,K} \qquad \forall\, v_p \in \widetilde{V}_p,$$

and summing up on all the mesh elements and applying the Poincarè inequality.

For the lower bound we observe that the *hp* polynomial inverse estimate (B.36) and the fact that $\Delta v_p \in \mathbb{P}_{p-1}(K)$ with $p \geq 1$ yield:

$$\begin{aligned} \|\Delta v_p\|_{0,K} \lesssim p^2\|\Delta v_p\|_{-1,K} &= p^2 \sup_{\Phi\in H^1_0(K)\setminus\{0\}} \frac{(\Delta v_p, \Phi)_{0,K}}{|\Phi|_{1,K}} \\ &= p^2 \sup_{\Phi\in H^1_0(K)\setminus\{0\}} \frac{(\nabla v_p, \nabla\Phi)_{0,K}}{|\Phi|_{1,K}} \lesssim p^2|v_p|_{1,K}, \end{aligned} \tag{9.22}$$

where the hidden constant depends solely on the shape-regularity of element K.

At this point, (3.33), (9.22) and a one dimensional *hp* inverse inequality [96, Theorem 3.91] along with interpolation theory [101, 102], yield:

$$|v_p|_{1,K} \lesssim p^3(\|v_p\|_{0,\partial K} + \|\Pi^0_{p-1} v_p\|_{0,K}),$$

where the hidden constant depends solely on the parameters ρ_0 and c introduced in assumptions (**G1**)-(**G2**)-(**G3**). From this, we duduce:

$$|v_p|^2_{1,K} \lesssim p^6 (v_p, v_p)_{p,\mathrm{aux};K}.$$

The assertion follows summing on all the elements. □

Lemma 9.2.3. *Let $(\cdot,\cdot)_{p,aux}$ and $(\cdot,\cdot)_p$ be defined as in* (9.19) *and* (9.15)*, respectively. Then it holds:*

$$p^{-2}(v_p, v_p)_{p,aux} \lesssim (v_p, v_p)_p \lesssim (v_p, v_p)_{p,aux} \qquad \forall\, v_p \in \widetilde{V}_p. \tag{9.23}$$

Proof. The proof is a straightforward modification of the one of Lemma 9.1.3. □

Remark 14. The choice (9.15) for the space-dependent inner product is crucial for the construction of the interspace operators, see Section 9.2.2. Moreover, we point out that it coincides with the usual choice for the space-dependent inner product in the *hp* DG-FEM framework, see [9, 11].

The FEM counterpart of Theorem 9.2.1 is much less technical, since it suffices to choose an L^2 orthonormal basis of polynomials as the canonical basis; via the Parseval identity, the (scaled) L^2 norm is spectrally equivalent to the space-dependent inner product (9.15); thus, the employment of polynomial inverse inequality implies a straightforward relation with the H^1 seminorm.

In the VEM framework, it is not possible to proceed similarly for two reasons. The first one is that, to the best of our knowledge, *hp* inverse inequalities for functions in virtual spaces are not available; the second reason is that an explicit L^2 orthonormal basis of functions in the virtual space is not computable, since such functions are not known in closed form.

9.2.2 Interspace operators

In this section, we introduce and construct suitable prolongation and restriction operators acting between the VE spaces $\widetilde{V}_{\ell-1}$ and $\widetilde{V}_\ell$, $\ell = p, p-1, \dots, 2$. First of all, we stress that the sequence of local spaces $\widetilde{V}_p(K)$, and thus the associated sequence of global spaces $\widetilde{V}_p$, are not nested. As a consequence, we cannot define the prolongation interspace operator simply as the natural injection, as done for instance in [9, 11, 48, 49]. In our context, the prolongation operator:

$$I^p_{p-1} : \widetilde{V}_{p-1} \to \widetilde{V}_p \tag{9.24}$$

associates to a function v_{p-1} in $\widetilde{V}_{p-1}$ a function $I^p_{p-1} v_{p-1}$ in $\widetilde{V}_p$, having the same values as v_{p-1} for all the dofs that are in common with space $\widetilde{V}_{p-1}$, while the remaining values of the dofs (i.e. the internal higher order ones) are computed using the enhancing constraints defined in (9.11).

More precisely, we define for $p \geq 2$ $I^p_{p-1} : \widetilde{V}_{p-1} \to \widetilde{V}_p$ as:

$$\begin{cases} I^p_{p-1} v_{p-1} = v_{p-1}, & \text{on } \partial K, \\ \displaystyle\int_K I^p_{p-1} v_{p-1}\, q^2_{\boldsymbol{\alpha}} = \int_K v_{p-1}\, q^2_{\boldsymbol{\alpha}} = \mathrm{dof}_{\boldsymbol{\alpha}}(v_{p-1}), & \text{if } |\boldsymbol{\alpha}| \leq p-3, \\ \displaystyle\int_K I^p_{p-1} v_{p-1}\, q^2_{\boldsymbol{\alpha}} = \int_K \Pi^0_{p-3} v_{p-1}\, q^2_{\boldsymbol{\alpha}} = 0, & \text{if } |\boldsymbol{\alpha}| = p-2, \end{cases} \tag{9.25}$$

since basis $\{q^2_{\boldsymbol{\alpha}}\}^{p-2}_{|\boldsymbol{\alpha}|=0}$ is $L^2(K)$-orthonormal by construction. We recall that the third equation in (9.25) follows from the enhancing constraints (9.12).

The restriction operator I^{p-1}_p is defined as the adjoint of I^p_{p-1} with respect to the space-dependent inner product defined in (9.15), i.e.:

$$(I^{p-1}_p v_p, w_{p-1})_{p-1} = (v_p, I^p_{p-1} w_{p-1})_p \quad \forall\, v_p \in \widetilde{V}_p,\ \forall\, w_{p-1} \in \widetilde{V}_{p-1}. \tag{9.26}$$

Importantly, we remark that, thanks to definition (9.15) of the space-dependent inner product, the matrix associated with I^{p-1}_p is the transpose of the matrix associated with the operator I^p_{p-1}.

9.2.3 Smoothing scheme and spectral bounds

In this section, we introduce and discuss the smoothing scheme entering in the multigrid algorithm. To this aim, we introduce the following space-dependent norms:

$$|||v_p|||_{s,p} = \sqrt{(A_p^s v_p, v_p)_p} \qquad \forall\, v_p \in V_p, \quad s \in \mathbb{R}^+. \tag{9.27}$$

We highlight that it holds:

$$|||v_p|||_{1,p}^2 = a_p(v_p, v_p).$$

Since the matrix $\mathbf{A}_p$ is symmetric positive definite, there exists an orthonormal (with respect to the inner product $(\cdot,\cdot)_p$) basis of eigenvectors of $\mathbf{A}_p$, and the associated eigenvalues are real and strictly positive. Let $\{\psi_i, \lambda_i\}_{i=1}^{\dim(V_p)}$ be the related set of eigenpairs. We show now a bound of the spectrum of $\mathbf{A}_p$ in terms of p.

Lemma 9.2.4. *The following upper bound Λ_p for the spectrum of $\mathbf{A}_p$ holds true:*

$$\Lambda_p \lesssim \frac{\alpha^*(p)}{\beta_*(p)}, \tag{9.28}$$

where $\alpha^*(p)$ and $\beta_*(p)$ are introduced in (9.14) *and* (9.18)*, respectively.*

Proof. Let λ_i be an eigenvalue of $\mathbf{A}_p$ and let $\boldsymbol{\psi}_i$ be the associated normalized eigenvector. Then:

$$\mathbf{A}_p \cdot \boldsymbol{\psi}_i = \lambda_i \boldsymbol{\psi}_i \Longrightarrow (A_p\psi_i, \psi_i)_p = \lambda_i(\psi_i, \psi_i)_p.$$

Owing to (2.15) and (9.18):

$$\lambda_i = \frac{(A_p\psi_i, \psi_i)_p}{(\psi_i, \psi_i)_p} = \frac{a_p(\psi_i, \psi_i)}{(\psi_i, \psi_i)_p} \lesssim \alpha^*(p)\frac{|\psi_i|_{1,\Omega}^2}{(\psi_i, \psi_i)_p} \lesssim \frac{\alpha^*(p)}{\beta_*(p)}.$$

□

As a smoothing scheme, we choose a Richardson scheme, which is given by:

$$B_p = \widetilde{\Lambda}_p \cdot Id_p, \tag{9.29}$$

where $\widetilde{\Lambda}_p \leq \Lambda_p$. A numerical study concerning the (sharp) dependence of Λ_p on p of the spectral bound Λ_p is presented in Section 9.4.

9.2.4 Error propagator operator

As in the classical analysis of the multigrid algorithms [49], in this section we introduce and analyze the error propagator operator. To this aim, we firstly consider a "projection" operator $P_p^{p-1} : \widetilde{V}_p \to \widetilde{V}_{p-1}$, defined for $p \geq 2$ as the adjoint of I_{p-1}^p with respect to inner product $a_p(\cdot,\cdot)$, i.e.:

$$a_{p-1}(v_{p-1}, P_p^{p-1} w_p) = a_p(I_{p-1}^p v_{p-1}, w_p) \qquad \forall\, v_{p-1} \in \widetilde{V}_{p-1},\, w_p \in \widetilde{V}_p. \tag{9.30}$$

The following auxiliary result holds.

Lemma 9.2.5. *Let $q_{p-1} \in \widetilde{V}_{p-1}$ be such that*

$$A_{p-1} q_{p-1} = r_{p-1}, \qquad \text{with } r_{p-1} = I_p^{p-1}(g_p - A_p z_p^{(0)}), \tag{9.31}$$

where I_p^{p-1} is defined in (9.26)*, while $z_p^{(0)}$ is the initial guess of the algorithm and A_p and A_{p-1} are defined in* (9.17)*. Then, it holds:*

$$q_{p-1} = P_p^{p-1}(z_p - z_p^{(0)}), \tag{9.32}$$

where P_p^{p-1} is defined in (9.30) *and where we recall that z_p is the solution to $A_p z_p = g_p$.*

Proof. As the proof is very similar to its analogous version in [49, Lemma 6.4.2], here we briefly sketch it. For all $v_{p-1} \in \widetilde{V}_{p-1}$:

$$a_{p-1}(q_{p-1}, v_{p-1}) = (A_{p-1}q_{p-1}, v_{p-1})_{p-1} = (r_{p-1}, v_{p-1})_{p-1} = (I_p^{p-1}(g_p - A_p z_p^{(0)}), v_{p-1})_{p-1}$$
$$= (A_p(z_p - z_p^{(0)}), I_{p-1}^p v_{p-1})_p = a_p(z_p - z_p^{(0)}, I_{p-1}^p v_{p-1}) = a_{p-1}(P_p^{p-1}(z_p - z_p^{(0)}), v_{p-1}).$$

□

We now introduce the error propagator operator:

$$\begin{cases} \mathbb{E}_{1,m_2} v_p = 0, \\ \mathbb{E}_{p,m_2} v_p = \left[G_p^{m_2} \left(Id_p - I_{p-1}^p (Id_{p-1} - \mathbb{E}_{p-1,m_2}^2) P_p^{p-1} \right) \right] v_p \quad \forall p \geq 2, \end{cases} \tag{9.33}$$

where the relaxation operator G_p is defined as:

$$G_p = Id_p - B_p^{-1} A_p, \qquad B_p \text{ being introduced in (9.29).} \tag{9.34}$$

The following result holds.

Theorem 9.2.6. *Let z_p and $z_p^{(m_2+1)}$ be the exact and the multigrid solutions associated with system* (9.16)*, respectively. Then, given $z_p^{(0)}$ initial guess of the algorithm, it holds:*

$$z_p - z_p^{(m_2+1)} = \mathbb{E}_{p,m_2}(z_p - z_p^{(0)}), \tag{9.35}$$

where $\mathbb{E}_{p,m_2}$ is defined in (9.33)*.*

Proof. We follow the guidelines of [49, Lemma 6.6.2] and proceed by induction on p. The initial step of the induction is straightforward since the system is solved exactly at the coarsest level. Therefore, we assume (9.35) true up to $p-1$ and we prove the claim for p.

Let e_{p-1} and $\overline{e}_{p-1}$ be introduced in Algorithm 1 and let q_{p-1} be introduced in (9.31). Owing to the induction hypothesis applied to the residual equation, we have:

$$q_{p-1} - e_{p-1} = \mathbb{E}_{p-1,m_2}(q_{p-1} - \overline{e}_{p-1}) = \mathbb{E}_{p-1,m_2}^2(q_{p-1} - 0) = \mathbb{E}_{p-1,m_2}^2(q_{p-1}),$$

whence:

$$e_{p-1} = q_{p-1} - \mathbb{E}_{p-1,m_2}^2(q_{p-1}) = (Id_{p-1} - \mathbb{E}_{p-1,m_2}^2) q_{p-1}. \tag{9.36}$$

Thus:

$$\begin{aligned} z_p - z_p^{(m_2+1)} &= z_p - z_p^{(m_2)} - B_p^{-1}(g_p - A_p z_p^{(m_2)}) = (Id_p - B_p^{-1}A_p)(z_p - z_p^{(m_2)}) \\ &= (Id_p - B_p^{-1}A_p)^{m_2}(z_p - z_p^{(1)}) = G_p^{m_2}(z_p - z_p^{(1)}) = G_p^{m_2}(z_p - z_p^{(0)} - I_{p-1}^p e_{p-1}). \end{aligned} \tag{9.37}$$

Inserting (9.32) and (9.36) in (9.37), we get:

$$\begin{aligned} z_p - z_p^{(m_2+1)} &= G_p^{m_2} \left(z_p - z_p^{(0)} - I_{p-1}^p (Id_{p-1} - \mathbb{E}_{p-1,m_2}^2) P_p^{p-1}(z_p - z_p^{(0)}) \right) \\ &= G_p^{m_2} \left(Id_p - I_{p-1}^p (Id_{p-1} - \mathbb{E}_{p-1,m_2}^2) P_p^{p-1} \right) (z_p - z_p^{(0)}). \end{aligned}$$

□

9.3 Convergence analysis of the multigrid method

We prove in Section 9.3.5 the convergence of the multigrid algorithm presented in Section 9.2. For the purpose, we preliminarily introduce some technical tools. In Section 9.3.1, we discuss the so-called smoothing property associated with the Richardson scheme (9.29). In Section 9.3.2, we show bounds related to the prolongation operator I_{p-1}^p defined in (9.24) and its adjoint with respect to the space-dependent inner product I_p^{p-1} defined in (9.15). Bounds concerning the error correction steps are the topic of Section 9.3.3. Finally, in Sections 9.3.4 and 9.3.5, we treat the convergence of the two-level and multilevel algorithm respectively.

9.3.1 Smoothing property

Lemma 9.3.1. *(smoothing property) For any $v_p \in \widetilde{V}_p$, it holds that:*

$$\begin{aligned} &\left|\!\left|\!\left| G_p^{m_2} v_p \right|\!\right|\!\right|_{1,p} \leq \left|\!\left|\!\left| v_p \right|\!\right|\!\right|_{1,p}, \\ &\left|\!\left|\!\left| G_p^{m_2} v_p \right|\!\right|\!\right|_{s,p} \lesssim \left(\frac{\alpha^*(p)}{\beta_*(p)} \right)^{\frac{s-t}{2}} (1+m_2)^{\frac{t-s}{2}} \left|\!\left|\!\left| v_p \right|\!\right|\!\right|_{t,p}, \end{aligned} \tag{9.38}$$

for some $0 \leq t \leq s \leq 2$, $m_2 \in \mathbb{N} \setminus \{0\}$, where $\alpha^*(p)$ and $\beta_*(p)$ are defined in (9.14) *and in* (9.18) *respectively.*

Proof. The proof is analogous to that in [11, Lemma 4.3]. For the sake of clarity, we report the details. To start with, we rewrite v_p in terms of the orthonormal basis of eigenvectors $\{\psi_i\}_{i=1}^{\dim(\widetilde{V}_p)}$ of $\mathbf{A}_p$ as follows:

$$v_p = \sum_{i=1}^{\dim(V_p)} v_i \psi_i, \qquad \forall\, v_p \in \widetilde{V}_p.$$

As a consequence,

$$G_p^{m_2} v_p = \left(Id_p - \frac{1}{\Lambda_p} A_p \right)^{m_2} v_p = \sum_{i=1}^{\dim(V_p)} \left(1 - \frac{\lambda_i}{\Lambda_p} \right)^{m_2} v_i \psi_i,$$

where Λ_p is the upper bound for the spectrum of $\mathbf{A}_p$ presented in Lemma 9.2.4. Then, owing to the orthonormality of ψ_i with respect to the inner product $(\cdot,\cdot)_p$, we have:

$$\begin{aligned} \left|\!\left|\!\left| G_p^{m_2} v_p \right|\!\right|\!\right|_{s,p}^2 &= \sum_{i=1}^{\dim(V_p)} \left(1 - \frac{\lambda_i}{\Lambda_p} \right)^{2m_2} v_i^2 \lambda_i^s = \Lambda_p^{s-t} \sum_{i=1}^{\dim(V_p)} \left(1 - \frac{\lambda_i}{\Lambda_p} \right)^{2m_2} \frac{\lambda_i^{s-t}}{\Lambda_p^{s-t}} \lambda_i^t v_i^2 \\ &\leq \Lambda_p^{s-t} \max_{x \in [0,1]} (x^{s-t}(1-x)^{2m_2}) \left|\!\left|\!\left| v_p \right|\!\right|\!\right|_{t,p}^2 \lesssim \left(\frac{\alpha^*(p)}{\beta_*(p)} \right)^{s-t} (1+m_2)^{t-s} \left|\!\left|\!\left| v_p \right|\!\right|\!\right|_{t,p}^2, \end{aligned}$$

where in the last inequality we used [11, Lemma 4.2] and (9.28). □

9.3.2 Prolongation and projection operators

In this section, we prove bounds in the $\left|\!\left|\!\left| \cdot \right|\!\right|\!\right|_{1,p}$ norm of the prolongation and the projection operators defined in (9.24) and (9.30), respectively. We stress that this set of results deeply relies on the enhancing strategy presented in the definition of the virtual space (9.11).

We start with a bound on the prolongation operator.

Theorem 9.3.2. *(bound on the prolongation operator) There exists c_{STAB}, positive constant independent of the discretization and multigrid parameters, such that:*

$$\left|\!\left|\!\left| I_{p-1}^p v_{p-1} \right|\!\right|\!\right|_{1,p} \leq c_{STAB} \sqrt{\frac{\alpha^*(p)\beta^*(p)}{\alpha_*(p)\beta_*(p)}} \left|\!\left|\!\left| v_{p-1} \right|\!\right|\!\right|_{1,p-1} \qquad \forall\, v_{p-1} \in \widetilde{V}_{p-1}, \tag{9.39}$$

where $\alpha_*(p)$, $\alpha^*(p)$ are introduced in (9.14) *whereas $\beta_*(p)$ and $\beta^*(p)$ are introduced in* (9.18)*.*

Proof. Recalling bounds (2.15), (9.21) and the definition of the auxiliary space-dependent inner product (9.19), we have:

$$\begin{aligned} \left|\!\left|\!\left| I_{p-1}^p v_{p-1} \right|\!\right|\!\right|_{1,p}^2 &= \sum_{K \in \mathcal{T}_h} \left|\!\left|\!\left| I_{p-1}^p v_{p-1} \right|\!\right|\!\right|_{1,p;K}^2 = \sum_{K \in \mathcal{T}_h} a_p^K (I_{p-1}^p v_{p-1}, I_{p-1}^p v_{p-1}) \\ &\lesssim \alpha^*(p) a(I_{p-1}^p v_{p-1}, I_{p-1}^p v_{p-1}) \lesssim \frac{\alpha^*(p)}{\beta_*(p)} (I_{p-1}^p v_{p-1}, I_{p-1}^p v_{p-1})_p. \end{aligned} \tag{9.40}$$

We recall that:

$$(I_{p-1}^p v_{p-1}, I_{p-1}^p v_{p-1})_p = \sum_{j=1}^{\dim(\widetilde{V}_p)} \mathrm{dof}_j^2(I_{p-1}^p v_{p-1}).$$

Since $\{\mathbb{B}_p(\partial K)\}_{p=1}^{+\infty}$ defined in (2.2) is a sequence of *nested* space for all $K \in \mathcal{T}_n$, we directly have:

$$\mathrm{dof}_{b,j}^2(I_{p-1}^p v_{p-1}) = \mathrm{dof}_{b,j}^2(v_{p-1}),$$

where $\mathrm{dof}_{b,j}(\cdot)$ denotes the j-th boundary dof.

Now, we deal with the internal degrees of freedom. We cannot use the above nestedness argument since we recall that the sequence $\{V_p\}_{p=1}^{\dim(V_p)}$ is made of non-nested spaces. In order to overcome this hindrance, recalling the definition of the prolongation operator (9.25), we write:

$$\mathrm{dof}_{i,j}(I_{p-1}^p v_{p-1}) = \frac{1}{|K|}\int_K I_{p-1}^p v_{p-1} q_{\boldsymbol{\alpha}} = \begin{cases} \frac{1}{|K|}\int_K v_{p-1} q_{\boldsymbol{\alpha}} & \text{if } |\boldsymbol{\alpha}| \leq p-3, \\ 0 & \text{if } |\boldsymbol{\alpha}| = p-2, \end{cases}$$

where $\mathrm{dof}_{i,j}(\cdot)$ denotes the j-th internal dof. As a consequence, it holds:

$$(I_{p-1}^p v_{p-1}, I_{p-1}^p v_{p-1})_p = (v_{p-1}, v_{p-1})_{p-1} = |||v_{p-1}|||_{0,p-1}^2. \tag{9.41}$$

Next, we relate $|||\cdot|||_{0,p-1}$ with $|||\cdot|||_{1,p-1}$. We note that:

$$|||v_{p-1}|||_{0,p-1}^2 \lesssim \beta^*(p)|v_{p-1}|_{1,K}^2 \lesssim \frac{\beta^*(p)}{\alpha_*(p)}|||v_{p-1}|||_{1,p-1}^2, \tag{9.42}$$

where we used in the last but one and in the last inequalities (9.18) and (2.15), respectively.

Combining (9.40), (9.41) and (9.42), we get the claim. □

We show an analogous bound for the "projection" operator P_p^{p-1} introduced in (9.30).

Theorem 9.3.3. *(bound on the "projection" operator) There exists c_{STAB}, positive constant independent of the discretization and multigrid parameters, such that:*

$$\left|\left|\left|P_p^{p-1} v_p\right|\right|\right|_{1,p-1} \leq c_{STAB}\sqrt{\frac{\alpha^*(p)\beta^*(p)}{\alpha_*(p)\beta_*(p)}}|||v_p|||_{1,p} \qquad \forall\, v_p \in \widetilde{V}_p, \tag{9.43}$$

where $\alpha_*(p)$, $\alpha^*(p)$ are introduced in (9.14) *whereas $\beta_*(p)$ and $\beta^*(p)$ are introduced in* (9.18)*. The constant c_{STAB} is the same constant appearing in the statement of Theorem 9.3.2.*

Proof. It suffices to note that:

$$\left|\left|\left|P_p^{p-1} v_p\right|\right|\right|_{1,p-1} = \max_{w_{p-1}\in V_{p-1}\setminus\{0\}} \frac{a_{p-1}(P_p^{p-1}v_p, w_{p-1})}{|||w_{p-1}|||_{1,p-1}} = \max_{w_{p-1}\in V_{p-1}\setminus\{0\}} \frac{a_p(v_p, I_{p-1}^p w_{p-1})}{|||w_{p-1}|||_{1,p-1}}$$

and then apply Theorem 9.3.2 along with a Cauchy-Schwarz inequality. □

9.3.3 Error correction step

In this section, we prove a bound for the error correction step discussed in the multigrid algorithm, see Algorithm 2.

Theorem 9.3.4. *(bound on the error correction step) There exists a positive constant c independent of the discretization parameters such that:*

$$\left|\left|\left|(Id_p - I_{p-1}^p P_p^{p-1})v_p\right|\right|\right|_{0,p} \leq c\frac{\alpha^*(p)}{\alpha_*(p)^{\frac{3}{2}}}\frac{\beta^*(p)^{\frac{3}{2}}}{\beta_*(p)}|||v_p|||_{1,p} \qquad \forall\, v_p \in \widetilde{V}_p, \tag{9.44}$$

where $\alpha_*(p)$, $\alpha^*(p)$ are introduced in (9.14) *whereas $\beta_*(p)$ and $\beta^*(p)$ are introduced in* (9.18)*.*

Proof. Applying (2.15) and (9.18), we have:

$$\begin{aligned}&\left|\!\left|\!\left|(Id_p - I_{p-1}^p P_p^{p-1})v_p\right|\!\right|\!\right|_{0,p}^2 \lesssim \beta^*(p)\left|(Id_p - I_{p-1}^p P_p^{p-1})v_p\right|_{1,\Omega}^2 \\ &\lesssim \beta^*(p)\alpha_*(p)^{-1}\sum_{K\in\mathcal{T}_h}\left\{a_p^K((Id_p - I_{p-1}^p P_p^{p-1})v_p,(Id_p - I_{p-1}^p P_p^{p-1})v_p)\right\}.\end{aligned}$$

Therefore, we deduce:

$$\begin{aligned}&\left|\!\left|\!\left|(Id_p - I_{p-1}^p P_p^{p-1})v_p\right|\!\right|\!\right|_{0,p}^2 \\ &\lesssim \beta^*(p)\alpha_*(p)^{-1}\sum_{K\in\mathcal{T}_h}\left\{a_p^K(v_p,v_p) + a_p^K(I_{p-1}^p P_p^{p-1}v_p, I_{p-1}^p P_p^{p-1}v_p) - 2a_p^K(v_p, I_{p-1}^p P_p^{p-1}v_p)\right\} \\ &= \beta^*(p)\alpha_*(p)^{-1}\sum_{K\in\mathcal{T}_h}\left\{a_p^K(v_p,v_p) + a_p^K(I_{p-1}^p P_p^{p-1}v_p, I_{p-1}^p P_p^{p-1}v_p) - 2a_{p-1}^K(P_p^{p-1}v_p, P_p^{p-1}v_p)\right\} \\ &\lesssim \beta^*(p)\alpha_*(p)^{-1}\sum_{K\in\mathcal{T}_h}\left\{a_p^K(v_p,v_p) + \frac{\alpha^*(p)\beta^*(p)}{\alpha_*(p)\beta_*(p)}a_p^K(P_p^{p-1}v_p, P_p^{p-1}v_p)\right\},\end{aligned}$$

where in the last inequality we applied Theorem 9.3.2 and we dropped the third term since it is negative. Finally, applying Theorem 9.3.3, we obtain:

$$\left|\!\left|\!\left|(Id_p - I_{p-1}^p P_p^{p-1})v_p\right|\!\right|\!\right|_{0,p}^2 \lesssim \frac{\alpha^*(p)^2}{\alpha_*(p)^3}\frac{\beta^*(p)^3}{\beta_*(p)^2}\left|\!\left|\!\left|v_p\right|\!\right|\!\right|_{1,p}^2,$$

whence the claim. □

9.3.4 Convergence of the two-level algorithm

In this section, we prove the convergence of the two-level algorithm.

Theorem 9.3.5. *There exists a positive constant c_{2lvl} independent of the discretization and multilevel parameters, such that:*

$$\left|\!\left|\!\left|\mathbb{E}_{p,m_2}^{2lvl}v_p\right|\!\right|\!\right|_{1,p} \le c_{2lvl}\Sigma_{p,m_2}\left|\!\left|\!\left|v_p\right|\!\right|\!\right|_{1,p} \qquad \forall\, v_p \in \widetilde{V}_p, \tag{9.45}$$

where

$$\Sigma_{p,m_2} = \left(\frac{\alpha^*(p)\beta^*(p)}{\alpha_*(p)\beta_*(p)}\right)^{\frac{3}{2}}\cdot\frac{1}{\sqrt{1+m_2}}$$

and $\mathbb{E}_{p,m_2}^{2lvl}$ is the two-level error propagator operator:

$$\mathbb{E}_{p,m_2}^{2lvl}v_p = \left[G_p^{m_2}\left(Id_p - I_{p-1}^p P_p^{p-1}\right)\right]v_p.$$

The constants $\alpha_*(p)$ and $\alpha^*(p)$ are introduced in (9.14)*, whereas the constants $\beta_*(p)$ and $\beta^*(p)$ are introduced in* (9.18)*.*

Proof. Using the smoothing property (9.38) and Theorem 9.3.4, we get:

$$\begin{aligned}&\left|\!\left|\!\left|\mathbb{E}_{p,m_2}^{2\text{lvl}}v_p\right|\!\right|\!\right|_{1,p} = \left|\!\left|\!\left|G_p^{m_2}(Id_p - I_{p-1}^p P_p^{p-1})v_p\right|\!\right|\!\right|_{1,p} \lesssim \frac{1}{\sqrt{1+m_2}}\cdot\sqrt{\frac{\alpha^*(p)}{\beta_*(p)}}\left|\!\left|\!\left|(Id_p - I_{p-1}^p P_p^{p-1})v_p\right|\!\right|\!\right|_{0,p} \\ &\lesssim \frac{1}{\sqrt{1+m_2}}\cdot\sqrt{\frac{\alpha^*(p)}{\beta_*(p)}}\cdot\frac{\alpha^*(p)}{\alpha_*(p)^{\frac{3}{2}}}\cdot\frac{\beta^*(p)^{\frac{3}{2}}}{\beta_*(p)}\left|\!\left|\!\left|v_p\right|\!\right|\!\right|_{1,p} = \left(\frac{\alpha^*(p)\beta^*(p)}{\alpha_*(p)\beta_*(p)}\right)^{\frac{3}{2}}\cdot\frac{1}{\sqrt{1+m_2}}\left|\!\left|\!\left|v_p\right|\!\right|\!\right|_{1,p}.\end{aligned}$$

□

As a consequence of Theorem 9.3.5, we deduce that taking m_2, the number of postsmoothing iterations, large enough, the two-level algorithm converges, since the two-level error propagator

operator $\mathbb{E}^{2\text{lvl}}_{p,m_2}$ is a contraction. We point out that a sufficient condition for the convergence of the two-level algorithm is that the number of postsmoothing iterations m_2 must satisfy:

$$\sqrt{1+m_2} > c_{2\text{lvl}}^{-1}\left(\frac{\alpha^*(p)\beta^*(p)}{\alpha_*(p)\beta_*(p)}\right)^{\frac{3}{2}}, \tag{9.46}$$

see Remark 15 for more details. We stress that (9.46) is a sufficient condition only, in practice the number of postsmoothing steps needed for the convergence of the algorithm is much smaller; see the numerical results in Section 9.4.

9.3.5 Convergence of the multilevel algorithm

In this section, we prove the main result of the paper, namely the convergence of our p-VEM multigrid algorithm.

Theorem 9.3.6. *Let Σ_{p,m_2} and c_{2lvl} be defined as in Theorem 9.3.5. Let c_{STAB} be defined as in Theorem 9.3.3. Let $\alpha_*(p)$ and $\alpha^*(p)$ be defined in* (9.14) *and $\beta_*(p)$ and $\beta^*(p)$ be defined in* (9.21)*. Then, there exists $\widehat{c} > c_{2lvl}$ such that, if the number of postsmoothing iterations satisfies:*

$$\sqrt{1+m_2} > \frac{c^2_{STAB}\widehat{c}^2}{\widehat{c}-c_{2lvl}}\left(\frac{\alpha^*(p)\beta^*(p)}{\alpha_*(p)\beta_*(p)}\right)^{\frac{5}{2}}, \tag{9.47}$$

then, it holds:

$$\|\mathbb{E}_{p,m_2}v_p\|_{1,p} \leq \widehat{c}\Sigma_{p,m_2}\|v_p\|_{1,p} \quad \forall v_p \in \widetilde{V}_p,$$

with $\widehat{c}\Sigma_{p,m_2} < 1$. As a consequence, this implies that the multilevel algorithm converges uniformly with respect to the discretization parameters and the number of levels provided that m_2 satisfies (9.47)*, since in that case $\mathbb{E}_{p,m_2}$ is a contraction.*

Proof. We proceed by induction in p. For $p = 1$, the assertion is trivially true owing to (9.33). Assume next that the following induction hypothesis is valid:

$$\left|\left|\left|E^2_{p-1,m_2}v_{p-1}\right|\right|\right|_{1,p-1} \leq \widehat{c}\Sigma_{p-1,m_2}|||v_{p-1}|||_{1,p-1} \quad \forall v_{p-1} \in \widetilde{V}_{p-1}. \tag{9.48}$$

We want to prove the assertion for induction step p.

From Theorem 9.3.5, we have that:

$$\Sigma_{p,m_2} = \left(\frac{\alpha^*(p)\beta^*(p)}{\alpha_*(p)\beta_*(p)}\right)^{\frac{3}{2}} \cdot \frac{1}{\sqrt{1+m_2}}.$$

Recalling (9.33), we decompose the error propagator operator as:

$$\mathbb{E}_{p,m_2}v_p = G_p^{m_2}(Id_p - I^p_{p-1}P^{p-1}_p)v_p + G_p^{m_2}I^p_{p-1}\mathbb{E}^2_{p-1,m_2}P^{p-1}_p v_p = \mathbb{E}^{2\text{lvl}}_{p,m_2}v_p + G_p^{m_2}I^p_{p-1}\mathbb{E}^2_{p-1,m_2}P^{p-1}_p v_p.$$

Thus:

$$|||\mathbb{E}_{p,m_2}v_p|||_{1,p} \leq \left|\left|\left|\mathbb{E}^{2\text{lvl}}_{p,m_2}v_p\right|\right|\right|_{1,p} + \left|\left|\left|G_p^{m_2}I^p_{p-1}\mathbb{E}^2_{p-1,m_2}P^{p-1}_p v_p\right|\right|\right|_{1,p} = I + II.$$

We bound the two terms separately. The first one is estimated directly applying the two-level error result, namely Theorem 9.3.5:

$$I \leq c_{2\text{lvl}}\Sigma_{p,m_2}|||v_p|||_{1,p}.$$

On the other hand, the second term can be bounded applying the smoothing property Lemma 9.3.1, the bounds regarding the interspace operator Theorem 9.3.2, the induction hypothesis (9.48) and Theorem 9.3.3. We can write:

$$II \leq \left|\left|\left|I^p_{p-1}\mathbb{E}^2_{p-1,m_2}P^{p-1}_p v_p\right|\right|\right|_{1,p} \leq c_{\text{STAB}}\sqrt{\frac{\alpha^*(p)\beta^*(p)}{\alpha_*(p)\beta_*(p)}}\left|\left|\left|\mathbb{E}^2_{p-1,m_2}P^{p-1}_p v_p\right|\right|\right|_{1,p-1}$$

$$\leq c_{\text{STAB}}\sqrt{\frac{\alpha^*(p)\beta^*(p)}{\alpha_*(p)\beta_*(p)}}\widehat{c}^2\Sigma^2_{p-1,m_2}\left|\left|\left|P^{p-1}_p v_p\right|\right|\right|_{1,p-1} \leq c^2_{\text{STAB}}\widehat{c}^2\frac{\alpha^*(p)\beta^*(p)}{\alpha_*(p)\beta_*(p)}\Sigma_{p-1,m_2}|||v_p|||_{1,p}.$$

We note that, owing to (9.1) and (9.18), the following holds true:

$$\Sigma^2_{p-1,m_2} = \left(\frac{\alpha^*(p-1)\beta^*(p-1)}{\alpha_*(p-1)\beta_*(p-1)}\right)^3 \cdot \frac{1}{1+m_2} \approx \left(\frac{\alpha^*(p)\beta^*(p)}{\alpha_*(p)\beta_*(p)}\right)^{\frac{3}{2}} \cdot \frac{1}{\sqrt{1+m_2}}\Sigma_{p,m_2}.$$

We deduce:

$$|||\mathbb{E}_{p,m_2} v_p|||_{1,p} \leq \underbrace{\left(c_{2\text{lvl}} + c^2_{\text{STAB}}\widehat{c}^2 \left(\frac{\alpha^*(p)\beta^*(p)}{\alpha_*(p)\beta_*(p)}\right)^{\frac{5}{2}} \cdot \frac{1}{\sqrt{1+m_2}}\right)\Sigma_{p,m_2}}_{\zeta} |||v_p|||_{1,p}.$$

We want that ζ is such that $\zeta < \widehat{c}\Sigma_{p,m_2}$. In particular, we require:

$$c_{2\text{lvl}} + c^2_{\text{STAB}}\widehat{c}^2 \left(\frac{\alpha^*(p)\beta^*(p)}{\alpha_*(p)\beta_*(p)}\right)^{\frac{5}{2}} \cdot \frac{1}{\sqrt{1+m_2}} < \widehat{c},$$

which is in fact equivalent to (9.47). □

Remark 15. We briefly comment on equations (9.46) and (9.47) highlighting the origin of the different terms:

* the term $\frac{\alpha^*(p)}{\alpha_*(p)} \approx p^9$ originates from the spectral property (2.12) of the stabilization term S^K; if it were possible to provide a discrete bilinear form (2.15) with continuity and coercivity constants provably independent of p, then $\frac{\alpha^*(p)}{\alpha_*(p)} \approx 1$;

* the term $\frac{\beta^*(p)}{\beta_*(p)} \approx p^6$ is related to (9.18) which is not p robust; again, if it were possible to provide space-dependent inner products spectrally equivalent to the H^1 seminorm, then $\frac{\beta^*(p)}{\beta_*(p)} \approx 1$.

The existence of a p independent stabilization of the method and the existence of a computable virtual L^2-orthonormal basis is still, to the best of our knowledge, an open issue.

It is worth to stress that the bounds on $\alpha_*(p)$, $\alpha^*(p)$, $\beta_*(p)$ and $\beta^*(p)$ that we provide in terms of p are extremely crude; we expect a much better practical behaviour as was observed in Sections 6.1 and 6.2.1 for what concerns the stability constants.

In addition, we highlight that the ratios $\frac{\alpha^*(p)}{\alpha_*(p)}$ and $\frac{\beta^*(p)}{\beta_*(p)}$ depend also on the shape of the elements of the decomposition. More precisely, from the proofs of Lemmata 9.1.2, 9.1.3, 9.2.2 and Theorem 9.2.1, we observe that such dependence appears when applying Neumann and trace inequalities. If the shape of the elements is allowed to be very general (small edges, collapsing bulks, ...), then the constants appearing in Neumann and trace inequalities may be very large. As a consequence, one expects that also the above mentioned ratios may get larger, see Remark 16.

9.4 Numerical results

In this section, we test the performance of the multigrid solver for the p-version of the VEM by studying the behaviour of the convergence factor:

$$\rho = \exp\left(\frac{1}{N}\ln\left(\frac{\|r_N\|_2}{\|r_0\|_2}\right)\right), \tag{9.49}$$

where N denotes the iteration counts needed to reduce the residual below a given tolerance of 10^{-8} and r_N, r_0 are the final and the initial residuals, respectively. We also show that our multigrid algorithm can be employed as a preconditioner for the PCG method. Throughout the section we fix the maximum number of iterations to 1000 and consider three different kind of decompositions: meshes made of squares, Voronoi-Lloyd polygons and quasi-regular hexagons; cf. Figure 1.3.

In Section 9.4.1, we present some tests aiming at assessing the performance of our multigrid scheme with different smoothers. In Section 9.4.2 we show that our multigrid method can be successfully employed as a preconditioner for the Conjugate Gradient (CG) iterative scheme, more precisely we consider a single iteration of the multigrid algorithm as a preconditioner to accelerate the Preconditioned CG method (PCG).

9.4.1 The p multigrid algorithm as an iterative solver

In this section we investigate the performance of our multigrid scheme with different smoothers. We consider both the Richardson scheme (9.29) as well as a symmetrized Gauß-Seidel scheme (on which in fact no theory has been developed) as a smoother.

The first set of numerical experiment has been obtained employing a Richardson smoother. Before presenting the computed estimates of the convergence factor, we investigate numerically the behaviour of the smoothing parameter Λ_p associated with the Richardson scheme (9.29), for which a far-from-being-sharp bound is given in Lemma 9.2.4. As shown in Figure 9.2, where Λ_p as a function of p is shown, the maximum eigenvalue of $\mathbf{A}_p$ seems to behave even better than p^2, which is the expected behaviour in standard FEM. The numerical tests presented in the following have been obtained with an approximation of Λ_p obtained (in a off line stage) with ten iterations of the power method.

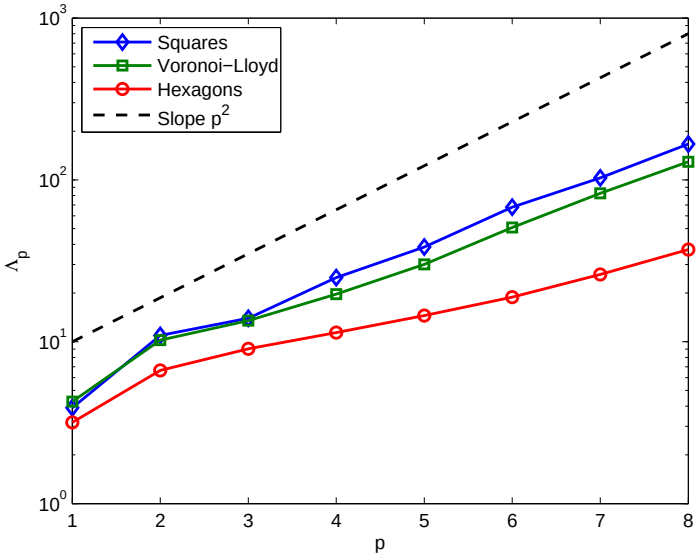

Figure 9.2: Maximum eigenvalue Λ_p of $\mathbf{A}_p$ as a function of p.

We numerically investigate the behaviour of the multigrid algorithm using a Richardson smoother. The results reported in Table 9.1 shows the computed convergence factor defined in ρ (9.49) as a function of the number of level K, the number of postsmoothing steps $m_2 = m$, and the degree of accuracy p employed at the "finest level" on a mesh made of squares, cf. Figure 1.3. Analogous results have been obtained on the other decompositions; such results are not reported here for the sake of brevity. As expected, increasing the number of postsmoothing m_2 implies a decreasing of the convergence factor ρ. Moreover, a minimum number of smoothing steps is required to guarantee the convergence of the underlying solver. We also observe that, as expected, even though both two-level and multilevel solvers converge for a fixed value of m, the number of iterations required to reduce the relative residual below the given tolerance grows with increasing p. A numerical es-

Table 9.1 Convergence factor ρ of the p–multigrid scheme as a function of K (number of levels), p ("finest" level) and m_2 (number of postsmoothing steps). Richardson smoother. Mesh of squares.

	$p=2$	$p=3$		$p=4$		$p=5$	
K	2	2	3	3	4	3	4
$m_2=2$	0.99	x	0.97	x	0.97	x	x
$m_2=4$	0.97	x	0.95	x	0.92	x	x
$m_2=6$	0.96	0.93	0.92	0.79	0.88	x	0.85
$m_2=8$	0.95	0.69	0.89	0.74	0.84	0.98	0.82

timate of the minimum number of postsmoothing steps needed in practice to achieve convergence

is reported in Table 9.2 for all the three meshes under consideration. This represents a *practical* indication for (9.47). As expected, such a minimum number depends on the polynomial degree employed on the finest level.

Table 9.2 Minimum number of postsmoothing steps needed to guarantee convergence.

	$p=2$	$p=3$		$p=4$			$p=5$			$p=6$		
K	2	2	3	2	3	4	2	3	4	2	3	4
Square	1	6	1	10	5	1	14	8	5	42	15	8
Voronoi-Lloyd	7	14	5	12	11	5	14	10	11	36	24	9
Hexagons	7	25	6	12	20	5	9	10	19	17	7	9

We next investigate the behaviour of our MG algorithm whenever a symmetrized Gauß-Seidel scheme as a smoother is employed. We recall that the smoothing matrix B_p associated with the symmetrized Gauß-Seidel operator now reads:

$$\mathbf{B_p} = \begin{cases} \mathbf{L_p} \text{ if the postsmoothing iteration is odd} \\ \mathbf{L_p^T} \text{ if if the postsmoothing iteration is even} \end{cases} \tag{9.50}$$

where $\mathbf{L_p}$ is the lower triangular part of $\mathbf{A}_p$ defined in (9.16). We have repeated the set of experiments carried out before employing the same same set of parameters: the results are are shown in Tables 9.3 and 0 9.4. Employing a symmetrized Gauß-Seidel smoother yields to an iterative scheme whose convergence factor is smaller than in the analogous cases with the Richardson smoother. In Table 9.4 we report the same results obtained on a mesh of Voronoi-Lloyd polygonal elements keep on increasing the number of post smoothing steps: as expected the performance of the algorithm improves further. The same kind of results have been obtained on a regular hexagonal grid; for the sake of brevity these results have been omitted.

Table 9.3 Convergence factor ρ of the p–multigrid scheme as a function of K (number of levels), P ("finest" level) and m_2 (number of postsmoothing steps). Gauß-Seidel smoother. Mesh of squares.

	$p=2$	$p=3$		$p=4$		$p=5$	
K	2	2	3	3	4	3	4
m= 2	0.96	0.90	0.92	x	0.75	0.97	x
m= 4	0.92	0.69	0.85	0.57	0.57	0.72	x
m = 6	0.88	0.60	0.78	0.43	0.44	0.60	0.85
m = 8	0.84	0.53	0.72	0.34	0.35	0.53	0.82

Table 9.4 Convergence factor ρ of the p–multigrid scheme as a function of K (number of levels), p ("finest" level) and m_2 (number of postsmoothing steps). Gauß-Seidel smoother. Mesh of Voronoi-Lloyd polygons.

	$p=2$	$p=3$		$p=4$		$p=5$	
K	2	2	3	3	4	3	4
$m=8$	0.91	0.63	0.81	0.45	0.61	0.49	0.46
$m=10$	0.89	0.57	0.77	0.37	0.54	0.44	0.43
$m=12$	0.87	0.52	0.73	0.31	0.47	0.40	0.40
$m=14$	0.86	0.48	0.69	0.25	0.42	0.37	0.37

Remark 16. We also carried out numerical tests employing meshes characterized by progressively increasing aspect ratios. We observed that the number of post-smoothing steps required for achieving convergence grows with such aspect ratio. This is consistent with what observed in Remark 15.

9.4.2 The p multigrid algorithm as a preconditioner for the PCG method

In this set of experiments we aim at demonstrating that *a single iteration* of the p–multigrid algorithm can be successfully employed to precondition the CG method. In this set of experiments,

the coarsest level is given by $p = 1$. In all the test cases, we have employed as a stopping criterion in order to reduce the (relative) residual below a tolerance of 10^{-6}, with a maximum number of iterations set equal to 1000. In Figure 9.3, we compare the PCG iteration counts with our multigrid preconditioner, which is constructed employing either a Richardson or a Gauß-Seidel smoother and $m = 8$ post-smoothing steps. For the sake of comparison, we report the same quantities computed with the unpreconditioned CG method and with the PCG method with preconditioner given by an incomplete Cholesky factorization. As before, the results reported in Figure 9.3 have been obtained on the computational grids considered in the foregoing section.

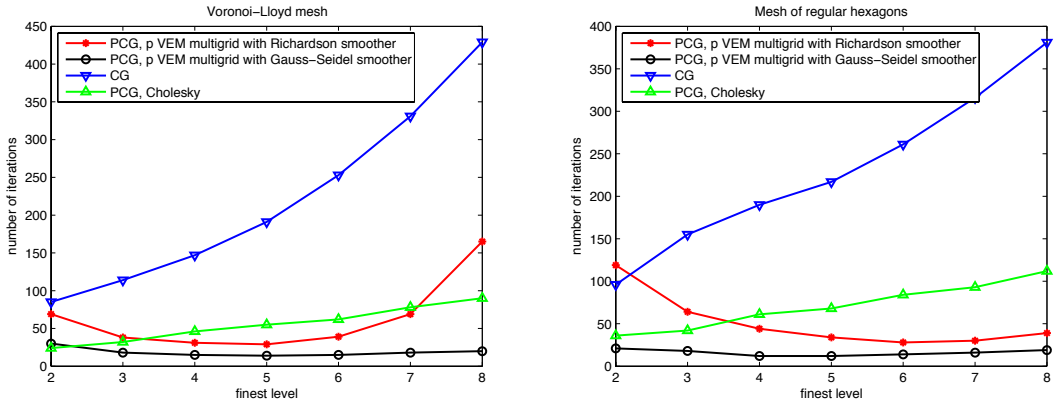

Figure 9.3: PCG iteration counts as a function of p with p–multigrid preconditioner (with either Richardson or Gauß-Seidel smoothers). For the sake of comparison the CG iteration counts without preconditioning and with an incomplete Cholesky preconditioner are also shown. For the p–multigrid preconditioner, the coarsest level is $p = 1$ and the number of post-smoothing steps is 8. Meshes made of: Voronoi-Lloyd polygons (left), quasi-regular hexagons (right).

Chapter 10

Future work

In this chapter, we suggest various topics which (are presently and) may be investigated, following both the theoretical and the numerical trail paved in the thesis.

1. A possible direction of interest is the extension of the results proven for 2D *hp* VEM to the 3D case. We believe that a possible way to deal with this extension is combining the ideas contained in the following works: [94, 95] for what concerns the 3D version of *hp* FEM part and the regularity issues of solutions to 3D elliptic problems; [4,33] for what concerns the 3D version of VEM; Chapter 3 and Section 6.2 for the construction of *hp* VEM with nonuniform degrees of accuracy.

2. The extension of *hp* VEM to general elliptic problems, see [28], is also of interest. Such extension is nontrivial since VE spaces for general elliptic problems are generally defined as in (9.11); in particular, they are defined through the enhancing constraints (9.12). At the present stage, one would need in particular to derive optimal error bounds in terms of p, when approximating a target function by means of functions in the VE enhanced space defined in (9.11).

   A possible way to overcome this lack of knowledge is considering larger spaces, defining for instance local VE spaces as:

   $$V_{hp}(K) = \left\{ v_{hp} \in H^1(K) \mid v_{hp} \in \mathbb{B}_{hp}(\partial K),\ \Delta v_{hp} \in \mathbb{P}_p(K) \right\}, \tag{10.1}$$

   where $\mathbb{B}_{hp}(\partial K)$ is defined in (2.2). The choice (10.1) allows us to compute higher order L^2 projectors that are needed in [28]. However, the dimension of space $V_{hp}(K)$ defined in (10.1) is larger than its counterpart in (9.11).

3. Having a better residual a-posteriori error analysis than the one presented in Chapter 5 is another important issue. What in particular we should do/improve is:

   - proving optimal local p estimates by functions in the VE space; in particular, we should improve Lemma 5.1.2;
   - proving lower and upper bounds that are provably independent of the stabilization constants $\alpha_*(p)$ and $\alpha^*(p)$, cf. Theorem 5.2.1;
   - discuss an *hp* refinement strategy and implement the adaptive *hp* VEM.

   These three topics above are in fact presently under investigations.

4. The best possible scenario would be, concerning the issue of stabilization, cf. Chapter 6, being able to show the existence of stabilizations that are provably spectrally equivalent to the H^1 seminorm.

5. The extension of *hp* VEM to other problems, such as linear and nonlinear elasticity, Stokes and Navier-Stokes equations, is intriguing. In our opinion, the main issue when tackling e.g.

Stokes equation is how to prove stability bounds that are explicit in terms of the degree of accuracy p.

Indeed, all the stability bounds we proved in Chapter 6 are based on the fact that the laplacian of functions in local VE spaces is a polynomial; instead, the definition of local "divergence free" VE spaces for Stokes, see [36], is more involved and it is not straightforward how to combine the definition of the space inside the theoretical stability bounds in terms of p proven in Chapter 6.

6. A particular mention is given to (for simplicity homogeneous) Helmholtz equation endowed (again for simplicity) with impedance (i.e. Robin) boundary conditions. In the unique (to the best of our knowledge) work available in VEM literature concerning Helmholtz equation, i.e. [91], the approximation spaces consist of *globally continuous* functions that locally are the product of low order VE functions (which form a harmonic partition of unity) and plane waves; nonetheless, the method is not really Trefftz.

   It is possible in fact to recover a full Trefftz method following the original spirit of VEM by relaxing the continuity of the global space and by requiring that local spaces contain plane waves plus other functions guaranteeing *only* the continuity of local impedance traces. Doing so, one is able to define local spaces as spaces of solutions to local homogeneous Helmholtz equations with "plane-waves impedance boundary conditions".

   Such a modification of [91] is currently under investigation.

7. Extending the p VEM multigrid algorithm of Chapter 9 to the 3D case is worth it, since iterative solvers are much more useful for large linear system , which typically stem from 3D Galerkin methods.

Assumptions

We collect here in one place all the assumptions that are employed throughout the thesis, concerning both the regularity of sequences of polygonal meshes and the distribution of "local polynomial degrees", recalling the pages where they were introduced.

We believe that this may be of help to the reader.

(**A**$_{hp}$**1**) (see page 17) for all $K \in \mathcal{T}_n$, it must hold:

$$a^K(q_p, v_{hp}) = a^K_{hp}(q_p, v_{hp}) \quad \forall\, q_p \in \mathbb{P}_p(K),\, \forall\, v_{hp} \in V_{hp}(K);$$

(**A**$_{hp}$**2**) (see page 17) for all $K \in \mathcal{T}_n$, it must hold:

$$\alpha_*(p)|v_{hp}|^2_{1,K} \leq a^K_{hp}(v_{hp}, v_{hp}) \leq \alpha^*(p)|v_{hp}|^2_{1,K}, \quad \forall v_{hp} \in V_{hp}(K),$$

where $0 < \alpha_*(p) \leq \alpha^*(p) < +\infty$ are two constants which may depend on p.

(**A**$_n$**1**) (see page 32) for all $K \in \mathcal{T}_n$, it must hold:

$$a^K(q_{p_K}, v_n) = a^K_n(q_{p_K}, v_n) \qquad \forall q_{p_K} \in \mathbb{P}_{p_K}(K), \quad \forall v_n \in V(K);$$

(**A**$_n$**2**) (see page 33) for all $K \in \mathcal{T}_n$, it must hold:

$$\alpha_*(p_K)|v_n|^2_{1,K} \leq a^K_n(v_n, v_n) \leq \alpha^*(p_K)|v_n|^2_{1,K} \qquad \forall v_n \in V(K)$$

where $\alpha_*(p_K) = \min(1, c\, p_K^{-r_1})$ and $\alpha^*(p_K) = \max(1, c\, p_K^{r_2})$, c, r_1 and r_2 being introduced in (3.12).

(**A**$^\Delta$**1**) (see page 46) for all $K \in \mathcal{T}_n$, it must hold:

$$a^K(q_{p,\Delta}, v_n) = a^K_\Delta(q_{p,\Delta}, v_n) \qquad \forall q_{p,\Delta} \in \mathbb{H}_p(K),\, \forall v_n \in V^\Delta(K),$$

where we recall that $\mathbb{H}_p(K)$ is the space of harmonic polynomials of degree p over K;

(**A**$^\Delta$**2**) (see page 46) for all $K \in \mathcal{T}_n$, it must hold:

$$\alpha_*(p)|v_n|^2_{1,K} \leq a^K_\Delta(v_n, v_n) \leq \alpha^*(p)|v_n|^2_{1,K} \quad \forall v_n \in V^\Delta(K),$$

where $\alpha_*(p) = \min(1, c\, p^{-r_3})$ and $\alpha^*(p) = \max(1, c\, p^{r_4})$.

(**G0**) (see page 9) $\mathcal{T}_n$ is a conforming polygonal decomposition of Ω, that is to say that each boundary edge $s \in \mathcal{E}^b_n$ belongs to the boundary of *only one* element $K \in \mathcal{T}_n$, whereas each internal edge $s \in \mathcal{E}_n \setminus \mathcal{E}^b_n$ belongs to the boundary of *exactly two* elements K_1 and K_2 of $\mathcal{T}_n$.

(**G1**) (see page 10) every $K \in \mathcal{T}_n$ is star-shaped (see [49]) with respect to a ball of radius greater than or equal to $\rho_0\, h_K$, where ρ_0 is a universal positive constant;

(**G2**) (see page 10) given any $K \in \mathcal{T}_n$, for all edges s of K, it holds that $h_s \geq \rho_0\, h_K$, where ρ_0 is a universal positive constant; without loss of generality, we assume that ρ_0 is the same constant of assumption (**G1**); besides, the number of edges in K is uniformly bounded independently of the geometry of the domain.

(**G3**) (see page 10) for all $K \in \mathcal{T}_n$, $h \leq ch_K$, being c a universal positive constant.

(**G4**) (see page 10) $\mathbf{0}$ is a vertex of Ω and is denoted by $\mathbf{A}_1$, see (1.17); moreover, the geometric refinements are performed only towards vertex $\mathbf{0}$ and not the other vertices. We also denote by $H^{m,\ell}_\beta(\Omega,\mathbf{0})$, $\beta \in \mathbb{R}$, the weighted Sobolev and Babuška spaces with a unique singular vertex, the spaces obtained by the completion of $\mathcal{C}^\infty(\overline{\Omega})$ using the norm:

$$\|u\|^2_{H^{m,\ell}_\beta(\Omega)} = \|u\|^2_{\ell-1,\Omega} + |u|^2_{H^{m,\ell}_\beta(\Omega)} = \|u\|^2_{\ell-1,\Omega} + \sum_{k=\ell}^{m} \|\Phi_{\beta+k-\ell}|D^k u|\|^2_{0,\Omega}$$

and:

$$\mathcal{B}^\ell_\beta(\Omega,\mathbf{0}) = \left\{u \in \mathcal{B}^\ell_{\boldsymbol{\beta}}(\Omega) \mid \boldsymbol{\beta} = (\beta,0,0,\ldots,0)\right\}$$

respectively, where the weight function Φ_β has been modified to:

$$\Phi_\beta(\mathbf{x}) = \min(1, |\mathbf{x}-\mathbf{0}|)^\beta).$$

(**G5**) (see page 11)

$$h_K \approx \begin{cases} \sigma^n & \text{if } K \in L_0 \\ \frac{1-\sigma}{\sigma}\text{dist}(K,\mathbf{0}) & \text{if } K \in L_j, \quad j = 1,\ldots,n \end{cases}.$$

(**G6**) (see page 24) for all $n \in \mathbb{N}$, there exists a positive universal constant $N \in \mathbb{N}$ such that there are at most N overlapping squares in the collection $\{Q(K)\}$ and N parallelograms in the collection $\{\widetilde{Q}(\widetilde{K})\}$, i.e. for all $Q(K)$ in $\{Q(K)\}$ and for all $\widetilde{Q}(\widetilde{K})$ in $\{\widetilde{Q}(\widetilde{K})\}$, given $I_{K'} := \{Q(K) \mid Q(K) \cap Q(K') \neq \emptyset\}$ and $\widetilde{I}_{\widetilde{K}'} := \{\widetilde{Q}(\widetilde{K}) \mid \widetilde{Q}(\widetilde{K}) \cap \widetilde{Q}(\widetilde{K}') \neq \emptyset\}$, it holds that $\text{card}(I_{K'})$, $\text{card}(\widetilde{I}_{\widetilde{K}'}) \leq N$, $\forall K \in \mathcal{T}_h$ and $\forall \widetilde{K} \in \widetilde{\mathcal{T}}_n$.

(**G7**) (see page 34) given $\mathcal{T}_n$ geometric polygonal decomposition, there exists a collection C^1_n of squares such that:

- $\text{card}(C^1_n) = \text{card}(\mathcal{T}^1_n)$; for each $K \in \mathcal{T}^1_n$, there exists $Q = Q(K) \in C^1_n$ such that $Q \supseteq K$ and $h_K \approx h_Q$, being $h_Q = \text{diam}(Q)$; in addition, it must hold $\text{dist}(\mathbf{0}, Q(K)) \approx h_K$;
- every $\mathbf{x} \in \Omega$ belong at most to a fixed number of squares Q, independently on all the discretization parameters;
- for all $K \in \mathcal{T}^0_n$, K is star-shaped with respect to $\mathbf{0}$; moreover, the subtriangulation of K obtained by joining $\mathbf{0}$ with the other vertices of the polygon is uniformly shape-regular.

(**G8**) (see page 47) the shape regularity constant ρ_0 introduced in assumptions (**G1**)-(**G2**) is such that $\rho_0 \in \left(0, \frac{1}{2}\right)$; moreover, for all $K \in \mathcal{T}_n$ abutting $\mathbf{0}$, it is possible to construct a subtriangulation $\widetilde{\mathcal{T}}_n = \widetilde{\mathcal{T}}_n(K)$ by joining the vertices of K to $\mathbf{0}$ is made of triangles that are star-shaped with respect to a ball of radius greater than or equal to $\rho_0 h_T$, h_T being $\text{diam}(T)$ for all $T \in \widetilde{\mathcal{T}}_n$. For all $T \in \widetilde{\mathcal{T}}_n(K)$, it holds $h_K \approx h_T$.

(**P1**) (see page 31) the following holds true:

$$p_{K_1} \approx p_{K_2} \text{ whenever } \overline{K_1} \cap \overline{K_2} \neq \emptyset.$$

Appendix A

Regularity of solutions to elliptic problems

In this appendix, we recall (without proofs) some important issues regarding the regularity of solutions to Poisson problems (and which remain valid also on general elliptic problems) on polygonal domains. For a deeper insight in the topic, we refer to [15, 16, 70, 73, 96].

In order to have a rather general presentation, we also allow for Dirichlet-Neumann conditions. For the purpose, given $\Omega \subset \mathbb{R}^2$ polygonal domain, we split its boundary $\partial\Omega$ into two (nonoverlapping) parts:

$$\Gamma_D \quad \text{(Dirichlet boundary)}, \qquad \Gamma_N \quad \text{(Neumann boundary)}. \tag{A.1}$$

We demand that both Γ_D and Γ_N consist of collections of full edges and that $\Gamma_D \neq \emptyset$.

The problem we consider is the following generalization of (1.26). Given data f, g_D and g_N regular enough, the aim is to find a function u such that:

$$\begin{cases} -\Delta u = f & \text{in } \Omega \\ u = g_D & \text{on} \Gamma_D \\ u = g_N & \text{on} \Gamma_N \end{cases}. \tag{A.2}$$

The weak formulation of (A.2) reads:

$$\begin{cases} \text{find } u \in V_g \text{ such that} \\ a(u,v) = (f,v)_{0,\Omega} + \int_{\Gamma_N} g_N v \quad \forall v \in V_{\Gamma_D} \end{cases}, \tag{A.3}$$

where $a(\cdot,\cdot)$ and V_g are defined in (1.28) and (1.30) respectively, while:

$$V_{\Gamma_D} = \big\{ v \in H^1(\Omega) \mid v = 0 \text{ on } \Gamma_D \big\}.$$

In the remainder of the appendix, we adopt the notation introduced in Section 1.2. More precisely, the names of the vertices of Ω, along with the magnitude of the associated angles, are given in (1.17).

We say that vertex $\mathbf{A}_i$ is a D (or N) vertex if $\mathbf{A}_i \in \Gamma_D^o$ (or Γ_N^o); otherwise, we say that $\mathbf{A}_i$ is D-N. Let us introduce the singular exponents $\alpha_{i,j}$ as:

$$\alpha_{i,j} = \begin{cases} j\frac{\pi}{\omega_i} & \text{if } \mathbf{A}_i \text{ is either D or N} \\ \big(j - \frac{1}{2}\big)\frac{\pi}{\omega_i} & \text{if } \mathbf{A}_i \text{ is D-N} \end{cases} \qquad \forall\, i = 1, \dots, N_\Omega, \quad j \in \mathbb{N}. \tag{A.4}$$

Assume that the set of edges $\{s_i\}_{i=1}^{N_\Omega}$ is counter-clockwise oriented; then, to each vertex $\mathbf{A}_i$, $i = 1, \dots, N_\Omega$, we can associate a couple of edges s_i and $s_{i+1,\mathrm{mod}(N_\Omega)}$ as in Figure A.1. Furthermore, to each vertex $\mathbf{A}_i$ of Ω, $i = 1, \dots, N_\Omega$, we associate a local set of polar coordinates:

$$\mathbf{A}_i \quad \longrightarrow \quad (r_i, \theta_i). \tag{A.5}$$

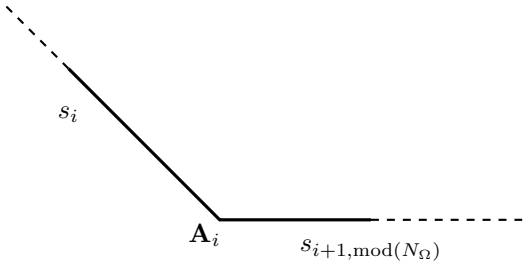

Figure A.1: Vertex $\mathbf{A}_i$ and edges s_i and $s_{i+1,\mathrm{mod}(N_\Omega)}$.

At this point, we are in business for defining the so-called singular functions. For $i = 1, \dots, N_\Omega$ and $j \in \mathbb{N}$, if the singular exponent $\alpha_{i,j}$ defined in (A.4) does not belong to $\mathbb{N}$, then we set:

$$S_{i,j}(r_i, \theta_i) = \begin{cases} r_i^{\alpha_{i,j}} \sin(\alpha_{i,j}\theta_i) & \text{if } \Gamma^{\mathrm{o}}_{i+1,\mathrm{mod}(N_\Omega)} \subset \Gamma^{\mathrm{o}}_D \\ r_i^{\alpha_{i,j}} \cos(\alpha_{i,j}\theta_i) & \text{if } \Gamma^{\mathrm{o}}_{i+1,\mathrm{mod}(N_\Omega)} \subset \Gamma^{\mathrm{o}}_N \end{cases}. \tag{A.6}$$

If instead $\alpha_{i,j} \in \mathbb{N}$, $i = 1, \dots, N_\Omega$, $j \in \mathbb{N}$, we set:

$$S_{i,j}(r_i, \theta_i) = \begin{cases} r_i^{\alpha_{i,j}} (\log(r_i) \sin(\alpha_{i,j}\theta_i) + \theta_i \cos(\alpha_{i,j}\theta_i)) & \text{if } \Gamma^{\mathrm{o}}_{i+1,\mathrm{mod}(N_\Omega)} \subset \Gamma^{\mathrm{o}}_D \\ r_i^{\alpha_{i,j}} (\log(r_i) \cos(\alpha_{i,j}\theta_i) + \theta_i \sin(\alpha_{i,j}\theta_i)) & \text{if } \Gamma^{\mathrm{o}}_{i+1,\mathrm{mod}(N_\Omega)} \subset \Gamma^{\mathrm{o}}_N \end{cases}. \tag{A.7}$$

Importantly, it is possible to prove two important issues regarding the singular functions $S_{i,j}$. The first one is that, if $\mathbf{A}_i$ is either a D or a N vertex, then:

$$S_{i,j} \in H^{1+j\frac{\pi}{\omega_i}-\varepsilon}(\Omega) \qquad \forall \varepsilon > 0 \quad \text{small enough.} \tag{A.8}$$

In fact, $S_{i,j} \in H^{m,2}_\beta(\Omega)$ for all $m \geq 2$, $\beta = \max\left(0, \frac{\pi}{2\,\omega_{i,1}}\right)$ for all $i = 1, \dots, N_\Omega$, where we recall that the weighted Sobolev space $H^{m,2}_\beta(\Omega)$ is defined in (1.35).

The second issue of interest that we highlight is that:

$$\Delta S_{i,j} = 0 \qquad \text{pointwise in } \overline{\Omega}. \tag{A.9}$$

Singular functions (A.6) and (A.7) are in a natural way part of the solutions to (A.3). More precisely, the following result holds true.

Theorem A.0.1. *Assume that the data of problem* (A.3) *satisfy, for some* $s > 0$*:*

$$f \in H^{s-1}(\Omega), \quad g_D|_{s_i} \in H^{\frac{1}{2}+s}(s_i) \quad \forall s_i^o \subset \Gamma_D^o, \quad g_D \in H^{\frac{1}{2}}(\Gamma_D),$$
$$g_N|_{s_i} \in H^{-\frac{1}{2}+s}(s_i) \quad \forall s_i^o \subset \Gamma_N^o, \quad g_D \in L^2(\Gamma_D).$$

Then, the following decomposition of the solution to (A.3) *holds true:*

$$u = u_0 + \sum_{\alpha_{i,j} < s} c_{i,j} S_{i,j}(r_i, \theta_i), \tag{A.10}$$

where $c_{i,j} \in \mathbb{R}$ *and* $u_0 \in H^{1+s}(\Omega)$*.*

Proof. See [15, 16]. □

Theorem A.0.1 states that, even for a Poisson problem with homogeneous pure Dirichlet boundary conditions and analytic right-hand side f, the solution is not in general analytic but has a prescribed singular behaviours at the vertices of the domain, which uniquely depend on the magnitudes of the associated angles.

Employing the notation of Section 1.2 and in particular the definition of weighted Sobolev and Babuška spaces (1.35) and (1.36) respectively, we can state the following results which in fact hinge upon decomposition (A.10). The first one concerns Dirichlet problems with homogeneous boundary conditions.

Theorem A.0.2. *Let us consider problem* (1.27) *with* $f \in H^{0,0}_{\boldsymbol{\beta}}(\Omega)$*, where the weight vector* $\boldsymbol{\beta}$ *is such that* $1 - \alpha_{i,1} < \beta_i$ *for all* $i = 1, \ldots, N_\Omega$*. Then,* u*, the solution to* (1.27)*, belongs to* $H^{2,2}_{\boldsymbol{\beta}}(\Omega)$ *and satisfies the a priori bound:*

$$\|u\|_{H^{2,2}_{\boldsymbol{\beta}}(\Omega)} \leq c\|f\|_{H^{0,0}_{\boldsymbol{\beta}}(\Omega)},$$

where c *is a positive constant independent of* u*,* f *and* $\boldsymbol{\beta}$*.*

Proof. See [96, Theorem 4.4]. □

The second one, instead, regards the regularity of Dirichlet boundary conditions and of the right-hand side f.

Theorem A.0.3. *Let* f *be an analytic function over* $\overline{\Omega}$*,* Ω *polygonal domain; then* $f \in \mathcal{B}^0_{\boldsymbol{\beta}}(\Omega)$*. Moreover, let* g *be a continuous function over* $\partial\Omega$ *and assume* $g|_{s_i}$ *analytic for all edge* s_i *of* Ω*; then,* $g \in \mathcal{B}^{\frac{3}{2}}_{\boldsymbol{\beta}}(\partial\Omega)$*.*

Proof. See [96, Lemma 4.43]. □

Finally, we state a regularity result in terms of Babuška spaces for Poisson problem with (possibly) nonhomogeneous boundary conditions.

Theorem A.0.4. *Let us consider problem* (1.32) *with* $f \in \mathcal{B}^0_{\boldsymbol{\beta}}(\Omega)$ *and* $g \in \mathcal{B}^{\frac{3}{2}}_{\boldsymbol{\beta}}(\partial\Omega)$*, where the weight vector* $\boldsymbol{\beta}$ *is such that* $1 - \alpha_{i,1} < \beta_i$ *for all* $i = 1, \ldots, N_\Omega$*,* $\alpha_{i,1}$ *being defined in* (A.4)*. Then, there exists a unique solution to problem* (1.32) *which belongs to space* $\mathcal{B}^2_{\boldsymbol{\beta}}(\Omega)$*.*

Proof. See [96, Lemma 4.44]. □

Appendix B

hp inverse estimates on triangles and general polygons

In this appendix, we collect and prove some *hp* polynomial inverse estimates over triangles and polygons. Such inverse estimates are instrumental for proving stability bounds in Chapter 6, see e.g. Theorem 6.2.2, and when carrying the *hp* a-posteriori error analysis for VEM, but it is worth to mention that they are interesting on their own.

We split the chapter into three parts. Firstly, in Section B.1, we prove a *hp* polynomial inverse estimate on triangles; although such inverse estimate is very well-known, we are not able to find an explicit proof in literature. Secondly, in Section B.2, we prove more involved *hp* polynomial inverse estimates on triangles involving weighted Lebesgue and Sobolev (semi)norms; such inverse estimates are aimed at proving the main result of the chapter, namely Theorem B.2.6, which is a *hp* polynomial inverse estimate on polygons which is used in Chapter 6. Finally, in Section B.3, we recall (and discuss) additional *hp* polynomial inverse estimates on triangles and general polygons that are instrumental in the a-posteriori *hp* error analysis for VEM performed in Chapter 5.

B.1 A simple *hp* polynomial inverse estimate

In this section, we discuss the following classical *hp* polynomial inverse estimate on triangles:

Theorem B.1.1. *Let $T \subset \mathbb{R}^2$ be a triangle and let h_T denote the diameter of T. Then:*

$$|q_p|_{1,T} \leq c_{inv} \frac{(p+1)^2}{h_T} \|q_p\|_{0,T} \quad \forall\, q_p \in \mathbb{P}_p(T), \quad p \in \mathbb{N}, \tag{B.1}$$

where c_{inv} is a positive constant independent of h_T, p and q_p.

We note that inequality (B.1) is a very well-known and widely used result. It is stated for instance in [96, Theorem 4.76]. Nonetheless, we were not able to find an explicit proof in literature.

Proof of Theorem B.1.1. We show the result on the reference triangle $\widehat{T}$ of vertices $(0,0)$, $(1,0)$, $(0,1)$. The statement will follow from a scaling argument.

We consider a decomposition of $\widehat{T}$ into the three overlapping parallelograms P_1, P_2 and P_3 depicted in Figure B.3. We can write:

$$|q_p|_{1,\widehat{T}} \leq |q_p|_{1,P_1} + |q_p|_{1,P_2} + |q_p|_{1,P_3}. \tag{B.2}$$

We only have to prove that:

$$|q_p|_{1,P_i} \leq c_1 p^2 \|q_p\|_{0,P_i}, \quad i = 1,2,3. \tag{B.3}$$

In particular, it suffices to prove the same inequality on the reference square $\widehat{Q} = [-1,1]^2$ and then using an affine transformation in order to deduce the assertion of the theorem from (B.2). Thus, we must prove:

$$|q_p|_{1,\widehat{Q}} \leq c p^2 \|q_p\|_{0,\widehat{Q}}, \quad \forall\, q_p \in \mathbb{P}_p(\widehat{Q}). \tag{B.4}$$

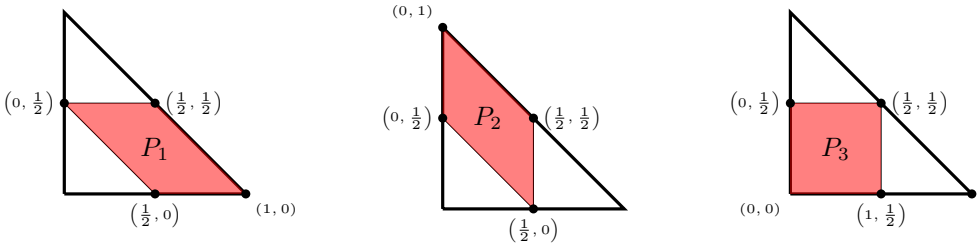

Figure B.1: Overlapping parallelograms covering the reference triangle $\widehat{T}$.

For the purpose, we have to show:

$$\|\partial_i q_p\|_{0,\widehat{Q}} \leq cp^2 \|q_p\|_{0,\widehat{Q}} \qquad \forall\, i = 1, 2.$$

Owing to [96, Theorem 3.96], that is a *hp* polynomial inverse inequality in 1D, we can write:

$$\|\partial_i q_p\|_{0,\widetilde{I}} \leq cp^2 \|q_p\|_{0,\widetilde{I}}, \tag{B.5}$$

where

$$\widetilde{I} = \begin{cases} [-1,1] \times \{\widetilde{y}\},\ \widetilde{y} \in [-1,1] & \text{if } i = 1, \\ \{\widetilde{x}\} \times [-1,1],\ \widetilde{x} \in [-1,1] & \text{if } i = 2. \end{cases}$$

Here, the constant c does not depend on $\widetilde{y}$. Integrating (B.5) in y (if $i = 1$) or in x (if $i = 2$) from -1 to 1, we get (B.4), whence the claim. □

B.2 A *hp* polynomial inverse estimate on polygons involving negative norms

In this section, we prove a *hp* polynomial inverse estimate on (sufficiently regular) polygons involving a negative norm, see Theorem B.2.6. For the purpose, we need some technical results.

We will use the properties of some particular Jacobi polynomials $\{J_n^{\alpha,\beta}(x)\}_{n=0}^{\infty}$, $\alpha, \beta \geq 0$, namely Legendre and shifted-ultraspherical polynomials. Henceforth, we denote by $\widehat{I}$ the reference interval $[-1, 1]$.

We begin with the following result which was firstly presented in [42]. We stress that Lemma B.2.1 holds for more general weights (i.e $-1 < \alpha \leq \beta$), nonetheless we discuss here only the case $0 \leq \alpha \leq \beta$ which is sufficient for our purpose.

Lemma B.2.1. *Given $0 \leq \alpha \leq \beta$, it holds:*

$$\int_{\widehat{I}} (1-x^2)^{\alpha} q_p(x)^2 dx \leq c(p+1)^{2(\beta-\alpha)} \int_{\widehat{I}} (1-x^2)^{\beta} q_p(x)^2 dx \qquad \forall\, q_p \in \mathbb{P}_p(\widehat{I}), \quad p \in \mathbb{N}, \tag{B.6}$$

where c is a positive contant depending on α and β, but not on p and q_p.

Proof. We split the proof into three parts. The first two are results dealing with ultraspherical polynomials properties, while in the last one we show the assertion.

For the properties of ultraspherical polynomials we refer to [1, 44, 68, 96, 97, 100]. We recall various facts that we will use throughout the proof about these polynomials.

* The n-th ultraspherical polynomial J_α^n, $\alpha \geq 0$, is the n-th Jacobi polynomial $J_n^{\alpha,\beta}$ with $\alpha = \beta \geq 0$; the sequence $\{J_\alpha^n\}_{n=0}^{+\infty}$ forms an orthogonal (but not normal) basis for the weighted Lebesgue space:

$$L_{\rho_\alpha}(\widehat{I}) := \left\{ u \text{ Lebesgue-measurable on } \widehat{I} \;\middle|\; \int_{\widehat{I}} \rho_\alpha(x) |u(x)|^2 dx < +\infty \right\},$$

where ρ_α is the weighted 1D bubble function $\rho_\alpha(x) = (1-x^2)^\alpha$.

* Each J_α^n is the n-th eigenfunction of the Sturm-Liouville problem:

$$(\rho_{\alpha+1}(x)J_\alpha^n(x)')' + n(n+2\alpha+1)\rho_\alpha(x)J_\alpha^n(x) = 0 \qquad \forall\, x \in \widehat{I}, \tag{B.7}$$

with appropriate Dirichlet conditions at the endpoints of $\widehat{I}$:

$$J_\alpha^n(\pm 1) = (-1)^n \binom{n+\alpha}{n}.$$

* The following orthogonality relation holds for $n \geq 1$, see e.g. [100, formula (4.3.3)]:

$$\int_{-1}^{1} J_\alpha^n(x)J_\alpha^n(x)\rho_\alpha(x)dx = \delta_{n,m}\frac{2^{2\alpha+1}\Gamma(n+\alpha+1)^2}{(2n+2\alpha+1)n!\Gamma(n+2\alpha+1)}, \tag{B.8}$$

where $\delta_{n,m}$ is the Kronecker delta and Γ is the Gamma function.

* The following asymptotic behaviour of the Gamma function holds:

$$\Gamma(t) = \sqrt{2\pi}e^{-t}t^{t-\frac{1}{2}}\left(1 + O(1/t)\right), \quad \text{for } t \to +\infty. \tag{B.9}$$

* The following relation between ultraspherical polynomials and their derivatives holds, see e.g. [44, Theorem 19.3]:

$$(2n+2\alpha+1)J_\alpha^n(x) = \frac{n+2\alpha+1}{n+\alpha+1}J_\alpha^{n+1}(x)' - \frac{n+\alpha}{n+2\alpha}J_\alpha^{n-1}(x)'. \tag{B.10}$$

We start now the proof of the theorem. As a last comment, the details of steps 1 and 2 are carried out here (although the estimates we prove therein are known), while step 3 is a detailed version of [42, Theorem 19.3].

Since the statement is straightforward for $\alpha = \beta$, we assume henceforth $\alpha < \beta$.
1st STEP We want to show here:

$$c_1 n \leq \int_{\widehat{I}} (J_\alpha^n(x)')^2\rho_{\alpha+1}(x)dx \leq c_2 n, \tag{B.11}$$

where c_1 and c_2 are two positive constants independent of n, but depending on α.

For the purpose, we observe that (B.7) and an integration by parts imply:

$$\int_{\widehat{I}} (J_\alpha^n(x)')^2\rho_{\alpha+1}(x)dx = n(n+2\alpha+1)\int_{\widehat{I}} (J_\alpha^n(x))^2\rho_\alpha(x)dx. \tag{B.12}$$

We stress that one could also show (B.12) by combining (B.8) with [100, formula (4.21.7)].

Next, we estimate $\int_{\widehat{I}} (J_\alpha^n(x))^2\rho_\alpha(x)dx$. We set for the purpose:

$$2^{-2\alpha-1}(2n+2\alpha+1)\int_{\widehat{I}} J_\alpha^n(x)^2\rho_\alpha(x)dx =: g(n,\alpha) = \frac{\Gamma(n+\alpha+1)^2}{\Gamma(n+1)\Gamma(n+2\alpha+1)}.$$

Function $g(n,\alpha)$ is increasing in n for every fixed $\alpha > -1$. Besides, $\lim_{n\to+\infty} g(n,\alpha) = 1$. Thus:

$$g(1,\alpha) \leq 2^{-2\alpha-1}(2n+2\alpha+1)\int_{\widehat{I}} J_\alpha^n(x)^2\rho_\alpha(x)dx \leq 1,$$

which implies:

$$\frac{\widetilde{c}_1}{n} \leq \int_{\widehat{I}} J_\alpha^n(x)^2\rho_\alpha(x)dx \leq \frac{\widetilde{c}_2}{n} \qquad \forall\, n \geq 1, \tag{B.13}$$

where $\widetilde{c}_1$ and $\widetilde{c}_2$ are two positive constants independent of n, but dependent on α. Using that $\alpha \geq$, an explicit representation for the two constants $\widetilde{c}_1$ and $\widetilde{c}_2$ is given by:

$$\widetilde{c}_1 = \frac{2^{2\alpha+1}}{2\alpha+3}\frac{\Gamma(2+\alpha)^2}{\Gamma(2)\Gamma(2+2\alpha)}, \qquad \widetilde{c}_2 = 2^{2\alpha}. \tag{B.14}$$

The claim, i.e. (B.11), follows by combining (B.12) and (B.13). An explicit choice for the two constants c_1 and c_2 in (B.12) is given by:

$$c_1 = \widetilde{c}_1 = \frac{2^{2\alpha+1}}{2\alpha+3}\frac{\Gamma(2+\alpha)^2}{\Gamma(2)\Gamma(2+2\alpha)}, \qquad c_2 = (2\alpha+2)2^{2\alpha}. \tag{B.15}$$

2nd STEP We show secondly the following bound:

$$\int_{\widehat{I}} (J_\alpha^n(x)')^2 \rho_\alpha(x)dx \leq bn^2, \tag{B.16}$$

for some positive constant b independent of n but depending on α. We will prove this fact by induction. The cases $n = 1$, 2 are obvious since we have positive left and right-hand sides. Assume then that (B.16) holds up to n and we show the inequality for $n+1$.

We observe that the following inequalities involving the coefficients in (B.10) are valid (we recall that $\alpha, \beta \geq 0$):

$$2n \leq 2n + 2\alpha + 1 \leq (2\alpha+3)n, \qquad 1 \leq \frac{n+2\alpha+1}{n+\alpha+1} \leq 2, \qquad \frac{1}{2} \leq \frac{n+\alpha}{n+2\alpha} \leq 1. \tag{B.17}$$

Then, using (B.8), (B.10) and (B.17), we get:

$$\begin{aligned}
&\int_{\widehat{I}} (J_{n+1}^\alpha(x)')^2 \rho_\alpha(x)dx \leq \int_{\widehat{I}} \left(\left(\frac{n+2\alpha+1}{n+\alpha+1} \right) J_{n+1}^\alpha(x)' \right)^2 \rho_\alpha(x)dx \\
&= \int_{\widehat{I}} \left((2n+2\alpha+1) J_\alpha^n(x) \right)^2 \rho_\alpha(x)dx + \int_{\widehat{I}} \left(\frac{n+\alpha}{n+2\alpha} J_{n-1}^\alpha(x)' \right)^2 \rho_\alpha(x)dx \\
&\leq \underbrace{(2\alpha+3)^2}_{=:c_\alpha} n^2 \int_{\widehat{I}} J_\alpha^n(x)^2 \rho_\alpha(x)dx + \int_{\widehat{I}} \left(J_{n-1}^\alpha(x)' \right)^2 \rho_\alpha dx.
\end{aligned} \tag{B.18}$$

We apply (B.13) and the induction hypothesis to the first and second term on the right-hand side of (B.18) respectively, obtaining:

$$\int_{\widehat{I}} (J_{n+1}^\alpha(x)')^2 \rho_\alpha(x)dx \leq c_\alpha \widetilde{c}_2 n + b(n-1)^2 =: \widetilde{c}n + b(n-1)^2,$$

where $\widetilde{c}_2$ is defined in (B.14). Taking b large enough, for instance $b \geq \frac{\widetilde{c}}{4}$, the following holds:

$$\widetilde{c}n + b(n-1)^2 \leq b(n+1)^2. \tag{B.19}$$

We point out that we have to take power 2 on the right-hand side of (B.16) because with smaller powers (B.19) would not be true.

3rd STEP We show (B.6). Given $q_p \in \mathbb{P}_p(\widehat{I})$, we expand it into a sum of derivatives of Jacobi polynomials:

$$q(x) = \sum_{n=1}^{p+1} a_n J_\alpha^n(x)'.$$

Then, noting from (B.7) and an integration by parts implies that the ultraspherical polynomials $J_n^{\alpha+1}$ are L^2 orthogonal with respect to the weight $\rho_{\alpha+1}$, we have:

$$\int_{\widehat{I}} q_p(x)^2 \rho_{\alpha+1}(x)dx = \sum_{n=1}^{p+1} a_n^2 \int_{\widehat{I}} (J_\alpha^n(x)')^2 \rho_{\alpha+1}(x)dx \geq c_1 \sum_{n=1}^{p+1} a_n^2 n, \tag{B.20}$$

where c_1 is defined in (B.15). On the other hand, (B.16) implies:

$$\int_{\widehat{I}} q_p(x)^2 \rho_\alpha(x)dx \leq 2 \left(\sum_{n=1}^{p+1} |a_n| \left(\int_{\widehat{I}} (J_\alpha^n(x)')^2 \rho_\alpha(x) \right)^{\frac{1}{2}} \right)^2 \leq b \left(\sum_{n=1}^{p+1} |a_n| n \right)^2, \tag{B.21}$$

where b is introduced in (B.16).

Combining (B.20) with (B.21) and using a Cauchy-Schwarz inequality for sequences, lead to:

$$\int_{\widehat{I}} q_p(x)^2 \rho_\alpha(x) dx \leq b \left(\sum_{n=1}^{p+1} a_n^2 n \right) \left(\sum_{n=1}^{p+1} n \right) \leq b c_1^{-1} (p+1)^2 \int_{\widehat{I}} q(x)^2 \rho_{\alpha+1}(x) dx. \tag{B.22}$$

This is in fact the assertion when $\beta - \alpha = 1$. The case $\beta - \alpha \in \mathbb{N}$ is straightforward; it suffices in fact to iterate enough time the above computations.

Assume now $\alpha \in (\beta - 1, \beta)$. Then:

$$\alpha = \frac{\beta - 1}{r} + \frac{\beta}{s}, \quad \text{with } \frac{1}{r} + \frac{1}{s} = 1 \quad \text{and } \frac{1}{r} = \beta - \alpha < 1.$$

In order to conclude, using an Holder inequality and (B.22):

$$\begin{aligned}
\int_{\widehat{I}} q_p(x)^2 \rho_\alpha(x) dx &= \int_{\widehat{I}} q_p(x)^{\frac{2}{r}} \rho_{\frac{\beta-1}{r}}(x) q_p(x)^{\frac{2}{s}} \rho_{\frac{\beta}{s}}(x) dx \\
&\leq \left(\int_{\widehat{I}} q_p(x)^2 \rho_{\beta-1}(x) dx \right)^{\frac{1}{r}} \left(\int_{\widehat{I}} q_p(x)^2 \rho_\beta(x) dx \right)^{\frac{1}{s}} \\
&\leq (b c_1^{-1})^{\frac{1}{r}} (p+1)^{\frac{2}{r}} \left(\int_{\widehat{I}} q_p(x)^2 \rho_\beta(x) dx \right)^{\frac{1}{r} + \frac{1}{s}} \\
&= (b c_1^{-1})^{\frac{1}{r}} (p+1)^{2(\beta-\alpha)} \int_{\widehat{I}} q_p(x)^2 \rho_\beta(x) dx.
\end{aligned}$$

We point out that in order to prove the case $\alpha \in (\beta - 1, \beta)$ one could also use interpolation theory, see [101, 102]. Nonetheless, we believe that a direct computation is easily readable. □

Corollary B.2.2. *Given $0 \leq \alpha \leq \beta$, it holds:*

$$\begin{aligned}
\int_{\widehat{I}} (1-x)^\alpha q_p(x)^2 dx &\leq c(p+1)^{\beta-\alpha} \int_{\widehat{I}} (1-x)^\beta q_p(x)^2 dx \\
\int_{\widehat{I}} (1+x)^\alpha q_p(x)^2 dx &\leq c(p+1)^{\beta-\alpha} \int_{\widehat{I}} (1+x)^\beta q_p(x)^2 dx
\end{aligned}$$

where c is a positive constant depending on α and β but not on h and p.

Proof. We only give a sketch of the proof. Let us denote by $b_{\widetilde{I}}$ the quadratic bubble function over an interval $\widetilde{I}$ extended to 0 on $\mathbb{R} \setminus \overline{\widetilde{I}}$. Then, it is possible to show for all $\gamma \geq 0$ that:

$$(1-x)^\gamma \approx b^0_{[-1,\frac{1}{2}]}(x) + b^{\frac{\gamma}{2}}_{[-\frac{1}{2},1]}(x), \tag{B.23}$$

$$(1+x)^\gamma \approx b^{\frac{\gamma}{2}}_{[-1,\frac{1}{2}]}(x) + b^0_{[-\frac{1}{2},1]}(x), \tag{B.24}$$

where we denoted with an abuse of notation $b^0_{\widetilde{I}}(x) = 0$ for all $x \in \mathbb{R} \setminus \widetilde{I}$.

In order to obtain the assertion one combines (B.23), (B.24), Lemma B.2.1 and simple algebra. □

The following lemma is a quasi-one dimensional result on trapezoids. The idea is pretty similar to that in [82, Lemma D.3], although our result employs a different class of weight functions. We also point out that Lemma B.2.3 can be generalized to the case $-1 < \alpha < \beta$, see [82].

Lemma B.2.3. *Given $d \in (0,1)$ and $a,\ b \in \mathbb{R}$ such that $-1 + a\,d < 1 + b\,d$. We set the (a,b,d)-trapezoid as:*

$$D(a,b,d) = D = \{(x,y) \in \mathbb{R}^2 \mid y \in [0,d],\ -1 + a\,y \leq x \leq 1 + b\,y\}.$$

We associate to each y^* the segment:

$$I(y^*) = I^* = [-1 + a\,y^*, 1 + b\,y^*]. \tag{B.25}$$

For every $\Phi \in \mathcal{C}^0(\overline{D})$ *such that:*

$$\Phi(\cdot, y^*) \in \mathbb{P}_3(I^*) \text{ is concave; } \Phi(x, y^*) \geq 0, \ \forall x \in I^*; \ \Phi = 0 \text{ only at the endpoints of } I^* \ \forall y^* \in [0, d], \tag{B.26}$$

the following quasi-one dimensional p polynomial inverse estimate holds:

$$\|\Phi^{\frac{\alpha}{2}} q_p\|_{0,D} \leq c\,(p+1)^{\beta-\alpha} \|\Phi^{\frac{\beta}{2}} q_p\|_{0,D} \qquad \forall\, q_p \in \mathbb{P}_p(D), \quad p \in \mathbb{N},$$

where c is a positive constant depending only on α *and* β*, but not on p, and where* $\beta > \alpha \geq 0$*.*

Proof. Let $\psi(x) = (1 - x^2)$ be the 1D bubble function associated to the reference interval $\widehat{I} := [-1, 1]$. Given $y^* \in [0, d]$, we set F the affine function mapping $\widehat{I}$ in I^* and $\psi^*(x) = \psi(F^{-1}(x)) : I^* \to \mathbb{R}$.

Then, there exist two positive constants c_1 and c_2 depending only on a, b and y^* such that:

$$c_1 \psi^*(x) \leq \Phi(x, y^*) \leq c_2 \psi^*(x) \qquad \forall\, x \in I^*. \tag{B.27}$$

This follows from the fact that both $\psi^*(\cdot)$ and $\Phi(\cdot, y^*)$ are two positive quadratic/cubic concave polynomials annihilating only at the endpoints of the segment for all $y^* \in [0, d]$, see (B.26).

Since Φ is by hypotesis a continuous function in y^*, then c_1 and c_2 depend continuously on y^*. Having that y^* lives in the compact set $[0, d]$, then c_1 and c_2 attain maximum and minimum respectively. Further, such extremal points are strictly positive due to the positiveness of c_1 and c_2 seen as functions of y^*, see (B.26). Therefore, we can write:

$$\overline{c}_1 \psi^*(x) \leq \Phi(x, y^*) \leq \overline{c}_2 \psi^*(x) \qquad \forall\, x \in I^*, \tag{B.28}$$

where $0 < \overline{c}_1 = \min_{y^* \in [0,d]}(c_1(y^*))$ and $\overline{c}_1 \leq \overline{c}_2 = \max_{y^* \in [0,d]}(c_2(y^*))$ are now independent of y^*.

We investigate a 1D inverse inequality. In particular, from Lemma B.2.1 and from (B.28), we have:

$$\int_{I^*} \Phi(x, y^*)^\alpha q_p(x, y^*)^2 dx \leq \overline{c}_2^\alpha \int_{I^*} \psi^*(x)^\alpha q_p(x, y^*)^2 dx \leq \frac{\overline{c}_2^\alpha}{\overline{c}_1^\beta} c (p+1)^{2(\beta-\alpha)} \int_{I^*} \Phi(x, y^*)^\beta q_p(x, y^*)^2 dx, \tag{B.29}$$

where c is independent of y^*.

The statement of the lemma is achieved by means of an integration of (B.28) over $y^* \in [0, d]$. □

We show now a global inverse estimate on triangles. Again, the following result can be generalized to the case of weights $-1 < \alpha \leq \beta$, see [82].

Theorem B.2.4. *Given* $\widehat{T}$ *the reference triangle of vertices* $(0,0)$*,* $(1,0)$ *and* $(0,1)$*, let* $b_{\widehat{T}}$ *be the cubic bubble function associated with* $\widehat{T}$*; in particular,* $b_{\widehat{T}} \in \mathbb{P}_3(\widehat{T})$ *is such that* $b_{\widehat{T}}|_{\partial \widehat{T}} = 0$*. Then, for all* $0 \leq \alpha \leq \beta$*:*

$$\|b_{\widehat{T}}^{\frac{\alpha}{2}} q_p\|_{0,\widehat{T}} \leq c\,(p+1)^{\beta-\alpha} \|b_{\widehat{T}}^{\frac{\beta}{2}} q_p\|_{0,\widehat{T}} \qquad \forall\, q_p \in \mathbb{P}_p(\widehat{T}), \quad p \in \mathbb{N}, \tag{B.30}$$

where c is a positive constant independent of p.

Proof. The proof is similar to that in [82, Theorem D2] and for this reason we only sketch it.

The idea consists in partitioning $\widehat{T}$ into an (overlapping) decomposition, prove the inverse inequality over each elements in the decomposition and then collect all the three terms together. In particular, we consider the following decomposition:

$$\widehat{T} = \left(\cup_{i=1}^6 D_i\right) \cup \left(\cup_{i=1}^3 P_i\right) \cup R, \tag{B.31}$$

where the $D_i, i = 1, \ldots, 6$, are the trapezoids depicted in Figure B.2, the P_i, $i = 1, 2, 3$, are the parallelograms depicted in Figure B.3, whereas $R = \widehat{T} \setminus \left((\cup_{i=1}^6 D_i) \cup (\cup_{i=1}^3 P_i)\right)$, depicted in Figure B.4, denotes a non-connected set having the property of being separated from $\partial \widehat{T}$.

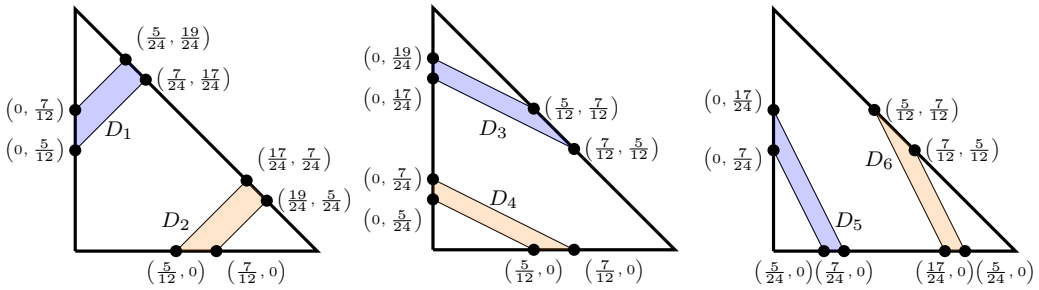

Figure B.2: Trapezoids D_i, $i = 1, \ldots, 6$.

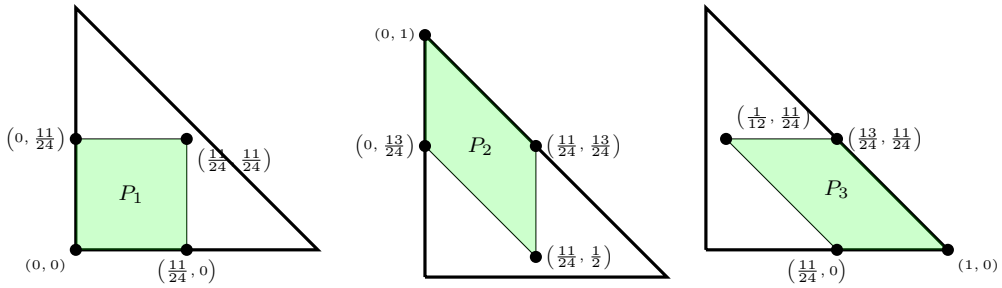

Figure B.3: Parallelograms P_i, $i = 1, 2, 3$.

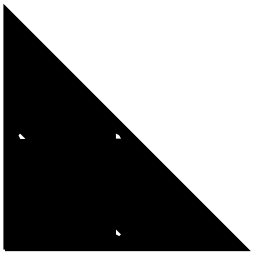

Figure B.4: The three white "small holes" inside triangle $\widehat{T}$ denote the remainder R.

At this point, one applies the inverse estimate of Lemma B.2.3 on the trapezoids, the inverse estimate (with a tensor product argument) of Corollary B.2.2 on the parallelograms, the fact that $b_{\widehat{T}}|_R \approx 1$ on the remainder R and simple algebra to get the assertion. □

Remark 17. In the proof of Theorem B.2.4 we considered the non-trivial decomposition (B.30) in lieu of a simpler one. The reason of this choice is that if, for instance, one consider instead the simpler covering depicted in Figure B.5, then the restriction of the cubic bubble function on the reference triangle is not concave along the directions of the bases of the trapezoids on the complete trapezoids and therefore Lemma B.2.3 can not be applied. On the other hand, such a concavity is valid on the trapezoids represented in Figure B.2.

We discuss also the following result, firstly presented in [22, Lemma 2].

Lemma B.2.5. *Given T a shape regular triangle, let b_T the associated cubic bubble function. Then:*

$$|q_p b_T|_{1,T} \leq c\frac{p+1}{h_T}\|q_p b_T^{\frac{1}{2}}\|_{0,T} \qquad \forall\, q_p \in \mathbb{P}_p(T), \quad p \in \mathbb{N},$$

where c is a positive constant independent of h_T and p, h_T being diam(T).

Proof. The proof is split into three parts; the first two of them are technical results dealing with Legendre-type approximations, while the third one deals with the proof of the lemma.
1st STEP The following estimate holds:

$$\|(1-x^2)q_p'(x)\|_{0,\widehat{I}} \leq c(p+1)\|(1-x^2)^{\frac{1}{2}}q_p(x)\|_{0,\widehat{I}} \qquad \forall\, q_p \in \mathbb{P}_p(\widehat{I}), \quad p \in \mathbb{N}, \tag{B.32}$$

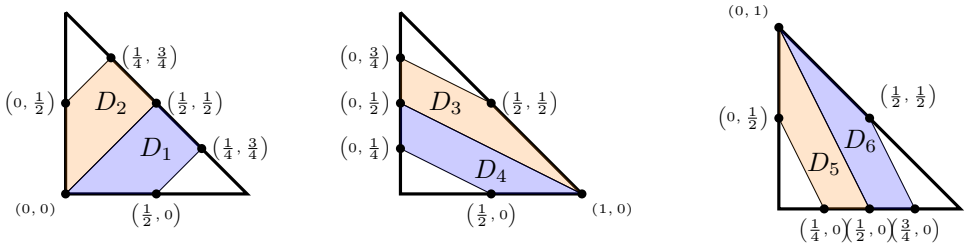

Figure B.5: Alternative covering the reference triangle $\widehat{T}$.

where c is a constant independent of p.

We recall that the following holds, see e.g. [96, formula (3.39)]:

$$\int_{\widehat{I}}(1-x^2)^k L_n^{(k)}(x)^2 dx = \begin{cases} \frac{2}{2n+1}\frac{(n+k)!}{(n-k)!} & \text{if } n \geq k, \\ 0 & \text{otherwise,} \end{cases}$$

where $L_n^{(k)}(x)$ denotes the k-th derivative of the n-th Legendre polynomial.

Then:

$$\int_{\widehat{I}}(1-x^2)^2 L_n''(x)^2 dx = \frac{2}{2n+1}\frac{(n+1)!}{(n-1)!}(n-1)(n+2) \leq \left(n+\frac{1}{2}\right)^2 \int_{\widehat{I}}(1-x^2)L_n'(x)^2 dx. \quad \text{(B.33)}$$

Therefore, expanding q_p into a sum of derivatives of Legendre polynomials:

$$q_p(x) = \sum_{n=1}^{p+1} c_n L_n'(x),$$

we have, owing to orthogonality of the second derivative of Legendre polynomials with respect to the L^2-$(1-x^2)^2$ weighted inner product and owing to (B.33):

$$\begin{aligned} \int_{\widehat{I}} q_p'(x)(1-x^2)^2 dx &= \sum_{n=1}^{p+1} c_n^2 \int_{\widehat{I}} L_n''(x)^2(1-x^2)^2 dx \leq \sum_{n=1}^{p+1} c_n^2 \left(n+\frac{1}{2}\right)^2 \int_{\widehat{I}} L_n'(x)^2(1-x^2)dx \\ &\leq \left(p+\frac{3}{2}\right)^2 \int_{\widehat{I}} q_p^2(x)(1-x^2)dx \leq \frac{3}{2}(p+1)^2 \int_{\widehat{I}} q_p^2(x)(1-x^2)dx. \end{aligned}$$

2nd STEP We show now the following 1D estimate. For $a < b$, let

$$b_{[a,b]}(x) := \frac{(x-a)(b-x)}{(b-a)^2}$$

be the 1D quadratic bubble function, then:

$$\left\|(b_{[a,b]}q_p)'\right\|_{0,[a,b]} \leq c\frac{p+1}{b-a}\left\|b_{[a,b]}^{\frac{1}{2}}q_p\right\|_{0,[a,b]}, \qquad \forall\, q_p \in \mathbb{P}_p([a,b]), \quad \text{(B.34)}$$

where c is a positive constant independent of p. It is sufficient to show (B.34) on the reference interval $\widehat{I}$, since the general result follows from a scaling argument.

Owing to $\|b_{\widehat{I}}'\|_{\infty,\widehat{I}} = \frac{1}{2} < 1$, the Leibniz derivation rule and a triangular inequality, we can write:

$$\|(b_{\widehat{I}}q_p)'\|_{0,\widehat{I}} \leq \|b_{\widehat{I}}'q_p\|_{0,\widehat{I}} + \|b_{\widehat{I}}q_p'\|_{0,\widehat{I}} \leq \|q_p\|_{0,\widehat{I}} + \|b_{\widehat{I}}q_p'\|_{0,\widehat{I}}. \quad \text{(B.35)}$$

Applying (B.6) (with $\alpha = 0$ and $\beta = 1$) and (B.32) to the first and second term of (B.35) respectively, we get (B.34).

3rd STEP We apply now (B.34) and we show the claim of the lemma. Without loss of generality, we work on the reference triangle $\widehat{T} = T$ of vertices $(0,0)$, $(1,0)$ and $(0,1)$. The statement follows from a scaling argument.

The cubic bubble function on $\widehat{T}$, which is given by the product of the barycentric coordinates, can be rewritten as:

$$b_{\widehat{T}} = b_{[0,1-x]}(y)(1-x)b_{[0,1]}(x).$$

We only show the bound on the partial derivative with respect to y. The general case is an easy consequence.

$$\begin{aligned}\|\partial_y(b_{\widehat{T}}q_p)\|^2_{0,\widehat{T}} &= \int_0^1 \int_0^{1-x} (\partial_y(b_{\widehat{T}}(x,y)q_p(x,y)))^2 dydx \\ &= \int_0^1 b^2_{[0,1]}(x)(1-x)^2 \int_0^{1-x} \left(\partial_y(b_{[0,1-x]}(y)q_p(x,y))\right)^2 dydx.\end{aligned}$$

We note that:

$$\begin{aligned}(1-x)^2 \int_0^{1-x} \left(\partial_y b_{[0,1-x]}(y)q_p(x,y)\right)^2 dy &= (1-x)^2 \|\partial_y(b_{[0,1-x]}(\cdot)q_p(x,\cdot))\|^2_{0,[0,1-x]} \\ &\underbrace{\leq}_{\text{(B.34)}} c(p+1)^2 \|b^{\frac{1}{2}}_{[0,1-x]}(\cdot)q_p(x,\cdot)\|^2_{0,[0,1-x]}.\end{aligned}$$

Since $b_{[0,1]} \leq 1-x$, we get $b^2_{[0,1]}(x)b_{[0,1-x]}(y) \leq b_{\widehat{T}}(x,y)$ and consequently:

$$\|\partial_2(b_{\widehat{T}}q_p)\|^2_{0,\widehat{T}} \leq (p+1)^2 \int_0^1 \int_0^{1-x} b^2_{[0,1]}(x)b_{[0,1-x]}(y)q_p^2(x,y)dydx \leq (p+1)^2 \|b^{\frac{1}{2}}_{\widehat{T}}q_p\|^2_{0,\widehat{T}}.$$

□

We are now ready for the inverse estimate involving the H^{-1} norm of polynomials (1.15).

Theorem B.2.6. *Let $K \subset \mathbb{R}^2$ be a polygon. Assume that there exists $\widetilde{\mathcal{T}}(K)$ subtriangulation of K such that $h_K \approx h_T$, where we have set as usual $h_\omega = diam(\omega)$ for all $\omega \subset \mathbb{R}^2$. Then:*

$$\|q_p\|_{0,K} \leq c\frac{(p+1)^2}{h_K}\|q_p\|_{-1,K} \qquad \forall\, q_p \in \mathbb{P}_p(K), \quad p \in \mathbb{N}, \tag{B.36}$$

where c is a positive constant independent of q_p, h_K and p, but depending on the shape-regularity of subtriangulation $\widetilde{\mathcal{T}}_n(K)$.

Proof. Let b_K be the "patch-bubble" function, defined on each $T \in \widetilde{\mathcal{T}}(K)$ as the local cubic bubble function b_T introduced in Lemma B.2.5. In particular, we write:

$$b_K|_T = b_T, \quad \text{where } b_T \text{ is the cubic bubble function on triangle } T \quad \forall\, T \in \widetilde{\mathcal{T}}(K). \tag{B.37}$$

Then:

$$\|q_p\|_{-1,K} = \sup_{\Phi \in H^1_0(K),\, \Phi \neq 0} \frac{(q_p,\Phi)_{0,K}}{|\Phi|_{1,K}} \geq \frac{(q_p, q_p b_K)_{0,K}}{|q_p b_K|_{1,K}} = \frac{\|q_p\sqrt{b}_K\|^2_{0,K}}{\left(\sum_{T\in\widetilde{\mathcal{T}}(K)} |q_p b_T|^2_{1,T}\right)^{\frac{1}{2}}}. \tag{B.38}$$

Using now Lemma B.2.5 and (B.38) , we obtain:

$$\|q_p\|_{-1,K} \geq c\frac{\min_{T\in\widetilde{\mathcal{T}}(K)} h_T}{p+1}\|q_p\sqrt{b_K}\|_{0,K} \geq c\frac{h_K}{p+1}\left(\sum_{T\in\widetilde{\mathcal{T}}(K)} \|q_p\sqrt{b_T}\|^2_{0,T}\right)^{\frac{1}{2}}, \tag{B.39}$$

where the constant c depends on the shape-regularity of subtriangulation $\widetilde{\mathcal{T}}_n(K)$.

Finally, we apply Theorem B.2.4 with $\alpha = 0$ and $\beta = 1$ and get:

$$\|q_p\|_{-1,K} \geq c\frac{h_K}{(p+1)^2}\left(\sum_{T\in\widetilde{\mathcal{T}}(K)} \|q_p\|^2_{0,T}\right)^{\frac{1}{2}} = c\frac{h_K}{(p+1)^2}\|q_p\|_{0,K}.$$

□

B.3 Additional *hp* polynomial inverse estimates on triangles and polygons

In this section, we recall an discuss other *hp* polynomial inverse estimates over triangles and polygons that are instrumental in the a-posteriori *hp* error analysis of Chapter 5.

We start by presenting a set of polynomial inverse estimates on triangles.

Theorem B.3.1. *Given T a triangle, let b_T be the associated cubic bubble function associated , i.e. the product of the barycentric coordinates of T. Then, for all $-1 < \alpha \leq \beta$ and $\delta \in [0,1]$, there exist positive constants c_i, $i = 1,2,3,4$, depending only on the shape of T, α, β and δ such that, for all $q_p \in \mathbb{P}_p(T)$, $p \in \mathbb{N}$:*

$$\int_T b_T |\nabla q_p|^2 \leq c_1 \frac{(p+1)^2}{h_T^2} \int_T |q_p|^2, \tag{B.40}$$

$$\int_T b_T^{\alpha} |q_p|^2 \leq c_2 (p+1)^{2(\beta-\alpha)} \int_T b_T^{\beta} |q_p|^2, \tag{B.41}$$

$$\int_T b_T^{2\delta} |\nabla q_p|^2 \leq c_3 \frac{(p+1)^{2(2-\delta)}}{h_T^2} \int_T b_T^{\delta} |q_p|^2. \tag{B.42}$$

If in addition $q_p = 0$ on ∂T, then:

$$\int_T |\nabla q_p|^2 \leq c \frac{(p+1)^2}{h_T^2} \int_T b_T^{-1} |q_p|^2. \tag{B.43}$$

Proof. For a complete proof, we refer to [84, Theorem 2.5] and the references therein. We only note that inequality (B.41) is proven also in Theorem B.2.4. □

The same sort of inverse estimates are valid on a polygon if we substitute the bubble function on a triangle with a function which is a piecewise bubble function on each triangle of the subtriangulation of a polygon $K \in \mathcal{T}_n$. Therefore, given $K \in \mathcal{T}_n$, we define b_K as in (B.37). The following set of polynomial inverse estimates over a polygon holds true.

Theorem B.3.2. *Given K a polygon, we assume that there exists $\widetilde{\mathcal{T}}(K)$ subtriangulation of K such that $h_K \approx h_T$, where we have set as usual $h_\omega = diam(\omega)$ for all $\omega \subset \mathbb{R}^2$. Let b_K be the piecewise bubble function associated with regular subtriangulation $\widetilde{\mathcal{T}}(K)$ of K defined in* (B.37). *Then, for all $-1 < \alpha \leq \beta$ and $\delta \in [0,1]$, there exists positive constants c_i, $i = 1,2,3$ depending only on the shape-regularity of subtriangulation $\widetilde{\mathcal{T}}_n(K)$ α, β and δ such that, for all $q_p \in \mathbb{P}_p(K)$, $p \in \mathbb{N}$:*

$$\int_K b_K |\nabla q_p|^2 \leq c_1 \frac{(p+1)^2}{h_K^2} \int_K |q_p|^2, \tag{B.44}$$

$$\int_K b_K^{\alpha} |q_p|^2 \leq c_2 (p+1)^{2(\beta-\alpha)} \int_K b_K^{\beta} |q_p|^2, \tag{B.45}$$

$$\int_K b_K^{2\delta} |\nabla q_p|^2 \leq c_3 \frac{(p+1)^{2(2-\delta)}}{h_K^2} \int_K b_K^{\delta} |q_p|^2. \tag{B.46}$$

Proof. It suffices to recall that $h_T \approx h_K$ for all $T \in \widetilde{\mathcal{T}}$, to split the integral over K as a sum of integrals over triangles and to apply Theorem B.3.1. □

Finally, we prove an additional *hp* polynomial inverse inequality which will be instrumental in the *hp* a-posteriori analysis, more precisely in Section 5.2.3.1. We stress that the triangular counterpart of this result was shown in [84, Lemma 3.4].

Lemma B.3.3. *Given K a polygon, we assume that there exists $\widetilde{\mathcal{T}}(K)$ subtriangulation of K such that $h_K \approx h_T$, where we have set as usual $h_\omega = diam(\omega)$ for all $\omega \subset \mathbb{R}^2$. Let b_K be the piecewise bubble function associated with polygon $K \in \mathcal{T}_n$; for an explicit definition of such function see* (B.37). *Then, for all $\frac{1}{2} < \alpha \leq 2$, the following holds true:*

$$|b_K^{\alpha} q_p|_{1,K} \lesssim \frac{(p+1)^{2-\alpha}}{h_K} \| b_K^{\frac{\alpha}{2}} q_p \|_{0,K} \qquad \forall\, q_p \in \mathbb{P}_p(K),\ p \in \mathbb{N}, \tag{B.47}$$

where the hidden constant depends on the shape-regularity of the subtriangulation $\widetilde{\mathcal{T}}(K)$.

Proof. Without loss of generality. We prove the lemma assuming $h_K = 1$. The general assertion follows from a scaling argument.

For $\alpha > \frac{1}{2}$, a direct computation yields:

$$|b_K^\alpha q_p|_{1,K}^2 = \int_K |\nabla(b_K^\alpha q_p)|^2 \leq 2\int_K |b_K|^{2\alpha}|\nabla q_p|^2 + 2\int_K |q_p|^2|\nabla b_K^\alpha|^2. \tag{B.48}$$

Simple algebra implies:

$$|\nabla b_K^\alpha|^2 \lesssim |b_K|^{2(\alpha-1)}. \tag{B.49}$$

Therefore, using the *hp* polynomial inverse estimate on polygons (B.46) with $\delta = \alpha$ on the first term and plugging (B.49) in (B.48), we get:

$$|b_K^\alpha q_p|_{1,K}^2 \lesssim p^{2(2-\alpha)} \int_K b_K^\alpha |q_p|^2 + \int_K b_K^{2(\alpha-1)}|q_p|^2.$$

Note that we can apply (B.46) since we are assuming that $\alpha > \frac{1}{2}$. Applying next the *hp* polynomial inverse estimate on polygons (B.45) to the second term (which is valid owing to $\alpha \leq 2$), we deduce:

$$|b_K^\alpha q_p|_{1,K}^2 \lesssim p^{2(2-\alpha)} \int_K b_K^\alpha |q_p|^2 = p^{2(1-\alpha)} p^2 \|b_K^{\frac{\alpha}{2}} q_p\|_{0,K}^2,$$

which is in fact (B.47). □

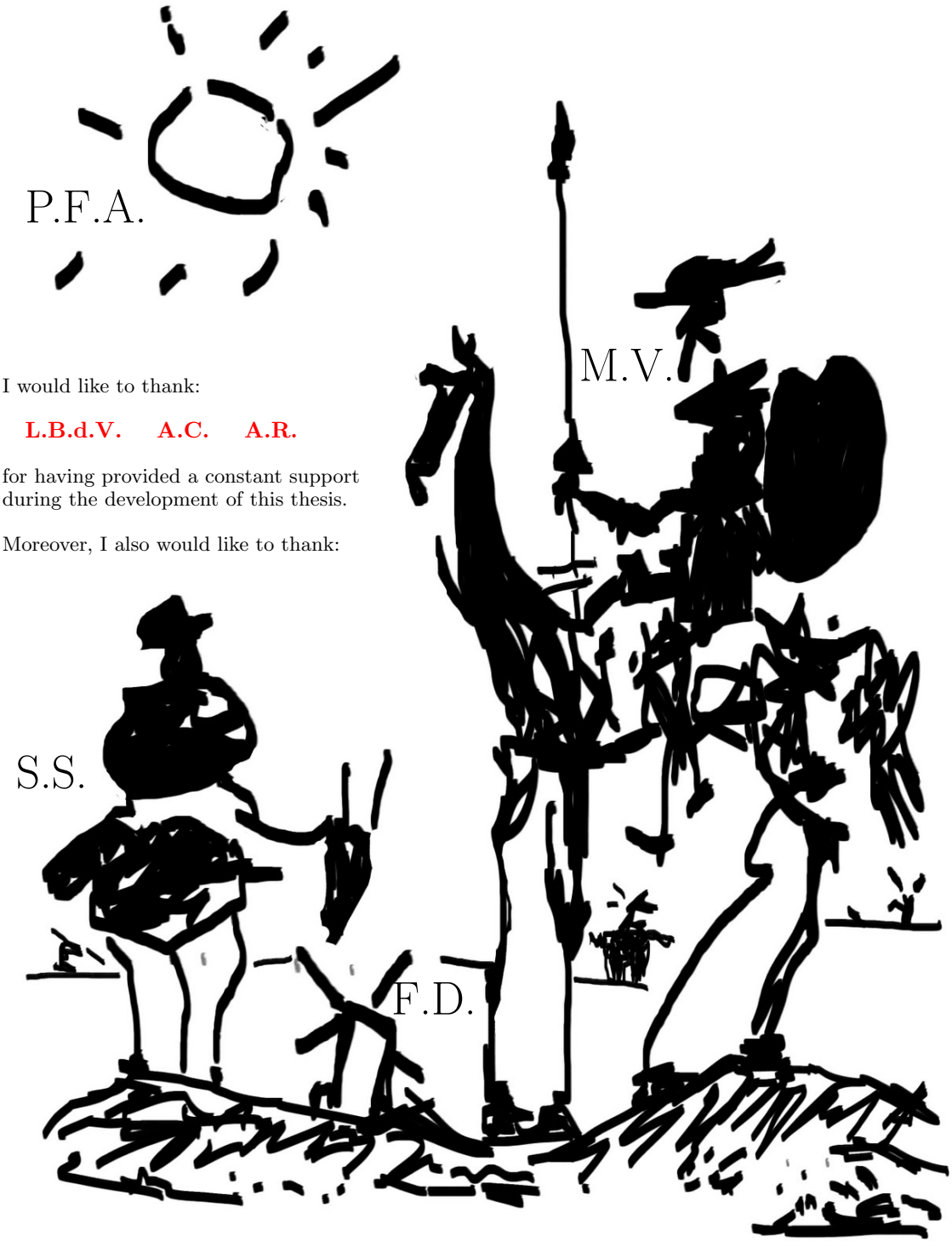

I would like to thank:

L.B.d.V. **A.C.** **A.R.**

for having provided a constant support during the development of this thesis.

Moreover, I also would like to thank:

Bibliography

[1] M. Abramowitz and I. A. Stegun. *Handbook of Mathematical Functions with Formulas, Graphs, and Mathematical Tables*. 1964.

[2] S. Adjerid, M. Aiffa, and J.E. Flaherty. Hierarchical finite element bases for triangular and tetrahedral elements. *Comput. Methods Appl. Mech. Engrg.*, 190(22):2925–2941, 2001.

[3] J. Aghili, D. Di Pietro, and B. Ruffini. A *hp*-hybrid high-order method for variable diffusion on general meshes. 2016.

[4] B. Ahmad, A. Alsaedi, F. Brezzi, L.D. Marini, and A. Russo. Equivalent projectors for virtual element methods. *Comput. Math. Appl.*, 66(3):376–391, 2013.

[5] O. Andersen, H.M. Nilsen, and X. Raynaud. Virtual element method for geomechanical simulations of reservoir models. *Comput. Geosci.*, pages 1–17, 2017.

[6] P. F. Antonietti, L. Beirão da Veiga, D. Mora, and M. Verani. A stream virtual element formulation of the Stokes problem on polygonal meshes. *SIAM J. Numer. Anal.*, 52(1):386–404, 2014.

[7] P. F. Antonietti, L. Beirão da Veiga, S. Scacchi, and M. Verani. A $\mathcal{C}^1$ virtual element method for the Cahn–Hilliard equation with polygonal meshes. *SIAM J. Numer. Anal.*, 54(1):34–56, 2016.

[8] P. F. Antonietti, A. Cangiani, J. Collis, Z. Dong, E. H. Georgoulis, S. Giani, and P. Houston. Review of discontinuous Galerkin finite element methods for partial differential equations on complicated domains. In *Building Bridges: Connections and Challenges in Modern Approaches to Numerical Partial Differential Equations*, pages 279–308. Springer, 2016.

[9] P. F. Antonietti, X. Hu, P. Houston, M. Sarti, and M. Verani. Multigrid algorithms for *hp*-version interior penalty discontinuous galerkin methods on polygonal and polyhedral meshes. *In press on Calcolo*, 2017.

[10] P. F. Antonietti, L. Mascotto, and M. Verani. A multigrid algorithm for the *p*-version of the virtual element method. `https://arxiv.org/abs/1703.02285`, 2017. Accepted for publication on ESAIM Math. Model. Numer. Anal.

[11] P. F. Antonietti, M. Sarti, and M. Verani. Multigrid algorithms for *hp*-discontinuous Galerkin discretizations of elliptic problems. *SIAM J. Numer. Anal.*, 53(1):598–618, 2015.

[12] P. F. Antonietti, M. Sarti, and M. Verani. Multigrid algorithms for high order discontinuous Galerkin methods. *Lect. Notes Comput. Sci. Eng.*, 104:3–13, 2016.

[13] S. Axler, P. Bourdon, and R. Wade. *Harmonic Function Theory*, volume 137. Springer Science & Business Media, 2013.

[14] I. Babuška and B. Guo. The *hp* version of the finite element method. *Comput. Mech.*, 1(1):21–41, 1986.

[15] I. Babuška and B. Q. Guo. Regularity of the solution of elliptic problems with piecewise analytic data. Part I. Boundary value problems for linear elliptic equation of second order. *SIAM J. Math. Anal.*, 19(1):172–203, 1988.

[16] I. Babuška and B. Q. Guo. Regularity of the solution of elliptic problems with piecewise analytic data. Part II: The trace spaces and application to the boundary value problems with nonhomogeneous boundary conditions. *SIAM J. Math. Anal.*, 20(4):763–781, 1989.

[17] I. Babuška and B.Q. Guo. The *hp* version of the finite element method for domains with curved boundaries. *SIAM J. Numer. Anal.*, 25(4):837–861, 1988.

[18] I. Babuška and J. M. Melenk. The partition of unity finite element method: basic theory and applications. *Comput. Methods Appl. Mech. Engrg.*, 139(1-4):289–314, 1996.

[19] I. Babuška and J.M. Melenk. Approximation with harmonic and generalized harmonic polynomials in the partition of unity method. *Comput. Assist. Methods Eng. Sci.*, 4:607–632, 1997.

[20] I. Babuška and M. Suri. The *hp* version of the finite element method with quasiuniform meshes. *ESAIM Math. Model. Numer. Anal.*, 21(2):199–238, 1987.

[21] I. Babuška and M. Suri. The optimal convergence rate of the *p*-version of the finite element method. *SIAM J. Numer. Anal.*, 24(4):750–776, 1987.

[22] R. E. Bank, A. Parsania, and S. Sauter. Saturation estimates for *hp*-finite element methods. *Comput. Vis. Sci.*, 16(5):195–217, 2013.

[23] F. Bassi, L. Botti, A. Colombo, D. A. Di Pietro, and P. Tesini. On the flexibility of agglomeration based physical space discontinuous Galerkin discretizations. *J. Comput. Phys.*, 231(1):45–65, 2012.

[24] L. Beirão da Veiga, C. Lovadina, and D. Mora. A virtual element method for elastic and inelastic problems on polytope meshes. *Comput. Methods Appl. Mech. Engrg.*, 295:327 – 346, 2015.

[25] L. Beirão da Veiga, F. Brezzi, A. Cangiani, G. Manzini, L.D. Marini, and A. Russo. Basic principles of virtual element methods. *Math. Models Methods Appl. Sci.*, 23(01):199–214, 2013.

[26] L. Beirao da Veiga, F. Brezzi, L. D. Marini, and A. Russo. Mixed virtual element methods for general second order elliptic problems on polygonal meshes. *ESAIM Math. Model. Numer. Anal.*, 50(3):727–747, 2016.

[27] L. Beirão da Veiga, F. Brezzi, L. D. Marini, and A. Russo. Serendipity nodal VEM spaces. *Comput. & Fluids*, 141:2–12, 2016.

[28] L. Beirão da Veiga, F. Brezzi, L. D. Marini, and A. Russo. Virtual element method for general second-order elliptic problems on polygonal meshes. *Math. Models Methods Appl. Sci.*, 26(4):729–750, 2016.

[29] L. Beirão da Veiga, F. Brezzi, and L.D. Marini. Virtual elements for linear elasticity problems. *SIAM J. Numer. Anal.*, 51:794–812, 2013.

[30] L. Beirão da Veiga, F. Brezzi, L.D. Marini, and A. Russo. The hitchhiker's guide to the virtual element method. *Math. Models Methods Appl. Sci.*, 24(8):1541–1573, 2014.

[31] L. Beirão da Veiga, A. Chernov, L. Mascotto, and A. Russo. Basic principles of *hp* Virtual Elements on quasiuniform meshes. *Math. Models Methods Appl. Sci.*, 26(8):1567–1598, 2016.

[32] L. Beirão da Veiga, A. Chernov, L. Mascotto, and A. Russo. Exponential convergence of the *hp* virtual element method with corner singularity. *Numerische Mathematik*, 2017. `https://doi.org/10.1007/s00211-017-0921-7`.

[33] L. Beirão da Veiga, F. Dassi, and A. Russo. High-order virtual element method on polyhedral meshes. *Comput. Math. Appl.*, 2017.

[34] L. Beirão da Veiga, K. Lipnikov, and G. Manzini. *The Mimetic Finite Difference Method for elliptic problems*, volume 11. Springer, 2014.

[35] L. Beirão da Veiga, C. Lovadina, and A. Russo. Stability analysis for the virtual element method. *Math. Models Methods Appl. Sci.*, 27(13):2557–2594, 2017.

[36] L. Beirão da Veiga, C. Lovadina, and G. Vacca. Divergence free virtual elements for the Stokes problem on polygonal meshes. *ESAIM Math. Model. Numer. Anal.*, 51(2):509–535, 2017.

[37] L. Beirão da Veiga and G. Manzini. A virtual element method with arbitrary regularity. *IMA J. Numer. Anal.*, 34(2):759–781, 2014.

[38] L. Beirão da Veiga and G. Manzini. Residual a posteriori error estimation for the virtual element method for elliptic problems. *ESAIM Math. Model. Numer. Anal.*, 49(2):577–599, 2015.

[39] M. F. Benedetto, S. Berrone, A. Borio, S. Pieraccini, and S. Scialò. A hybrid mortar virtual element method for discrete fracture network simulations. *J. Comput. Phys.*, 306:148 – 166, 2016.

[40] M.F. Benedetto, S. Berrone, S. Pieraccini, and S. Scialò. The virtual element method for discrete fracture network simulations. *Comput. Meth. Appl. Mech. Engrg.*, 280:135–156, 2014.

[41] M.F. Benedetto, S. Berrone, and S. Scialò. A globally conforming method for solving flow in discrete fracture networks using the virtual element method. *Finite Elem. Anal. Des.*, 109:23 – 36, 2016.

[42] C. Bernardi, N. Fiétier, and R. G. Owens. An error indicator for mortar element solutions to the Stokes problem. *IMA J. Numer. Anal.*, 21(4):857–886, 2001.

[43] C. Bernardi and Y. Maday. Polynomial interpolation results in Sobolev spaces. *J. Comput. Appl. Math.*, 43(1):53–80, 1992.

[44] C. Bernardi and Y. Maday. Spectral methods, in the Handbook of Numerical Analysis V, P.G Ciarlet & J.-L. Lions eds, 1997.

[45] S. Berrone and A. Borio. Orthogonal polynomials in badly shaped polygonal elements for the virtual element method. *Finite Elem. Anal. Des.*, 129:14–31, 2017.

[46] S. Berrone and A. Borio. A residual a posteriori error estimate for the virtual element method. *Math. Models Methods Appl. Sci.*, 2017.

[47] L. Boutet de Monvel and P. Krée. Pseudo-differential operators and Gevrey classes. *Ann. Inst. Fourier (Grenoble)*, 17(1):295–323, 1967.

[48] J. H. Bramble. *Multigrid methods*, volume 294. CRC Press, 1993.

[49] S. C. Brenner and L. R. Scott. *The mathematical theory of Finite Element Methods*, volume 15. Texts in Applied Mathematics, Springer-Verlag, New York, third edition, 2008.

[50] F. Brezzi, K. Lipnikov, and M. Shashkov. Convergence of the mimetic finite difference method for diffusion problems on polyhedral meshes. *SIAM J. Numer. Anal.*, 43(5):1872–1896, 2005.

[51] F. Brezzi and L.D. Marini. Virtual element method for plate bending problems. *Comput. Methods Appl. Mech. Engrg.*, 253:455–462, 2013.

[52] E. Cáceres and G. N. Gatica. A mixed virtual element method for the pseudostress-velocity formulation of the Stokes problem. *IMA J. Numer. Anal.*, 37(1):296–331, 2017.

[53] A. Cangiani, E. H Georgoulis, and P. Houston. *hp*-version discontinuous Galerkin methods on polygonal and polyhedral meshes. *Math. Models Methods Appl. Sci.*, 24(10):2009–2041, 2014.

[54] A. Cangiani, E. H. Georgoulis, T. Pryer, and O. J. Sutton. A posteriori error estimates for the virtual element method. *Numer. Math.*, 137:857–893, 2017.

[55] A. Cangiani, V. Gyrya, and G. Manzini. The non-conforming virtual element method for the Stokes equations. *SIAM J. Numer. Anal.*, 54(6):3411–3435, 2016.

[56] A. Cangiani, G. Manzini, and O. J. Sutton. Conforming and nonconforming virtual element methods for elliptic problems. *IMA J. Numer. Anal.*, 37:1317–1354, 2016.

[57] C. Canuto, M. Y. Hussaini, A. Quarteroni, and T. A. Zhang. *Spectral Methods in Fluid Dynamics*. Springer Science & Business Media, 2012.

[58] A. Chernov and L. Mascotto. The harmonic virtual element method: Stabilization and exponential convergence for the Laplace problem on polygonal domains. `https://arxiv.org/abs/1705.10049`, 2017.

[59] A. Chernov and C. Schwab. Exponential convergence of Gauss–Jacobi quadratures for singular integrals over simplices in arbitrary dimension. *SIAM J. Numer. Anal.*, 50(3):1433–1455, 2012.

[60] B. Cockburn, J. Gopalakrishnan, and R. Lazarov. Unified hybridization of discontinuous Galerkin, mixed, and continuous Galerkin methods for second order elliptic problems. *SIAM J. Numer. Anal.*, 47(2):1319–1365, 2009.

[61] F. Dassi and L. Mascotto. Exploring high-order three dimensional virtual elements: bases and stabilizations. `https://arxiv.org/abs/1709.04371`, 2017.

[62] D. A. Di Pietro and A. Ern. Hybrid high-order methods for variable-diffusion problems on general meshes. *C. R. Math. Acad. Sci. Paris*, 353(1):31–34, 2015.

[63] M. Dubiner. Spectral methods on triangles and other domains. *J. Sci. Comput.*, 6(4):345–390, 1991.

[64] M. G. Duffy. Quadrature over a pyramid or cube of integrands with a singularity at a vertex. *SIAM J. Numer. Anal.*, 19(6):1260–1262, 1982.

[65] T. Dupont and L. R. Scott. Polynomial approximation of functions in Sobolev spaces. *Math. Comp.*, 34(150):441–463, 1980.

[66] A.L. Gain, G.H. Paulino, S.D. Leonardo, and I.F.M. Menezes. Topology optimization using polytopes. *Comput. Methods Appl. Mech. Engrg.*, 293:411–430, 2015.

[67] A.L. Gain, C. Talischi, and G.H. Paulino. On the virtual element method for three-dimensional elasticity problems on arbitrary polyhedral meshes. *Comput. Methods Appl. Mech. Engrg.*, 282:132–160, 2014.

[68] A. Ghizzetti and A. Ossicini. *Quadrature Formulae*. Birkhäuser, 1970.

[69] A. Gillette, A. Rand, and C. Bajaj. Error estimates for generalized barycentric interpolation. *Adv. Comput. Math.*, 37(3):417–439, 2012.

[70] P. Grisvard. *Elliptic problems in nonsmooth domains*. SIAM, 2011.

[71] B. Guo and L. Wang. Jacobi approximations in non-uniformly Jacobi-weighted Sobolev spaces. *J. Approx. Theory*, 128(1):1–41, 2004.

[72] R. Hiptmair, A. Moiola, I. Perugia, and C. Schwab. Approximation by harmonic polynomials in star-shaped domains and exponential convergence of Trefftz *hp*-dGFEM. *ESAIM Math. Model. Numer. Anal.*, 48(3):727–752, 2014.

[73] V. A. Kondrat'ev. Boundary value problems for elliptic equations in domains with conical or angular points. *Trudy Moskovskogo Matematicheskogo Obshchestva*, 16:209–292, 1967.

[74] T. Koornwinder. Two-variable analogues of the classical orthogonal polynomials. *Theory and applications of special functions*, pages 435–495, 1975.

[75] F. Li. On the negative-order norm accuracy of a local-structure-preserving LDG method. *J. Sci. Comput.*, 51(1):213–223, 2012.

[76] F. Li and C.-W. Shu. A local-structure-preserving local discontinuous Galerkin method for the Laplace equation. *Methods Appl. Anal.*, 13(2):215, 2006.

[77] H. Li and W. Shan. The triangular spectral element method for Stokes eigenvalues. *Math. Comp.*, 2017.

[78] H. Li and J. Shen. Optimal error estimates in Jacobi-weighted Sobolev spaces for polynomial approximations on the triangle. *Math. Comp.*, 79(271):1621–1646, 2010.

[79] L. Mascotto. Ill-conditioning in the virtual element method: stabilizations and bases. `https://arxiv.org/abs/1705.10581`, 2017. Accepted for publication on Numer. Methods Partial Differential Equations.

[80] W. C. H. McLean. *Strongly Elliptic Systems and Boundary Integral Equations*. Cambridge university press, 2000.

[81] J. M. Melenk. Operator adapted spectral element methods I: harmonic and generalized harmonic polynomials. *Numer. Math.*, 84(1):35–69, 1999.

[82] J. M. Melenk. *hp*–interpolation of non–smooth functions. *SIAM J. Numer. Anal.*, 43:127–155, 2005.

[83] J. M. Melenk, A. Parsania, and S. Sauter. General DG-methods for highly indefinite Helmholtz problems. *J. Sci. Comput.*, 57(3):536–581, 2013.

[84] J. M. Melenk and B. I. Wohlmuth. On residual-based a posteriori error estimation in *hp*-FEM. *Adv. Comput. Math.*, 15(1-4):311–331, 2001.

[85] M. Melenk. *On Generalized Finite Element Methods*. PhD thesis, University of Maryland, 1995.

[86] I. F. M. Menezes, G. H. Paulino, A. Pereira, and C. Talischi. Polygonal finite elements for topology optimization: A unifying paradigm. *Internat. J. Numer. Methods Engrg.*, 82(6):671–698, 2010.

[87] D. Mora, G. Rivera, and R. Rodríguez. A virtual element method for the Steklov eigenvalue problem. *Math. Models Methods Appl. Sci.*, 25(08):1421–1445, 2015.

[88] D. Mora, G. Rivera, and R. Rodriguez. A posteriori error estimates for a virtual elements method for the Steklov eigenvalue problem. *Comput. Math. Appl.*, 74:2172–2190, 2017.

[89] S. Natarajan, S.PA Bordas, and E.T. Ooi. Virtual and smoothed finite elements: a connection and its application to polygonal/polyhedral finite element methods. *Internat. J. Numer. Methods Engrg.*, 104(13):1173–1199, 2015.

[90] R. Pasquetti and F. Rapetti. Spectral element methods on triangles and quadrilaterals: comparisons and applications. *J. Comput. Phys.*, 198(1):349–362, 2004.

[91] Perugia, I., Pietra, P., and Russo, A. A plane wave virtual element method for the Helmholtz problem. *ESAIM Math. Model. Numer. Anal.*, 50(3):783–808, 2016.

[92] S. Rjasanow and S. Weißer. Higher order BEM-based FEM on polygonal meshes. *SIAM J. Numer. Anal.*, 50(5):2357–2378, 2012.

[93] S. A. Sauter and C. Schwab. Boundary Element Methods. In *Boundary Element Methods*, pages 183–287. Springer, 2010.

[94] D. Schötzau, Ch. Schwab, and T. P. Wihler. *hp*-DGFEM for second-order elliptic problems in polyhedra I: Stability on geometric meshes. *SIAM J. Numer. Anal.*, 51(3):1610–1633, 2013.

[95] D. Schötzau, Ch. Schwab, and T. P. Wihler. *hp*-dGFEM for second order elliptic problems in polyhedra II: Exponential convergence. *SIAM J. Numer. Anal.*, 51(4):2005–2035, 2013.

[96] C. Schwab. *p- and hp- Finite Element Methods: Theory and Applications in Solid and Fluid Mechanics*. Clarendon Press Oxford, 1998.

[97] J. Shen, T. Tang, and L.-L. Wang. *Spectral Methods: algorithms, analysis and applications*, volume 41. Springer Science & Business Media, 2011.

[98] E. M. Stein. *Singular integrals and differentiability properties of functions*, volume 2. Princeton University Press, 1970.

[99] N. Sukumar and A. Tabarraei. Conforming polygonal finite elements. *Internat. J. Numer. Methods Engrg.*, 61:2045–2066, 2004.

[100] G. Szegő. *Orthogonal polynomials*, volume 23. American Mathematical Soc., 1939.

[101] L. Tartar. *An introduction to Sobolev spaces and interpolation spaces*, volume 3. Springer Science & Business Media, 2007.

[102] H. Triebel. *Interpolation theory, function spaces, differential operators*. North-Holland, 1978.

[103] J. Wang and X. Ye. A weak Galerkin finite element method for second-order elliptic problems. *J. Comput. Appl. Math.*, 241:103–115, 2013.

[104] T. P. Wihler. *Discontinuous Galerkin FEM for elliptic problems in polygonal domains*. PhD thesis, Swiss Federal Institute of Technology Zurich, 2002.

[105] P. Wriggers, W. T. Rust, and B. D. Reddy. A virtual element method for contact. *Comput. Mech.*, 58(6):1039–1050, 2016.